PREDICTION OF REGENERATOR THERMAL PERFORMANCE USING A NON-ITERATIVE METHOD OF COMPUTATION

by

Ronald Evans, B.Sc.,
Department of Mathematics and Computer Science,
The Polytechnic of Wales.

This thesis is submitted for the degree of Doctor of Philosophy of the Council for National Academic Awards.

September, 1984.

DECLARATION

I hereby declare that while registered as a candidate for the C.N.A.A. degree of Doctor of Philosophy, I have not been registered as a candidate for another award of the C.N.A.A. or of a University. I further declare that, apart from the previous studies in this field, which are appropriately referenced in the text, the material contained in this thesis has not been used for any other academic award.

K. Evans.

Acknowledgements

I would like to thank The Polytechnic of Wales for permitting this research study to be undertaken and also for the use of the Polytechnic computing equipment.

I am also deeply indebted to my Director of Studies, Professor S.D. Probert, School of Mechanical Engineering, Cranfield Institute of Technology, and to my Supervisor, the late Dr. J.V. Edwards, formerly of the Department of Chemical Engineering at The Polytechnic of Wales.

The co-operation, advice and encouragement afforded to me by Professor Probert throughout the entire course of this study have been factors of immense value and are greatly appreciated.

Prior to his untimely death, the keen interest taken in this research by Dr. John Edwards resulted in many helpful discussions which were of particular benefit.

Finally, I would like to acknowledge the valuable contribution made by Mrs. Barbara Rees, who has typed the complicated mathematical manuscript with consummate skill.

Ronald Evans, Ph.D. Thesis, 1984.

SUMMARY

Prediction of Regenerator Thermal Performance Using a Non-iterative Method of Computation

This research study has undertaken the further development of a non-iterative method for predicting the fluid temperature variations in a counterflow regenerator operating at cyclic equilibrium. The method utilises the closed-form solutions derived by earlier workers from the equations of the regenerator, finite-conductivity thermal model.

The numerical techniques required to compute the fluid temperature histories from these 'closed' solutions are detailed, and it is noted that in a previous attempt to apply this method, many computations had serious numerical errors. Also, the theory developed to cater for heating and cooling periods of unequal duration was incomplete and virtually untested.

As a result of the present investigation, all of the previously reported computational difficulties have been resolved satisfactorily. In addition, techniques have been developed which have enabled regenerator performance to be predicted for a wide range of dimensionless regenerator parameters, including cases of unequal heating and cooling periods.

The successful application of this method has been shown to depend on the ability to control, to suitably small values, the numerical errors which can arise during the summation of infinite series and in the application of methods for numerical quadrature and for the numerical integration of differential equations.

The application of the techniques developed to achieve the necessary error control has enabled thermally well-balanced solutions to be attained consistently although, in many cases, the need to resort to small step sizes in the time dimension has reflected the relatively poor accuracy of the method adopted for numerical quadrature. This, in turn, has necessitated the development of an extrapolation method for predicting the regenerator effectiveness.

The use of a more accurate quadrature formula is suggested in order to realise the full potential of this computational approach.

CONTENTS

LIST OF TABLES AND FIGURES

APPENDICES

NOMENCLATURE OF THE MOST FREQUENTLY-USED SYMBOLS

a	Semi-thickness of regenerator wall.	..... m
a_1	$= \frac{N_1}{N_1-1}$	
a_2	$= \frac{N_2}{N_2-1}$	
a_3	$= \frac{1}{N_2-1} - \frac{1}{N_1-1}$	
a_4	$= \frac{1}{N_1-1} + \frac{1}{N_2-1}$	
A	A constant used in equation (A2.1-10).	
$\underline{A}_1', \underline{A}_2'$	Matrices which occur when numerical methods are used to approximate each of the integro-differential equations (2-5) and (2-6) by a system of ordinary differential equations; the elements of these matrices are given in equations (A2.1-16) and (A2.1-20).	
$\underline{A}_1, \underline{A}_2$	Matrices related to $\underline{A}_1'$ and $\underline{A}_2'$ as shown in equations (2-27) and (2-28).	
b_s	$= \frac{2\beta_s}{2+\beta_s}$	
$\bar{b}_i$	Gradient of regression line relating $\dot{H}_i$ and $\frac{1}{n}$, as specified in equation (4-1).	
B	A constant introduced in equation (A2.1-10).	

$\underline{B}_1, \underline{B}_2$ Matrices which occur when numerical methods are used to approximate each of the integro-differential equations (2-13) and (2-14) by a system of ordinary differential equations; the elements of these matrices are given in equations (A2.2-1), (A2.2-3) and (A2.2-4).

c Specific heat capacity of regenerator wall material. ..... $Jkg^{-1}K^{-1}$

C A particular value of z'.

C_1 A constant (for a particular regenerator) introduced in equation (2-49).

$\underline{C}_1, \underline{C}_2, \underline{C}_3, \underline{C}_4$ Matrices defined in equations (7-23) to (7-26).

d_1 $= \frac{1}{\Omega_1(N_1-1)}$

d_2 $= \frac{1}{\Omega_2(N_2-1)}$

$\underline{D}_1, \underline{D}_2$ Matrices which occur when numerical methods are used to approximate each of the integro-differential equations (2-13) and (2-14) by a system of ordinary differential equations; the elements of these matrices are given in equations (A2.2-2) to (A2.2-4).

e_1 Acceptable limit of fractional error.

$E(\xi, \zeta, z)$ Wall temperature referred to the dimensionless variables ξ, ζ, z ..... Dimensionless

$E\dot{H}^*$ Maximum numerical error in $\dot{H}^*$, as estimated by equation (4-4).

EH_T^* Maximum numerical error in H_T^*, as estimated by equations (8-4), (8-6) or (8-8).

$E_{T_s}[H_j]$ Maximum fractional error in the s-th term of the infinite series, H_j.

$Eq_s(u)$;$Er_s(u)$ Quantities which are known to be greater than the fractional errors of the terms $q_s(u)$ and $r_s(u)$, respectively.

$E\eta_R$ Estimated value of the maximum percentage error in the predicted value of η_R.

$f_i(\zeta,z')$ Dimensionless fluid temperature referred to variables ζ,z'; occurs in equal-period theory.

$f_i(\zeta,v)$ Dimensionless fluid temperature referred to variables ζ,v; occurs in generalised theory.

$f_{m,j}^{(s)}$ j-th element of solution vector $\underline{F}_m^{(s)}$.

$\underline{F}_i(\zeta)$ Column matrix containing the values of $f_i(\zeta)$ at (n+1) equally-spaced values of z' (or v), as appropriate, for $0 \leqslant z' \leqslant \Omega$ (or $0 \leqslant v \leqslant 1$).

$\underline{F}_{i,r}$ $\underline{F}_i(\zeta)$ at $\zeta = \frac{r}{m}$; $-m \leqslant r \leqslant m$.

$\underline{F}(\zeta)$ Column matrix of order (2n+2)x1 defined in equation (2-23).

$\underline{F}_r$ $\underline{F}(\zeta)$ at $\zeta = \frac{r}{m}$; $-m \leqslant r \leqslant m$.

$\underline{F}_r^{(s)}$ Solution vector of the coupled difference equations (A3-1) at $\zeta = \frac{r}{m}$, $-m \leqslant r \leqslant m$, computed using the hypothetical boundary condition $\underline{F}_{-m}^{(s)}$.

$\underline{F}_{-m}^{(s)}$ Hypothetical boundary condition used in the solution of equations (A3-1) and defined in equations (A3-4) to (A3-6); $1 \leqslant s \leqslant n+2$.

$\underline{F}_{1,-m}^{(s)}$ Sub-matrix of $\underline{F}_{-m}^{(s)}$, as defined in equation (A3-5).

$g(v)$ A function defined in equation (2-18).

$\underline{G}_1, \underline{G}_2, \underline{G}_3, \underline{G}_4$ Matrices defined in equations (3-11) to (3-14).

h Dimensionless step size used for numerical quadrature in the time domain; $h = \frac{\Omega}{n}$ for equal-period theory, $h = \frac{1}{n}$ for generalised theory.

h_i Heat-transfer coefficient between the fluid and the regenerator wall surface, in period i. ..... $Wm^{-2}K^{-1}$

$\bar{h}_i$ Bulk heat-transfer coefficient between the fluid and the regenerator wall in period i - see equation (1-15) ..... $Wm^{-2}K^{-1}$

h_L Dimensionless step size used for finite-difference approximations in the distance domain, $h_L = \frac{1}{m}$.

H_j Functions defined in equations (A2.1-17) to (A2.1-19) and (A2.1-21) to (A2.1-23); $1 \leqslant j \leqslant 6$.

$\underline{H}_1, \underline{H}_2$ Matrices defined in equations (3-15) and (3-16).

$\dot{H}_i$ Dimensionless mean rate of heat transfer for period i, see equations (2-45) and (2-46).

$\dot{H}_i^r$ Value of $\dot{H}_i$ computed with program parameter n=r.

$\dot{H}_i^\infty$ Value of $\dot{H}_i^r$ predicted for the case $r \to \infty$.

$\dot{H}^*$ Value of $\dot{H}_i$ which would be obtained in a computation not affected by numerical errors (equal-period theory only).

$H_{T,i}$ Dimensionless quantity of heat transferred in heating and cooling periods; see equations (8-1) and (8-2).

H_T^* Dimensionless value of $H_{T,i}$ which would be obtained in a computation not affected by numerical errors.

$H_{T,i}^r$ Value of $H_{T,i}$ computed with program parameter n=r.

i Subscript used to distinguish the hot and cold periods; i=1 represents the hot period, i=2, the cold period.

$\underline{I}$ The identity matrix.

$I_{1,r}, I_{2,r}$ Definite integrals defined in equations (A2.1-1) and (A2.1-3).

$\delta I'_{l,r'}, \delta I''_{l,r'}$ Definite integrals taken over a single time-step, as defined in equations (A2.1-6) and (A2.1-7).

j An integer.

k_x, k_y Thermal conductivity of the regenerator wall material in directions perpendicular to and parallel to the fluid flow, respectively. (When $k_y=0$, for simplicity k_x is written as k). ..... $Wm^{-1}K^{-1}$

K_s Constants introduced in equation (A3-7); $1 \leqslant s \leqslant n+2$.

$\underline{K}$ Column matrix containing the values of K_s; see (A3-12).

$\underline{K}_1, \underline{K}_2, \underline{K}_3, \underline{K}_4$ Matrices defined in equations (7-19) to (7-22).

L Length of a regenerator channel. ..... m

$2m$ Integral number of equal distance steps dividing the regenerator channel length.

M_i $= \frac{2W_i S_i a}{kpL}$; Dimensionless parameter characteristic of period i.

n Integral number of time-steps dividing each period.

N_i $= \frac{h_i a}{k}$; Dimensionless parameter, (i.e. the Biot modulus), characteristic of period i.

p	Perimeter of equivalent single channel regenerator. ..... m
P_i	Duration of appropriate period i. ..... s
$\underline{P}, \underline{P}_1, \underline{P}', \underline{P}'_1$	Matrices defined in equations (2-25), (2-38), (3-22) and (7-16).
q	A positive integer.
$q_s(u)$	s-th term of the series $Q_1(u)$ or $Q_2(u)$, as appropriate.
$Q_1(u), Q_2(u)$	Functions defined in equation (A2.2-3).
Q'_i	Total quantity of heat transferred during appropriate period i. ..... J
$\underline{Q}$	Matrix defined in equation (2-34).
r, r', r_1	Integers.
$r_s(u)$	s-th term of series $R_1(u)$ or $R_2(u)$, as appropriate.
$R_1(u), R_2(u)$	Functions defined in equation (A2.2-4).
$\overline{R}$	Value of $\overline{R}_s\,[R_i(0)]$ estimated from equation (7-7).
$\overline{R}_s$	Estimated value of residue of slowly converging H-series; see (A5-7).

$\overline{R}_r[Y]$ Residue of any infinite series Y, after the first r terms have been summed.

$\underline{R}, \underline{R}_1$ Matrices defined in equations (3-18) and (7-17).

s A positive integer.

S_i Specific heat capacity of regenerator fluid in appropriate period i. ..... $Jkg^{-1}K^{-1}$

$\underline{S}, \underline{S}_1$ Matrices defined in equations (3-19) and (7-18).

$\overline{S}_r[Y]$ Sum of the first r terms of the infinite series Y.

$t(y,\theta)$ Temperature of the fluid during the heating or cooling period. ..... ^oC

$t_i(y,\theta)$ Temperature of fluid during the appropriate period i. ..... ^oC

$\overline{t}_i(y)$ Chronological mean temperature during the appropriate period i. ..... ^oC

$t'(y,\theta)$ Temperature of fluid measured on a dimensionless scale, (see equation (2-1)). ..... Dimensionless

$T(x,y,\theta)$ Temperature of the regenerator wall in heating or cooling period. ..... ^oC

$\underline{T}_1, \underline{T}_2$ Matrices defined in equation (2-26).

u, u' Independent variables.

v Dimensionless time measured on a dimensionless scale, such that $0 \leqslant v \leqslant 1$ in each period, (see equation 2-20).

v_s s-th root of $[v_s+(s-1)\pi]\tan v_s=1$, (Program 2 only).

$\underline{V}_1, \underline{V}_2$ Matrices defined in equations (2-41) and (2-42).

w_i Mass of fluid occupying unit length of the equivalent single-channel regenerator, in period i. ..... kg

W_i Mass flow rate of fluid in equivalent single-channel regenerator, in period i. ..... kg s^{-1}

x Perpendicular distance into the regenerator wall measured from the wall surface. ..... m

$X_1(\zeta,z'), X_2(\zeta,z')$ Functions defined in equations (2-7) and (2-8).

$X_{1,s}, X_{2,s}$ Values of $X_1(\zeta,z')$ and $X_2(\zeta,z')$ at $z'=sh$; $0 \leqslant s \leqslant n$.

$\underline{X}_1(\zeta), \underline{X}_2(\zeta)$ Column matrices containing the (n+1) values of $X_{1,s}$ and $X_{2,s}$, respectively.

y	Distance along regenerator channel, measured from its mid-point. ..... m
z	Dimensionless time measured on a dimensionless scale, such that $0 \leqslant z \leqslant 2\Omega$ for a complete cycle (see equation (2-2)).
z'	Dimensionless time measured on a dimensionless scale such that $0 \leqslant z' \leqslant \Omega$ in each period.
$\underline{Z}_1, \underline{Z}_2$	Matrices defined in equations (2-39) and (2-40).

Greek Symbols

α	Thermal diffusivity of regenerator wall material. ..... $m^2 s^{-1}$
α_s	s-th element of column matrix $\underline{\alpha}$; $1 \leqslant s \leqslant n+2$.
$\underline{\alpha}$	Column matrix defined in equation (A3-11).
β_s	The s-th root of $\sqrt{\beta} \tan \sqrt{\beta} = 1$.
$\beta_{s\ min}$	A lower bound of β_s.
$\beta_{s\ max}$	An upper bound of β_s.
$\underline{\beta}$	A matrix defined in equation (A3-13).
$\underline{\gamma}_1, \underline{\gamma}_2$	Matrices defined in equations (2-26).
ϵ_2	Upper bound for local truncation error in Runge-Kutta program.

ζ $= \frac{2y}{L}$. Dimensionless distance along the regenerator channel, such that $-1 \leqslant \zeta \leqslant +1$.

$\eta_1(\tau), \eta_2(\tau)$ Functions defined in equations (2-9) and (2-10).

η_R Regenerator effectiveness, defined in equation (4-5).

$\eta_{R,C}$ Regenerator cooling-period effectiveness, defined in equation (8-11).

θ Time, measured from the start of a heating period. ..... s

Λ_i $= \frac{2N_i}{M_i}$. Dimensionless regenerator parameter ('Reduced length').

ν_s s-th root of $\nu \tan \nu = 1$.

$\nu_{s\ min}, \nu_{s\ max}$ Lower and upper bounds of ν_s, respectively.

$\nu_{s,0}, \nu_{s,1}$ Successive estimates of ν_s obtained from equation (A5-1).

ξ $= \frac{x}{a}$. Non-dimensional distance orthogonal to regenerator wall, such that $0 \leqslant \xi \leqslant 1$.

Π_i $= \Omega_i N_i$. Dimensionless regenerator parameter ('Reduced Period').

$\sigma_r[S]$ Sum of the first r terms of infinite series S.

$\tau, \bar{\tau}$ Particular values of z' and v, respectively.

$\phi_1(\zeta,v), \phi_2(\zeta,v)$ Functions defined in equations (2-16) and (2-17).

$\underline{\phi}_1(\zeta), \underline{\phi}_2(\zeta)$ Column matrices containing the values of ϕ_1 and ϕ_2 obtained with $v=sh$; $0 \leqslant s \leqslant n$.

$\chi_i(\zeta,z)$ Fluid temperature $t'_i(y,\theta)$ transformed to axes ζ, z. ..... Dimensionless

Ω_i $= \frac{a P_i}{a^2}$. Dimensionless parameter (i.e. the Fourier number), characterising the duration of period i.

Ω Used for Ω_1 or Ω_2 when these are equal.

GLOSSARY OF TECHNICAL TERMS

For convenience of reference, certain frequently used technical terms are explained:-

Balanced regenerator - a thermally symmetrical regenerator (see below).

Cold fluid - a fluid whose temperature increases as it passes through a regenerator.

Cooling (cold) period - the time interval between starting and stopping the cold fluid flow.

Counterflow - describes a heat exchanger design in which the hot and cold fluid streams flow in parallel but opposite directions.

Cross-flow - describes a heat exchanger design in which the hot and cold fluid streams flow in orthogonal directions.

Cycle - the sequence of operations in a fixed-bed regenerator, namely the start of the hot fluid flow followed successively by stopping the hot fluid flow, starting the cold fluid flow, stopping the cold fluid flow and continuing until the start of the hot fluid flow once again.

Cyclic equilibrium - the state attained in a regenerator when fluid and solid temperature-time histories, at all regenerator positions, are repeated identically in all cycles.

Equal-period theory - the non-iterative (closed) theory developed to enable a regenerator's thermal performance to be computed for the case when the hot and cold periods are of equal duration.

Example - regenerator example: a regenerator design computation which requires the solution of the equations of the regenerator, 3-D, thermal model, for a particular combination of the dimensionless regenerator parameters.

Fixed-bed regenerator - a regenerator which operates with a static matrix.

Fractional error - the ratio $\frac{|S_E - S|}{S_E}$, where S is an estimated value and S_E the exact value of the considered quantity (usually the sum of an infinite series).

Fluid temperature - the temperature of the prescribed hot or cold fluid.

Generalised theory - the non-iterative (closed) theory developed to enable a regenerator's performance to be computed for the case when the hot and cold periods are of unequal duration.

Harmonic mean - the harmonic mean A_H of any two numbers A_1 and A_2 is defined to be $A_H = \frac{2}{\frac{1}{A_1} + \frac{1}{A_2}}$.

Heat-balance discrepancy (H.B.D.) - the ratio $\frac{|Q'_1 - Q'_2|}{Q'_{MIN}}$ expressed as a percentage, where Q'_1 and Q'_2 are the computed values of the amounts of heat transferred during the hot and cold periods, and Q'_{MIN} is the smaller of Q'_1 or Q'_2.

Heating (hot) period - the time interval between starting and stopping the hot fluid flow.

Hot fluid - a fluid whose temperature <u>decreases</u> as it passes through a regenerator.

Invert example - if a given regenerator example is defined by the parameters $M_1 = m_1$, $M_2 = m_2$, $N_1 = n_1$, $N_2 = n_2$, $\Omega_1 = w_1$, $\Omega_2 = w_2$, then its invert example is defined by the parameters $M_1 = m_2$, $M_2 = m_1$, $N_1 = n_2$, $N_2 = n_1$, $\Omega_1 = w_2$ and $\Omega_2 = w_1$.

Matrix (mathematical) - a rectangular array of numbers which are arranged in r rows and s columns, where r and s are integers $\geqslant 1$.

Matrix (physical) - the solid medium in a regenerator, which absorbs heat from the hot fluid and gives out heat to the cold fluid: synonymous terms are regenerator walls, packing, filling and chequers.

Memory usage - the amount of computer memory (e.g. number of bytes) needed to store and run a given computer program.

Model - mathematical model: a collection of mathematical equations (usually differential equations and associated boundary conditions) which relate the physical variables pertinent to a particular physical process, e.g. those relating the temperatures in a regenerator operating at cyclic equilibrium.

2-D Model - a mathematical model of a regenerator in which the fluid and solid temperatures are functions of one space co-ordinate and time (hence the phrase 'two-dimensional' model).

3-D Model - as for the 2-D model, but with the solid temperature being a function of two space co-ordinates as well as time (hence the phrase 'three-dimensional' model).

Parallel flow - describes a heat exchanger in which the hot and cold fluid streams flow in the same direction.

Program parameters - computer program variables which are assigned from input data and which control the numerical accuracy of a regenerator computation.

Recuperator - a heat exchanger in which heat is transferred directly and continuously from the hot fluid, through a separating wall, to a colder fluid.

Regenerator - a heat exchanger in which, for a given interval, heat is transferred from the hot fluid to a suitable heat store (matrix), and subsequently, for a further period, from the heat store to the cold fluid; these operations being repeated continuously.

Regenerator effectiveness - the ratio Q'/Q'_{MAX}, where Q' is the quantity of heat transferred per cycle in a given regenerator, and Q'_{MAX} is the maximum possible value of Q', consistent with the heat-transfer laws.

Regenerator parameters - dimensionless groups which characterise the mathematical model of a given regenerator, e.g. Λ, Π, N, M, Ω.

Residue - the sum of the remaining terms of an infinite series $\sum_{r=1}^{\infty} u_r$, after the first s terms have been summed, where s is any positive integer.

Reversal condition - a mathematical condition which expresses the fact that a regenerator operates in cyclic equilibrium (but often taken to be the condition that the matrix temperature distribution at the start of a period is equal to that at the end of the preceding period).

Rotary regenerator - a regenerator in which the matrix rotates about a central axis, so that a given proportion of the matrix is always in contact with the hot fluid, the remainder being in contact with the cold fluid.

Solid temperature - the temperature of the regenerator matrix.

Thermally symmetrical regenerator - a regenerator whose operating parameters are identical for both periods. This would occur, for example, if the fluid heat capacity rates, the heat-transfer coefficients and heating and cooling times were equal for successive periods.

CHAPTER 1

REGENERATIVE HEAT EXCHANGERS (REGENERATORS): A REVIEW OF THEIR APPLICATIONS AND THE THERMAL ASPECTS OF THEIR DESIGN

1.1 HEAT EXCHANGERS: RECUPERATORS AND REGENERATORS

The technical success and economic viability of many modern industrial processes often depend on the installation of suitable heat exchangers to transfer heat energy between two fluid streams, whose temperatures are at different levels. In many applications heat exchangers make a significant contribution to industrial energy conservation, by recovering heat energy which would otherwise be wasted, an aspect which has been treated in depth by Reay [1]. Heat exchangers are also vital components in many engineering systems.

Depending on the particular practical application, the transfer of heat through a heat exchanger can occur between two liquid streams, or two gas streams or a liquid stream and a gas stream. For this reason, heat exchangers are often simply classified as 'liquid-to-liquid', 'gas-to-gas' or 'liquid-to-gas' types.

Other more comprehensive classification schemes have been advanced by Shah [2]. One such scheme, which is particularly useful for industrial applications, is to classify heat exchangers according to the general process by which the heat transfer is effected. Using this approach, the majority of heat exchangers fall into two broad categories, namely recuperators and regenerators. Put very simply, the essential difference between these two types is that regenerators involve the storage of heat, whereas recuperators do not.

Recuperators are usually constructed to allow both fluids to flow continuously and simultaneously through the same unit, without coming into direct contact with one another. This is achieved by passing one or both fluids through different leak-proof passages. In such an arrangement, heat is transferred directly from one fluid to the other, through the walls of the passages separating the two fluids. Heat exchangers of this type are therefore often referred to as 'separating-wall', 'conductance' or 'direct-transfer' heat exchangers.

By contrast, in a regenerator - alternative names are thermal regenerator, regenerative heat exchanger or periodic-flow exchanger - the same flow passages are occupied by each of the two fluids, but at different times. In the simplest form of regenerator, an initially hotter fluid passes through the unit for a certain time interval known as the heating or hot period, during which it transfers a proportion of its sensible heat to a heat-storing mass[+] placed within the regenerator. At the end of the heating period, the flow of the hotter gas is terminated and an initially colder fluid is then passed through the regenerator for a time interval known as the cooling or cold period. During this latter period, heat is recovered from the heat-storing mass, thereby heating the colder fluid.

+ alternatively called the regenerator 'filling', 'packing', 'matrix' or 'chequers'.

It is useful to recognise at this point, that in practice regenerators are used only for the transfer of heat between gases. Also, in a great number of applications, the heated gas is air. Because of this, the terms 'air', 'gas', 'air period' and 'gas period' will be used synonymously with the terms cold fluid, hot fluid, cold period and hot period, respectively.

Both recuperators and regenerators can be designed so that the hot and cold fluids flow either in the same direction or in opposite directions. These two flow arrangements are described as 'parallel-flow' and 'counter-flow', respectively. For a given heat exchanger of either type, the latter mode is usually preferred, because it results in a better heat-transfer performance. A third arrangement, viz., 'cross-flow', in which the fluid flow paths are not parallel - in pure cross-flow they are orthogonal - occurs only in recuperators. With recuperators, combinations of these three arrangements are also possible [3] .

Many different forms of recuperators have been developed over the years, and standard types such as plate heat exchangers, shell-and-tube heat exchangers, radiators and coolers are applied over a broad spectrum of technological processes. The texts by Reay [1] , Hausen [3] and Fraas [4] are useful reference sources, covering the design and application of these different recuperator types.

Since their invention over a century ago, regenerators have also been developed in several different forms. However, the majority of practical applications are confined to two major types, namely fixed-bed regenerators and rotary regenerators. In the first type, the heat-storing mass is static within a particular structure, whereas in the second type, the heat-storing mass is constructed in the form of a cylindrical wheel or disc, which rotates continuously about its longitudinal axis.

Industrial processes which employ fixed-bed regenerators to provide a continuous supply of heated fluid, necessarily require the installation of at least two regenerators, as well as a number of valves. The latter are needed to switch the hot and cold fluids from one regenerator to another. Installations of this kind are traditionally associated with the high-temperature furnace applications which occur in the fields of ferrous metallurgy and glass manufacture. A typical arrangement of the use of two static regenerators for providing a continuous supply of preheated air, is shown diagrammatically in FIG. 1(A). In this arrangement, a process waste gas is used for heating regenerators A and B during successive periods.

Rotary regenerators are used principally as air preheaters, a typical arrangement for such an application is given in FIG. 1(B). In the arrangement shown, the hot and cold fluids pass in counter-flow directions through adjacent ducts, the regenerator matrix being mounted so as

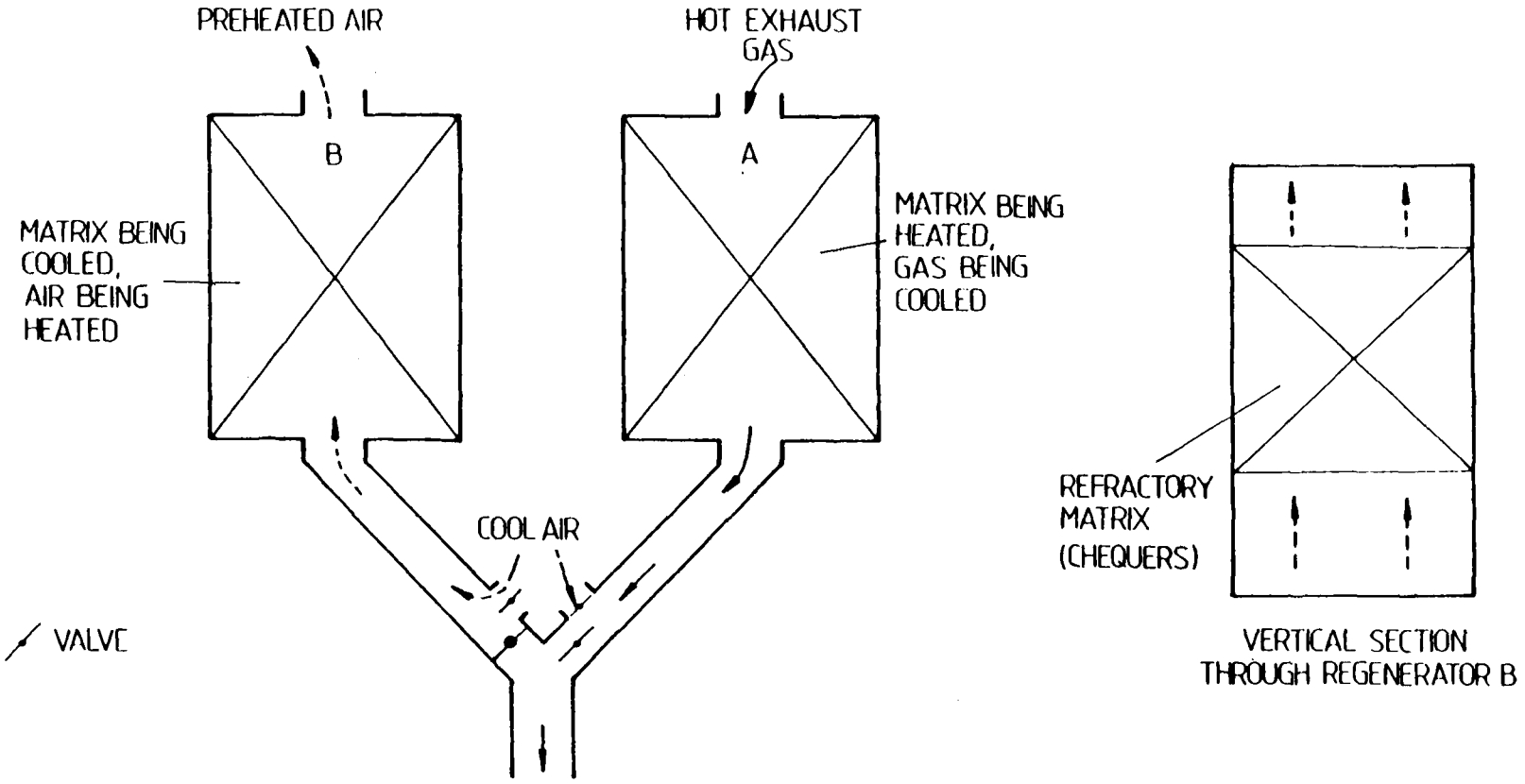

NOTE. GAS AND AIR FLOWS THROUGH THE SYSTEM ARE SWITCHED PERIODICALLY TO GIVE EITHER THE ARRANGEMENT SHOWN OR AN ALTERNATIVE ARRANGEMENT IN WHICH MATRIX B IS HEATED BY THE HOT GAS, THE AIR THEN BEING HEATED IN MATRIX A.

FIG. 1(A) SCHEMATIC DIAGRAM SHOWING FIXED-BED REGENERATOR SYSTEM FOR PREHEATING AIR

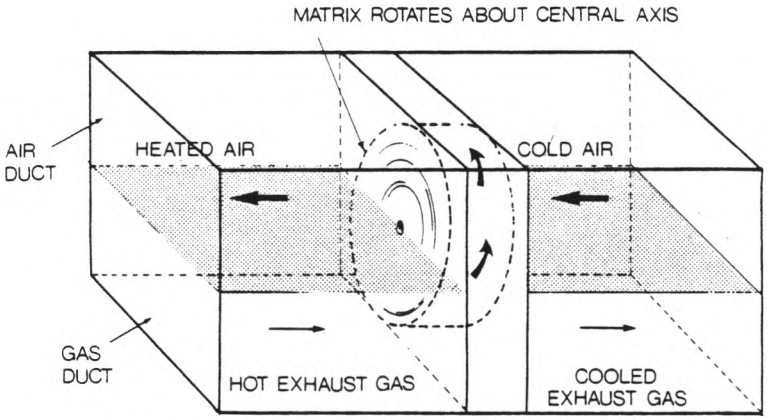

(B) ROTARY REGENERATOR

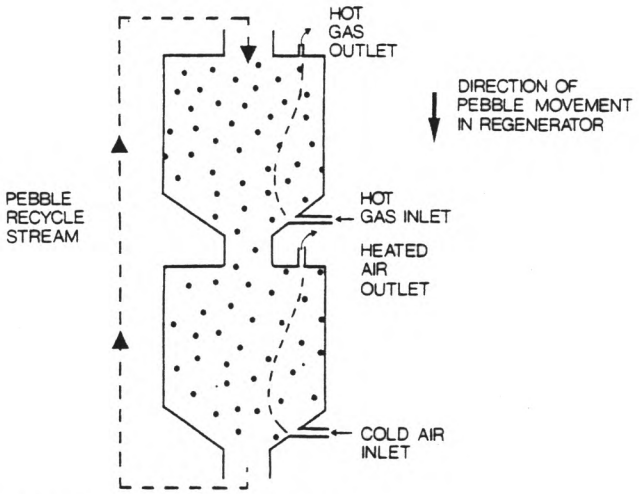

(C) PEBBLE-BED REGENERATOR

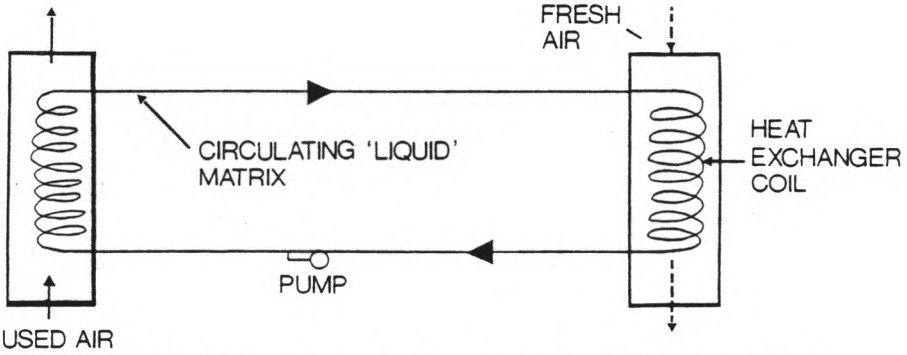

(D) RUN-AROUND COIL FOR AIR-CONDITIONING SYSTEM

FIGURE 1. (B), (C), (D) SCHEMATIC DIAGRAMS OF REGENERATORS WITH MOVING MATRICES

to intercept both fluid streams. For simplicity, the diagram depicts a symmetrical arrangement in which the hot gas flows through one half of the matrix, the colder air flowing through the other half. In many applications, however, the proportions of the matrix in contact with the hot and cold streams are not equal. As the matrix rotates, each element of the matrix is alternately heated, as it passes through the gas stream, and then cooled as it traverses the air stream. It then follows that, in passing through the matrix, the gas temperature decreases, whereas that of the air increases. Two other forms of heat exchanger which employ the regenerator principle are the pebble-bed heater and the liquid-coupled regenerator.

Pebble-bed regenerators are constructions in which the matrix is a moving bed of refractory pellets, spheres or similar small bodies. In a typical installation, shown diagrammatically in FIG. 1(C), the pebbles descend under gravity through two chambers. In the upper chamber the pebbles are heated by a hot gas, this heat being partially released to an air stream when the pebbles pass through the lower chamber. The design and application of such heaters have been discussed by Norton [5], Fraas [4] and Schneller[6].

In a liquid-coupled regenerator, the heat-storing mass is a liquid which circulates continuously, picking-up heat from the fluid being cooled and subsequently transferring it

to the fluid being heated. Installations of this type have been applied successfully for cooling purposes in nuclear reactors and also in air-conditioning systems, where they are known as run-around coils [1]. As shown in FIG. 1(D), an advantage of this arrangement is that the 'hot' and 'cold' fluids need not flow through the same or even adjacent paths.

1.2 REGENERATOR APPLICATIONS

Although the regenerators used for most practical purposes are either of the fixed-bed or rotary type, the very wide range of applications over which regenerators are now used has given rise to many different designs within these two categories.

No set procedure exists for designing a regenerator (or any other type of heat exchanger) to meet a given specification, although Fraas and Ozisik [4], Edwards and Probert [7] and Shah [8] have each suggested various approaches to the overall design problem. Whichever approach is used, the type of regenerator selected for a particular application is usually based on a consideration of many factors. These could include pressure loss requirements, mechanical design and structural considerations including reliability, safety and maintenance, size and/or weight, ease and cost of manufacture, tolerance for cross-contamination between fluids, and many others. Depending on the application, one or more of these factors usually takes precedence over the others and will govern not only

the type of regenerator selected, but also the design and construction of the regenerator matrix. The review of current regenerator applications presented next will illustrate this point.

As a first example, we consider the regenerators used in certain metallurgical and glass-smelting processes. For these applications, the over-riding needs are to ensure long-term structural stability, to minimise the occurrence of blocked ducts and to withstand the high fluid temperatures (up to 1500°C). These requirements have led to the evolution of large, high-mass, fixed-bed regenerators containing a matrix constructed from specially-selected refractory bricks (chequers). When assembled these chequers provide a system of ducts each having a relatively large cross-sectional area, through which the hot and cold fluids pass in successive periods.

Historically, regenerators of this type were probably the first to be applied to industrial processes, and the pioneering work of Siemens over 120 years ago in developing such regenerators for pre-heating the combustion air required for steel-making and glass-making furnaces, has been well documented by Schofield [9]. Fixed-bed regenerators of this type - see FIG. 1(A) - continue to form an integral part of certain glass-making furnaces to the present day [10,11], although their use in the steel-making process has diminished over the past twenty years or so, following the introduction of more economical steel-making practices.

Regenerators with fixed matrices have also retained their importance in the iron-making process, and modern iron-making blast furnaces still feature an array of regenerators - usually called blast-furnace or Cowper stoves - for preheating the air (blast) supplied to the furnace. FIG. 2 is a representation of a typical blast-furnace stove. Unlike the regenerators installed on glass-melting furnaces, which are heated by the process exhaust gas, blast-furnace stoves are heated by burning an appropriate fuel in an adjacent combustion chamber. In certain stove designs, positioning the combustion chamber adjacent to the stove chequers has given rise to large differential expansions in the bridge-wall (see FIG. 2), leading to its eventual collapse and hence to premature stove failure. However, Evans [12] has indicated that this problem has been eliminated successfully by appropriate design changes.

In low-temperature gas-processing systems, design considerations have also favoured the use of fixed-bed regenerators. A particular feature of the regenerators used in this field of application is their relatively small size. The ability to construct such 'compact' regenerators, i.e. regenerators in which a large surface for heat transfer is contained within a relatively small volume, is directly attributable to the use of a suitable all-metal packing. Frankl, circa 1926, was the first to demonstrate this advantage when he used a packing of 'pancakes' wound from aluminium ribbon, to achieve a

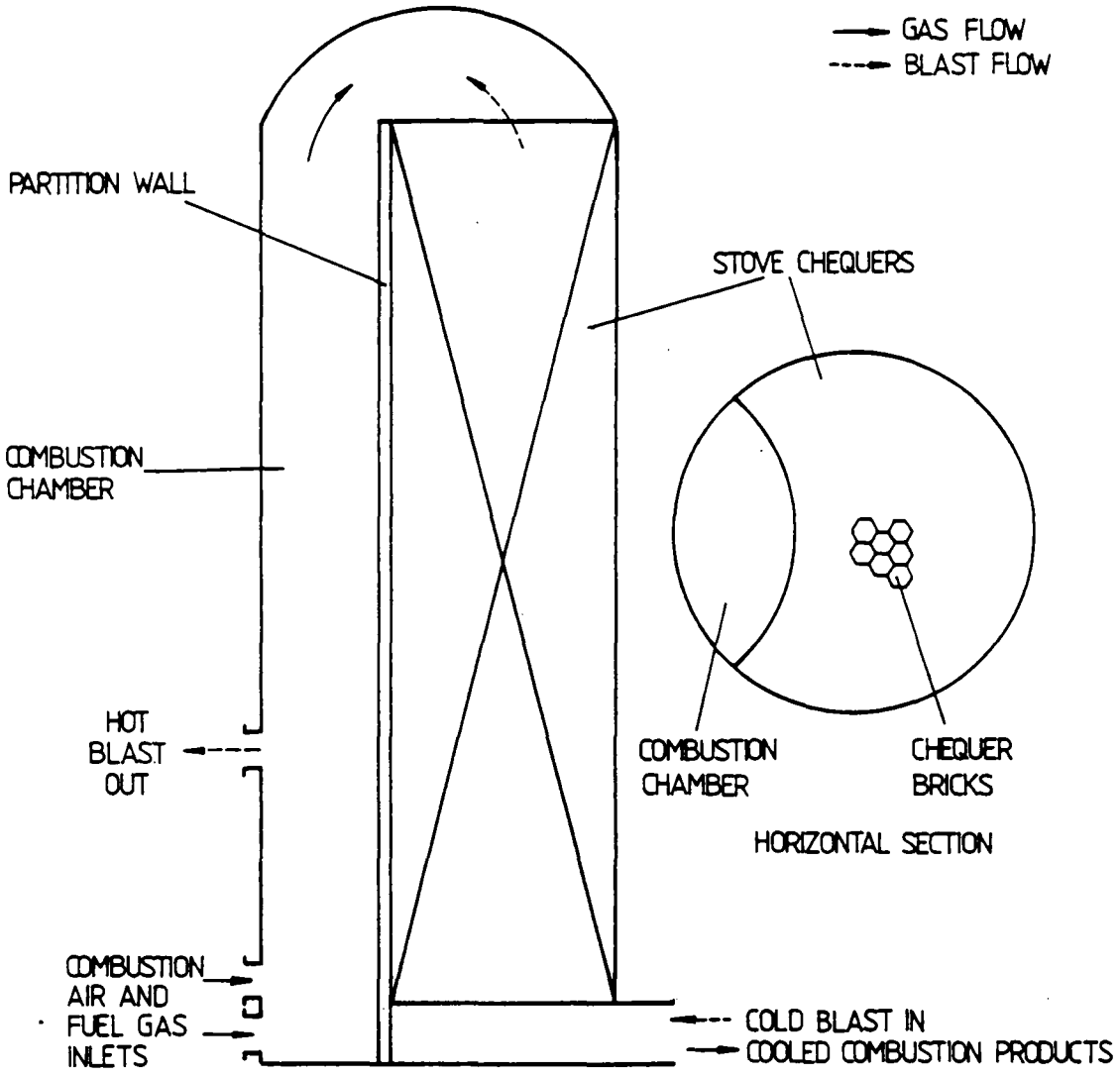

NOTE. THE STOVE IS EITHER 'ON-GAS', IN WHICH CASE HOT GAS FLOWS FROM THE COMBUSTION CHAMBER AND HEATS THE CHEQUER BRICKS AS IT PASSES DOWNWARDS THROUGH THE STOVE. OR 'ON AIR', IN WHICH CASE AIR (BLAST) FLOWS UPWARDS THROUGH THE STOVE AND IS HEATED BY THE HOTTER CHEQUER BRICKS. THE SEQUENCE OF AN 'ON-GAS' PERIOD FOLLOWED BY AN 'ON AIR' PERIOD IS REPEATED CONTINUOUSLY

FIG. 2. SCHEMATIC DIAGRAM OF A HOT BLAST STOVE.

heating surface area per unit volume of around 2000 m^2/m^3 (c.f. 25 to 50 m^2/m^3 for blast-furnace stoves).

The Frankl regenerator was developed as part of a system for the liquefaction of air, and regenerators of this type continue to be used in plant for the liquefaction and separation of gases at very low temperatures. In these applications, the use of a metal packing has the additional advantage that impurities in the inlet gas stream condense on the cold metal surface as the stream traverses the regenerator. These impurities are either drained-off immediately, or if left as deposits on the metal packing, are evaporated and removed in the succeeding period by the exhaust-gas stream [13].

Also in the low-temperature field, the superior thermal performance and compactness of regenerators has made them crucial components in modern cryogenic refrigerators. Scott [13] points out that, because the specific heat of metals becomes very small at very low temperatures, the packing material for cryogenic applications needs careful selection, to ensure that its total heat capacity is large enough to store the required heat. He suggests the use of lead for this purpose. Hausen [3], however, notes that a packing formed from coils of thin copper wire is used in the regenerator fitted to the Phillips low-temperature refrigerator.

For many industrial applications in which the fluid temperatures are not extreme, design considerations often favour the use of rotary regenerators of the type designed by Ljungstrom (1926). Typically, these feature a cylindrical matrix fabricated from alternate layers of flat and corrugated mild-steel sheets, and built around a central hub, as indicated in FIG. 1(B). As shown in this diagram, the fluids flow axially through the matrix in a counter-flow arrangement. Regenerators of this type are commonly used for pre-heating the combustion air for steam boilers and gas-turbine power plant [1,3], as well as for a range of smaller-scale industrial processes, which need a supply of pre-heated air [14,15].

In certain installations, in which the gas used to heat this form of regenerator is corrosive, the regenerator designer is faced with conflicting demands. On the one hand, for optimal heat-transfer performance, the gas temperature at the outlet (i.e. the cold side) needs to be as low as possible. On the other hand, allowing the gas temperatures to fall below the acid dew-point would result in corrosion of the metal matrix. Faced with this dilemma, one manufacturer [14] has found it more economical to design for the lower gas outlet temperatures, and combat the inevitable corrosion by manufacturing matrices with an easily replacable tier of corrosion-resistant material at the cold side.

A significant contribution to both the practical and theoretical aspects of regenerator technology has resulted from the development of compact rotary regenerators for gas-turbine engines, of the type used for vehicle propulsion. The main thrust of this development was carried out in the 'Fifties and 'Sixties, and was primarily motivated by the automobile industry.

The choice and design of a heat exchanger for vehicle turbine-systems were significantly influenced by the need for a small volume and mass, low-cost unit, offering a small pressure loss, and capable of withstanding high operating temperatures (800°C to 1000°C) combined with rapid thermal cycling. A major factor in assuring the successful development of a rotary regenerator for this application was undoubtedly the advance of ceramics technology to enable the fabrication of cellular glass-ceramic 'disc' matrices. Such units can achieve heat-transfer area densities of up to 6600 m^2/m^3 [2], and have a proven capability of 10,000 hours operation at 800°C, [16].

An account of the pioneering work carried out with the 'first-generation' ceramic disc regenerators for vehicle gas-turbines has been given by Penny [17]. A more up-to-date report on their mechanical design and performance capabilities has been given by Rahnke [16]. The application and design of both recuperators and regenerators for gas-turbine systems has also been considered by Hryniszak [18].

Within this field, rotary regenerators have been applied to gas-turbine engines used in aircraft and in various forms of surface transportation, although their use in the motor industry appears to be restricted to large commercial vehicles.

In a completely different field - the building industry - both Thornley [19] and Reay [1] note that for space-heating and air-conditioning systems, the rotary regenerator (often called a thermal wheel) competes favourably with alternative types of heat exchanger, such as the run-around coil, heat pipe and recuperator. An interesting development in this area is that of the 'hygroscopic' wheel, in which the matrix transfers both sensible and latent heat between the fresh and exhaust air streams [1,20] . Thornley [19] states that commercially available wheels are made with diameters ranging from 0.75 m to 4 m, and are capable of dealing with exhaust gases up to 980°C.

A common difficulty with all types of rotary regenerators is that of minimising fluid leakage from the hot stream to the cold stream or vice versa. Details of particular systems devised to inhibit the leakages on industrial pre-heaters, air-conditioning regenerators and vehicle gas-turbine regenerators have been reported by Orr [14] , Reay [1] and O'Neill [21] , respectively.

To complete this review of regenerator applications, one recent development programme which, if successful, will significantly extend the role of rotary regenerators, is

worthy of mention. This work has been initiated by the British Steel Corporation and concerns the development of a rotary regenerator equipped with a refractory matrix. The aim is to produce an air preheater for steelworks reheating and other high-output furnaces [22] .

1.3 REGENERATOR THERMAL DESIGN

1.3.1 MATHEMATICAL MODELS

The problem usually considered in the context of regenerator thermal design is that of predicting, by some form of theoretical analysis, the thermal performance of a regenerator operating in a particular state. Three operating conditions are of interest to the designer. These are the 'single-blow' or 'first-heating' of a regenerator, the condition of cyclic equilibrium, and thirdly, the state of disturbed equilibrium, i.e. the transient-response problem.

The 'first-heating' problem considers a regenerator matrix, whose temperature is known initially at all positions. Gas at a known constant temperature and flow rate is then passed through the regenerator, the mathematical problem being to predict the gas and matrix temperature distributions for all subsequent times. Although the single-blow conditions do not correspond with normal regenerator operation, the availability of theoretical methods for providing such predictions is important for the evaluation of heat-transfer coefficients from practical experimentation [23] .

Normal regenerator operation is usually taken to correspond to the state of cyclic equilibrium. This term refers to the condition which is attained in a regenerator after the regenerator matrix has been repeatedly heated and cooled for a very large number of identical cycles; the heating and cooling periods of each cycle being of fixed, but not necessarily equal, duration.

In the state of cyclic equilibrium, at any particular instant, the temperatures of each fluid and of the matrix, at any position in the regenerator, are identical with their values a full cycle earlier. Expressing this more rigorously, we say the temperatures are periodic, with a period equal to the duration of a complete cycle. Under these conditions the problem then is to predict the total amount of heat exchanged during each period and also the complete temperature histories of the two fluids and of the matrix everywhere in the regenerator for a full cycle.

For the third of the states mentioned above, the objective is to predict the effect on regenerator performance of a sudden change in operating conditions.

Whilst all three of these theoretical problems are relevant to the design of regenerator systems, because of its far greater practical importance - and relevance to this research study - the review of regenerator theories

presented below is directed almost exclusively to those relating to the cyclic equilibrium problem.

As will be evident from the next section, modern methods of predicting the thermal performance of regenerators in the equilibrium condition usually involve the analysis of an appropriate mathematical model. Such models are formulated so as to describe, in mathematical terms, the heat-transfer processes occurring within a regenerator, and usually comprise several differential equations and associated boundary conditions.

Examination of the literature on this subject reveals that four different mathematical models are of interest for the design of the various regenerator types considered in the preceding section. Other models have been considered, for example, by Nusselt [24] , but although these are mathematically interesting (see Jakob [25]), they are of no practical significance.

The four models which are of practical importance are based on the conditions presented in Cases (A) to (D) below. For convenience, these descriptions are referred to a plane-wall regenerator, of the type shown in FIG. 3(a).

Case (A). This case is appropriate to regenerators having metallic and/or thin-walled matrices. In this type of regenerator, at any position and at any instant, the temperature gradient within the matrix in a direction perpendicular to that of the fluid flow, is negligibly small.

The component of the matrix thermal conductivity in this direction, k_x, can therefore be taken to be infinitely large. Also, provided the flow-path through the regenerator is relatively long, the component of the wall conductivity parallel to the flow direction, k_y, may reasonably be taken to be zero. Hence, Case (A), assumes $k_x = \infty$, $k_y = 0$.

Case (B). For high-temperature regenerators with thick-walled refractory matrices, the temperature distributions measured within the cross-section of the matrix wall [3] are consistent with a finite value of the conductivity component k_x. However, due to the construction of these refractory matrices, the assumption $k_y = 0$ is still a valid approximation. Case (B) is therefore based on k_x = finite, $k_y = 0$.

Case (C). For the thin-walled, short-flow-path matrices used in vehicle gas-turbine regenerators, heat conduction along the matrix, i.e. parallel to the fluid flow, cannot be neglected [23] , as in Case (A). Appropriate assumptions for this type of matrix are therefore $k_x = \infty$, k_y = finite.

Case (D). This simply assumes that the duration of each period is infinitesimally small. This extreme condition is one that is approached when a rotary regenerator is operated with high rotor speeds.

The mathematical description of a regenerator operating under the conditions specified in Case (D) was considered by Nusselt, and was the first of five regenerator problems presented in his 1927 paper [24]. For this particular problem, Nusselt obtained exact solutions for the fluid and solid temperatures throughout the regenerator. These solutions are of some interest in design work and may be used either, directly for the approximate calculation of rotary regenerator performance [4,26], or as the basis for more sophisticated methods giving more accurate predictions. The exact solutions for this limiting case also provide a useful check on the validity of numerical solutions of more elaborate regenerator models [26].

For the first three cases above, in order to formulate mathematical models which do not present insurmountable mathematical and computational problems for their solution, but at the same time provide realistic predictions, the following further idealisations are usually made. These are also stated with reference to a plane-wall regenerator of the type illustrated in FIG. 3(a):-

(i) All channels are physically identical.

(ii) No heat is lost from the regenerator exterior walls.

(iii) There is no leakage or mixing of the two fluids.

(iv) In either period, the fluid flow rates and the heat-transfer processes are the same in all

channels. The flow is assumed to be incompressible and also to be sufficiently turbulent within each channel, to achieve a uniform fluid temperature in any channel cross-section perpendicular to the fluid flow.

(v) In both periods, the heat-transfer rate is assumed to be proportional to the temperature difference between the matrix wall surface and the adjacent fluid.

(vi) Fluid entry temperatures are constant throughout each period.

(vii) Fluid mass flow rates are constant throughout each period.

(viii) The thermal properties of both fluids and of the matrix are invariant, as also are the heat-transfer coefficients.

The first six of these idealisations are justifiable for most regenerator applications and have been adopted by most investigators. However, because in practice physical properties are not constant but vary with temperature, and also because in certain applications (e.g. blast-furnace stoves), the cold fluid flow rate varies with time, the use of (vii) and (viii) are more contentious.

If items (vii) and (viii) are adopted when setting-up the mathematical models for any of the cases (A), (B) or (C), the heat-transfer processes in each case will be described by a linear system of differential equations. The model itself is then called 'linear'. Exclusion of (vii) and/or (viii) in the formulation process leads to non-linear differential equations, that is to a 'non-linear' model. For a given regenerator type, the non-linear model provides a more accurate mathematical representation of the heat-transfer processes involved, than the corresponding linear model does. However, this advantage is off-set by the fact that the descriptive equations of the non-linear model require more extensive mathematical techniques and considerably longer computation times for their solution.

Many of the currently-available regenerator theories have been developed from models of these two types. Before reviewing the various alternative theories, and in order to clarify the discussion of their relative merits and weaknesses, it will be useful at this stage to present the descriptive equations of the linear models for cases (A) and (B), above. For reference purposes, these will be called the two-dimensional (2-D) or 'infinite-conductivity' model, and the three-dimensional (3-D) or 'finite-conductivity' model, respectively. Again it is convenient to derive the mathematical equations for both models for the type of regenerator depicted in FIG. 3(a).

For both cases, we assume the regenerator to be in a state of cyclic equilibrium such that in any arbitrary cycle, for a period of duration P_1, the hot fluid with a mass flow rate W_1 and specific heat S_1 enters the regenerator at a temperature $t_{1,IN}$. At the end of this period, the fluid flow is instantaneously reversed so that for a further period P_2, colder fluid enters the regenerator, with a massflow rate W_2, specific heat S_2 and temperature $t_{2,IN}$.

Positions within the regenerator are specified with reference to the co-ordinate axes Ox, Oy, which are arranged so that the origin of the co-ordinates in each period is located at the point of fluid entry. Restricting the derivation to the more important counterflow arrangement, the origin is therefore positioned at opposite ends of the regenerator in successive periods: this differs from the fixed origin shown in FIG. 3(b), which refers to an analysis presented in a later chapter. Thus, the x-coordinate of any point in the matrix measures the distance normal to the fluid flow direction as shown in FIG. 3(b), but the y-coordinate indicates the distance along the regenerator length, in the direction of fluid flow. The origin of time is taken to be at the start of the heating period.

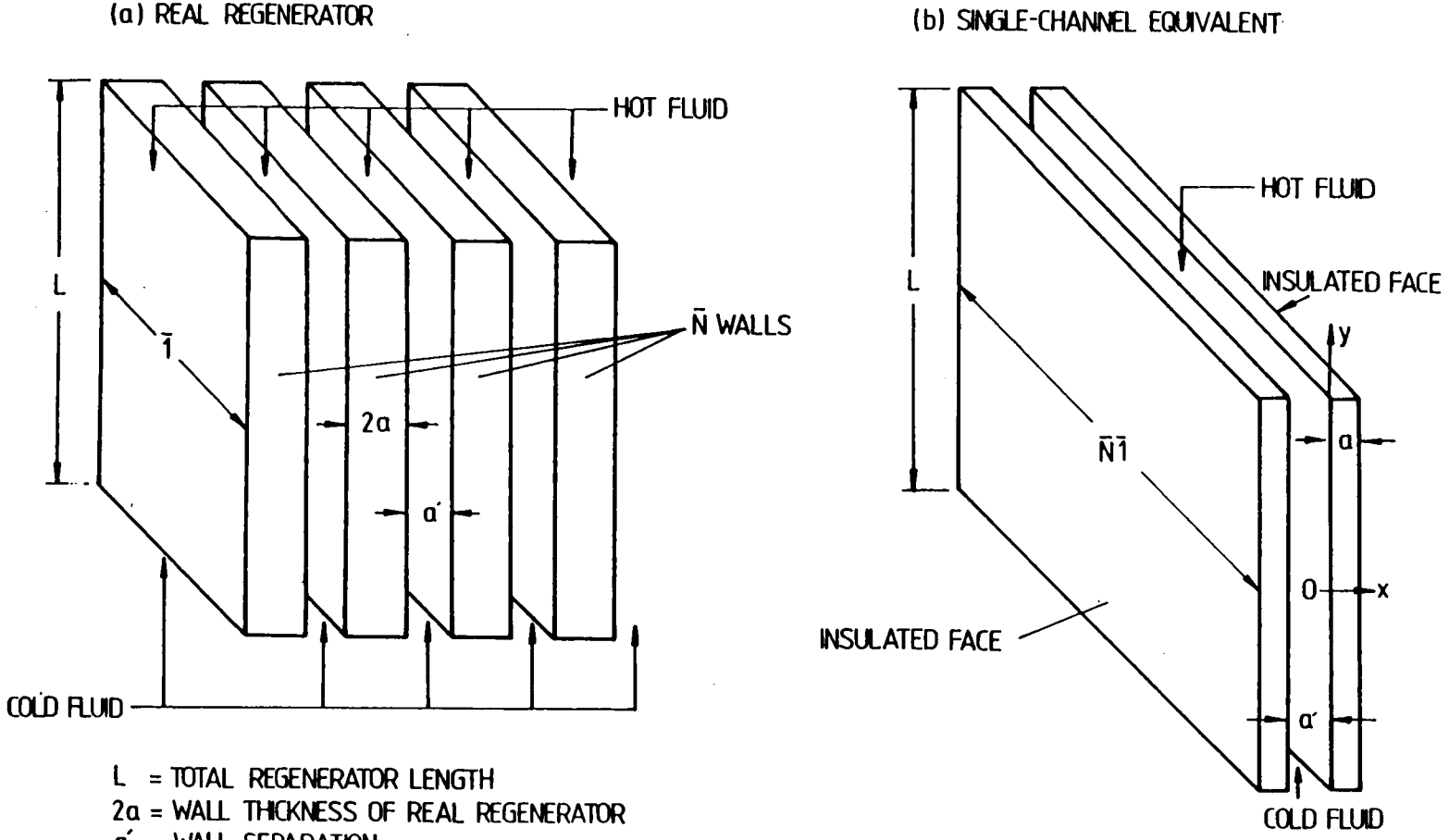

L = TOTAL REGENERATOR LENGTH
2a = WALL THICKNESS OF REAL REGENERATOR
a' = WALL SEPARATION
$\bar{l}$ = WIDTH OF WALL
$\bar{N}$ = NUMBER OF WALLS IN REAL REGENERATOR
0 = ORIGIN OF CO-ORDINATE AXES Ox AND Oy

FIG. 3 RELATION BETWEEN REAL REGENERATOR AND EQUIVALENT SINGLE-CHANNEL REGENERATOR

2-D (Infinite-Conductivity) Model - Case (A)

In this case, the matrix and fluid temperatures are functions of distance, y, and time, θ, only and are represented by T and t respectively.

Heat balances for elementary volumes within the fluid and also in the matrix (at a distance y along the regenerator) lead to the following equations.

$$W_1 S_1 \frac{\partial t_1}{\partial y} + w_1 S_1 \frac{\partial t_1}{\partial \theta} = h_1 p(T-t_1) \quad \text{..... (1-1)}$$

$$\bar{M}c \frac{\partial T}{\partial \theta} = h_1 pL(t_1-T) \quad \text{..... (1-2)}$$

$$0 \leqslant y \leqslant L, \quad 0 \leqslant \theta \leqslant P_1$$

$$W_2 S_2 \frac{\partial t_2}{\partial y} + w_2 S_2 \frac{\partial t_2}{\partial \theta} = h_2 p(T-t_2) \quad \text{..... (1-3)}$$

$$\bar{M}c \frac{\partial T}{\partial \theta} = h_2 pL(t_2-T) \quad \text{..... (1-4)}$$

$$0 \leqslant y \leqslant L, \quad P_1 \leqslant \theta \leqslant P_1+P_2$$

In these equations suffices 1 and 2 are used to distinguish the heating and cooling periods, respectively: h represents the surface heat-transfer coefficient, $\bar{M}$ the matrix mass, c the specific heat of the matrix material, and p and L the perimeter and length of the regenerator channel respectively.

In addition, we have

$$t_1(0,\theta) = t_{1,IN}, \quad 0 \leqslant \theta \leqslant P_1$$

$$t_2(0,\theta) = t_{2,IN}, \quad P_1 \leqslant \theta \leqslant P_1+P_2 \quad \text{..... (1-5)}$$

and

$$T(y,\theta) = T\left[y,\theta+\bar{n}(P_1+P_2)\right],\ 0\leq y\leq L, 0\leq\theta\leq P_1+P_2, \bar{n}=1,2,\ldots \quad \ldots\ldots (1\text{-}6)$$

These two equations specify the conditions that the fluid entry temperatures have known constant values, and that the regenerator operates at cyclic equilibrium.

Equations (1-1) to (1-4), coupled with the boundary conditions stated in equations (1-5) and (1-6) constitute the 2-D linear model. When solving these equations, the equilibrium condition given in equation (1-6) is often replaced by the 'reversal condition'. This states that, at any regenerator position, the temperature of the matrix at the end of either period is equal to that at the start of the following period.

3-D (Finite Conductivity) Model - Case (B)

Taking an arbitrary cycle as before, the fluid temperatures in this case are again functions of y and θ only. However, because of the assumption of a finite value for k_x, the matrix temperature depends on x, y and θ. Moreover, because the heat flow within the matrix is always parallel to Ox, the matrix temperature $T(x,y,\theta)$ satisfies the one-dimensional heat conduction equation

$$\frac{\partial T}{\partial \theta} = \alpha \frac{\partial^2 T}{\partial x^2}\ ,\quad 0\leq x\leq a,\ 0\leq \theta\leq P_1+P_2 \qquad \ldots\ldots (1\text{-}7)$$

The boundary conditions associated with this equation are

$$\frac{\partial T}{\partial x}(a,y,\theta) = 0 \ , \ 0 \leqslant \theta \leqslant P_1+P_2 \qquad \ldots\ldots (1\text{-}8)$$

$$k\frac{\partial T}{\partial x}(0,y,\theta) = h_1 \left[T(0,y,\theta)-t_1\right], \ 0 \leqslant \theta \leqslant P_1 \qquad \ldots\ldots (1\text{-}9)$$

$$k\frac{\partial T}{\partial x}(0,y,\theta) = h_2 \left[T(0,y,\theta)-t_2\right], \ P_1 \leqslant \theta \leqslant P_1+P_2 \qquad \ldots\ldots (1\text{-}10)$$

Equation (1-8) expresses the condition of zero heat flow at the wall's mid-plane, whereas equations (1-9) and (1-10) equate the conductive and convective heat-transfer rates at the matrix surface, in each period.

A heat balance in the fluid phase as before, gives

$$W_1 S_1 \frac{\partial t_1}{\partial y} + w_1 S_1 \frac{\partial t_1}{\partial \theta} = h_1 p \left[T(0,y,\theta)-t_1\right] \ , \ 0 \leqslant \theta \leqslant P_1 \qquad \ldots\ldots (1\text{-}11)$$

and

$$W_2 S_2 \frac{\partial t_2}{\partial y} + w_2 S_2 \frac{\partial t_2}{\partial \theta} = h_2 p \left[T(0,y,\theta)-t_2\right], \ P_1 \leqslant \theta \leqslant P_1+P_2 \qquad \ldots\ldots (1\text{-}12)$$

The fluid entry temperature condition, in this case, is as previously stated in equation (1-5). However the equilibrium condition is now described by the equation

$$T(x,y,\theta) = T\left[x,y,\theta+\bar{n}(P_1+P_2)\right] \ , \ 0 \leqslant x \leqslant a, \ 0 \leqslant \theta \leqslant P_1+P_2$$
$$\bar{n} = 1,2,\ldots \qquad \ldots\ldots (1\text{-}13)$$

In equations (1-7) to (1-13), the range of y is $0 \leqslant y \leqslant L$. These equations, together with equation (1-5), form the more detailed 3-D model. As with the 2-D model, solutions to the above equations are often determined using the reversal condition, as stated above, rather than equation (1-13).

1.3.2 EARLY REGENERATOR THEORIES

The earliest regenerator theories for predicting regenerator thermal performances were almost all developed in Germany over fifty years ago. At that time, practical interest centred on high-temperature regenerators used in the iron and steel industry, and also on those used for low-temperature processes. As such, the provision of solutions for both the two and three-dimensional models described above, was of particular relevance.

Amongst the earliest publications in this field were those by Anzelius [27], Schumann [28] and Nusselt [24], who each developed analytical methods for solving the single-blow problem. Mathematically, this required the solution of equations (1-1) and (1-2) but with the fluid entry temperature and initial matrix temperature distribution as known boundary conditions. Both Anzelius and Schumann derived solutions for the case of a uniform initial matrix temperature distribution, whereas Nusselt's solution catered for the more general case of an arbitrary (known) initial temperature distribution. The solutions obtained by all three workers were given in terms of Bessel functions.

In a subsequent paper, Nusselt [29] obtained the first solution to the equations representing a regenerator operating in cyclic equilibrium. His analysis was carried out for a thin-wall regenerator, Case (A), and was restricted to the case of thermal symmetry ($W_1S_1 = W_2S_2$; $P_1=P_2$, $h_1=h_2$). Because, in this special case, the temperature solutions in successive periods are related by symmetry, all required regenerator temperatures may be obtained from one application of the single-blow theory, provided the correct matrix temperature distribution at the start of the operation is known. To determine this initial temperature distribution, Nusselt commenced with his single-blow solution for the matrix temperature. He then introduced into this solution, the particular form of the reversal condition relevant to the case of thermal symmetry. This gave an integral equation, which was then solved by an approximation method, to determine the required initial matrix temperature distribution. A full account of Nusselt's work on this problem has been given by Jakob [25]. Later discussions will confirm that Nusselt's technique of using a closed-form of solution to calculate the regenerator's performance, has been the basis of many subsequent theoretical studies of this problem.

Using a completely different analysis, Hausen [30] published, in 1929, an exact solution to the same, Case (A), problem. This work has similarly had an important influence on later theories of regenerator behaviour.

Hausen first simplified the basic equations, which were equivalent to equations (1-1) to (1-6), by transforming to dimensionless distance and time co-ordinates. In terms of these new variables, and for given fluid entry temperatures, only four dimensionless parameters, Λ_1, Λ_2, Π_1 and Π_2, are needed to describe a particular regenerator operation - as opposed to the fourteen required in equations (1-1) to (1-6). Hausen used the terms 'reduced length' and 'reduced period' to describe the parameters Λ and Π.

Also restricting his analysis to the simpler case of thermal symmetry, for which $\Lambda_1 = \Lambda_2$ and $\Pi_1 = \Pi_2$, he then showed that the transformed equations had an infinite number of particular solutions for the fluid and matrix temperatures. These solutions were termed 'eigenfunctions', each eigenfunction being characterised by an integer number 0, 1, 2, ..., specifying its order. The zero-order eigenfunction corresponds to fluid and solid temperature changes which are linear in both space and time, conditions which closely correspond to those in the middle regions of a long regenerator some time after reversal. However the cumulative effect of all the higher-order eigenfunctions is negligible in these middle regions but increases in magnitude towards the ends of the regenerator. Every one of these solutions, for the matrix temperature, satisfied the reversal condition.

The analysis was completed by expressing the required fluid temperature as a linear combination of the full set of relevant eigenfunctions, the combination being selected so as to satisfy the constant fluid entry temperature boundary condition. Finally the method was applied to produce a set of curves; plotting regenerator effectiveness against Λ and Π, for $0 \leqslant \Lambda \leqslant 50$, $0 \leqslant \Pi \leqslant 50$.

An attractive feature of this theory is that temperature changes in a regenerator can be regarded as a forced oscillation - analagous to the oscillations of an elastic string, composed of the zero-order eigen-function (corresponding to the fundamental oscillation) combined with the higher-order eigenfunctions (the higher harmonics).

Hausen also derived an alternative method, called the 'heat-pole' method [31], for solving the same problem. In comparing these two approaches, Hausen considered the heat-pole method simpler to apply, but felt the eigenfunction theory provided a far better insight into regenerator temperature variations.

The earliest attempts at dealing with the more difficult problem of a regenerator having a finite wall-conductivity perpendicular to the fluid flow, Case (B), were based on the simpler and well-known theory for calculating the thermal performance of a steady-state recuperator [3]. This approach is possible provided the mathematical equations describing the heat transfer between the fluids

in a regenerator are formed using periodic mean temperatures. However, application of the recuperator theory for regenerator calculations, requires the calculation of an overall (fluid to fluid) heat-transfer coefficient per cycle, h_p.

Several noteworthy methods for evaluating such a coefficient, for a given regenerator operation, were developed by Heiligenstaedt [32], Schmeidler [33], Rummel [34], Schack [35] and Hausen [36]. Apart from their original papers, detailed accounts of these methods have been given by Edwards [37], Hausen [3], Schack [38] and Razelos [39], and as such, only the work of Hausen which is particularly relevant to this review, is examined here.

Hausen adopted a completely analytical approach to determine h_p. He commenced by solving the heat-conduction equation (1-7) for the special case of a constant heat flux at the solid surface. This condition is consistent with both the fluid's temperature and the average wall-temperature (averaged across the entire wall cross-section) varying linearly along the regenerator length, with the same gradient, and also with the average wall-temperature (at any section) varying linearly with time. Hausen then selected the arbitrary constants in the solution to equation (1-7) to be consistent with this latter condition and also to satisfy the reversal condition and equation (1-8). On the basis of this 'zero-order eigenfunction' solution, so called

because of the linear variation of the fluid and solid mean temperatures (c.f. his first theory), he obtained an expression for the overall heat-transfer coefficient, k_0, in the form

$$\frac{1}{k_0} = (P_1+P_2)\left[\frac{1}{h_1P_1} + \frac{1}{h_2P_2} + \left(\frac{1}{P_1} + \frac{1}{P_2}\right)\frac{a}{3k}\,\phi_H\right] \qquad \ldots\ldots \text{(1-14)}$$

where ϕ_H is essentially a function of the dimensionless expression $\frac{2a^2}{\alpha}\left(\frac{1}{P_1} + \frac{1}{P_2}\right)$. However, the zero-eigenfunction solution does not satisfy the condition of constant fluid entry temperature and, as such, k_0 does not represent accurately the true overall heat-transfer coefficient. To overcome these difficulties Hausen re-formulated the finite conductivity model using the average wall-temperatures and the modified (bulk) heat-transfer coefficients to express the heat transfer between the fluid and the wall, at any section. With this approach, the equations describing a regenerator with a finite wall conductivity (k_x = finite, k_y = 0) achieve an identical form to those of the 2-D, infinite-conductivity model given in equations (1-1) to (1-6). However for the finite-conductivity model, T has to represent the average wall-temperature, and the surface heat-transfer coefficients h_1 and h_2 have to be replaced by bulk coefficients $\bar{h}_1$ and $\bar{h}_2$ given by

$$\frac{1}{\bar{h}_i} = \frac{1}{h_i} + \frac{a}{3k}\,\phi_H \quad , \; i=1,\; 2 \qquad \ldots\ldots \text{(1-15)}$$

Hence, by adapting his first theory [30], in which the zero-order eigenfunction solutions for the fluid and solid temperatures were entirely consistent with the solution of equation (1-7) used to calculate k_0, the constant fluid entry temperature condition was then satisfied using the complete set of fluid eigenfunction solutions. In addition, by re-defining the dimensionless parameters Λ and Π in terms of $\bar{h}_1$ and $\bar{h}_2$, rather than in terms of h_1 and h_2, Hausen was able to apply his previously obtained effectiveness graphs to produce a further set of curves of a correction factor, which could be used to multiply k_0, and so determine the true coefficient h_p for any combination of Λ and Π in the range $0 \leqslant \Lambda \leqslant 200$ and $0 \leqslant \Pi \leqslant 50$.

Finally, although the entire analysis was carried out for the thermally symmetrical case $\Lambda_1 = \Lambda_2$, $\Pi_1 = \Pi_2$, Hausen considered that the method could be used in the more general case, provided the appropriate graphs are read using the harmonic means of the two values of Λ and of Π.

1.3.3 MORE RECENT THEORIES

Although somewhat dated, the 'recuperator analogy' methods referred to in the previous section, remain useful for rapid estimations of overall regenerator performance. Other simplified theories for approximating the effectiveness of a regenerator have been given by Tipler [40], Schalkwijk [41] and Traustel [42].

More modern techniques for solving the regenerator problem, however, usually employ a high-speed digital computer in conjunction with a specially written computer program, to calculate the solutions to the full set of regenerator equations. This approach not only provides a more accurate prediction of the regenerator effectiveness, but also provides complete fluid and solid temperature histories at all regenerator positions.

In broad terms, these digital computation methods for solving the differential equations of a given regenerator model, fall into two categories viz., 'open' methods of solution and 'closed' methods of solution.

In an open method of solution, finite-difference methods are used to transform the relevant differential equations and boundary conditions into corresponding difference equations. Then, using a 'guessed' initial matrix temperature distribution, the difference equations are applied to calculate all fluid and matrix temperatures at a discrete number of positions along the regenerator, at each of a discrete number of times during a complete cycle. The entire computation scheme is then repeated iteratively, using the matrix temperatures calculated at the end of any period, as the initial matrix temperature distribution for the next period, until successive sets of calculations agree to within some prescribed accuracy. When this happens, the reversal condition is therefore satisfied, and the 'latest' set of results are taken to be

the required solutions. These methods are often called simulation methods.

In the second class of methods, following Nusselt's approach, the differential equations forming the mathematical model are solved analytically, to obtain a closed form of solution. Such closed solutions usually take the form of one or more integral equations, (see equations (1-16) and (1-17), below), and numerical approximation techniques are still needed to calculate the required regenerator temperature distributions from these equations. However, a major advantage of the closed approach arises from the fact that the reversal condition is satisfied in the mathematical derivation of the closed solution. This means that just one set of calculations is sufficient to provide the full set of solutions, compared with the large number of repeated 'cycles' of calculations required by the open methods. It follows therefore that for a given regenerator model, the amount of computer time needed for a closed method of solution is generally far less than that for an open method.

Because both 'closed' and 'open' methods require a specially-written computer program incorporating particular techniques of numerical approximation, the concepts of numerical accuracy and computational efficiency assume a particular importance. As such, the following common objectives apply to either method of solution:-

(i) the selected numerical algorithm and associated step sizes must provide valid predictions of a satisfactory numerical accuracy over as wide a range of regenerator examples as possible, i.e. for combinations of the dimensionless regenerator parameters covering the entire range of practical interest.

(ii) computation time per example should be the least possible.

(iii) the computer memory usage should also be as small as possible.

Many different mathematical and numerical schemes have been investigated in the continuing attempt to find the optimal way of satisfying these demands. Inevitably these have involved some duplication of results in certain areas. Before examining the various theories which have arisen from these investigations, it is worth noting at this point that, as far as the above objectives are concerned, the theoretical developments relating to the infinite-conductivity model, Case (A), and the associated Case (C) model, have currently reached an advanced state. However, as will be explained later, developments relating to the finite-conductivity model are still open to improvement.

Examination of the literature relating to the application of digital computation methods reveals that far greater attention has been given to the solution of the 2-D regenerator model, Case (A), than to the 3-D model, Case (B), with the majority of investigators favouring open methods of solution. This concentration of effort on solving the 2-D model equations is to be expected, not only because they are mathematically simpler to deal with and require considerably less computation time per example, but also because, with suitable interpretation, the 2-D mathematical model can be used to investigate regenerators for which $k_x = \infty$ and also those for which k_x has a finite value. Although the mathematical equations in each case are identical in form, for greater clarity those relating to the case $k_x = \infty$ will, as before, be referred to as the 'infinite-conductivity' model, whereas the alternative case will be referred to as the 2-D, 'finite-conductivity' model.

2-D Model Theories

The first to apply an open method of solution to the 2-D, infinite-conductivity model were Saunders and Smoleniec [43]. They used an approximation technique suggested by Allen [44], to obtain results for both the single-blow and cyclic equilibrium problems. In the latter case, results were presented mostly for the thermally symmetrical case, for Hausen's parameters Λ and Π in the ranges $4 \leqslant \Lambda \leqslant 100$, $0 \leqslant \Pi \leqslant 10$. Some results were also calculated for examples for which $\frac{\Lambda_1}{\Pi_1} \neq \frac{\Lambda_2}{\Pi_2} \neq 1$.

The advantages of using a high-speed digital computer for carrying out regenerator calculations were first exploited by Lambertson [45] (circa 1958), and a little later by Willmott [46] . Both used finite differences to approximate the differential equations of the two-dimensional regenerator model, and computed the required solutions using an iterative (open) scheme. Willmott, whose interest was in high-temperature regenerators, used a trapezoidal method to represent the equations of the 2-D, finite-conductivity model. Lambertson, on the other hand, was concerned with predicting the performance of rotary regenerators, and as such solved the infinite-conductivity model.

The mathematical equations describing the heat-transfer in a rotary regenerator subject to the conditions of Case (A), are identical with equations (1-1) to(1-6), i.e. the infinite-conductivity model. However for design work in this field, the dimensionless parameters of Hausen are not the most useful, and an alternative set of parameters (the effectiveness-NTU_0 system) is generally used. Lambertson presented his results as a series of tables of regenerator effectiveness values computed for a range of these alternative parameters.

Many investigators have subsequently sought to improve the accuracy and range of applicability of rotary regenerator thermal predictions. Individual contributors are too numerous to detail separately, but the work of Bahnke and

Howard [47] and Mondt [23] are particularly noteworthy. The latter author, whose paper, reference [23], provides a comprehensive review of investigations in this field, points out that for automotive disc regenerators, a satisfactory correlation between theoretically predicted and measured performance has only been achieved from a model which includes the effect of heat conduction along the matrix, as specified in the Case (C) model.

Concurrently with the development of open methods for solving the regenerator problem, theories based on closed methods of solution were also being investigated. Thus at roughly the same time that Saunders and Smoleniec published their open-method solutions to the infinite-conductivity model, Iliffe [48] reported results for the same model, but calculated using a closed method. Iliffe's analysis commenced by applying the reversal condition to Nusselt's single-blow solution for the matrix temperature. This gave the two integral equations:-

$$F'(\xi') = \exp(-\Pi'')F''(\xi'') + \int_0^{\xi''} K''(\xi''-\epsilon)F''(\epsilon)\,d\epsilon \quad . \qquad \ldots\ldots \text{(1-16)}$$

and

$$F''(\xi'') = 1-\exp(-\Pi')\left[1-F'(\xi')\right] + \int_0^{\xi'} K'(\xi'-\epsilon)\left[1-F'(\epsilon)\right] d\epsilon \qquad \ldots\ldots \text{(1-17)}$$

where

$$K(\xi-\epsilon) = -i\,\frac{J_1\left[2i\sqrt{(\xi-\epsilon)\Pi}\right]}{\sqrt{(\xi-\epsilon)\Pi}}\cdot\Pi\exp\left[-(\xi-\epsilon)-\Pi\right] \qquad \ldots\ldots \text{(1-18)}$$

and $0\leqslant\xi\leqslant\Lambda$ and $i=\sqrt{-1}$.

These equations are given using Iliffe's original notation, in which F and ξ represent the initial matrix temperature and dimensionless heating surface (measured from the point of fluid entry), respectively. The single and double primes indicate the heating and cooling periods.

Using appropriate quadrature formulae to approximate the integrals, equations (1-16) and (1-17) were applied to give a set of linear algebraic equations. These were then solved simultaneously to give firstly, the initial matrix temperatures (F' and F") at selected points along the regenerator, and thence the amount of heat transferred per period. Iliffe applied this technique to produce performance curves for the two thermally un-symmetrical cases given by $\frac{\Lambda_1}{\Pi_1}=\frac{\Lambda_2}{\Pi_2}=2$ and 3, respectively.

In an alternative treatment, Nahavandi and Weinstein [49] derived essentially the same integral equations as Iliffe. However, these were solved by first representing the unknown initial matrix temperatures by a polynomial of degree N, and then applying the integral equations at (N+1) equally-spaced points along the regenerator. The resulting system of linear algebraic equations were then solved to give

the matrix temperatures at the selected points, at the start of each period. Results calculated from this 'closed' theory were in close agreement with Lambertson's 'open-method' results.

More detailed investigations of the closed-solution techniques originated by Iliffe and Nahavandi and Weinstein have subsequently been carried out by several workers. Kulakowski et al [50] performed a series of numerical experiments to investigate the range of applicability of each method and to compare their computational efficiency. The comparison, which was limited to the simpler case of thermal symmetry, indicated that to compute the regenerator effectiveness to the same degree of accuracy, Iliffe's method required considerably less computer time per example than that of Nahavandi and Weinstein, particularly at large values of Λ. However, as the value of Λ increased, the computer memory usage became considerably greater for the Iliffe method.

In an earlier study, Willmott and Thomas [51] had concluded that Iliffe's method was not suitable for evaluating the performance of long regenerators, i.e. those for which $\Lambda > 10$ and $\frac{\Lambda}{\Pi} > 3$. The authors attributed this to ill-conditioning of the system of algebraic equations to be solved and suggested that such cases should be treated using an extrapolative method devised by Hausen [3]. It is interesting to note, however, that Kulakowski et al [50], who used Crout's procedure [52] for

solving the system of algebraic equations generated by Iliffe's method, found no cases of ill-conditioning for computations covering the ranges $1 \leqslant \Lambda \leqslant 100$ and $0.5 \leqslant \Pi \leqslant 15$.

In a further study [53] , Willmott and Duggan have shown that slightly more rapid convergence is obtained when applying Nahavandi and Weinstein's method, by using points which are not equally-spaced along the regenerator, but which are more closely distributed near the regenerator ends.

Romie [54] has also developed a quite different closed-form solution for the infinite-conductivity model. Results calculated by this theory were presented in terms of dimensionless groups which are suitable for evaluating the performances of regenerators for thermal-storage applications.

The regenerator theories reported up to this point have all been based on the use of linear models, which are formulated on the assumption that the heat-transfer coefficients, the solid and fluid thermal properties and the fluid flow rates are all invariant with respect to time and temperature. However, certain investigations have also been carried out using the more comprehensive non-linear models, obtained when some or all of these parameters are treated as functions of temperature, or time.

As part of the work referred to earlier [50] , Kulakowski and Anielewski demonstrated that a closed method of solution can be applied iteratively to obtain solutions to the 2-D model equations in which the heat-transfer coefficients and fluid and solid physical properties are taken to be functions of distance and time. The authors concluded that the closed approach has useful advantages in terms of shorter computer times for certain regenerator parameters, but was not capable of dealing with time-dependent fluid flow rates. In this latter respect open methods of solution have proved more versatile, as they are not limited by this restriction.

Variable fluid flow rates occur in the operation of blast-furnace stoves and are necessary in order to maintain a constant blast temperature to the furnace. In separate studies, Willmott [55, 56] , Hofmann and Kappelmayer [57] and Razelos and Benjamin [58, 59] each applied a digital simulation method to estimate the performance of a blast-furnace stove. In each case the 2-D finite-conductivity model was modified to simulate the air-flow variations experienced in actual stove systems.

In Willmott's calculations, the air flow rate through the stove at selected times during the cold period was evaluated from a heat-balance equation involving the 'latest' computed values of the air pre-heat temperature and the eventual blast temperature (by-pass main system). The entire cycle of calculations proceeded iteratively until

solutions became repetitive. The air-period heat-transfer coefficients, being functions of the flow rate, also took different values at the pre-selected times. Hofmann and Kappelmayer devised a computer program to carry out similar calculations, but included the effect of flow maldistribution within the stove chequerwork. More recently, Razelos and Benjamin undertook a similar, but more detailed, study to that of Willmott [55,59]

Increasing the generality of a regenerator model to include non-linearities inevitably incurs a considerable penalty in terms of the computer time needed for each example. This point is amply illustrated by Razelos, who found that one full set of calculations for a four-stove staggered arrangement, which included the effects of a variable air flow rate and with the heat-transfer coefficients evaluated at each of 30 x 20 space-time nodes, required over nine minutes of computer time on an IBM 360/75. The use of mean heat-transfer coefficients (averaged over the complete stove height for each period) reduced this time to just over 1.5 minutes, with little sacrifice in the accuracy of the predicted pre-heat temperature. With a view to speeding up this type of computational scheme, Willmott and Kulakowski [60] have reported a numerical procedure for accelerating the convergence of successive 'cycles' of calculations.

For the more conventional three-stove 'series' arrangement, it is interesting to note that the cooling-period effectiveness values calculated by Willmott [55] using a variable-flow model were at most just over two per cent higher than those obtained from the corresponding constant-flow model. In an equivalent exercise, Razelos [58] detected virtually no difference in the performance predicted for these two cases.

3-D Model Theories

It is clear from the foregoing discussion that, apart from the recuperator analogy methods, the thermal performance of a regenerator having a finite wall-conductivity ($k_x \neq 0, k_y = 0$) can be predicted either from the 2-D, finite-conductivity model, using the bulk heat-transfer coefficients of equation (1-15), or from the 3-D model presented in equations (1-7) to (1-13). The advantages of using the 2-D model are that the associated mathematical and computational techniques are simpler, the computer memory requirement is smaller and more importantly, the time for computing each example is much shorter. Balanced against these, however, are the uncertainties which arise because the gas temperatures calculated from the simpler model can differ significantly from those obtained from the more comprehensive 3-D model; an aspect that is examined in more detail below.

Several different finite-difference methods have been examined for solving the 3-D counterflow model by the digital simulation approach. Manrique and Cardenas [61] applied an explicit scheme, incorporating forward and central differences, to calculate the temperature histories of the solid and fluids in a high-temperature regenerator, throughout a complete cycle. To ensure the numerical stability of the calculations, the choice of step sizes in all three dimensions were required to satisfy certain mathematical conditions. In a more recent study, Khandwawala and Chawla [62] compared two fairly-new methods, viz. the Dufort and Frankel scheme [63] and the Alternating Direction Approximation [63]. While both methods were said to be stable for any step size, the latter method was found to be simpler to apply and required slightly less computer time. The authors considered that both these methods were superior, in terms of computational efficiency, to the more established Crank-Nicolson [64] and Mitchell-Pearce [65] implicit methods.

The latter method was used by Heggs and Carpenter [66,67] and also by Willmott [68] in studies involving a comparison of results computed by the 2-D and 3-D regenerator models. The former authors produced a set of charts to indicate, for any combination of the dimensionless parameters Λ, Π and Bi (the Biot number) whether, for a given design calculation, it is necessary to use the more elaborate 3-D model or whether results of sufficient accuracy could be obtained from the simpler 2-D infinite-conductivity model.

Willmott's work [68] was of particular significance, as it compared the results obtained from the two alternative methods for predicting the performance of a regenerator with a finite wall-thermal conductivity. The comparison was carried out for the thermally-symmetrical case only, and showed that considerable errors can occur in the pre-heat temperatures predicted by the 2-D, finite-conductivity model. Willmott attributes these deviations to the fact that the bulk heat-transfer coefficients are calculated using a constant, rather than a time-varying value of the Hausen factor ϕ_H (defined in equation (1-15) for the plane-wall matrix, and in references [3] and [69] for different matrix geometries). Subsequently, amended theories have improved the accuracy of predictions from the 2-D models [70,71], although it appears that further studies are needed to enable these theories to be applied for the complete range of regenerator parameters.

Discarding the 2-D model in favour of the more complete 3-D model would clearly avoid any uncertainties arising in the results from the simpler model. However, the use of open methods to solve the equations of the 3-D model are considered to be too expensive in computer time.

One way of avoiding all of these difficulties is to use the closed-form solution to the full 3-D model, derived by Collins and Daws [72]. As far as the author is aware, this solution is the only one of its type to be derived for a counterflow regenerator, although Kardas [73] has obtained an analytical solution for the uni-directional regenerator problem.

Unlike the corresponding open method of solution, which requires an iterative computation of both fluid and solid temperatures in two space and one time dimensions, the closed theory of Collins and Daws only involves the non-iterative computation of fluid temperatures in one space and one time dimension. Thus, in addition to the advantage obtained from the use of the more detailed 3-D model, programming the closed theory for regenerator calculations should result in shorter and more predictable computation times. Another advantage of the Collins and Daws method is that, as with all closed methods, the equilibrium condition is satisfied mathematically in the theoretical analysis. The problem which arises in open methods of solution, viz. that of judging when a given set of calculations satisfies the equilibrium condition, particularly in cases of slow convergence, does not arise when the non-iterative method is used.

A feasibility study of this method of regenerator computation has been carried out by the writer and colleagues [37,74]. Whilst this served to confirm the validity of the method, it also revealed the need for considerable further development to enable the technique to be applied successfully over a wide range of regenerator parameters. In view of the potential benefits to be gained from its use as a design tool, the research programme reported hereunder was undertaken, in order to carry out the necessary development.

CHAPTER 2

PREVIOUS COMPUTER SOLUTIONS OF THE REGENERATOR, 3-D MODEL, USING A NON-ITERATIVE METHOD

2.1 REVIEW OF THE NON-ITERATIVE METHOD FOR REGENERATOR COMPUTATION

Both the original theory of Collins and Daws, and its development and trial application by Edwards et al, have been reported in the open literature [37, 74]. However, because of the relationship of this further research to these earlier investigations, it is expedient to include at this point a summary of the regenerator theory derived by Collins and Daws, together with a detailed review of the additional techniques developed in the earlier analysis [74] for the application of their method of regenerator solution.

The Regenerator Theory of Collins and Daws

As previously stated, the mathematical analysis developed by these authors resulted in a closed-form solution for the equations of the 3-D, finite-conductivity, regenerator model.

In formulating the equations of the 3-D model, Collins and Daws considered a plane-wall regenerator of the type shown in FIG. 3(a), or, more correctly, its representation as an equivalent, single-channel regenerator as shown in FIG. 3(b). The regenerator depicted in FIG. 3(b) is a hypothetical structure which is thermally equivalent to the adjacent real regenerator. The convenience of using the latter representation and its exact relationship to the corresponding real regenerator is fully discussed in reference [74]. In particular, it is noted that by using this concept, the regenerator problem can be specified in terms of one time and only two space dimensions.

As shown in FIG. 3(b), positions inside the regenerator are specified in relation to two perpendicular axes Ox and Oy, the origin O of the co-ordinates being located in a wall surface at the mid-length of the regenerator channel. The Oy axis is parallel to the direction of the fluid flow, the positive y-direction being defined arbitrarily by the hot fluid entry end. The positive x-direction is taken into the chequer wall.

Considering the regenerator to be in a state of cyclic equilibrium, hot fluid with a mass flow rate W_1, specific heat S_1 and temperature $t_1(\frac{1}{2}L, \theta)$, is assumed to enter the regenerator at $y = \frac{1}{2}L$ for a period P. The flows are then instantaneously reversed so that for a further period P, a cold fluid with a mass flow rate W_2, specific heat S_2 and temperature $t_2(-\frac{1}{2}L, \theta)$, enters the regenerator at $y = -\frac{1}{2}L$. In the equilibrium state, the fluid and solid temperatures throughout the regenerator are therefore periodic functions of time, with a period 2P. The origin of time, θ, is taken to be at the start of an arbitrarily selected heating period.

Using similar procedures to those described to obtain equations (1-7) to (1-13), the mathematical equations describing this particular regenerator operation were then formulated. However, as a result of using the same (fixed) origin of co-ordinates for both periods, together with the assumption of equal reversal periods, the regenerator equations derived by Collins and Daws were similar in form but not identical to those given by equations (1-7) to (1-13).

For greater generality, Collins and Daws first made the fluid and the wall temperatures dimensionless by substitutions of the type

$$t'(y,\theta) = \frac{2t(y,\theta)}{\bar{t}_1(\frac{1}{2}L)-\bar{t}_2(-\frac{1}{2}L)} - \frac{\bar{t}_1(\frac{1}{2}L)+\bar{t}_2(-\frac{1}{2}L)}{\bar{t}_1(\frac{1}{2}L)-\bar{t}_2(-\frac{1}{2}L)} \quad \ldots\ldots (2\text{-}1)$$

The independent variables were also made dimensionless by the normalising substitutions:-

$$x = a\xi \quad , \quad y = \tfrac{1}{2}L\zeta \quad , \quad \theta = \frac{a^2 z}{\alpha} \quad \ldots\ldots (2\text{-}2)$$

These changes introduced the dimensionless groups

$$\left.\begin{aligned} M_1 &= \frac{2W_1 S_1 a}{kpL} \quad , \quad M_2 = \frac{2W_2 S_2 a}{kpL} \\ N_1 &= \frac{h_1 a}{k} \quad , \quad N_2 = \frac{h_2 a}{k} \quad , \quad \Omega = \frac{\alpha P}{a^2} \end{aligned}\right\} \quad \ldots\ldots (2\text{-}3)$$

A further change in the time variable to z', where

$$\left.\begin{aligned} z' &= z, \text{ in the heating period} \\ \text{and } z' &= z-\Omega, \text{ in the cooling period} \end{aligned}\right\} \quad \ldots\ldots (2\text{-}4)$$

resulted in the fluid temperature $t'(y,\theta)$ eventually transforming to $f(\zeta,z')$.

When expressed in terms of the dimensionless variables of equations (2-1), (2-2) and (2-4), the distance, ζ, along the regenerator length varies in the range $-1 \leqslant \zeta \leqslant +1$, the distance ξ normal to the wall surface varies from zero to a, and time z' varies from zero at the start to Ω at the end of each period. All 'dimensionless' temperatures vary in the range -1 to +1, which are the mean values of the dimensionless fluid temperatures entering the regenerator matrix in the cooling and heating periods, respectively.

Using these dimensionless variables, Collins and Daws obtained the mathematical equations describing a regenerator operating at cyclic equilibrium in the forms stated in Appendix 1. They then derived an analytical solution of the heat-conduction equation (A1-1) which satisfied the boundary condition stated in equation (A1-2) and also the reversal condition. From the solution obtained, the fluid temperatures $f_1(\zeta,\tau)$ and $f_2(\zeta,\tau)$ at any position ζ and at any instant $z'=\tau$, were shown to satisfy the following integro-differential equations:-

$$a_1 f_1(\zeta,\tau) + a_2 f_2(\zeta,\tau) + a_4 X_1(\zeta,\tau) + a_3 X_2(\zeta,\tau)$$

$$+ 2\int_{z'=0}^{\tau} X_1(\zeta,z')\eta_1(\tau-\Omega-z')dz' + 2\int_{z'=\tau}^{\Omega} X_1(\zeta,z')\eta_1(\tau-z')dz'=0$$

..... (2-5)

and

$$-a_1 f_1(\zeta,\tau) + a_2 f_2(\zeta,\tau) + a_3 X_1(\zeta,\tau) + a_4 X_2(\zeta,\tau)$$

$$+ 2\int_{z'=0}^{\tau} X_2(\zeta,z')\eta_2(\tau-\Omega-z')dz' - 2\int_{z'=\tau}^{\Omega} X_2(\zeta,z')\eta_2(\tau-z')dz' = 0$$

..... (2-6)

where

$$2X_1(\zeta,z') = -\left[\frac{M_1}{a_1}\frac{\partial f_1}{\partial \zeta} + f_1\right] + \left[\frac{M_2}{a_2}\frac{\partial f_2}{\partial \zeta} - f_2\right]$$

..... (2-7)

$$2X_2(\zeta,z') = \left[\frac{M_1}{a_1}\frac{\partial f_1}{\partial \zeta} + f_1\right] + \left[\frac{M_2}{a_2}\frac{\partial f_2}{\partial \zeta} - f_2\right] \quad \text{..... (2-8)}$$

$$\eta_1(\tau) = \sum_{s=1}^{\infty} \frac{b_s \exp\left[-\beta_s(\tau+\Omega)\right]}{1 - \exp(-\beta_s\Omega)} \quad \text{..... (2-9)}$$

$$\eta_2(\tau) = \sum_{s=1}^{\infty} \frac{b_s \exp\left[-\beta_s(\tau+\Omega)\right]}{1 + \exp(-\beta_s\Omega)} \quad \text{..... (2-10)}$$

Also $$b_s = \frac{2\beta_s}{2+\beta_s} \quad , \; s=1,2,3,..... \quad \text{..... (2-11)}$$

where β_s is the s^{th} root of

$$\sqrt{\beta}\tan\sqrt{\beta} = 1 \quad \text{..... (2-12)}$$

The coefficients a_1, a_2, a_3 and a_4 in equations (2-5) and (2-6) are functions of the parameters N_1 and N_2 and are defined in the list of symbols.

It is useful to note at this point that the closed-form solution stated in equations (2-5) and (2-6) is completely specified when the five dimensionless parameters M_1, M_2, N_1, N_2 and Ω are known. According to this theory therefore, for any given fluid entry temperatures, the thermal behaviour of a particular regenerator is governed by the values of these five parameters, with M_1 and M_2 characterising the fluid mass flow rates, N_1 and N_2 the heat transfer and Ω the duration of each reversal period.

Because the reversal boundary condition has been satisfied in the derivation of the closed-form solution stated in equations (2-5) and (2-6), the required fluid temperatures throughout a given regenerator can therefore be obtained, for any appropriate values of M_i, N_i and Ω, by solving these equations numerically, with the known fluid entry temperatures $f_1(1,z')$ and $f_2(-1,z')$, $0 \leqslant z' \leqslant \Omega$, as boundary conditions.

The Theory of Edwards et al for Non-Equal Reversal Periods

As part of the earlier investigation [37, 74], Edwards generalised the 'equal-period' theory of Collins and Daws in order to allow for heating and cooling periods of dissimilar duration. The fluid temperatures in a regenerator operating in this more general mode were again shown to satisfy a pair of simultaneous integro-differential equations. These are given as equations (2-13) and (2-14) below.

$$a_1 f_1(\zeta,\bar{\tau}) + d_1 \phi_1(\zeta,\bar{\tau}) + \int_{v=0}^{\bar{\tau}} \phi_1(\zeta,v)\, g\left[\Omega_1(\bar{\tau}-v)\right] dv$$

$$+\int_{v=\bar{\tau}}^{1} \phi_1(\zeta,v)\, g\left[\Omega_1(\bar{\tau}+1+\frac{\Omega_2}{\Omega_1}-v)\right]dv + \int_{v=0}^{1} \phi_2(\zeta,v)\, g\left[\Omega_2(\frac{\Omega_1}{\Omega_2}\bar{\tau}+1-v)\right] dv=0$$

..... (2-13)

and

$$a_2 f_2(\zeta,\bar{\tau}) + d_2 \phi_2(\zeta,\bar{\tau}) + \int_{v=0}^{\bar{\tau}} \phi_2(\zeta,v)\, g\left[\Omega_2(\bar{\tau}-v)\right] dv$$

$$+\int_{v=\bar{\tau}}^{1} \phi_2(\zeta,v)\, g\left[\Omega_2(\bar{\tau}+1+\frac{\Omega_1}{\Omega_2}-v)\right] dv + \int_{v=0}^{1} \phi_1(\zeta,v)\, g\left[\Omega_1(\frac{\Omega_2}{\Omega_1}\bar{\tau}+1-v)\right] dv=0$$

..... (2-14)

In these equations $\bar{\tau}$ is an instantaneous value of v, given by

$$\bar{\tau} = \frac{\tau}{\Omega_1} \quad , \quad 0 \leqslant \tau \leqslant \Omega_1 \qquad \text{..... (2-15)}$$

and

$$\phi_1(\zeta,v) = \Omega_1 \left[-\frac{M_1}{a_1}\frac{\partial f_1}{\partial \zeta} - f_1 \right] \qquad \text{..... (2-16)}$$

$$\phi_2(\zeta,v) = \Omega_2 \left[\frac{M_2}{a_2}\frac{\partial f_2}{\partial \zeta} - f_2 \right] \qquad \text{..... (2-17)}$$

$$g(v) = \sum_{s=1}^{\infty} \frac{b_s \exp(-\beta_s v)}{1-\exp\left[-\beta_s(\Omega_1+\Omega_2)\right]} \qquad \text{..... (2-18)}$$

$$d_1 = \frac{1}{\Omega_1(N_1-1)} \quad \text{and} \quad d_2 = \frac{1}{\Omega_2(N_2-1)} \qquad \text{..... (2-19)}$$

Also in these equations Ω_1 and Ω_2 are the values of Ω in the heating and cooling periods respectively, and v is the dimensionless time variable defined by

$$v = \frac{z}{\Omega_1} \quad , \quad 0 \leqslant z \leqslant \Omega_1$$

$$v = \frac{z-\Omega_1}{\Omega_2} \quad , \quad \Omega_1 \leqslant z \leqslant \Omega_1 + \Omega_2 \qquad \text{..... (2-20)}$$

For this time scale, v varies linearly from zero at the start to unity at the end of each period. Thus in either period, a particular value of v in the range $0 \leqslant v \leqslant 1$, represents the same proportion of the appropriate total period time.

All other symbols in equations (2-13) to (2-19) are as defined previously, the range of ζ again being $-1 \leqslant \zeta \leqslant +1$.

In this more general case, it can be seen that the six dimensionless parameters M_i, N_i, Ω_i, i=1,2, are needed to specify equations (2-13) and (2-14). The thermal behaviour of a regenerator working in this mode is therefore governed by the values of these six parameters. With these six values given, the problem is then to solve equations (2-13) and (2-14), with $f_1(1,\bar{\tau})$ and $f_2(-1,\bar{\tau})$ known, to determine $f_i(\zeta,\bar{\tau})$ for $0 \leqslant \bar{\tau} \leqslant 1$.

The solution obtained by Edwards et al (1971) for $\Omega_1 \neq \Omega_2$, viz. equations (2-13) and (2-14), has many similar features to that obtained by Collins and Daws for $\Omega_1 = \Omega_2 = \Omega$, i.e. equations (2-5) and (2-6). However, even though the latter problem is a special case of that considered by Edwards et al, it has not been found possible to deduce equations (2-5) and (2-6) by an algebraic simplification of equations (2-13) and (2-14). For this reason, the numerical

computation of solutions for each of these two cases requires a completely separate treatment, as described in the following sections.

2.2 SOLUTION OF THE INTEGRO-DIFFERENTIAL EQUATIONS DERIVED FOR THE CASE $\Omega_1 = \Omega_2 = \Omega$.

The scheme proposed by Collins and Daws [72] for the numerical solution of equations (2-5) and (2-6), commenced by dividing the dimensionless period Ω into (n+1) equally-spaced times. Equations (2-5) and (2-6) are then applied at each of these times to obtain the two matrix equations:-

$$a_1\underline{F}_1(\zeta) + a_2\underline{F}_2(\zeta) + a_3\underline{X}_2(\zeta) + (a_4\underline{I} + \underline{A}_1')\underline{X}_1(\zeta) = 0 \qquad \ldots\ldots \text{(2-21)}$$

and

$$-a_1\underline{F}_1(\zeta) + a_2\underline{F}_2(\zeta) + a_3\underline{X}_1(\zeta) + (a_4\underline{I} + \underline{A}_2')\underline{X}_2(\zeta) = 0 \qquad \ldots\ldots \text{(2-22)}$$

In these equations $\underline{F}_1$, $\underline{F}_2$, $\underline{X}_1$ and $\underline{X}_2$ are column matrices containing the values of f_1, f_2, X_1 and X_2 at the (n+1) discrete values of time. Also $\underline{A}_1'$ and $\underline{A}_2'$ are square matrices of order (n+1) which arise when the integrals in equations (2-5) and (2-6) are approximated numerically.

Defining $\underline{F}(\zeta)$ to be the (2n+2)x1 column matrix

$$\underline{F}(\zeta) = \begin{bmatrix} \underline{F}_2(\zeta) \\ \underline{F}_1(\zeta) \end{bmatrix} \qquad \ldots\ldots \text{(2-23)}$$

and using equations (2-7) and (2-8), equations (2-21) and (2-22) can be arranged ultimately as the system of (2n+2) ordinary differential equations which is expressed in matrix form in equation (2-24), (see [74] for mathematical details).

$$\frac{d\underline{F}(\zeta)}{d\zeta} + \underline{P}\,\underline{F}(\zeta) = 0, \quad -1 \leqslant \zeta \leqslant +1 \qquad \ldots\ldots (2\text{-}24)$$

In equation (2-24)

$$\underline{P} = \left[\begin{array}{c|c} \underline{\gamma}_1 & \underline{\gamma}_2 \\ \hline \underline{T}_2 & \underline{T}_1 \end{array}\right] \qquad \ldots\ldots (2\text{-}25)$$

and the (n+1)x(n+1) sub-matrices $\underline{\gamma}_1$, $\underline{\gamma}_2$, $\underline{T}_1$ and $\underline{T}_2$ are given by

$$\left.\begin{aligned}
\underline{\gamma}_1 &= \frac{a_2}{M_2}\left\{(\underline{A}_2\underline{A}_1 - a_3^2\underline{I})^{-1}a_2(\underline{A}_2 - a_3\underline{I}) + (\underline{A}_1\underline{A}_2 - a_3^2\underline{I})^{-1}a_2 \times (\underline{A}_1 - a_3\underline{I}) - \underline{I}\right\} \\
\underline{\gamma}_2 &= \frac{a_2}{M_2}\left\{(\underline{A}_2\underline{A}_1 - a_3^2\underline{I})^{-1}a_1(\underline{A}_2 + a_3\underline{I}) - (\underline{A}_1\underline{A}_2 - a_3^2\underline{I})^{-1}a_1 \times (\underline{A}_1 + a_3\underline{I})\right\} \\
\underline{T}_1 &= \frac{-a_1}{M_1}\left\{(\underline{A}_2\underline{A}_1 - a_3^2\underline{I})^{-1}a_1(\underline{A}_2 + a_3\underline{I}) + (\underline{A}_1\underline{A}_2 - a_3^2\underline{I})^{-1}a_1 \times (\underline{A}_1 + a_3\underline{I}) - \underline{I}\right\} \\
\underline{T}_2 &= \frac{-a_1}{M_1}\left\{(\underline{A}_2\underline{A}_1 - a_3^2\underline{I})^{-1}a_2(\underline{A}_2 - a_3\underline{I}) - (\underline{A}_1\underline{A}_2 - a_3^2\underline{I})^{-1}a_2 \times (\underline{A}_1 - a_3\underline{I})\right\}
\end{aligned}\right\} \ldots (2\text{-}26)$$

where $\underline{A}_1 = \underline{A}_1' + a_4 \underline{I}$ ..... (2-27)

and $\underline{A}_2 = \underline{A}_2' + a_4 \underline{I}$ ..... (2-28)

The problem is then solved by numerical integration of equations (2-24), with the known fluid entry temperatures as boundary conditions. Assuming the fluid entry temperatures remain invariant at their mean values during their respective periods, the boundary conditions can be written in terms of (n+1)x1 column matrices:-

$$\underline{F}_1(+1) = \left\{(f_1)_j\right\} \text{ , where } (f_1)_j = +1 \text{ for } 1 \leqslant j \leqslant n+1 \quad \text{..... (2-29)}$$

and

$$\underline{F}_2(-1) = \left\{(f_2)_j\right\} \text{ , where } (f_2)_j = -1 \text{ for } 1 \leqslant j \leqslant n+1 \quad \text{..... (2-30)}$$

Numerical Computation

In the original investigation the above solution scheme was split into three main stages. The first stage involved the development of mathematical techniques for approximating the definite integrals in equations (2-5) and (2-6). The particular method developed by Edwards et al [37, 74] is outlined in Appendix 2, Section A2.1, which also defines, in equations (A2.1-16) to A2.1-23), the mathematical forms derived for each element of matrices $\underline{A}_1'$ and $\underline{A}_2'$. These latter formulae were then programmed to enable each element of these matrices to be computed to a known accuracy.

These elements were then used in the second stage of the process to calculate the elements of matrix $\underline{P}$. This stage involved extensive matrix calculations but required no additional mathematics.

The third stage, which with stage two was carried out by the writer, entailed the numerical integration of the system of differential equations (2-24). In the scheme adopted to do this, the regenerator length was sub-divided into 2m equal intervals, the interval boundaries being at the points $\zeta = \frac{r}{m} = rh_L$, where $-m \leqslant r \leqslant +m$, and $h_L = \frac{1}{m}$ is the distance step size.

Considering a typical interval $rh_L \leqslant \zeta \leqslant (r+1)h_L$, the Crank-Nicolson [64, 78] finite-difference approximation

$$\frac{\underline{F}_{r+1} - \underline{F}_r}{h_L} \simeq \frac{1}{2}\left[\left(\frac{d\underline{F}}{d\zeta}\right)_{\zeta=rh_L} + \left(\frac{d\underline{F}}{d\zeta}\right)_{\zeta=(r+1)h_L}\right] \quad \ldots\ldots (2\text{-}31)$$

where $\underline{F}_r = \underline{F}(rh_L)$, was applied in conjunction with equation (2-24) to give

$$\underline{F}_{r+1} - \underline{F}_r + \frac{h_L}{2}(\underline{P}\,\underline{F}_{r+1} + \underline{P}\,\underline{F}_r) = 0, \quad -m \leqslant r \leqslant m \quad \ldots\ldots (2\text{-}32)$$

The latter equation incorporates the assumption that physical properties, and therefore the elements of $\underline{P}$, remain invariant along the regenerator. Simplifying this equation gives

$$\underline{F}_{r+1} = \underline{Q}\,\underline{F}_r \quad , \quad -m \leqslant r \leqslant m \quad \ldots\ldots (2\text{-}33)$$

where $\underline{Q} = (2m\underline{I} + \underline{P})^{-1}(2m\underline{I} - \underline{P})$ $\ldots\ldots (2\text{-}34)$

The system of differential equations (2-24) is therefore replaced by the coupled difference equations (2-33), which then have to be solved subject to the boundary conditions given in (2-29) and (2-30).

Because of the particular form of the boundary conditions, equation (2-33) cannot be applied recursively to calculate the required fluid temperatures. Moreover, the particular method used to solve these equations has only previously been stated [74] for the case where n=5. Hence for completeness the more general treatment needed for this further study is presented in Appendix 3.

After first forming the elements of matrices $\underline{P}$ and $\underline{Q}$ using equations (2-25) to (2-28), incorporation of the method described in Appendix 3 into a second computer program enabled the fluid temperatures to be computed at each of the (2m+1) points along the regenerator for each of the selected (n+1) times in each period.

2.3 SOLUTION OF THE INTEGRO-DIFFERENTIAL EQUATIONS DERIVED FOR THE CASE $\Omega_1 \neq \Omega_2$

The equations to be solved in this case are equations (2-13) and (2-14). Following a similar procedure to that described in the preceding section, but with the range of $\bar{\tau}$, $0 \leqslant \bar{\tau} \leqslant 1$, divided into (n+1) equally-spaced times, Edwards et al [74] showed that at any value of ζ, these equations could be approximated by

$$a_1 \underline{F}_1(\zeta) + (\underline{B}_1 + d_1\underline{I})\underline{\phi}_1(\zeta) + \underline{D}_1\underline{\phi}_2(\zeta) = 0 \qquad \ldots\ldots (2\text{-}35)$$

and

$$a_2 \underline{F}_2(\zeta) + (\underline{B}_2 + d_2\underline{I})\underline{\phi}_2(\zeta) + \underline{D}_2\underline{\phi}_1(\zeta) = 0 \qquad \ldots\ldots (2\text{-}36)$$

where $\underline{F}_1$, $\underline{F}_2$, $\underline{\phi}_1$ and $\underline{\phi}_2$ are column matrices containing the values of f_1, f_2, ϕ_1 and ϕ_2 at the (n+1) selected values of time. Also, $\underline{B}_1$, $\underline{B}_2$, $\underline{D}_1$ and $\underline{D}_2$ are (n+1)x(n+1) matrices whose elements, for a given n, depend on the method used to approximate the definite integrals in equations (2-13) and (2-14).

Combining equations (2-35) and (2-36) with equations (2-16) and (2-17) gives the system of differential equations

$$\frac{d\underline{F}(\zeta)}{d\zeta} + \underline{P}_1 \underline{F}(\zeta) = 0, \quad -1 \leqslant \zeta \leqslant +1 \qquad \ldots\ldots (2\text{-}37)$$

where

$$\underline{P}_1 = \left[\begin{array}{c|c} \underline{Z}_1 & \underline{Z}_2 \\ \hline \underline{V}_2 & \underline{V}_1 \end{array}\right] \qquad \ldots\ldots (2\text{-}38)$$

$\underline{F}$ is as defined by equation (2-23) and the (n+1)x(n+1) matrices $\underline{Z}_1$, $\underline{Z}_2$, $\underline{V}_1$ and $\underline{V}_2$ are given by

$$\underline{Z}_1 = \frac{1}{\Omega_2 M_2}\left\{a_2^2\left[(\underline{B}_2 + d_2\underline{I}) - \underline{D}_2(\underline{B}_1 + d_1\underline{I})^{-1}\underline{D}_1\right]^{-1} - a_2\Omega_2\underline{I}\right\} \qquad \ldots\ldots (2\text{-}39)$$

$$\underline{Z}_2 = \frac{-a_1 a_2}{\Omega_2 M_2} \left[(\underline{B}_1 + d_1\underline{I})\underline{D}_2^{-1}(\underline{B}_2 + d_2\underline{I}) - \underline{D}_1 \right]^{-1} \quad \ldots\ldots (2\text{-}40)$$

$$\underline{V}_1 = \frac{-1}{\Omega_1 M_1} \left\{ a_1^2 \left[(\underline{B}_1 + d_1\underline{I}) - \underline{D}_1(\underline{B}_2 + d_2\underline{I})^{-1}\underline{D}_2 \right]^{-1} - \Omega_1 a_1 \underline{I} \right\} \quad \ldots\ldots (2\text{-}41)$$

$$\underline{V}_2 = \frac{a_1 a_2}{\Omega_1 M_1} \left[(\underline{B}_2 + d_2\underline{I})\underline{D}_1^{-1}(\underline{B}_1 + d_1\underline{I}) - \underline{D}_2 \right]^{-1} \quad \ldots\ldots (2\text{-}42)$$

In this case the system of differential equations (2-37) has to be solved subject to the boundary conditions stated in equations (2-29) and (2-30).

Computation Process

The computation process needed to apply the above scheme follows similar lines to that described in Section 2.2, and also contains three main stages.

Firstly, the integrals of equations (2-13) and (2-14) are approximated using techniques developed by Edwards et al [37, 74]. These are summarised in Appendix 2, Section A2.2 which specifies in equations (A2.2-1) to (A2.2-4) the mathematical forms derived for the elements of the matrices $\underline{B}_1$, $\underline{B}_2$, $\underline{D}_1$ and $\underline{D}_2$. Using these forms the first stage of the computation is arranged to calculate the elements of these four matrices.

With these matrices known, the second stage involves the computation of matrices $\underline{Z}_1$, $\underline{Z}_2$, $\underline{V}_1$ and $\underline{V}_2$ and then matrix $\underline{P}_1$ of equation (2-38).

Now it is readily seen that equation (2-37) has exactly the same form as equation (2-24). Moreover, the boundary conditions remain as specified in equations (2-29) and (2-30). The system of (2-37) may therefore be integrated numerically in exactly the same way as that described in Section 2.2, to obtain the required fluid temperature histories throughout the regenerator.

2.4 LIMITATIONS OF THE INITIAL DEVELOPMENT : AIMS OF THE CURRENT INVESTIGATION

The initial development and application of the non-iterative method for regenerator computation by Edwards et al had two principal aims. These were:-

(a) to generalise the theoretical model proposed by Collins and Daws to include reversal periods of unequal duration, and

(b) to develop and apply appropriate computational techniques in order to test the validity of this method of regenerator computation.

As may be seen from the published account [74], both of these aims were successfully completed, and it was concluded that the non-iterative method produced valid results for regenerators operating with equal or with unequal heating and cooling periods.

Although the study carried out at that time was therefore quite encouraging, the treatment of certain aspects - the testing of the more general theory, for example - had been

limited and of a preliminary nature only. Also serious difficulties relating to the numerical accuracy of some computations had been noted. It was clear therefore, that a further, more extensive investigation would be needed to complete the development of this 'closed' method to the stage where it could usefully be applied for design and/or optimisation studies on regenerators in current practice. In order to clarify the extent and nature of the necessary further development, the difficulties and shortcomings highlighted by the feasibility study will be considered next.

Dealing firstly with the tests carried out with the 'equal-period' theory, two particular problems were noted:-

(i) the computed heat-balance discrepancy, which is the percentage difference in the heat-transfer rates computed for the hot and cold periods, increased with increasing values of Ω. (For a numerically correct computation the heat-balance discrepancy should be zero); and

(ii) for isolated examples, even with low values of Ω, the program had produced absurd results in the sense that the computed temperatures, f_i, were not contained within the permitted range $-1 \leqslant f_i \leqslant +1$.

Because the majority of examples tested at that time had been computed with a heat-balance discrepancy of below 1%, it was considered that a computation which had a heat-balance discrepancy of less than 1% was of an acceptable accuracy. The point being made in (i) above is, that for examples

having large values of Ω, the heat-balance discrepancy increased well above 1%, so that in these cases the computed results were not of an acceptable accuracy. It was suspected that this effect was due to a lack of accuracy in the numerical techniques used to approximate the various integrals in equations (2-5) and (2-6), but this hypothesis was not tested.

It was not as easy to speculate on the possible cause of the difficulty noted in item (ii), because this particular effect was restricted to only a few examples, and occurred unpredictably. However, it was found, for all examples in this category, that sensible results were obtained for the corresponding 'invert' example. The 'invert' of a given example is obtained by interchanging the values of M_1 and N_1 with those of M_2 and N_2, the solution of the original problem then being deduced from the solution of its invert, on the basis of thermal symmetry. Although sensible solutions were obtained by this technique, the reasons for this computational difficulty were unclear and needed investigation. It was also felt that a rigorous derivation of the relationships between the solutions for a given example and those of its 'invert' example ought to be attempted.

In the earlier investigation, the calculations required for the first stage of the computation process and those required for the remaining two stages were performed by two separate programs. At that time, such a scheme had certain advantages and was adequate for an initial assessment of the

'closed' method. However, such a split arrangement is too cumbersome for a more extensive application of the method. Also due to the rapid developments in computer technology, the original programs are now outdated and are useless for modern digital computers. In this context, therefore, a single program written in a universal, high-level language is required for the entire computation process. Furthermore, the program design should be such as to allow the size of the time step and that of the distance step to be specified in the program input data. (The original programs were restricted in this respect).

Dealing next with the investigation of the more general theory; this was in fact limited to just a single computation. Although the results obtained for this example were not particularly accurate, they were considered to be encouraging. However, the example selected had only tested the theory in a case for which $\Omega_1 = \Omega_2 = 0.4176$ and since modern blast-furnace stoves, for which the theory had been prepared, operate with much larger and unequal values of Ω, there was a clear need for a more detailed assessment to cover such values.

On the programming side, such an assessment was seen to require the development of a single program embodying the more general theory. Because of the differences in the two underlying theories, this second program would be quite distinct from the 'equal-period' program, but would need the same general requirements, as specified above.

On the mathematical side, Edwards et al [37, 74] pointed out the need to develop techniques to ensure the accurate summation of all the infinite series $Q_i(u)$ and $R_i(u)$ defined by equations (A2.2-1) to (A2.2-4). These techniques would also need to be incorporated in the second, more generally applicable computer program.

One final, but nevertheless important weakness in the initial development concerns the reliance on a final heat-balance test to assess the numerical accuracy of a given computation. While it is evident, from the heat-transfer laws, that a small heat-balance discrepancy is a necessary condition for accurate solutions, such a result does not provide a direct measure of the numerical accuracy of the predicted heat-transfer rates.

To clarify this point, the procedure used to calculate the heat-balance discrepancy in this and in the previous investigation has been considered, for an example having equal heating and cooling periods. Calculation of the actual quantities of heat transferred in each period, in commonly used energy units, would require the evaluation of

$$Q'_1 = W_1 S_1 \left[\bar{t}_1(\tfrac{1}{2}L) - \bar{t}_1(-\tfrac{1}{2}L) \right] P_1 \qquad \ldots\ldots (2\text{-}43)$$

and

$$Q'_2 = W_2 S_2 \left[\bar{t}_2(\tfrac{1}{2}L) - \bar{t}_2(-\tfrac{1}{2}L) \right] P_2 \qquad \ldots\ldots (2\text{-}44)$$

where $P_1 = P_2 = P$ when the reversal periods are of equal duration.

Because each regenerator computation is carried out for a particular set of values of the dimensionless parameters M_1, M_2, N_1, N_2 and Ω, the variables required for the evaluation of Q_1' and Q_2' are not usually known explicitly. Consequently direct evaluation of these quantities is not possible. However the dimensionless quantities $\dot{H}_1$ and $\dot{H}_2$ defined by equations (2-45) and (2-46) can be readily calculated.

$$\dot{H}_1 = M_1 \left[\bar{f}_1(+1) - \bar{f}_1(-1) \right] = M_1 \left[1 - \bar{f}_1(-1) \right] \quad \ldots\ldots (2\text{-}45)$$

$$\dot{H}_2 = M_2 \left[\bar{f}_2(+1) - \bar{f}_2(-1) \right] = M_2 \left[\bar{f}_2(+1) + 1 \right] \quad \ldots\ldots (2\text{-}46)$$

where $\bar{f}_1(-1)$ and $\bar{f}_2(+1)$ are the time-mean fluid exit temperatures in the heating and cooling periods.

Using equations (2-1) to (2-3), the equations for $\dot{H}_1$ and $\dot{H}_2$ can be written

$$\dot{H}_1 = C_1 Q_1' \quad \ldots\ldots (2\text{-}47)$$

$$\dot{H}_2 = C_1 Q_2' \quad \ldots\ldots (2\text{-}48)$$

where $C_1 = 4a / \left\{ kpLP \left[\bar{t}_1(\tfrac{1}{2}L) - \bar{t}_2(-\tfrac{1}{2}L) \right] \right\}$ $\ldots\ldots (2\text{-}49)$

Equation (2-49) shows that C_1 is a constant for a given regenerator operation and it follows that the percentage difference between $\dot{H}_1$ and $\dot{H}_2$ is the same as that between Q_1'

and Q_2'. Each program computation therefore calculates the heat-balance discrepancy (H.B.D.) as the value of the maximum percentage difference between $\dot{H}_1$ and $\dot{H}_2$. That is

$$\text{H.B.D.} = \frac{\dot{H}_1 - \dot{H}_2}{(\dot{H}_i)_{min}} \times 100 \qquad \ldots\ldots (2\text{-}50)$$

where $(\dot{H}_i)_{min}$ is the smaller of $\dot{H}_1$ and $\dot{H}_2$.

The quantities $\dot{H}_1$ and $\dot{H}_2$ may be thought of as dimensionless heat-transfer rates, which although not measured in commonly used units, are related to such units by the same numerical factor.

In a given computation, because of the many numerical techniques involved, it is inevitable that the computed values of $\dot{H}_1$ and $\dot{H}_2$ will each be subject to some numerical error. What was not clear at the outset of this investigation was how, for any given example, the $\dot{H}_1$ and $\dot{H}_2$ values computed with different combinations of time and distance steps are related to the 'true', i.e. the numerically correct heat-transfer rate $\dot{H}^*$. It is this latter quantity together with its numerical accuracy that we really need to know, and the fact that $\dot{H}_1$ and $\dot{H}_2$ agree to within a given percentage figure does not provide this information. In fact, an assumption made in the earlier study [74] that $\dot{H}^*$ always lies between the computed values of $\dot{H}_1$ and $\dot{H}_2$ has been shown in this further investigation to be untrue, in many cases (see Chapter 4).

On the basis of these earlier findings, the aims and objectives of this further research are stated as follows.

The overall aim is to complete the development of the non-iterative method for solving the regenerator, 3-D, thermal model so as to produce a suite of computer programs capable of rapid and accurate evaluation of regenerator thermal behaviour.

To achieve this aim the following particular objectives were identified:-

1. To develop a technique for predicting, for any given example, the 'true' heat-transfer rate $\dot{H}^*$, together with its numerical accuracy.

2. To develop techniques firstly, to ensure that computed solutions are thermally well-balanced and secondly, to ensure that the predicted heat-transfer rate, $\dot{H}^*$, is of a satisfactory numerical accuracy. These objectives should apply to as wide a range of regenerator parameters as possible, and the reduction of the large heat-balance discrepancies which occurred for examples with large Ω values was a particular target.

3. To overcome the problem of absurd solutions being computed for some isolated examples.

4. To derive the theoretical relationships assumed by symmetry to exist between the temperatures computed for a given regenerator example and those obtained from the corresponding 'invert' example.

5. To continue and complete the development of the mathematical and programming techniques needed for the computation of regenerators with unequal heating and cooling periods. This development should incorporate items 1, 2 and 4 above.

6. To comprehensively test both the 'equal-period' theory and the 'generalised' theory for an appropriate and wide range of regenerator parameters.

The investigations carried out in pursuance of these objectives are described in the following chapters. The work was not undertaken in the sequence listed above, but concentrated initially on completing the development of the 'equal-period' theory, before moving on to the more general theory catering for unequal reversal periods.

CHAPTER 3

INITIAL INVESTIGATION OF THE NUMERICAL ACCURACY OF PREDICTIONS OBTAINED USING THE 'EQUAL-PERIOD' THEORY

3.1 IDENTIFICATION OF ERROR SOURCES IN THE COMPUTATION PROCESS

The discussion of the previous chapter clearly pointed to two groups of examples for which the original programs could not produce acceptable predictions (items (i) and (ii) of Section 2.4). The problems arising in both of these cases were thought to be due to the effect of unidentified numerical errors. For this reason, it was decided to commence this follow-up development by first identifying all possible sources of numerical error in each of the three main stages of the computational process. These were determined as follows.

Stage 1

This evaluates the elements of matrices $\underline{A}_1'$ and $\underline{A}_2'$ which arise from the numerical integration of the integrals in equations (2-5) and (2-6).

Examination of the Edwards et al method, given in Appendix A2.1, for carrying out the numerical integration showed that the computed values of these matrix elements are subject to errors arising from the following sources:-

(a) The errors introduced by the assumption, stated in equation (A2.1-10), that the functions $X_i(\zeta, z')$ are linear in z' within each of the n intervals which sub-divide the reversal period Ω .

(b) The errors arising in the evaluation and summation of successive terms of each infinite series defining the elements of $\underline{A}_1'$ and $\underline{A}_2'$.

(c) An accumulation of round-off errors, which affect almost all calculations carried out on a digital computer.

Stage 2

Errors in this stage are entirely the round-off errors which arise in the matrix calculations needed to compute the matrix $\underline{P}$ as defined by equation (2-25). These errors could become large if any of the matrices inverted in the computation of $\underline{\gamma}_1$, $\underline{\gamma}_2$, $\underline{T}_1$ and $\underline{T}_2$ of equation (2-26), are ill-conditioned [75].

Stage 3

The final stage of the computation involves the step-by-step numerical integration (i.e. solution) of the system of ordinary differential equations (2-24).

The main errors arising in each step of the integration process are truncation (i.e. discretization) errors. Over many integration steps these errors normally accumulate so that we refer to 'accumulated' truncation errors.

In addition to accumulated truncation errors, there is also an accumulation of round-off errors.

On the basis of this analysis, the effect of the numerical errors from each of the above listed sources was then investigated in greater depth. The objective in each case was to minimise the effect of the errors concerned in order to improve and control the numerical accuracy of the final computed solutions. A single FORTRAN program was written for this purpose, based on the computational procedures described in Section 2.2. However, appropriate sections of this program were modified during the course of these investigations. A brief description of the investigations is reported next.

3.2 CONTROL OF ROUND-OFF ERRORS

Since round-off errors affect each stage of the computational process, these were considered first.

Two approaches have been used to control the build-up of round-off errors during the computation. The first applies to all three parts of the computation, whereas the second is aimed specifically at minimising the error build-up during the intermediate stage.

3.2.1 Round-Off Errors in the Complete Calculation

Round-off errors are an unwanted feature of almost all digital computer calculations and arise because only a finite number of digits are available for storing each number. Most digital computers store real numbers in floating-point form, the floating-point approximation $fl(\bar{x})$ to a real number $\bar{x}$ being given by

$$fl(\bar{x}) = \bar{a}.b^{\bar{e}} \qquad \ldots\ldots (3\text{-}1)$$

where $\bar{a}$ is the mantissa (or fraction), b is the number base and $\bar{e}$ the exponent. In equation (3-1), the mantissa takes the form

$$\bar{a} = \sum_{j=1}^{r} d_j.b^{-j} \qquad \ldots\ldots (3\text{-}2)$$

where $0 \leqslant d_j \leqslant b-1$, $j=1,2,\ldots,r$, and the exponent is such that $\bar{L} \leqslant \bar{e} \leqslant \bar{K}$. The parameters b, r, $\bar{L}$ and $\bar{K}$ are design constants for a given computer.

We see from equation (3-2) that the value of r specifies the number of digits in the mantissa. This means that, before it is stored in the computer memory, the result of any arithmetic operation has to be 'rounded-off', i.e. curtailed to 'fit' into the available r digits. In this way each stored result is normally subject to some round-off error. While these errors are small for individual operations, it is possible in certain types of calculations for errors of this type to accumulate to such an extent that they seriously affect the accuracy of the final predictions.

It follows from this explanation that the larger the value of r, the smaller will be the individual round-off errors. For this reason computers are usually designed to enable the user to make a choice from at least two values of r. For example, on the three computers used in this study, the user has the choice of working with single-precision

(i.e. a lower value of r) or double-precision (i.e. a higher value of r). Selecting an appropriate precision therefore provides a simple way of controlling the general magnitude of round-off errors.

The selection of which precision setting to work with on the various computers used for this study was based on an examination of the relative accuracy of its arithmetic in each mode, using a method suggested by Forsythe et al [76]. This involves a comparison of a quantity called the 'machine epsilon', ϵ. The value of ϵ characterises the precision of the floating-point arithmetic on a given computer, and is defined to be the smallest floating-point number for which $1 \oplus \epsilon > 1$, where $\oplus$ denotes floating-point addition.

Table 1 shows the ϵ values determined for the computers used in this study. Use of the higher precision levels on all three computers have clear advantages in terms of lowering the level of round-off errors. However, their use increases the computer memory usage and also increases computer run times. In view of the relatively poor accuracy of single precision on the IBM 1130, these were felt to be necessary sacrifices, and double precision was used for all computations on this machine.

By contrast, Table 1 confirms that single precision on both the B1726 and the DEC-20 computers was only slightly less accurate than double precision on the IBM equipment. Moreover the use of double precision on the Burroughs and

TABLE 1

RELATIVE ACCURACY OF FLOATING-POINT ARITHMETIC
ON POLYTECHNIC OF WALES DIGITAL COMPUTERS

COMPUTER	PRECISION MODE	MACHINE EPSILON ε	SIGNIFICANT DECIMAL DIGITS*
IBM 1130	SINGLE	1.19×10^{-7}	6 to 7
	DOUBLE	4.66×10^{-10}	9 to 10
BURROUGHS B1726	SINGLE	2.98×10^{-8}	7 to 8
	DOUBLE	4.33×10^{-19}	18 to 19
DEC-20	SINGLE	3.73×10^{-9}	8 to 9
	DOUBLE	1.08×10^{-19}	16 to 18

* VALUES QUOTED IN RELEVANT USER MANUALS

DEC computers corresponded to precision increases of from about 8 to 18 decimal digits. Such increases were considered to be unnecessary for the proposed application - predicting the performance of the considered heat exchanger - and so single precision was used on both of these machines.

3.2.2 A Simplified Matrix Analysis for Stage 2

The build-up of round-off errors in this intermediate stage is directly related to the number and type of matrix operations needed to obtain the matrix $\underline{P}$ of equation (2-25). It can be seen that the matrix arithmetic needed to calculate the sub-matrices $\underline{\gamma}_1$, $\underline{\gamma}_2$, $\underline{T}_1$ and $\underline{T}_2$ of equations (2-26) is considerable, and involves many matrix multiplications and several matrix inversions. Since extremely large errors can occur if any of the matrices being inverted are ill-conditioned, and bearing in mind that extremely large errors had occurred in some isolated examples, there was reasonable motivation to try to simplify the matrix analysis needed to obtain the final set of differential equations to be solved. Such a simplification was made, and because the simpler theory has been used in all ensuing investigations, it is reported at this point.

To derive the simpler forms, we note that the expressions defining matrices $\underline{\gamma}_1$, $\underline{\gamma}_2$, $\underline{T}_1$ and $\underline{T}_2$ are a direct consequence of the analysis used by Collins and Daws to derive equations (2-24) from equations (2-21) and (2-22). We commence therefore with these two equations which can be written as

$$a_1\underline{F}_1 + a_2\underline{F}_2 + a_3\underline{X}_2 + a_4\underline{X}_1 + \underline{A}_1'\underline{X}_1 = 0 \qquad \ldots\ldots (3\text{-}3)$$

and

$$-a_1\underline{F}_1 + a_2\underline{F}_2 + a_3\underline{X}_1 + a_4\underline{X}_2 + \underline{A}_2'\underline{X}_2 = 0 \qquad \ldots\ldots (3\text{-}4)$$

where

$$2\underline{X}_1 = -\underline{F}_1 - \underline{F}_2 - \frac{M_1}{a_1}\frac{d\underline{F}_1}{d\zeta} + \frac{M_2}{a_2}\frac{d\underline{F}_2}{d\zeta} \qquad \ldots\ldots (3\text{-}5)$$

and

$$2\underline{X}_2 = \underline{F}_1 - \underline{F}_2 + \frac{M_1}{a_1}\frac{d\underline{F}_1}{d\zeta} + \frac{M_2}{a_2}\frac{d\underline{F}_2}{d\zeta} \qquad \ldots\ldots (3\text{-}6)$$

Substituting for $\underline{X}_1$ and $\underline{X}_2$ in (3-3) and (3-4) leads to

$$\left(\frac{M_2}{N_2}\underline{I} + \frac{1}{2}\frac{M_2}{a_2}\underline{A}_2'\right)\frac{d\underline{F}_2}{d\zeta} + \left(\frac{M_1}{N_1}\underline{I} + \frac{1}{2}\frac{M_1}{a_1}\underline{A}_2'\right)\frac{d\underline{F}_1}{d\zeta} =$$

$$-(\underline{I} - \tfrac{1}{2}\underline{A}_2')\underline{F}_2 + (\underline{I} - \tfrac{1}{2}\underline{A}_2')\underline{F}_1 \qquad \ldots\ldots (3\text{-}7)$$

and

$$-\left(\frac{M_2}{N_2}\underline{I} + \frac{1}{2}\frac{M_2}{a_2}\underline{A}_1'\right)\frac{d\underline{F}_2}{d\zeta} + \left(\frac{M_1}{N_1}\underline{I} + \frac{1}{2}\frac{M_1}{a_1}\underline{A}_1'\right)\frac{d\underline{F}_1}{d\zeta} =$$

$$(\underline{I} - \tfrac{1}{2}\underline{A}_1')\underline{F}_2 + (\underline{I} - \tfrac{1}{2}\underline{A}_1')\underline{F}_1 \qquad \ldots\ldots (3\text{-}8)$$

These may be written more simply as

$$\underline{G}_2\frac{d\underline{F}_2}{d\zeta} + \underline{G}_1\frac{d\underline{F}_1}{d\zeta} = -\underline{H}_2\underline{F}_2 + \underline{H}_2\underline{F}_1 \qquad \ldots\ldots (3\text{-}9)$$

and

$$\underline{G}_4\frac{d\underline{F}_2}{d\zeta} + \underline{G}_3\frac{d\underline{F}_1}{d\zeta} = \underline{H}_1\underline{F}_2 + \underline{H}_1\underline{F}_1 \qquad \ldots\ldots (3\text{-}10)$$

where

$$\underline{G}_1 = \frac{M_1}{N_1}\underline{I} + \frac{1}{2}\frac{M_1}{a_1}\underline{A}'_2 \qquad \ldots\ldots (3\text{-}11)$$

$$\underline{G}_2 = \frac{M_2}{N_2}\underline{I} + \frac{1}{2}\frac{M_2}{a_2}\underline{A}'_2 \qquad \ldots\ldots (3\text{-}12)$$

$$\underline{G}_3 = \frac{M_1}{N_1}\underline{I} + \frac{1}{2}\frac{M_1}{a_1}\underline{A}'_1 \qquad \ldots\ldots (3\text{-}13)$$

$$\underline{G}_4 = -\left[\frac{M_2}{N_2}\underline{I} + \frac{1}{2}\frac{M_2}{a_2}\underline{A}'_1\right] \qquad \ldots\ldots (3\text{-}14)$$

$$\underline{H}_1 = \underline{I} - \frac{1}{2}\underline{A}'_1 \qquad \ldots\ldots (3\text{-}15)$$

$$\underline{H}_2 = \underline{I} - \frac{1}{2}\underline{A}'_2 \qquad \ldots\ldots (3\text{-}16)$$

As before, by defining $\underline{F}$ to be the column matrix $\{\underline{F}_2, \underline{F}_1\}$, then equations (3-9) and (3-10) may be further simplified to

$$\underline{R}\,\frac{d\underline{F}}{d\zeta} = \underline{S}\,\underline{F} \qquad \ldots\ldots (3\text{-}17)$$

where $\underline{R}$ and $\underline{S}$ are the $(2n+2)\times(2n+2)$ matrices defined by

$$\underline{R} = \left[\begin{array}{c|c} \underline{G}_2 & \underline{G}_1 \\ \hline \underline{G}_4 & \underline{G}_3 \end{array}\right] \qquad \ldots\ldots (3\text{-}18)$$

and

$$\underline{S} = \begin{bmatrix} -\underline{H}_2 & \vdots & \underline{H}_2 \\ \cdots\cdots & \vdots & \cdots\cdots \\ \underline{H}_1 & \vdots & \underline{H}_1 \end{bmatrix} \qquad \ldots\ldots \text{(3-19)}$$

Pre-multiplying (3-17) by $\underline{R}^{-1}$ and re-arranging gives

$$\frac{d\underline{F}}{d\zeta} - \underline{R}^{-1}\,\underline{S}\,\underline{F} = 0 \qquad \ldots\ldots \text{(3-20)}$$

or, more concisely

$$\frac{d\underline{F}}{d\zeta} + \underline{P}'\underline{F} = 0 \qquad \ldots\ldots \text{(3-21)}$$

where

$$\underline{P}' = -\underline{R}^{-1}\,\underline{S} \qquad \ldots\ldots \text{(3-22)}$$

Equation (3-21) has the same form, and is equivalent to equation (2-24). However, the sub-matrices $\underline{G}_1$, $\underline{G}_2$, $\underline{G}_3$, $\underline{G}_4$, $\underline{H}_1$ and $\underline{H}_2$ which are used to define $\underline{P}'$ in (3-22), only require the simple matrix operations of addition, subtraction and scalar multiplication for their formulation. Matrix inversion is required just once to form $\underline{R}^{-1}$.

Application of the Simplified Analysis

The principal reason for using the re-arranged forms shown in equation (3-21) was a preventative one; that is, to limit

the possibility of error build-up in the matrix arithmetic required to form the matrix $\underline{P}'$. It was anticipated therefore, that the effect of the change would be marginal for examples which had previously given good results. Example 1 of Table 2 was such an example [74], and all temperatures computed using the simpler analysis agreed to five decimal places with those previously obtained.

The seven examples, referred to as numbers 2 to 8 in Table 2, were those for which the original programs had produced absurd and/or poorly balanced results. In five of the seven cases, the values of the dimensionless temperatures f_1 and f_2 computed by the original programs were outside the range -1.0 to +1.0 required by the heat-transfer laws. Example 2 in which f_1 and f_2 values ranged from -10^3 to 10^8 was the worst case found.

Table 2 compares the results obtained from the earlier study using the original matrix analysis, with those computed by a FORTRAN program incorporating the simplified matrix algebra.

The table shows that sensible output temperatures were obtained for examples 4 to 8 inclusive when the simplified analysis was used. It is also evident that the computed heat-balance discrepancies were significantly lowered in these examples.

The relatively high heat-balance values obtained for examples 7 and 8, even with the simplified analysis, is a

TABLE 2

COMPARISON OF HEAT-BALANCE DISCREPANCIES COMPUTED WITH THE ORIGINAL AND SIMPLIFIED MATRIX ANALYSES

Program Parameters:- n=5, m=3, e_1=0.002

Example Number	Regenerator Parameters					H.B.D.	
	N_1	N_2	M_1	M_2	Ω	Original Analysis	Simplified Analysis
1	1.363459	0.232786	0.514943	0.33658	0.4176	0.06%	0.13%
2	0.6	0.45	0.1	0.5	0.015	$0.2\times10^{4}\%^{+}$	N.P.$^{+}$
3	2.0	0.5	0.3	0.2	0.1	N.P.$^{+}$	-180%$^{+}$
4	0.9	2.0	0.1	0.11	0.1	222%$^{+}$	0.05%
5	0.6	0.3	0.7	0.7	0.1	223%	0.005%
6	0.6	0.3	0.4	0.4	0.1	232%	0.014%
7	10.0	0.1	0.6666667	0.25	3.0	24%$^{+}$	3.2%
8	10.0	0.1	0.6666667	0.25	6.0	9%$^{+}$	7.8%

Notes

1. Examples 2 to 8 were those for which absurd results were obtained in the original studies.
2. H.B.D. ≡ Heat-Balance Discrepancy.
3. N.P. ≡ Result not printed-out (value being too large for the specified field-width).
4. + Absurd results obtained. Values of f_i were outside the permitted range of $-1 \leq f_i \leq +1$.

consequence of the high Ω values used. This aspect is dealt with in the next section where it is shown how discrepancies in the heat balances for both these examples can be reduced to less than 1 per cent.

Disappointingly however, absurd results were again printed out for examples 2 and 3, despite the simplified algebra. This indicated that the reasons for such uncontrolled error growth lay elsewhere in the computational procedure. This in fact was confirmed by the work reported in Section 3.4. It is shown there, that sensible results were obtained for both examples by suitable modification to the third stage of the computation scheme.

3.3 ACCURACY OF THE NUMERICAL INTEGRATION IN THE TIME DOMAIN (Stage 1)

Apart from round-off errors, two other factors were identified in Section 3.1, as influencing the accuracy of this stage of the computational process. The first of these concerned the assumption, stated mathematically in equation (A2.1-10) that the functions X_1 and X_2 vary linearly with dimensionless time z', throughout each time step.

Reference to the integration procedure developed by Edwards et al, in Section A2.1 of Appendix 2, confirms that this assumption governs the particular formulae derived for the elements of $\underline{A}_1^!$ and $\underline{A}_2^!$. Consequently, the linear approximations stated in equations (A2.1-10) inevitably affect the accuracy of the numerical integrations in the time domain.

Therefore what we needed to assess was the extent to which these approximations affected the accuracy of the integration and thereby that of the overall computation.

The simplest approach to this, was to note that the accuracy of these linear approximations improves as h, the size of each time step, is made smaller and smaller. Since, in a given example, Ω is fixed and because $h = \frac{\Omega}{n}$, repeating a given computation with successively increasing values of n and noting the heat-balance values achieved, provided a fairly straight-forward way of carrying out the required assessment.

The effect of keeping n fixed and changing Ω was also considered, because this was the arrangement, (n=5), which prevailed in the original investigation. With a fixed value of n, the X_1 and X_2 approximations obviously lose accuracy as Ω increases, since h becomes larger and larger. For instance, when Ω increases from 0.5 to 5.0 the step size h increases from 0.1 to unity, the latter value being very large in the context of a quadrature computation. Recalling that, with the fixed n arrangement, the final heat-balance values had also increased with increasing Ω, it was reasonable to attribute this loss of overall accuracy to the diminished accuracy of the linear approximations for X_1 and X_2. This hypothesis was specifically tested by including examples covering a range of Ω values up to $\Omega = 6$.

Coming to the second factor affecting the accuracy of the first stage computations, Edwards et al had developed techniques

[37] , for ensuring that the sum of each of the required infinite series was calculated to a pre-selected accuracy. In fact, the fractional error in the calculated sum of each series was kept below a value e_1, where e_1 was set as a program input parameter.

In the earlier work, the value of e_1 was always set at 0.001 and the effect of changing the value of e_1, on the computed heat-balance discrepancy, was not investigated. As such it remained a possibility that even at the low level of 0.001, e_1 was still large enough to make a considerable contribution towards the overall heat-balance discrepancy. While this was thought to be unlikely, this contention clearly needed confirmation.

In the light of these considerations, an investigation was carried out to examine the effect, on the final heat-balance discrepancy, of variations in both the number of time intervals n, and also in the values of the parameter e_1.

Computed Results

The examples used in this investigation consisted of selected combinations of the following parameter values:- Ω = 0.1, 0.5, 1.0, 2.0, 3.0, 4.5 or 6.0; n = 5, 10, 15 or 20; and e_1 = 0.0005, 0.001, 0.002, 0.005 or 0.010. The other regenerator parameters were set equal to the values given for example 1, Table 2.

The influence of the parameter e_1 on the computed heat-balance discrepancy is shown graphically in FIG. 4. For each

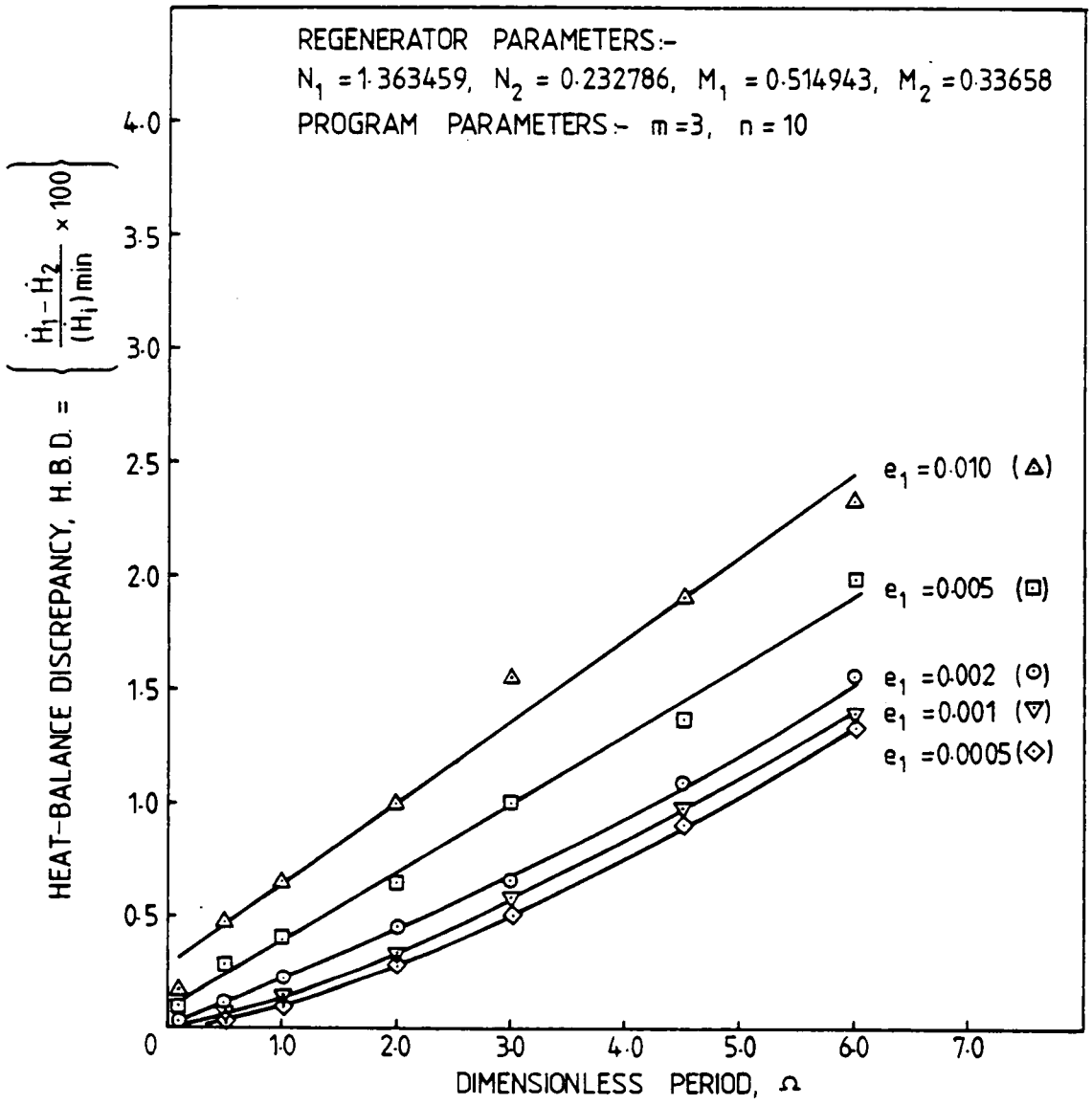

FIG. 4 EFFECT OF ERROR BOUND, e_1 ON HEAT-BALANCE DISCREPANCY

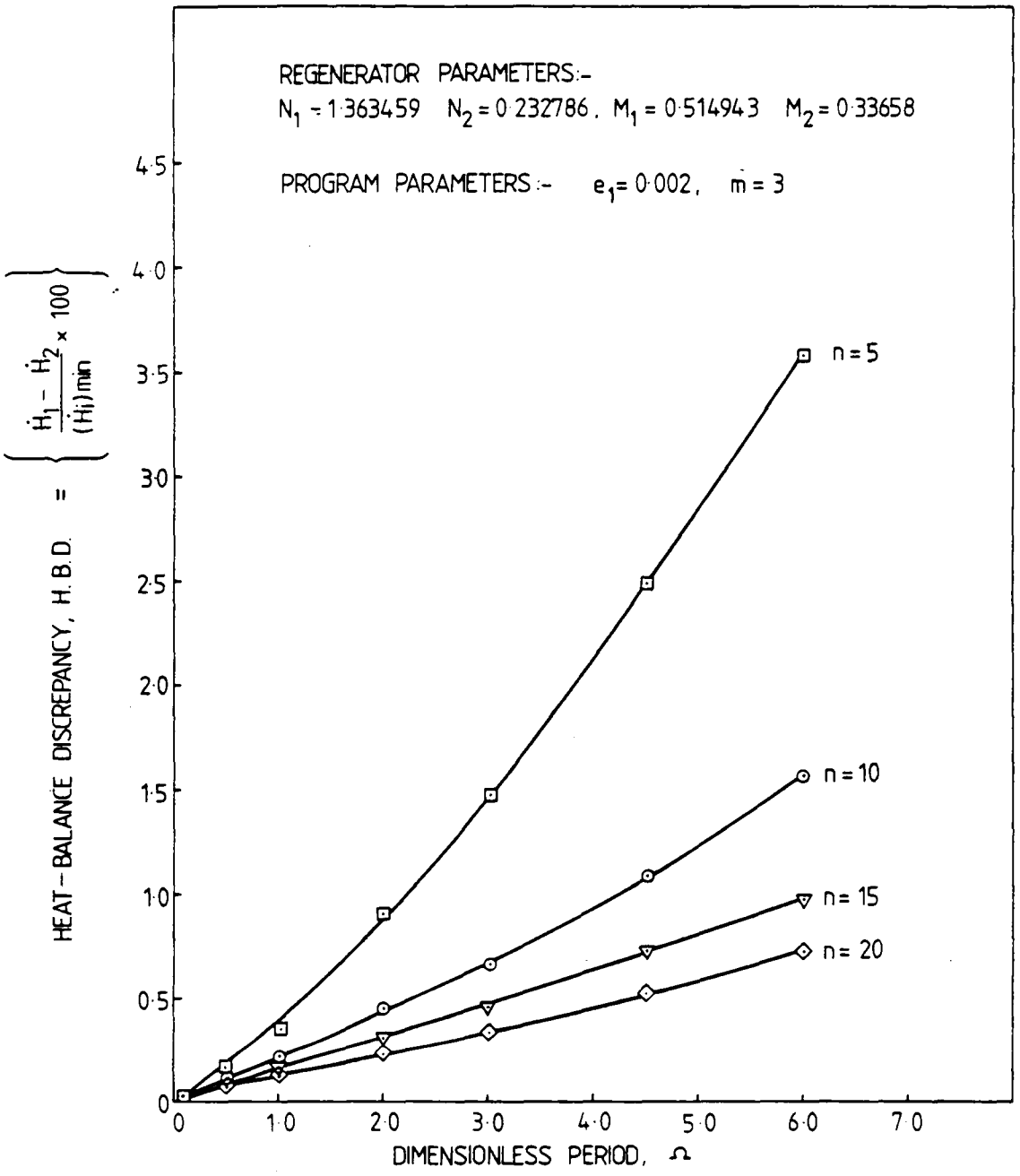

FIG. 5 EFFECT OF NUMBER OF TIME STEPS, n, ON HEAT-BALANCE DISCREPANCY.

plotted result (i.e. each example), n and m were fixed at 10 and 3, respectively.

Examination of these curves confirms that, at a given Ω, improving the accuracy of each series summation by decreasing e_1, results in correspondingly lower heat-balance discrepancies. However it is evident from the three lower curves, that the improvement in the overall heat balance obtained by decreasing e_1 below 0.002 is very slight. In practice this means that for Ω greater than about 4.0, it is not possible to achieve heat balances of less than one per cent by just decreasing the value of e_1.

Also, on the basis of these results, it is felt that $e_1 = 0.002$ is an appropriate setting for this parameter for normal computations.

The effect of varying n, on the computed heat-balance discrepancy is shown graphically in FIG. 5. All computations for this figure were carried out with $e_1 = 0.002$ and $m = 3$.

The previously observed trend, for the heat-balance discrepancies to increase as Ω increases, is still evident on all the curves on FIG. 5.

Of far greater consequence however, is the considerable decrease in the heat-balance discrepancies achieved by increasing the value of n. This improved accuracy was obtained for all values of Ω, but was most pronounced at the higher Ω values. Thus, with n = 15, the heat-balance

discrepancies computed for all Ω values up to $\Omega = 6$ were within the target range of 0 to 1%. Subsequent tests have verified that by adjusting n, we can ensure the results of the final heat-balance check lie within this target range for Ω values up to $\Omega = 10$, which is considered to be the maximum value of practical interest.

The results of FIG. 5 are therefore taken as confirmation of the above hypothesis, i.e. that the large heat-balance discrepancies previously reported for examples with large Ω values, were a direct consequence of the inadequacy of the approximations of (A2.1-10), when these were applied with a small number of time steps.

One final point of interest concerns examples 7 and 8 of Table 1. Computing these examples with n = 15 and n = 30, respectively, reduced the heat-balance discrepancies to below the target maximum of one per cent.

3.4 ACCURACY OF NUMERICAL INTEGRATION ALONG THE REGENERATOR (Stage 3)

3.4.1 Scope of the Investigation

We are concerned in this section with the errors that arise when the system of ordinary differential equations defined by the matrix equation (2-24) is solved by a numerical approximation method.

Before looking in detail at the numerical method of solution, it is useful to note that an analytic solution of the actual

differential equations can be obtained as long as the matrix $\underline{P}$, of equation (2-25), is constant along the regenerator length [77]. When this is the case, the analytic solutions are then given in terms of the eigenvalues and eigenvectors of $\underline{P}$. For these solutions to be of any practical value, however, these eigenvalues and eigenvectors would have to be calculated, and because this would also require the use of numerical techniques, there appeared to be no clear advantage over the method previously adopted. Nevertheless, the existence of this alternative computational approach was noted for possible use, if circumstances warranted it.

The approximation procedure for solving the system of equations (2-24) has been outlined in Section 2.2, and we restrict this discussion to methods of the type shown there, viz. single-step methods.

As far as errors are concerned, the important feature of such methods is that of 'discretization'. That is, we seek solutions not of the original differential equations at all points in the interval $-1 \leqslant \zeta \leqslant +1$, but of an equivalent set of coupled difference equations, at the discrete points $\zeta = rh_L$, $-m \leqslant r \leqslant m$.

Many methods (algorithms) exist for replacing a given system of differential equations by a corresponding set of difference equations [77, 78]. The analysis presented in Section 2.2 illustrates one method for replacing the differential equations (2-24) by a set of difference equations, (2-33).

Whatever the algorithm used to achieve this replacement, solutions are then computed for the resulting difference equations at equi-spaced points along the regenerator length.

We then assume that the solutions obtained from the difference equations are equal to the corresponding (exact) solutions of the differential equations. In general, however, this will not be true and there will be discrepancies between the difference equations solutions and the corresponding differential equations solutions. Within the context of this investigation these discrepancies will be called truncation errors. When referred to one step of the integration range, any such error is termed a local truncation error (L.T.E.) - a strict mathematical definition of these terms may be found in most standard texts [77, 78] .

The concept of stability, which relates to the way in which errors committed in a single step are propagated over subsequent steps is an important factor in this application. This is because the presence of instability in this section of the solution process could produce a catastrophic growth of errors, rendering the final solutions meaningless. Some form of instability could be a possible explanation therefore, for the absurd results obtained for examples 2 and 3 - see Table 2. Even so, this third set of tests concentrated initially on investigating ways of controlling the magnitude of truncation errors, with the aim of improving the numerical accuracy of the final solutions.

For a given system of differential equations, two factors affect the magnitude of truncation errors. These are firstly the algorithm used to 'convert' the differential equations into a corresponding set of coupled difference equations, and secondly h_L, the size of the distance step along the regenerator length. Both of these factors have been examined.

The opportunity was taken to compare three different algorithms. These were the Crank-Nicolson method, as specified in equation (2-31), and also the well-known methods of Euler and Runge-Kutta [78] .

Adopting the O(h) notation [78] , reference texts [78] show that the magnitudes of the local truncation errors associated with each of these algorithms are of $O(h_L^3)$, $O(h_L^2)$ and $O(h_L^5)$, respectively. For normal computations this means, that for a given (small) h_L, solutions calculated by the Crank-Nicolson method will be more accurate than those calculated by the Euler method, but less accurate than those obtained using the Runge-Kutta method.

In applying Euler's method to equation (2-24), each derivative contained in $\frac{dF}{d\zeta}$ in this equation, is approximated at a given value of ζ , by its corresponding first forward difference. This procedure leads to the coupled difference equations

$$\underline{F}_{r+1} = (\underline{I} - \frac{1}{m}\underline{P})\underline{F}_r \qquad \ldots\ldots (3\text{-}23)$$

The third of the methods studied was the version of the classical fourth-order Runge-Kutta scheme programmed in the subroutine RKGS of the IBM Scientific Subroutine Package [79].

The availability of this item of software was one of the reasons for including this method in these comparison tests. More powerful attractions, however, were the incorporation of techniques to control the magnitude of truncation errors to below a pre-set value ϵ_2, and also to compensate for accumulated round-off errors. The first of these functions was achieved by automatically adjusting the step size [79], whereas the second relied on the use of Gill's modifications [79] to the basic Runge-Kutta formulae. With the inclusion of these features, this method was clearly the most sophisticated of those used.

In all three cases, the corresponding set of difference equations were solved by the procedure described in Appendix 3.

3.4.2 Computed Results

The three examples used for these tests are examples 1, 2, and 3 of Table 2. Of these, only the first example had been computed successfully.

For the Euler and Crank-Nicolson tests these examples were, in most cases, computed with the regenerator length divided into successively smaller steps, corresponding to m values of 3, 6, 12, 24 and 48. The results obtained for each m value are presented in Tables 3 and 4 and also in FIGS. 6 and 7.

Dealing with example 1 first: Table 3 indicates that both methods produced well-balanced results for all values of m. The tabulated values of the mean fluid exit temperatures $\bar{f}_1(-1)$ and $\bar{f}_2(+1)$, for example 1, are plotted in FIG. 6 for easier comparison. These curves show that the mean temperatures computed by the Euler method, exhibit a definite convergence with increasing m. Corresponding results from the Crank-Nicolson method, however, showed only the slightest variation as m was changed, probably reflecting the smaller truncation errors of this method.

It was interesting here, to compare the most accurate results computed by each of these two methods, i.e. for m=48, with those computed by the Runge-Kutta method. A full comparison of the computed cold fluid exit temperatures is given in Table 4. It is clear that all of the values computed with the Crank-Nicolson algorithm agreed to five places of decimals, with the corresponding Runge-Kutta results. The Euler solutions were obviously less accurate, although we note that the cold period heat-transfer rate $\dot{H}_2$ was only about 0.1% higher than that from the other methods. So, as far as the heat-transfer rate predictions are concerned there is little to chose between the three methods.

It was for examples 2 and 3 however, that these tests provided the most interesting and useful results. For both these examples, we recall that all previous computations with the Crank-Nicolson formulae had produced absurd results.

It is immediately apparent from Table 3, however, that sensible and well-balanced results were obtained for example 2 both by the Euler method, for all values of m used, and also by the Crank-Nicolson method, for $m \geqslant 6$.

A similar success was obtained for example 3. The results for this example are also given in Table 3. These confirm that, as for example 2, by increasing the number of distance steps to 12 or greater (i.e. $m \geqslant 6$), the Crank-Nicolson method again yields sensible solutions with a very low heat-balance discrepancy.

Returning to the example 2 results, the $\bar{f}_1(-1)$ and $\bar{f}_2(+1)$ values computed from the Euler and Crank-Nicolson solutions are plotted in FIG. 7. The graphs of these mean temperatures show similar convergence patterns to those displayed on FIG. 6, for example 1. In this case, however, a comparison with the Runge-Kutta method is not possible, because the Runge-Kutta computation, on the IBM 1130 computer, had to be aborted, due to the excessive computation time.

3.5 DISCUSSION OF RESULTS

With the completion of this preliminary investigation, several of the objectives of this further development, as identified in Section 2.4 of Chapter 2, had been satisfactorily accomplished.

In programming terms, the development of a new high-level language program to meet the specifications laid down in

TABLE 3

EFFECT OF ALGORITHM AND STEP SIZE
ON THE COMPUTED SOLUTIONS OF EQUATIONS (2-24)

Program Parameters:- $n=5$, $e_1=0.001$

Example		1		2		3	
m	Method	E	C-N	E	C-N	E	C-N
3	H.B.D.%	0.051	0.069	0.046	*	N.A.	*
	$\bar{f}_1(-1)$	0.2437	0.2559	-0.9257	*	N.A.	*
	$\bar{f}_2(+1)$	0.1564	0.1376	-0.6147	*	N.A.	*
6	H.B.D.%	0.059	0.069	0.043	0.040	N.A.	0.064
	$\bar{f}_1(-1)$	0.2500	0.2560	-0.9498	-0.9722	N.A.	-0.1716
	$\bar{f}_2(+1)$	0.1468	0.1375	-0.6099	-0.6054	N.A.	0.7585
12	H.B.D.%	0.064	0.068	0.042	0.040	N.A.	0.052
	$\bar{f}_1(-1)$	0.2530	0.2560	-0.9609	-0.9714	N.A.	-0.1720
	$\bar{f}_2(+1)$	0.1421	0.1374	-0.6077	-0.6056	N.A.	0.7571
24	H.B.D.%	0.066	0.068	0.041	0.040	N.A.	0.041
	$\bar{f}_1(-1)$	0.2545	0.2560	-0.9661	-0.9711	N.A.	-0.1719
	$\bar{f}_2(+1)$	0.1397	0.1374	-0.6066	-0.6056	N.A.	0.7572
48	H.B.D.%	0.067	0.068	0.040	0.040	N.A.	0.032
	$\bar{f}_1(-1)$	0.2553	0.2560	-0.9686	-0.9711	N.A.	-0.1719
	$\bar{f}_2(+1)$	0.1386	0.1374	-0.6061	-0.6056	N.A.	0.7572

Notes (1) * means absurd results obtained.

(2) E ≡ Euler Method; C-N ≡ Crank-Nicolson Method.

(3) H.B.D. ≡ Heat-Balance Discrepancy.

(4) N.A. ≡ Computation not attempted.

TABLE 4

COMPARISON OF COLD FLUID EXIT TEMPERATURES COMPUTED BY DIFFERENT INTEGRATION METHODS

Regenerator Parameters:- Example 1 parameters used (see Table 2)

Program Parameters:- n=5; e_1=0.001

Method	m	Cold Fluid Temperatures at ζ = +1							Dimensionless Heat Transfer Rate $\dot{H}_2$
		Fraction of Period						Mean Value $\bar{f}_2(+1)$	
		0	0.2	0.4	0.6	0.8	1.0		
E	48	0.23802	0.16459	0.13902	0.12202	0.10850	0.09654	0.13857	0.38322
C-N	48	0.23645	0.16332	0.13786	0.12093	0.10747	0.09555	0.13741	0.38283
R-K	*	0.23645	0.16332	0.13786	0.12093	0.10747	0.09555	0.13741	0.38283

Notes 1. * indicates variable step size method with a local truncation error tolerance set equal to 1×10^{-7}.

2. E ≡ Euler method.

C-N ≡ Crank-Nicolson method.

R-K ≡ Runge-Kutta method.

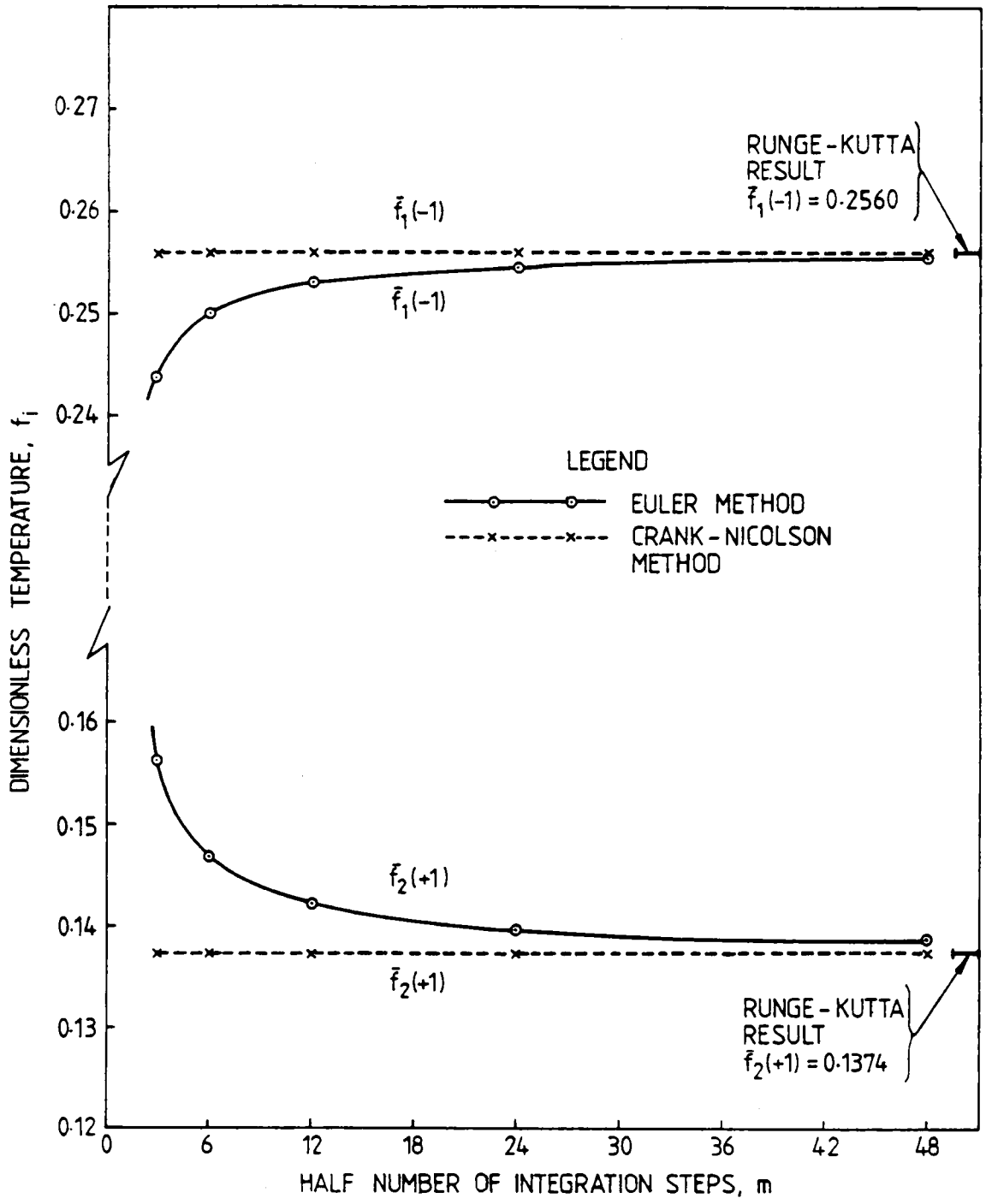

FIG. 6. EFFECT OF ALGORITHM AND NUMBER OF INTEGRATION STEPS ON THE TEMPERATURES COMPUTED FOR EXAMPLE 1.

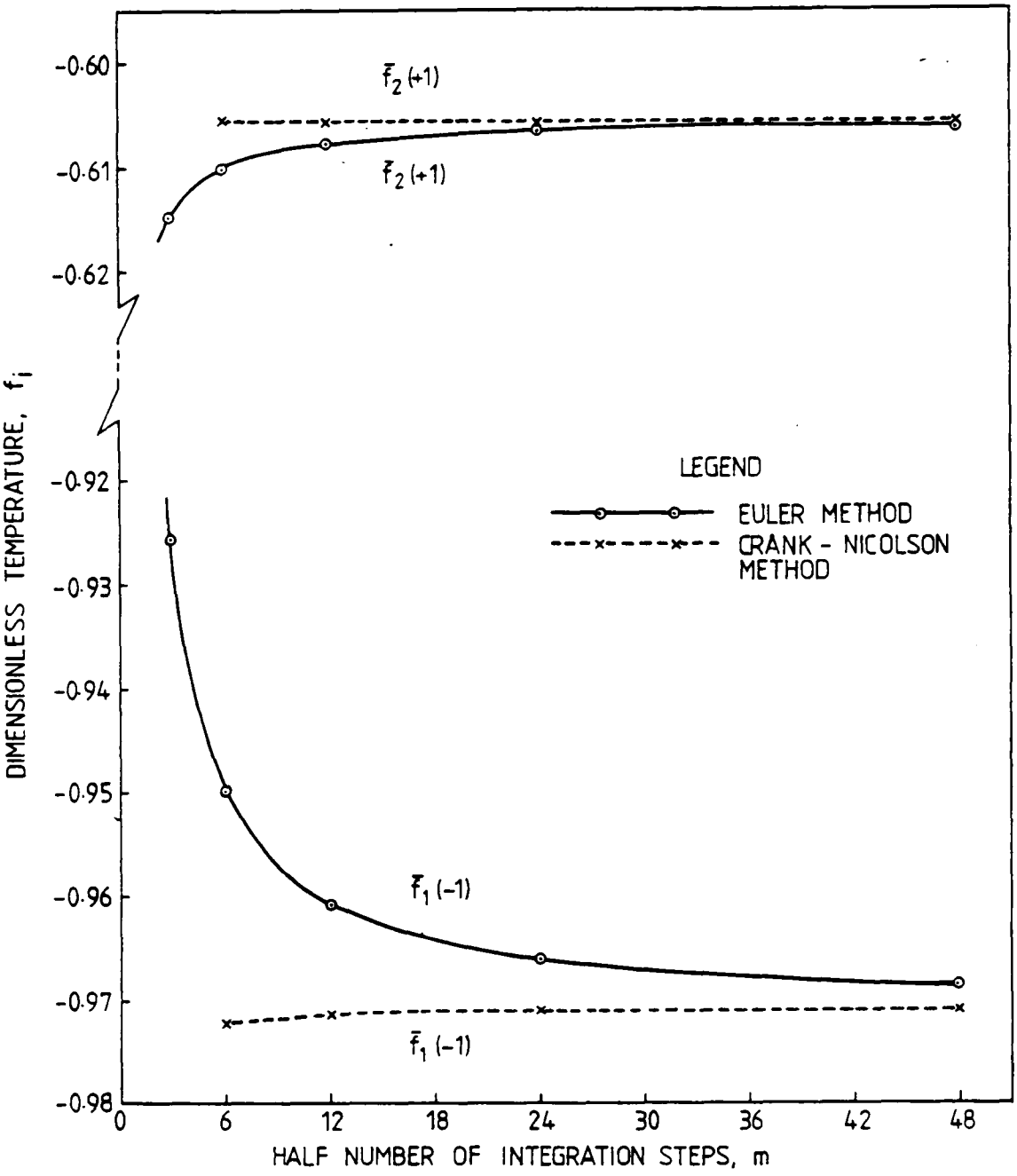

FIG. 7. EFFECT OF ALGORITHM AND NUMBER OF INTEGRATION STEPS ON THE TEMPERATURES COMPUTED FOR EXAMPLE 2.

Section 2.4 had been completed. The program was written to allow the number of steps in both the distance and time domains, and also the parameter e_1, to be pre-set by the user. A simplified matrix analysis was also included. A full description of the program is given in Chapter 6.

With this new program, the computational accuracy was greatly improved. In particular the ability to vary the parameters e_1, m and n, enabled the computed heat-balance discrepancy to be controlled, and more importantly, to be maintained within the target range of from 0% to 1%. This latter capability had been demonstrated for all examples tested but most convincingly so for those examples having Ω values ranging up to $\Omega = 6$.

The ability of the new program to improve computational accuracies was further demonstrated by the computation of technologically sensible solutions for all of the examples for which absurd, unrealistic results had been obtained previously.

In this way, two of the principal difficulties encountered in the original application of this method were resolved.

On the basis of the results obtained, the parameter values needed to ensure sensible results, and also to ensure that the final heat-balance discrepancy falls within the target range, were as follows:-

For $0.1 \leqslant \Omega \leqslant 2$, set $e_1 = 0.002$, m = 6 and n = 5

For $2 \leqslant \Omega \leqslant 4$, set $e_1 = 0.002$, m = 6 and n = 10

For $4 \leqslant \Omega \leqslant 6$, set $e_1 = 0.002$, m = 6 and n = 15.

The extent to which the values of these parameters would need to be adjusted to cater for different combinations of the other four regenerator parameters remained to be investigated.

As far as the choice of method for integration along the regenerator length was concerned, the tests reported in Section 3.4 had shown the Crank-Nicolson method to have clear advantages over the Runge-Kutta method in terms of simplicity of programming and also of shorter computation times. Since the accuracy of the Crank-Nicolson results, even at small values of m, were comparable with those from the Runge-Kutta program, it was decided to continue using the former method. While a case could be argued for the even simpler Euler method, the need to use a large value of m to attain the necessary computational accuracy was felt to be a feature best avoided.

One aspect of these results which was still not explained adequately was the cause of the absurd solutions computed for examples 2 and 3. However, this particular aspect is considered further in Chapter 9.

CHAPTER 4

PREDICTION OF THE CONVERGED HEAT-TRANSFER RATE, $\dot{H}^*$, AND THE REGENERATOR EFFECTIVENESS, η_R

4.1 CONVERGENCE AND NUMERICAL ACCURACY OF COMPUTED HEAT-TRANSFER RATES

We have seen in the preceding chapter that the numerical accuracy of the regenerator solutions computed by this non-iterative method can be simply and effectively controlled by setting the program parameters e_1, m and n to appropriate values at the commencement of a particular computation.

In stating this it has to be made clear, however, that up to this point, the accuracy of a given computation has been assessed solely by the final heat-balance calculation. In practice this has meant that a regenerator computation has been considered to be of a satisfactory numerical accuracy whenever the computed mean heat-transfer rates $\dot{H}_1$ and $\dot{H}_2$ differed by less than one per-cent.

As mentioned previously, close agreement between the computed values of $\dot{H}_1$ and $\dot{H}_2$ is an essential condition for accurate solutions to be obtained, because energy conservation is thereby ensured. However it was not immediately obvious that the computation of a heat-balance discrepancy of less than some selected tolerance would also guarantee the corresponding accuracy of the relevant $\dot{H}_1$ and $\dot{H}_2$ values. Even if, as seems likely, this is the case, certain important questions remained unanswered. These were:-

(a) In the heat-balance test, how small must the tolerance be to ensure that the corresponding heat-transfer rates are of an acceptable numerical accuracy?

(b) When such a test has been satisfied, is it valid to take the 'true' heat-transfer rate, $\dot{H}^*$, as the average of the 'closest' $\dot{H}_1$ and $\dot{H}_2$ results?

(c) What is the numerical accuracy of this, or any other, estimate?

To try to answer these questions, it was decided to examine the computed values of $\dot{H}_1$ and $\dot{H}_2$ in greater detail. In this context, it follows from the error analysis given in Chapter 3, that if all the calculations were performed with exact arithmetic, then as the number of steps are made infinitely large (i.e. m and $n \rightarrow \infty$) and as the series error bound e_1 is made infinitely small ($e_1 \rightarrow 0$), the principal numerical errors affecting the accuracy of the computed solutions will each tend to zero. In these 'ideal' circumstances, the computed values of $\dot{H}_1$ and $\dot{H}_2$ would converge to a common value, which is the required 'converged' or 'true' mean heat-transfer rate, $\dot{H}^*$.

It appeared relevant therefore to examine the extent to which this convergence happens in practice when e_1, m and n are varied in manners similar to those described above. In particular, a technique was sought for predicting the value of $\dot{H}^*$, and also its numerical accuracy, from the values of $\dot{H}_1$ and $\dot{H}_2$ computed with finite values of e_1, m and n.

An assessment of the extent to which a given sequence of computed solutions has converged to a 'true' solution is always required whenever numerical approximation techniques are applied to regenerator calculations.

Prior to the introduction of electronic digital computers, consideration of the effect of step sizes on the accuracy of results was severely limited by the considerable computational effort required. This point is well illustrated in Iliffe's paper [48] in which he records that times ranging from four to nine hours were needed to complete a regenerator computation by the closed method described in Chapter 1. The calculations were carried out using five-figure logarithms and a 20-inch slide rule. The total computation time was directly proportional to the number of steps taken along the regenerator, and as such, the convergence aspect was restricted to one example, with solutions being compared for just 4, 5, 7 and 9 steps.

Naturally, access to modern computers has eliminated the type of restriction faced by Iliffe and earlier workers. However, as far as the regenerator problem is concerned, this advantage has been off-set, to some extent by the fact that more recent workers have used the increased computing power to consider more realistic and therefore, more complex, regenerator models. Under certain conditions, e.g. with small step sizes, computation of predictions via such models can still lead to problems both with computing times and with the amount of memory needed to store intermediate results.

It is worth noting in this respect, that the study described in the next section, which was carried out on a DEC-20 computer, would not have been practicable on the smaller and older IBM 1130 machine used in the early parts of this investigation.

4.2 CONVERGENCE TESTS : ESTIMATION OF $\dot{H}^*$

It was evident from the heat-balance studies reported in Chapter 3, that for a given regenerator system and a fixed value of Ω , the computed heat-transfer rates $\dot{H}_1$ and $\dot{H}_2$ were principally affected by the pre-set value of n. Initially, therefore, a series of test computations were carried out, with e_1 and m fixed at 0.002 and 3 respectively, to examine the convergence of the $\dot{H}_1$ and $\dot{H}_2$ results as n was set successively to the values 5, 10, 15, 20, 25 and 30. The tests were arranged to cover the full range of dimensionless periods of practical interest, viz. $0 < \Omega \leqslant 10$. In all the computations, the other four regenerator parameters N_1, N_2, M_1 and M_2, were set equal to the values specified for example 1 in Table 2.

The values of $\dot{H}_1$ and $\dot{H}_2$ computed for $\Omega = 1$, 6 and 10 are presented graphically in FIG. 8. The curves on this figure clearly illustrate the general convergence of both $\dot{H}_1$ and $\dot{H}_2$ as n increases. Also, it is interesting to note that, for given values of Ω and n, the value of $\dot{H}_1$ always exceeds that of $\dot{H}_2$, so that each $\dot{H}_1$ versus n curve always lies above the corresponding $\dot{H}_2$ curve.

A technique often used in this type of numerical prediction to assess the extent to which solutions have converged, is to test the difference between the values of a selected parameter, which have been computed with successive step sizes. If the difference obtained exceeds a specified

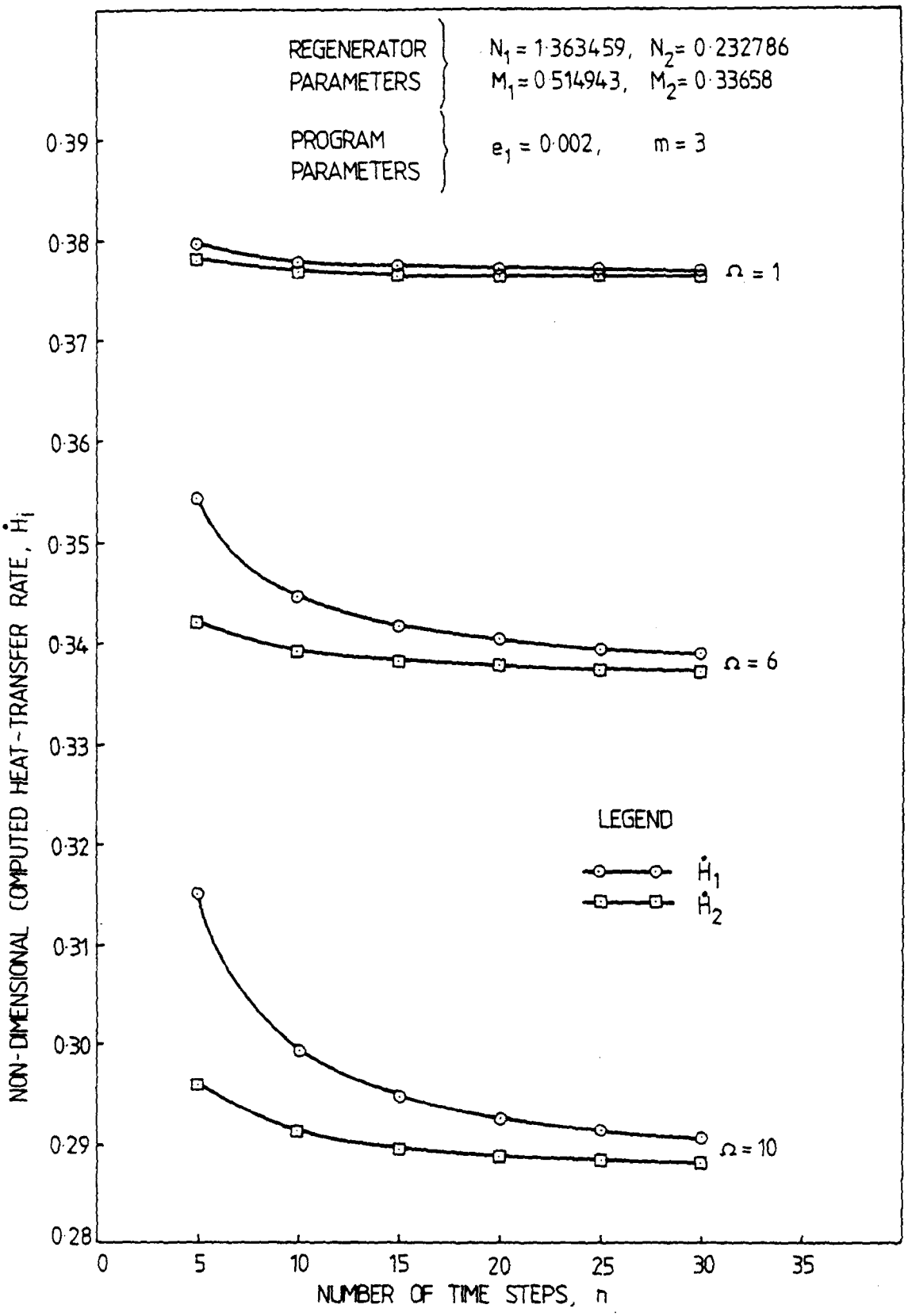

FIG. 8. VARIATION OF COMPUTED HEAT-TRANSFER RATE, $\dot{H}_i$ WITH NUMBER OF TIME STEPS, n

amount, step sizes are decreased repeatedly, until it is. When this difference test is satisfied, the 'latest' computed value is then taken as the 'converged' result. This was essentially the approach used by Carpenter [66] , who tested successive values of the computed mean fluid exit temperature.

Introducing the notation $\dot{H}_i^r$ to denote the mean heat-transfer rate computed using r time intervals, it can be confirmed that the values of $\dot{H}_2^{25}$ and $\dot{H}_2^{30}$, plotted on FIG.8, differ by less than 0.1%, (for each Ω). In this respect, it was tempting to take $\dot{H}_2^{30}$ as the converged value, $\dot{H}^*$. This approach was not adopted for two reasons. Firstly, it was felt that the method used to estimate $\dot{H}^*$ should take account of both the $\dot{H}_1$ and $\dot{H}_2$ results. Also, and more importantly, it was obvious from the curves on FIG.8, that the values of $\dot{H}_1$ and $\dot{H}_2$ were still decreasing, even at n=30. It was essential, therefore, to determine the extent to which these heat-transfer rates would continue to decrease with increasing n. Unfortunately, the curves of FIG.8 were of no use for this purpose.

As will be seen, a much more useful set of curves, from this point of view, was obtained when the $\dot{H}_1$ and $\dot{H}_2$ results were plotted against $\frac{1}{n}$. Examples of these plots are given in FIG.9, for a range of Ω values.

It is immediately evident that these curves give a far clearer picture of the convergence of the $\dot{H}_i$ values with increasing n, principally because of the exactly linear nature of these graphs.

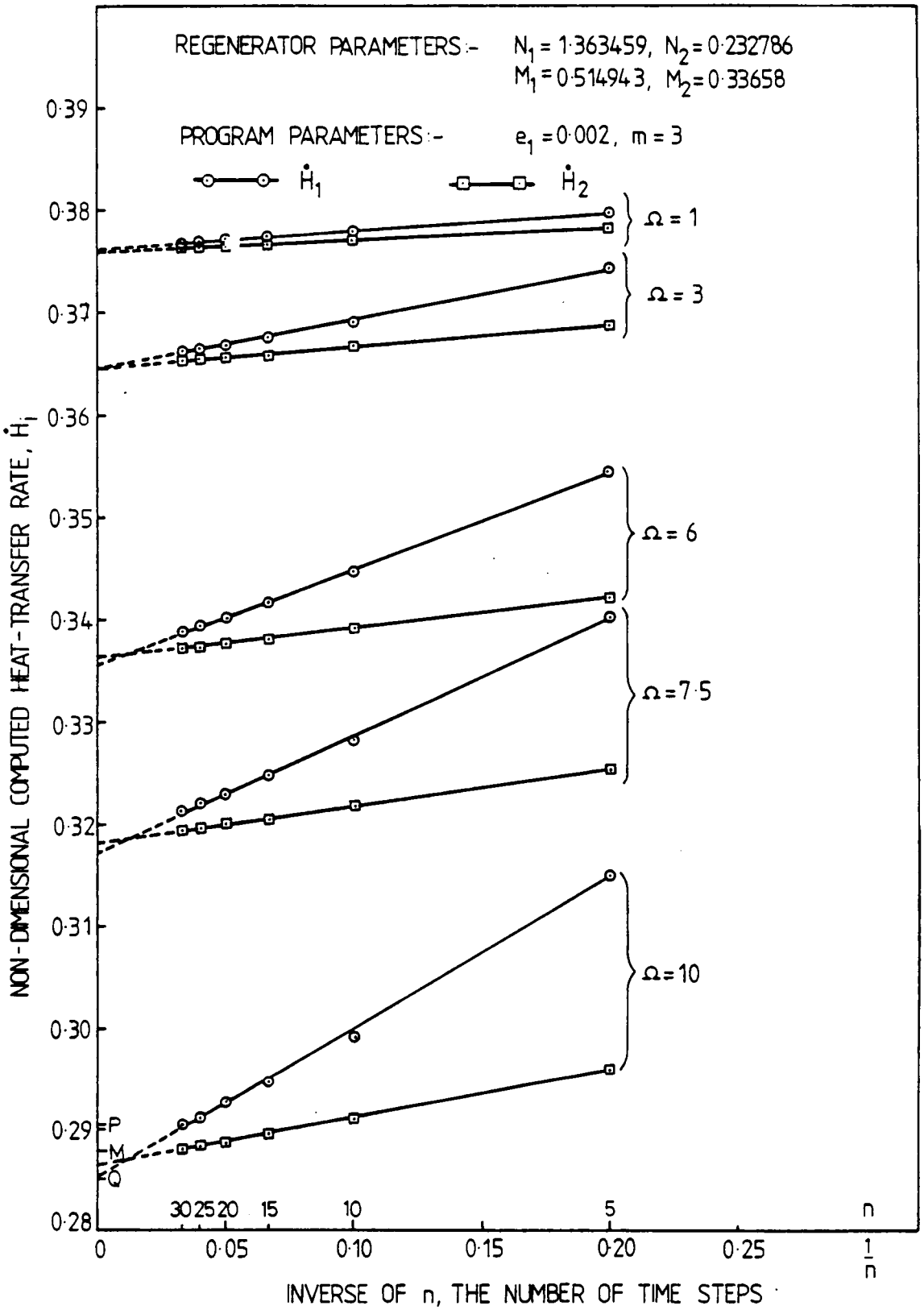

FIG. 9. CONVERGENCE OF COMPUTED VALUES OF $\dot{H}_i$ AS THE NUMBER OF TIME STEPS, n, INCREASES.

To examine the relationship between $\dot{H}_i$ and $\frac{1}{n}$ in more depth, a linear regression analysis was carried out for every set of $\dot{H}_1$ and $\dot{H}_2$ results (not all of which are shown in FIG.9).

For each set of data analysed, the regression program calculated the equation of the 'best' straight line through the data points, using the conventional least-squares method. The equation of each line was specified by the calculated values of its intercept on the $\dot{H}_i$ axis, denoted by $\dot{H}_i^{\infty}$ and by the slope of the line, denoted by $\bar{b}_i$. Each line of FIG.9 was then drawn from this information.

It will be seen from FIG.9, that the calculated values of $\dot{H}_1^{\infty}$ and $\dot{H}_2^{\infty}$ were always in fairly close agreement. However, the slope of each $\dot{H}_1$ line always exceeded that of the corresponding $\dot{H}_2$ line, the disparity between these slopes increasing as Ω increases. These have been consistent features of the results obtained from the 'equal-period' theory, both in these tests and in all later computations. In other words the convergence 'patterns' for $\dot{H}_i$ with increasing n have always been of the forms shown in FIG.9.

We also see, from the regression analysis, that each of the lines of FIG.9 has an equation of the form

$$\dot{H}_i = \dot{H}_i^{\infty} + \bar{b}_i\left(\frac{1}{n}\right) \qquad \ldots\ldots (4\text{-}1)$$

Moreover, if we consider a particular value of Ω and note that the time step $h = \frac{\Omega}{n}$, we may re-write equation (4-1) as

$$\dot{H}_i = \dot{H}_i^{\infty} + \frac{\bar{b}_i}{\Omega} . h \qquad \ldots\ldots (4-2)$$

which shows the computed values of $\dot{H}_i$ are linearly related to the time step h.

Two conclusions can be made concerning equation (4-2). Firstly, for each such line, the regression program calculated the correlation coefficient between $\dot{H}_i$ and $\frac{1}{n}$. In every case, the correlation coefficient exceeded 0.99, and as such the coefficients were extremely close to the theoretical maximum of unity. (A correlation coefficient of unity between two variables indicates that an exact linear relationship exists between them). For all practical purposes, therefore, the relationships given by equations (4-1) and (4-2) can be assumed to be exact for $n \leqslant 30$.

Secondly, we recall from the error analysis of Section 3.3, that the accuracy of the numerical integrations in the time domain, and hence in the predicted $\dot{H}_i$ values, are dependent upon the accuracy of equation (A2.1-10), which in turn depends upon the magnitude of the time-step, h. The type of relationship obtained in equation (4-2) is, therefore, entirely consistent with the numerical errors expected to arise from the use of equation (A2.1-10). When we couple this, with the high statistical significance of each regression line, then there seems little doubt that the

relationships given by equation (4-2) are a direct consequence of the use of equation (A2.1-10), and as such would apply for all values of n. It is on this basis that each line of FIG.9 has been extended to cover values of $\frac{1}{n}$ from 0.03 to zero, (indicated by the broken lines), to show the further convergence of the $\dot{H}_i$ results.

Theoretically, according to the 'ideal' computational scheme described above, each pair of $\dot{H}_1$ and $\dot{H}_2$ lines in FIG.9 should intersect at a common point on the $\dot{H}_i$ axis, which would then correspond to the converged value $\dot{H}^*$. In fact slightly different values of $\dot{H}_1^\infty$ and $\dot{H}_2^\infty$ were obtained in most of the examples tested, as can be seen from FIG.9. This is probably due to the use of finite values of e_1 and m, together with the effect of round-off and other small numerical errors.

To allow for these small deviations, and also to take both the $\dot{H}_1$ and $\dot{H}_2$ results into consideration, the converged heat-transfer rate $\dot{H}^*$, has been calculated from the following equation

$$\dot{H}^* = \frac{1}{2}\left[\dot{H}_{min}^\infty + \dot{H}_1^{30}\right] \qquad \ldots\ldots (4\text{-}3)$$

where $\dot{H}_{min}^\infty$ represents the smaller of the two values $\dot{H}_1^\infty$ and $\dot{H}_2^\infty$.

Referring to FIG.9, the value of $\dot{H}^*$ calculated for Ω =10, would therefore be at the point M, mid-way between the points P, $(\dot{H}_1^{30})$, and Q, $(\dot{H}_1^\infty)$, giving $\dot{H}^*$ = 0.2877. Thus it follows

that the maximum numerical error of this prediction, $\dot{EH}^* = \pm MP = \pm 0.0027$, which corresponds to a fractional error of $\pm 0.93\%$. More generally, $\dot{EH}^*$ is given by

$$\dot{EH}^* = \pm \frac{1}{2}\left[\dot{H}_1^{30} - \dot{H}_{min}^{\infty}\right] \qquad \ldots\ldots (4\text{-}4)$$

Although other formulae can be suggested for estimating $\dot{H}^*$, it is felt that the above scheme should provide a realistic prediction of $\dot{H}^*$, which reflects both the $\dot{H}_1$ and $\dot{H}_2$ results, and is also of an acceptable numerical accuracy.

Before applying equations (4-3) and (4-4), it was necessary to check the extent to which changes in e_1 and m affected the computed $\dot{H}_i$ values and thence also the value obtained for $\dot{H}^*$. This check was made by repeating the computations for $\Omega = 10$, but with e_1 reduced to 0.001 and m increased to 48 (ninety-six distance increments).

The $\dot{H}_1$ and $\dot{H}_2$ values computed with these new settings were virtually indistinguishable from the corresponding previous results, and could not be shown in FIG.9. The comparison is therefore summarised in Table 5, which compares both sets of regression results and also the predicted values of $\dot{H}^*$ and its fractional error.

It is quite clear from the entries in Table 5 that the influences of e_1 and m on $\dot{H}^*$ are extremely small, the changes in these parameters producing a decrease of only 0.07% in $\dot{H}^*$. The addition of 0.1% to the percentage error in $\dot{H}^*$ should thus be sufficient to cater for the effect of using the usual finite values of e_1 and m, viz. $e_1 = 0.002$ and m=3.

TABLE 5

INFLUENCE OF e_1 AND m ON THE ESTIMATED VALUE OF $\dot{H}^*$

Regenerator Parameters used:-

$\Omega=10$, $N_1=1.363459$, $N_2=0.232786$, $M_1=0.514943$, $M_2=0.33658$

m	e_1	Regression Results			$\dot{H}_1^{30}$	$\dot{H}^*$	Difference in $\dot{H}^*$ values	Maximum Fractional Error in $\dot{H}^*$ (%)
		i	Intercept $\dot{H}_i^{\infty}$	Gradient $\bar{b}_i$				
3	0.002	1	0.28500	0.14855	0.29036	0.28768		± 0.93
		2	0.28637	0.04795				
48	0.001	1	0.28483	0.14662	0.29013	0.28748	0.07%	± 0.92
		2	0.28650	0.04842				

The way was then clear to apply equation (4-3) in order to determine the values of $\dot{H}^*$ from the results obtained with these original settings. The values of $\dot{H}^*$ so obtained are plotted against Ω in FIG.10. This graph clearly illustrates the significant decrease in the predicted mean heat-transfer rate as the duration of the reversal period is increased.

Computation of the maximum numerical error $E\dot{H}^*$, for each $\dot{H}^*$ value, confirmed that $E\dot{H}^*$ increases as Ω increases, to attain a maximum fractional error of $\pm$ 0.93% at Ω=10. Including an additional 0.1% to account for the finite values used for e_1 and m, the results shown in FIG.10 have a maximum error of just over $\pm$ 1%.

4.3 CALCULATION OF REGENERATOR EFFECTIVENESS, η_R

Although the form of presentation given in FIG.10 is quite acceptable, most workers in this field, express the calculated performance of a regenerator in terms of what is variously called the 'regenerator effectiveness', 'regenerator efficiency', [36], or 'regenerator thermal ratio', [46]. In adopting this practice, we shall use the first of these terms.

The formula given by Edwards and Probert [7], when written in terms of the symbols used in this study, defines the regenerator effectiveness, η_R, as

$$\eta_R = \frac{W_1 S_1 P_1 \left[\bar{t}_1(\tfrac{1}{2}L) - \bar{t}_1(-\tfrac{1}{2}L)\right]}{(W_i S_i P_i)_{min}\left[\bar{t}_1(\tfrac{1}{2}L) - \bar{t}_2(-\tfrac{1}{2}L)\right]} = \frac{W_2 S_2 P_2\left[\bar{t}_2(\tfrac{1}{2}L) - \bar{t}_2(-\tfrac{1}{2}L)\right]}{(W_i S_i P_i)_{min}\left[\bar{t}_1(\tfrac{1}{2}L) - \bar{t}_2(-\tfrac{1}{2}L)\right]} \quad \ldots\ldots (4\text{-}5)$$

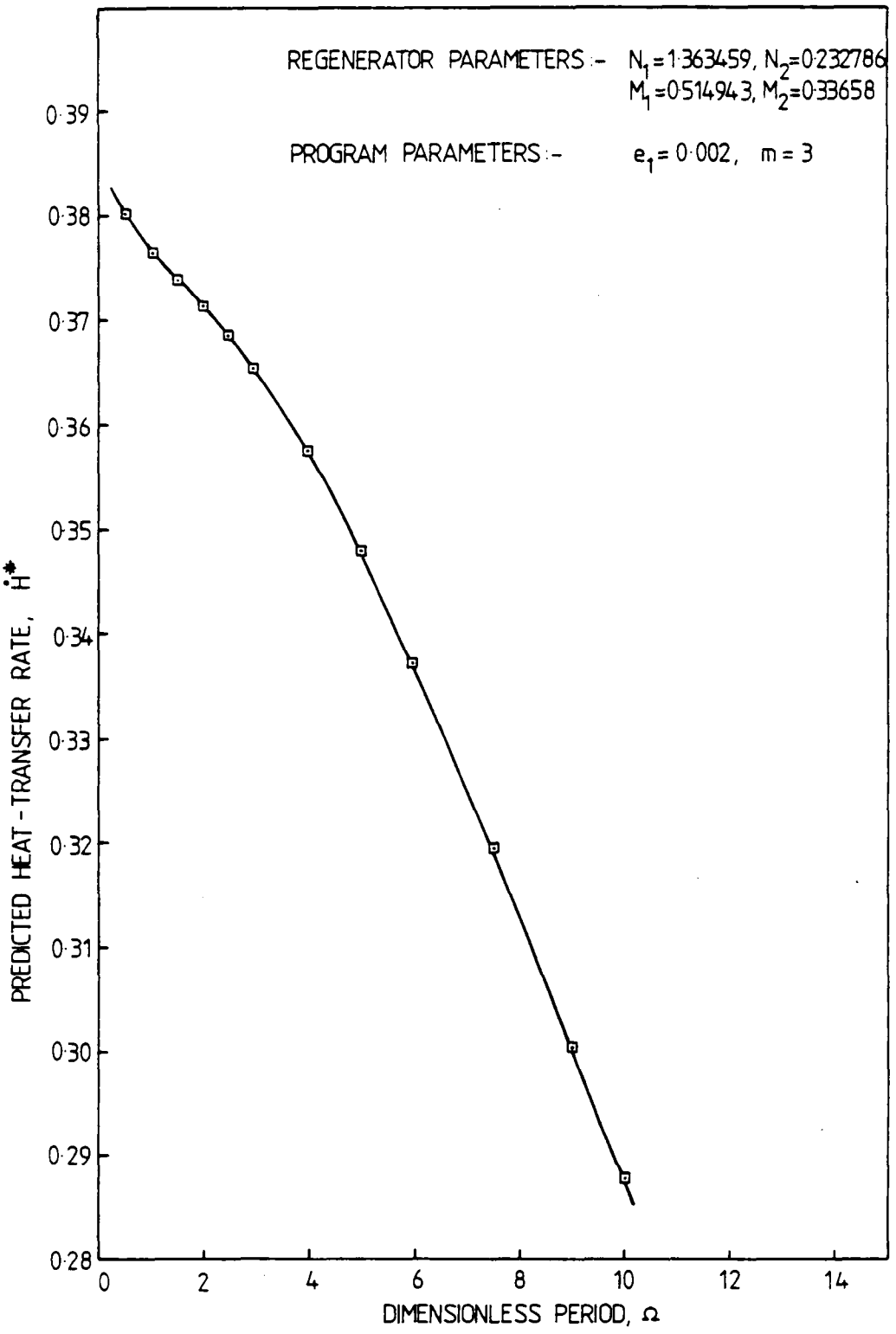

FIG. 10. VARIATION OF PREDICTED HEAT-TRANSFER RATE, $\dot{H}^*$, WITH DIMENSIONLESS PERIOD, Ω

where $(W_i S_i P_i)_{min}$ represents the smaller of $W_1 S_1 P_1$ and $W_2 S_2 P_2$.

The regenerator effectiveness is therefore the ratio of Q'_i, the actual quantity of heat transferred in a given period to Q'_{max} the theoretical maximum value of Q'_i. It follows that η_R varies in the range from zero to unity, this latter value representing the ideal case when $Q'_i = Q'_{max}$. An effectiveness of unity would occur, for example, if the mean temperature of the cold fluid leaving the regenerator was equal to that of the hot fluid entering the regenerator and $(W_i S_i P_i)_{min} = W_2 S_2 P_2$.

When the reversal periods are of equal duration, equation (4-5) simplifies to

$$\eta_R = \frac{W_1 S_1 \left[\bar{t}_1(\tfrac{1}{2}L) - \bar{t}_1(-\tfrac{1}{2}L)\right]}{(W_i S_i)_{min}\left[\bar{t}_1(\tfrac{1}{2}L) - \bar{t}_2(-\tfrac{1}{2}L)\right]} = \frac{W_2 S_2 \left[\bar{t}_2(\tfrac{1}{2}L) - \bar{t}_2(-\tfrac{1}{2}L)\right]}{(W_i S_i)_{min}\left[\bar{t}_1(\tfrac{1}{2}L) - \bar{t}_2(-\tfrac{1}{2}L)\right]} \quad \ldots\ldots (4\text{-}6)$$

where $(W_i S_i)_{min}$ is the smaller of $W_1 S_1$ and $W_2 S_2$.

Expressing this equation in terms of the dimensionless variables defined in equations (2-1) to (2-4), we obtain

$$\eta_R = \frac{M_1}{2(M_i)_{min}}\left[1 - \bar{f}_1(-1)\right] = \frac{M_2}{2(M_i)_{min}}\left[\bar{f}_2(+1) + 1\right] \quad \ldots\ldots (4\text{-}7)$$

where $(M_i)_{min}$ is the smaller of M_1 and M_2.

Using equations (2-45) and (2-46), we may then write

$$\eta_R = \frac{\dot{H}_1}{2(M_i)_{min}} = \frac{\dot{H}_2}{2(M_i)_{min}} \qquad \ldots\ldots (4\text{-}8)$$

Finally, using $\dot{H}_1 = \dot{H}_2 = \dot{H}^*$, we have

$$\eta_R = \frac{\dot{H}^*}{2(M_i)_{min}} \qquad \ldots\ldots (4\text{-}9)$$

Applying this latter equation, with $(M_i)_{min} = M_2$, and using the $\dot{H}^*$ results obtained for FIG.10, we obtain a corresponding set of η_R values. These are plotted against Ω in FIG.11, which illustrates the well-known tendency for the regenerator effectiveness to decrease for increased dimensionless periods.

The curve of FIG.11 is only applicable to the particular regenerator system defined by the parameters $N_1 = 1.363459$, $N_2 = 0.232786$, $M_1 = 0.514943$, $M_2 = 0.33658$. Quite different curves would be obtained for other systems; that is, for other values of N_i and M_i. This aspect is considered in Chapter 6.

Regarding the question of numerical accuracy, we note from equation (4-9) that η_R is a constant multiple of $\dot{H}^*$, and as such the fractional error in the computed value of η_R is equal to that for the corresponding value of $\dot{H}^*$. The values of η_R shown in FIG.11, therefore have the same maximum numerical error as the values of $\dot{H}^*$ contained in FIG.10, viz. just over $\pm$ 1%.

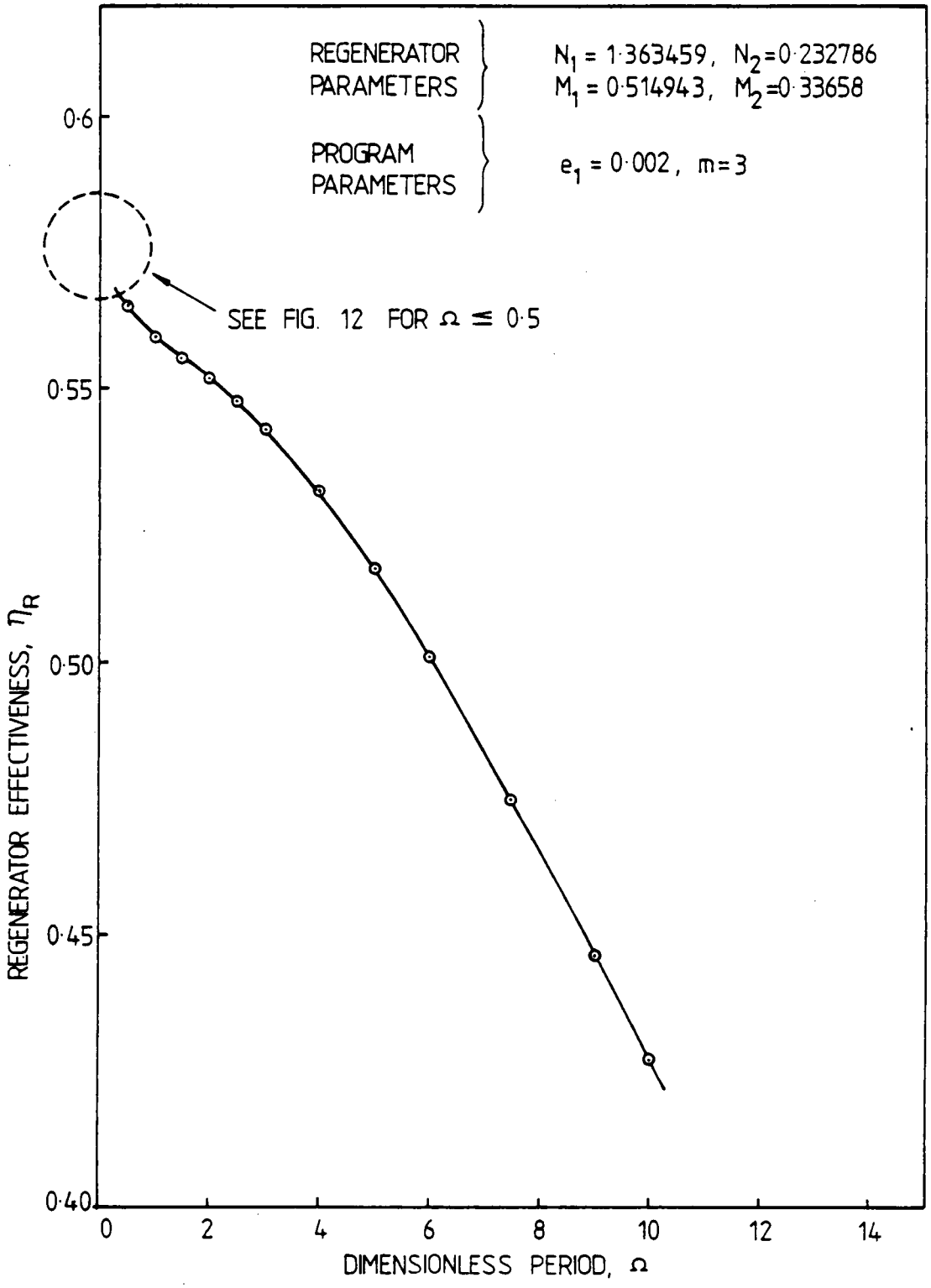

FIG. 11. VARIATION OF REGENERATOR EFFECTIVENESS, η_R, WITH DIMENSIONLESS PERIOD, Ω

One intriguing observation concerning the η_R versus Ω curve given on FIG.11, is the change in the concavity of the curve at about $\Omega = 1.0$. On first consideration such an inflexion did not seem to have any practical significance (or explanation). However, values of Ω of less than unity can occur in the practical operation of certain types of regenerator [61] and initially, for just this reason, some additional computations were carried out to establish the nature of the η_R curve at such low Ω values. However, it was then realised that the limiting case of infinitely-frequent reversal periods, (that is, reversal periods of infinitely-short duration) had been considered by Nusselt. He had in fact derived a completely analytic solution for the equations describing a regenerator operating in this mode [24] (see Chapter 1). As such, it was felt that the computation of the effectiveness values by Nusselt's theory and also by this non-iterative theory as Ω approached zero, would provide an interesting comparison of the two rival theories.

4.4 COMPARISON WITH NUSSELT'S ANALYTICAL SOLUTION FOR THE LIMITING CASE OF INFINITESIMALLY-SHORT REVERSAL PERIODS

The case of a regenerator operating with infinitesimally-short reversal periods was the first of the five regenerator problems considered by Nusselt and reported in his 1927 paper [24]. In this extreme case, the time coordinate is not involved as a variable, and the temperatures of the regenerator wall and fluids are functions of position along the regenerator length only.

The equations derived by Nusselt for the fluid temperatures and the quantity of heat exchanged in each period, for this particular problem, are given, using his original notation, in Appendix 4.

The regenerator effectiveness is given by equation (A4-10), which if re-written, in terms of the dimensionless variables N_1, N_2, M_1 and M_2, takes the form:-

$$\eta_R = \frac{1 - \exp\left[-u\right]}{\frac{M_2}{M_1} - \exp\left[-u\right]} \qquad \ldots\ldots (4\text{-}10)$$

where $$u = 2 \frac{\left[\frac{1}{M_1} - \frac{1}{M_2}\right]}{\left[\frac{1}{N_1} + \frac{1}{N_2}\right]} \qquad \ldots\ldots (4\text{-}11)$$

For the regenerator system being studied, we have $N_1 = 1.363459$, $N_2 = 0.232786$, $M_1 = 0.514943$ and $M_2 = 0.33658$. Substituting these values into equations (4-10) and (4-11) gives the value of the regenerator effectiveness as $\eta_R = 0.5935$.

This 'Nusselt' value is then plotted in FIG.12, which also contains for comparison purposes, the effectiveness values computed by the non-iterative theory for the same regenerator system, but for the following values of the dimensionless period:- Ω = 1.5, 1.0, 0.5, 0.25, 0.1, 0.05 and 0.02.

The convergence of the latter results to the Nusselt prediction is clearly depicted in FIG.12. The difference,

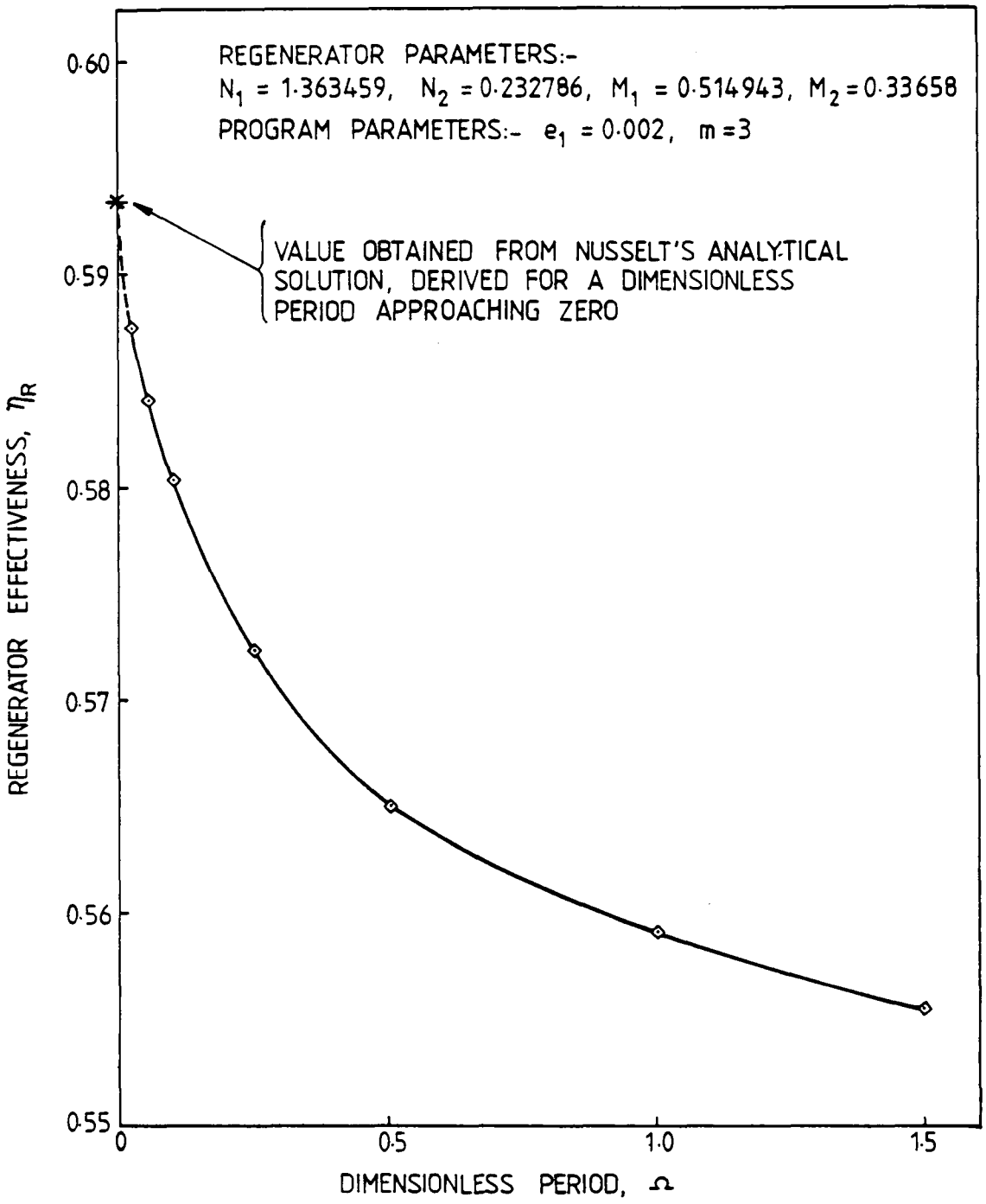

FIG. 12. CONVERGENCE OF COMPUTED REGENERATOR EFFECTIVENESS, η_R TOWARDS NUSSELT'S ANALYTICAL SOLUTION, AS $\Omega \to 0$

between the non-iterative result at $\Omega = 0.02$ and the Nusselt effectiveness, is just less than one per cent. This is a convincing demonstration of the agreement between the results obtained from the non-iterative theory (using several different numerical approximation techniques), and that calculated directly from a completely analytical solution.

The results plotted in FIG.12 also provide a clear confirmation of the suspected inflexion in the effectiveness curve of FIG.11, at low values of Ω. Subsequent computations, (see Chapter 6, FIGS. 14 and 15), indicate that this is a consistent feature for regenerators operating with equal heating and cooling periods. Additional, independent evidence for the rapid upturn in the effectiveness curve at low values of Ω is provided by one example computed by Heggs and Carpenter [67] using a completely numerical (i.e. 'open') method to solve the regenerator, 3-D model.

There is little doubt, therefore, that this change in the concavity of the effectiveness curve reflects a change in the heat-transfer mechanism which occurs within a regenerator, as the duration of the reversal periods is made smaller. The factor which alters is probably the extent to which heat is conducted into the solid walls of the regenerator. In this respect, it seems likely that the distance to which heat penetrates into the regenerator wall becomes successively smaller as the period time decreases, to affect only an infinitesimally-thin, superficial layer as the period time approaches zero.

This limiting case of infinitesimally-short periods is regarded by some research workers as being only of theoretical interest [25] . However, this view is not endorsed by Bayley et al [80] who point out, based on the study by Cox and Stevens [81],that this limiting theory may be used to predict the thermal performance of a rotary regenerator. Also, as previously mentioned, Fraas [4] , Coppage and London [26] and Lambertson[45] have all referred to the usefulness of the limiting theory for the design of rotary regenerators.

One final point concerns the results obtained by the non-iterative method for $\Omega = 0.02$, which was the smallest value of Ω tested. These results have proved to be somewhat exceptional in that the $\dot{H}_1$ and $\dot{H}_2$ values were not well correlated with the corresponding $\frac{1}{n}$ values, the correlation coefficients in this instance being 0.31 and 0.14. Because this was the only example found to have such low correlation coefficients, the particular reasons for these low values has not been pursued.

CHAPTER 5

RELATIONSHIP BETWEEN THE HEAT-BALANCE DISCREPANCY AND THE ERRORS IN THE COMPUTED MEAN HEAT-TRANSFER RATES, $\dot{H}_1$ AND $\dot{H}_2$

5.1 COMPARISON OF 'NEW' AND 'ORIGINAL' METHODS OF PREDICTING THE MEAN RATE OF HEAT TRANSFER IN A GIVEN REGENERATOR

Application of the techniques reported in Chapter 4, Section 4.2, has enabled the mean rate of heat transfer in a given regenerator to be predicted with far greater accuracy than was possible in the original 'trial' application of this non-iterative method [74]. These more recently developed techniques also enable the numerical error in the predicted heat-transfer rate to be estimated.

The ability to provide this latter information has overcome one of the major weaknesses in the computational procedure reported by Edwards et al [74], and as such, the non-iterative method can now be used for predicting regenerator performance with greater confidence.

It will be observed from Section 4.2, that the predicted mean rate of heat transfer, for any regenerator, is taken to be the value obtained for $\mathring{H}^*$, which is defined to be the mean rate of heat transfer that would be obtained in an ideal computation, free from all numerical errors.

The method developed for predicting $\dot{H}^*$, first requires several separate computer evaluations of the same regenerator example. In each of these evaluations, the regenerator parameters N_1, N_2, M_1, M_2 and Ω remain invariant, as do the program parameters, m and e_1. However each evaluation uses a different number of time steps n. The pairs of values of $\mathring{H}_1$ and $\mathring{H}_2$ obtained from each evaluation (i.e.

each n), are then used to establish the linear relationships between $\dot{H}_1$, $\dot{H}_2$ and $\frac{1}{n}$, of the form given in equation (4-1), and as depicted in FIG. 9.

During the studies reported in Section 4.2, six evaluations were undertaken for each regenerator example examined, although later tests have revealed that half this number of runs would usually be sufficient to determine the required relationships. Once these relationships are known, the predicted value of $\dot{H}^*$ and the maximum error in this estimate are then obtained using equations (4-3) and (4-4), respectively.

This improved procedure for calculating the overall performance of a regenerator, differs considerably from that originally used by Edwards et al [74]. Their technique simply predicted the mean rate of heat transfer for a given regenerator, as the average of the values of $\dot{H}_1$ and $\dot{H}_2$ obtained from a single computer evaluation using five time steps. However, as previously noted in this dissertation, the only method available for assessing the accuracy of such an estimate was by checking the extent to which the computed solutions were thermally balanced. A prediction obtained in this way was considered to be of reasonable accuracy only if the associated heat-balance discrepancy was less than one per cent, this somewhat arbitrary percentage being incorporated as a matter of judgement by the investigators concerned.

In applying this latter method of accuracy assessment, it was tacitly assumed that, in any computation having a heat-balance discrepancy of less than one per cent, the numerical errors in the heat transfer rates $\dot{H}_1$ and $\dot{H}_2$ would be suitably small. However, at that time (and during the early stages of this investigation) no method existed for checking this point: that is for checking whether the heat-balance discrepancy was explicitly related to the numerical errors in the computed values of $\dot{H}_1$ and $\dot{H}_2$.

An investigation of this issue only became a realistic possibility following the development of a technique for obtaining the 'true' mean rate of heat transfer, $\dot{H}^*$. Moreover, it appeared from FIG. 9, that the heat-balance discrepancy (which for any value of $\frac{1}{n}$ is approximately measured by the ordinate separation between a given pair of lines in FIG. 9), was almost certain to have a definite relationship with the accuracy of the corresponding heat-transfer rates. It was also evident that confirmation of this point would simply involve further analysis of the results depicted in FIG. 9. Thus, even though the heat-balance discrepancy was not involved explicitly in the improved prediction technique described earlier, the examination of a possible link between the heat-balance discrepancy and the corresponding heat-transfer errors was considered to be of sufficient interest retrospectively to merit the following brief study.

5.2 RELATIONSHIP BETWEEN THE HEAT-BALANCE DISCREPANCY AND THE ERRORS IN THE COMPUTED VALUES OF $\dot{H}_1$ AND $\dot{H}_2$

To provide the necessary quantitative data for the analysis, the terms $E\dot{H}_1$ and $E\dot{H}_2$ were defined by the following equation:-

$$E\dot{H}_i = \frac{(\dot{H}_i - \dot{H}^*)}{\dot{H}^*} \times 100 \ , \quad i = 1,2. \qquad \ldots\ldots \ (5\text{-}1)$$

It is clear from equation (5-1) that $E\dot{H}_1$ and $E\dot{H}_2$ are the percentage errors in the computed mean heat-transfer rates $\dot{H}_1$ and $\dot{H}_2$, relative to the 'true' rate of heat transfer $\dot{H}^*$. For convenience, the values of $E\dot{H}_i$, will be referred to as 'heat-transfer' errors.

To obtain the widest possible range of heat-transfer errors, this examination concentrated on those results for the three highest values of Ω shown in FIG. 9. Applying equations (5-1) and (2-50) to every pair of $\dot{H}_1$ and $\dot{H}_2$ values on each pair of lines depicted for Ω = 6, 7.5 and 10, a set of heat-transfer errors $E\dot{H}_i$, i = 1, 2 and corresponding heat-balance discrepancies were deduced. To increase the amount of data for analysis, the $\dot{H}_1$ and $\dot{H}_2$ results obtained from Ω = 9, but not shown in FIG. 9, were also treated in this way. The complete set of values of $E\dot{H}_i$ and the associated heat-balance discrepancies are plotted in FIG. 13.

Inspection of FIG. 13 confirms immediately that the heat-balance discrepancy is related linearly to the heating-period heat-transfer errors, $E\dot{H}_1$, (Line 1), and also to

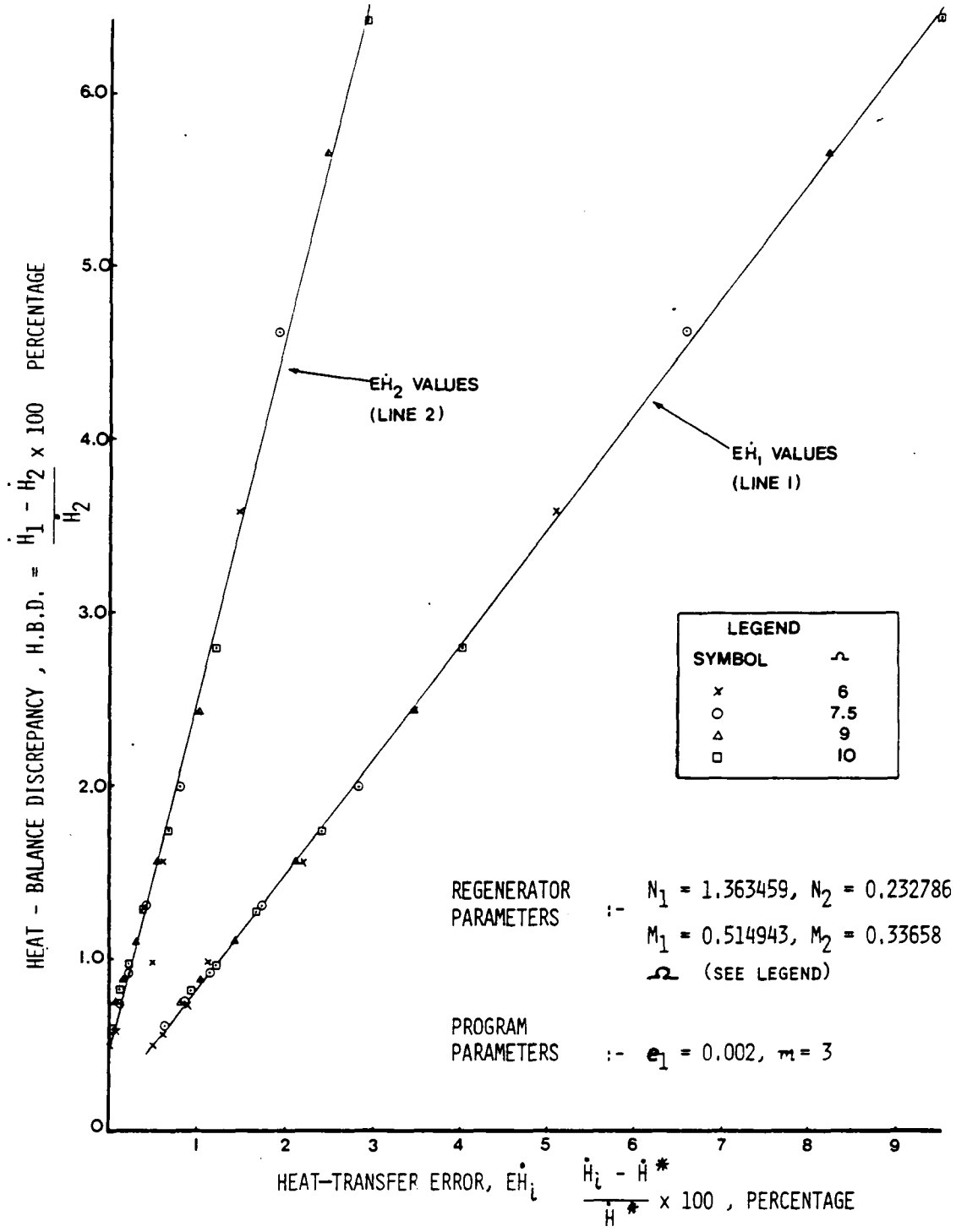

FIG 13 RELATIONSHIP BETWEEN HEAT-BALANCE DISCREPANCY, (H.B.D.) AND THE HEAT-TRANSFER ERRORS, $E\dot{H}_i$

those for the cooling period, $\dot{EH}_2$, (Line 2). However, the two relationships are clearly different.

While certain aspects of FIG. 13 were to some extent anticipated from the linear plots of FIG. 9, the fact that just two lines were needed to 'fit' the results from all four values of Ω, was totally unexpected.

Linear regression analyses carried out for the "Line 1" and "Line 2" results shown in FIG. 13, gave the best straight lines (using a least-squares approach) through each data set as:-

$$\underline{\text{Line 1}}, \quad (\text{H.B.D.}) = 0.663\ \dot{EH}_1 + 0.17 \quad \ldots\ldots \quad (5\text{-}2)$$

and

$$\underline{\text{Line 2}}, \quad (\text{H.B.D.}) = 2.08\ \dot{EH}_2 + 0.46 \quad \ldots\ldots \quad (5\text{-}3)$$

The calculated correlation coefficients between $\dot{EH}_i$ and the H.B.D. values for each of these lines were extremely high, being 0.999 and 0.996, respectively.

Because of these latter values, it was interesting to consider whether the relationships given in equations (5-2) and (5-3) could have been deduced from the equations for each of the lines in FIG. 9. Using certain reasonable approximations, the following mathematical analysis confirms that such a deduction is in fact possible.

We commence by recalling that the heat-transfer rates plotted as each pair of lines in FIG. 9 satisfy an equation of the form (given in equation (4-1)),

$$\dot{H}_1 = \dot{H}_1^{\infty} + \bar{b}_1\left(\frac{1}{n}\right) \qquad \ldots\ldots (5\text{-}4)$$

or

$$\dot{H}_2 = \dot{H}_2^{\infty} + \bar{b}_2\left(\frac{1}{n}\right) \qquad \ldots\ldots (5\text{-}5)$$

as appropriate.

If we use these equations to eliminate $\dot{H}_1$ and $\dot{H}_2$ from equations (2-50) and (5-1), then introduce the approximations $\dot{H}_1^{\infty} \simeq \dot{H}_2^{\infty} \simeq \dot{H}^{*}$ and $\frac{\bar{b}_2}{n} \simeq 0$, and finally combine the resulting equations, we obtain

$$(\text{H.B.D.}) \simeq \left(1 - \frac{\bar{b}_2}{\bar{b}_1}\right) E\dot{H}_1 \qquad \ldots\ldots (5\text{-}6)$$

and

$$(\text{H.B.D.}) \simeq \left(\frac{\bar{b}_1}{\bar{b}_2} - 1\right) E\dot{H}_2 \qquad \ldots\ldots (5\text{-}7)$$

corresponding to each pair of lines in FIG. 9.

Equations (5-6) and (5-7) clearly confirm the existence of two separate, almost linear relationships between the heat-balance discrepancy and the errors $E\dot{H}_1$ and $E\dot{H}_2$.

However, by examining the gradients of the lines on FIG. 9, we see that the values of $\bar{b}_1$ and $\bar{b}_2$ are quite different for each pair of lines. This implies that equations (5-6) and (5-7) should 'predict' two different linear relationships for each value of Ω. Nevertheless a check has shown that for the four values of Ω considered, the ratio of $\frac{\bar{b}_2}{\bar{b}_1}$ had the values 0.313, 0.310, 0.320 and 0.322.

Because of the small variation in these values it is reasonable to substitute their mean value of 0.317 into equations (5-6) and (5-7) to give

$$(H.B.D.) \simeq 0.68\ \dot{EH}_1 \qquad \ldots\ldots\ (5\text{-}8)$$

and

$$(H.B.D.) \simeq 2.16\ \dot{EH}_2 \qquad \ldots\ldots\ (5\text{-}9)$$

These latter equations are then applicable to the error data obtained from all four Ω values, and as such predict the two lines observed on FIG. 13. Furthermore, comparison of equations (5-8) and (5-9) with equations (5-2) and (5-3) shows these predicted equations to be in good agreement with the actual regression equations. Both of the investigations described above have convincingly demonstrated that the heat-balance discrepancy not only checks the thermal balance of a given computation, but also gives an indication of the numerical errors in the computed heat-transfer rates. However, the magnitude of these errors can only be found from the heat-balance discrepancy, by first obtaining relationships such as those in equations (5-2) and (5-3).

While in practice this would not be a practicable approach, it is interesting to note from FIG. 13, that whenever the H.B.D. was less than one per cent neither of the corresponding errors $\dot{EH}_1$ and $\dot{EH}_2$ exceeded 1.25%. This indicates that, for the regenerator systems to which FIG. 13 applies, the numerical error in the mean heat-

transfer rate predicted by the 'original' method referred to earlier, was less than one per cent. Hence, for these cases the original procedure would predict results of an acceptable accuracy.

Another deduction from FIG. 13 is that the value of $\dot{H}_2$ is a more accurate estimate of the 'true' heat-transfer rate, than the average of $\dot{H}_1$ and $\dot{H}_2$.

The particular relationships obtained in equations (5-2) and (5-3) are, of course, only applicable to those regenerator systems defined by the regenerator parameters quoted on FIG. 13. However, it will be seen in Chapter 6, that similar convergence graphs to those of FIG. 9 have been obtained from several hundred examples, covering a wide range of regenerator parameters. It is highly likely, therefore, that relationships of the same form as those of equations (5-2) and (5-3) exist for each different regenerator system, but there seemed little practical purpose in extending this investigation to examine different regenerator systems.

In concluding this particular aspect, it is perhaps worth recalling that, for any computation, the 'final' heat-transfer errors are an accumulation of errors propagated from three principal sources. These are, firstly, errors arising from the use of equation (A2.1-10) in the process for numerical integration in the time domain; secondly, the residual errors affecting the sum

of each infinite series required by the method; and thirdly, errors arising in the solution of the final set of differential equations (2-24).

For the examples considered in the preceding analysis, the heat-transfer errors were due almost entirely to errors from the first of these sources.

The question of whether the heat-transfer errors and the heat-balance discrepancies are also related when these 'final' errors originate from just the second or third sources, was given some consideration. However, this was not examined in depth, principally because the 'final' errors from both of these sources, were much smaller than those displayed in FIG. 13. There was, therefore, little of practical value to be gained by pursuing these particular aspects still further.

As we have seen, in terms of practical application, the relationships established in this brief study are not of any direct benefit to the present investigation. However their derivation has served to resolve a dilemma of long-standing interest, as well as providing a much better insight into the assessment of the accuracy of the solutions obtained using this non-iterative method of computation.

CHAPTER 6

PROGRAM 1 : DEVELOPMENT; ASSESSMENT; OPERATION

6.1 DEVELOPMENTS LEADING TO PROGRAM 1

The entire investigative effort reported so far, has concentrated on the further development of the theory derived for regenerators operating with heating and cooling periods of equal duration. All of the studies have fallen into two broad categories viz. mathematical and programming.

The mathematical investigations, whose specific aims were to eliminate the various weaknesses and difficulties which had affected the numerical accuracy of solutions obtained in the original Edwards et al research [74], have led to the successful development of techniques. These ensure that the solutions for a given regenerator example are thermally well-balanced, i.e. that the heat-balance discrepancy has a suitably small value. They also provide a means for the prediction of the regenenerator effectiveness η_R, together with an estimate of the maximum numerical error of the predicted value.

As a result of these developments, the first three objectives of this research, as listed in Section 2.4 of Chapter 2, have been successfully accomplished.

Fulfilment of another of the specified objectives, required an extensive redevelopment and updating of the original computer programs. In order to maximise its usefulness for design or optimisation studies, the requirement was for a single program, written in a commonly used high-level language, and suitable for use on modern digital computers.

The development of such a program, in FORTRAN (one of the standard computer languages for scientific computations), proceeded in parallel with, and as an integral part of, the above mentioned accuracy investigations. In this way, the final version of the program, which for reference purposes is called Program 1, has therefore incorporated all of the improved techniques, for controlling computational accuracy, that have been described in the preceding chapters.

As previously noted, a particular feature of the re-designed program is the facility for allowing the number of time and distance steps, and also the infinite series error bound e_1, to be changed from one computation to another, simply by altering the input data to the program. More comprehensive details of this, and other features of Program 1, are reported in Appendix 5 and also in Section 6.3 below.

With the completion of the scheduled programming and mathematical developments, it remained to assess the capabilities of Program 1 for predicting regenerator performance over a wide range of regenerator parameters.

In this context, it has probably been appreciated that most of the preceding investigations have been conducted with reference to Example 1 of Table 2. Consequently, the results obtained are, strictly speaking, relevant only for regenerator systems whose five dimensionless parameters Ω, N_1, N_2, M_1 and M_2 are identical to those of Example 1.

In the sense that the parameters defining Example 1 were calculated for an actual industrial regenerator of the type used in high-temperature smelting processes, and are therefore typical of such regenerators, this investigative approach is perfectly justified. The fact that most of the tests have involved the use of Ω values spanning the whole range of practical interest, provides further justification. Even so, before concluding the investigations relating to the 'equal-period' theory, it was considered essential to make a wider assessment of Program 1, and of the procedures developed for predicting overall regenerator performance. Such an assessment would require that all five dimensionless parameters be varied to cover the ranges of interest to the practical designer.

6.2 APPLICATION AND ASSESSMENT OF PROGRAM 1

6.2.1 Method of Assessment

For the non-iterative theory, when the heating and cooling periods are of equal duration, five dimensionless parameters are needed to define the thermal performance of any regenerator system. In principle therefore, this additional assessment was seen to require a repetition of the type of analyses described in Sections 4-2 and 4-3 of Chapter 4, so as to predict $\dot{H}^*$, η_R and their numerical accuracies, for a wide range of regenerator parameters. An ideal outcome of such an exercise would be the preparation of a set of design curves (or tables) covering all regenerators of likely practical interest.

In terms of practical implementation, however, even when each parameter varies through quite small ranges, the number of different combinations of the five parameters (i.e. examples) needed to prepare a comprehensive set of such curves, would be excessively large. Despite the relatively small times needed to compute each individual example (see Section 6.3, Table 10), the total computation time required for such an exercise would be impracticably large.

This particular difficulty is familiar to many investigators in the field of regenerator computation, who have needed to demonstrate the capabilities of, or the results from, a particular mathematical or computational solution process.

One approach, which virtually circumvents the problem of computational effort, is simply to restrict the demonstration to one specific example. This was the technique adopted by Manrique and Cardenas [61] , and more recently by Khandwawala and Chawla [62] . Both pairs of authors have reported solutions of the full three-dimensional, regenerator model using 'open', i.e. finite-difference procedures. In each case, particular solution techniques were demonstrated by computing detailed thermal histories of both fluids and the matrix filling for a selected 'typical' regenerator. Because of this restriction, the results reported in these cases, are of little direct use for general design purposes. However, as well as demonstrating the solution methods they also give a useful indication of the type of detailed

temperature histories which would be needed for the later stages of a design study.

For the earlier stages of a design study, a much broader picture of regenerator performance is usually required, and a number of investigators have produced design curves or tables, summarising overall regenerator performance, for a wide range of parameters.

The particular techniques applied by individual investigators have been reviewed in Chapter 1, where it was noted that almost all investigations were confined to the simpler 2-D model and also to the special case of 'balanced'[+] or 'thermally symmetrical' regenerators.

For the three-dimensional model given in Appendix 1, the condition of thermal symmetry corresponds to the case in which the dimensionless parameters which characterise the heating and cooling periods are equal in value. For the non-iterative theory, this implies $N_1=N_2$, $M_1=M_2$ and $\Omega_1=\Omega_2$. It follows that just three parameters (N,M,Ω) are needed to describe any balanced regenerator, as opposed to the five needed for an unbalanced regenerator having equal reversal periods (i.e. $N_1\neq N_2$, $M_1\neq M_2$). Considering only balanced systems obviously leads to a significant diminution in the overall computational effort needed to produce a set of design curves. As previously noted, however, this approach

---

+ Some authors define these terms differently (see Shah [82]).

only provides a partial solution to the design problem, for the simple reason that in practice, regenerator systems are not of the 'balanced' type.

For the simpler two-dimensional regenerator theory, Hausen's [30] recommendation that the performance of unbalanced regenerators be determined by applying the 'balanced' performance curves, but with the harmonic mean values of the unbalanced dimensionless parameters Λ and Π (see Symbols list), has been validated by Iliffe [48] . However, for the more general three-dimensional model, no results have been obtained to determine whether the application of harmonic or arithmetic means to the performance curves obtained for 'balanced' regenerators (both have been suggested [36, 67]), would give a useful estimate of the performance of the unbalanced system.

Taking the above points into consideration, it did not seem appropriate to limit any assessment of Program 1 to the computation of thermally-symmetrical regenerators. An assessment scheme was therefore devised to examine, as far as was practicable, the effect on the predicted regenerator effectiveness, of changes in all five dimensionless parameters N_1, N_2, M_1, M_2 and Ω . These computations, together with certain supplementary examples, are reported next.

6.2.2 Assessment of Results from Program 1

(a) Regenerator Parameters Covering Ranges of Practical Interest

Values of $\dot{H}^*$ and the corresponding regenerator effectiveness η_R, have been determined for selected combinations of the five parameters N_1, N_2, M_1, M_2 and Ω , when these parameters were varied in the following ranges:- $0.15 \leqslant N_1 \leqslant 1.5$; $0.15 \leqslant N_2 \leqslant 0.3$; $0.3 \leqslant M_1 \leqslant 0.6$; $M_2 = 0.3$; $0 < \Omega \leqslant 10$. As far as the author is aware, the values considered for each parameter, are representative of those which occur in high-temperature industrial regenerators, which operate with equal reversal periods. A computation with a selected combination of these parameters is called an 'example'.

In terms of procedure, we recall that the convergence graphs of $\dot{H}_i$ versus $\frac{1}{n}$ which were used to determine $\dot{H}^*$, were established using six different values of n. However in these latest tests, the required convergence graphs were based on the results from just three values of n viz. 5, 10 and 30. Apart from this one slight variation, the procedures used to predict $\dot{H}^*$ and η_R were exactly as previously described.

The particular examples used for these assessment tests were drawn up using the parameter values tabulated in FIGS. 14 and 15, the regenerator effectiveness values predicted for each example being plotted as a series of curves in these figures.

The form of presentation used in FIGS. 14 and 15 shows, for the range of examples studied, the variations in the predicted effectiveness η_R, brought about by changes in individual regenerator parameters.

To explain the layout of these results, we first note that all the curves of FIG.14 were obtained with $M_1=M_2=0.3$, whereas those of FIG.15 were obtained with $M_1=0.6$ and $M_2=0.3$.

Next we observe that each figure contains two corresponding sets of curves. For both lower sets of curves (A_2 to E_2), in addition to M_1 and M_2 being fixed, N_2 is also fixed at 0.15, whereas for the upper sets of curves (A_1-E_1), M_1, M_2 and N_2 are again fixed, but with the latter at the higher value of 0.3.

Finally, on each figure, the individual curves within each set (A to E), correspond to five different values of N_1 determined by the ratios $\frac{N_1}{N_2}$ = 5,3,2,1.5 and 1, respectively.

The effect of the individual parameters on the overall regenerator performance can now be explained as follows.

Firstly, we observe that moving from left to right along any curve of FIG.14 or FIG.15 again exhibits the decrease in regenerator effectiveness brought about by increasing just the dimensionless period Ω. For a given regenerator, this corresponds to increasing the duration of each reversal period. Examination of the entire set of curves indicates that such changes in η_R are greatest when N_1 and N_2 are largest and $\frac{M_1}{M_2}$ = 2; that is for curve A_1 of FIG.15.

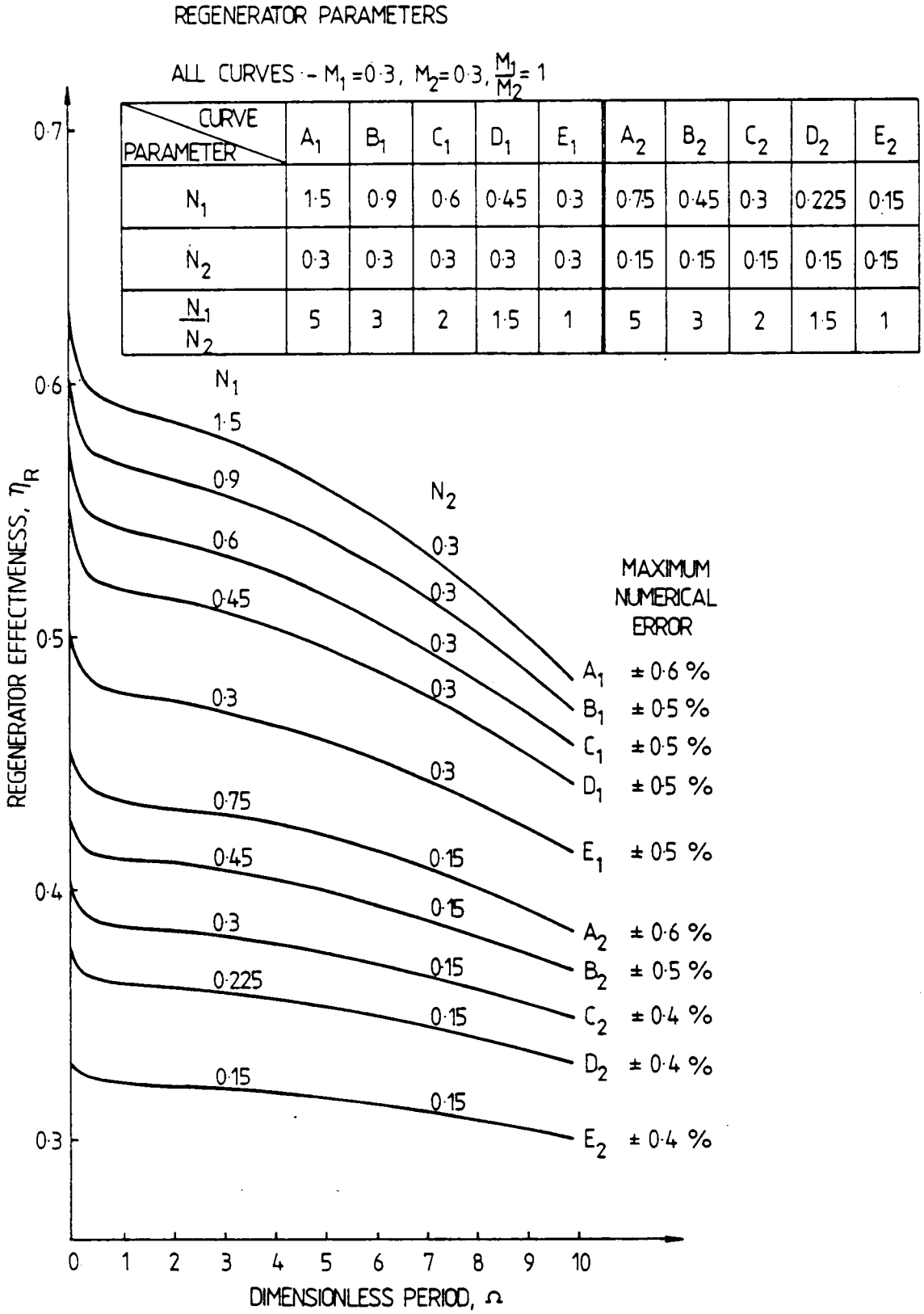

CURVE / PARAMETER	A_1	B_1	C_1	D_1	E_1	A_2	B_2	C_2	D_2	E_2
N_1	1·5	0·9	0·6	0·45	0·3	0·75	0·45	0·3	0·225	0·15
N_2	0·3	0·3	0·3	0·3	0·3	0·15	0·15	0·15	0·15	0·15
$\frac{N_1}{N_2}$	5	3	2	1·5	1	5	3	2	1·5	1

FIG. 14. REGENERATOR EFFECTIVENESS, η_R, COMPUTED BY PROGRAM 1, FOR A RANGE OF REGENERATOR PARAMETERS.

REGENERATOR PARAMETERS

ALL CURVES:- $M_1 = 0.6$, $M_2 = 0.3$, $\frac{M_1}{M_2} = 2$

CURVE / PARAMETER	A_1	B_1	C_1	D_1	E_1	A_2	B_2	C_2	D_2	E_2
N_1	1·5	0·9	0·6	0·45	0·3	0·75	0·45	0·3	0·225	0·15
N_2	0·3	0·3	0·3	0·3	0·3	0·15	0·15	0·15	0·15	0·15
$\frac{N_1}{N_2}$	5	3	2	1·5	1	5	3	2	1·5	1

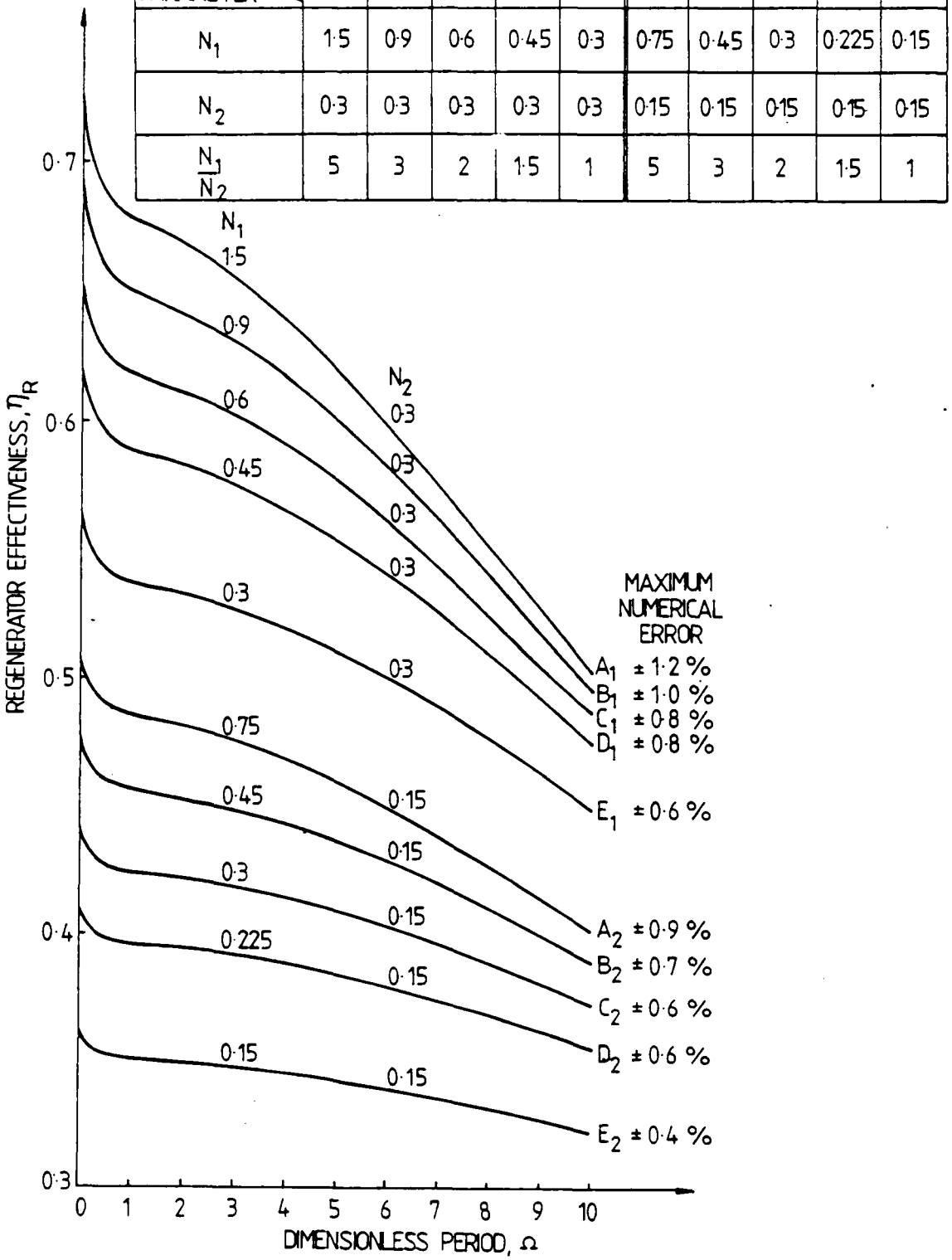

FIG. 15 REGENERATOR EFFECTIVENESS, η_R, COMPUTED BY PROGRAM 1, FOR A RANGE OF REGENERATOR PARAMETERS.

It is also interesting to note that the marked upswing in the η_R versus Ω curve previously observed when the values of Ω decreased below about 1.0 (see FIG.11) is again evident with all of the curves on these figures, the effect being most marked for curve A_1 of FIG.15. As before, the effectiveness values for the limiting case of infinitesimally-short periods ($\Omega \rightarrow 0$) have been determined using Nusselt's theory [24], and are included on each curve.

Considering next the results on either FIG.14 or FIG.15, and restricting observations to any one set of curves, we see that, for any selected value of Ω, the η_R values read from curves E to A, specify the change in regenerator effectiveness due to alterations in the Biot number N_1 only. The plotted results show the effect of up to a fivefold increase in the Biot number which, for a given regenerator operating under fixed conditions, corresponds to an equivalent increase in the heating period heat-transfer coefficient (h_1). Inspection of each set of curves indicates that the effect of such changes on η_R is greatest at the lower values of N_1 (c.f. the increases in η_R when $\frac{N_1}{N_2}$ changes from 1 to 1.5, with those when $\frac{N_1}{N_2}$ increases from 3 to 5).

To observe the result upon predicted effectiveness due to doubling both N_1 and N_2, we need to compare the η_R readings at a given point on either of the lower sets of curves (i.e. at the same Ω on any curve), with that from the equivalent point on the corresponding upper set curves (e.g. curve C_2 to C_1). In practical terms, doubling N_1 and N_2 corresponds

to doubling both the heating and cooling period heat-transfer coefficients in a given regenerator. Both FIG.14 and FIG.15 confirm the significant increases in η_R expected from changes of this type.

Finally, we note that the difference in η_R values determined from corresponding points on FIGS.14 and 15 (i.e. same curve, same Ω) determines the increase in regenerator effectiveness which occurs when M_1 is doubled from 0.3 to 0.6. For a given regenerator, this corresponds to a doubling of the mass flow rate of the hotter fluid.

Numerical Accuracy of the Predictions

An aspect of particular interest in these assessment tests was the extent to which the estimated numerical error in the predicted effectiveness values varied for different combinations of the dimensionless parameters. Using the convergence graphs of $\dot{H}_i$ versus $\frac{1}{n}$, together with equation (4-4) the maximum numerical error, $E\dot{H}^*$, in the predicted values of $\dot{H}^*$, and hence of η_R, (due to the use of finite values of n) was calculated for each example.

For each of the curves of FIGS.14 and 15, these errors were found to increase as Ω increased, the maximum error occurring at Ω = 10. For each set of curves, the largest errors occurred on the A-curves.

Using a similar procedure to that adopted in the preparation of Table 5 (of Chapter 4), further tests were

carried out for the $\Omega = 10$ examples on curves A_2 of FIG.14 and A_1 of FIG.15, to estimate the additional numerical error due to the use of finite values of m and e_1. As in Table 5 these additional errors were found to be very small, the addition of an extra $\pm$ 0.1% to the calculated values of $\dot{E}H^*$ being sufficient to cater for these effects. The maximum combined numerical error obtained for each curve is quoted in FIGS.14 and 15.

It is evident from these latter values that, with the exception of curve A_1 of FIG.15, all of the effectiveness values were determined to within a maximum error of $\pm$ 1%. However, those for curve A_1 of FIG.15 were slightly less accurate, having a maximum error of $\pm$ 1.2%.

On the basis of the results presented in FIGS.14 and 15, it is concluded therefore, that the application of the techniques developed in these studies to the solutions computed by Program 1, enables regenerator effectiveness values to be predicted to an acceptable numerical accuracy for the entire range of parameter values considered.

(b) Results for Balanced and Unbalanced Regenerators

It will be observed from the parameters used, that curves E_1 and E_2 of FIG.14 depict the overall performances of two balanced regenerators (each for Ω ranging from zero to 10). All other curves on these two figures indicate the change in the regenerator effectiveness which occurs when one or more of the regenerator parameters are changed from their balanced values.

Because of the points made in 6.2.1 above, it was of some interest to compare the effectiveness values predicted for an unbalanced regenerator, with those obtained for a 'corresponding' balanced regenerator defined firstly using the arithmetic means of parameters N_1 and N_2 and of M_1 and M_2, and secondly using the harmonic means of these parameters.

A limited comparison of this type has been carried out for three examples taken from curve A_1 of FIG.15. The values of η_R obtained for the balanced and unbalanced systems are summarised in Table 6.

The contents of Table 6 indicate that the regenerator effectiveness values obtained for balanced regenerators defined by either arithmetic or harmonic means differ considerably from the corresponding unbalanced results. Some measure of agreement is evident between the $\dot{H}^*$ values obtained for a balanced regenerator formed using harmonic means although even these differed by up to 6% from the corresponding, unbalanced values.

On the basis of this admittedly small sample, it seems unlikely that, for the non-iterative theory, the use of balanced results with either type of mean, would provide a sufficiently accurate basis for predicting the performance of unbalanced regenerators.

TABLE 6

COMPARISON OF THE THERMAL PERFORMANCES
OF UNBALANCED AND 'CORRESPONDING' BALANCED REGENERATORS

Program Parameters:- $e_1 = 0.002$, $m = 3$.

Type	N_1	N_2	M_1	M_2	Ω	$\dot{H}^*$	Difference (U-B)/U	η_R	Difference (U-B)/U
U	1.5	0.3	0.6	0.3	1	0.4073		0.6788	
B(A.M.)	0.9	0.9	0.45	0.45	1	0.5482	35%	0.6091	10.3%
B(H.M.)	0.5	0.5	0.4	0.4	1	0.4158	2.1%	0.5197	23.4%
U	1.5	0.3	0.6	0.3	6	0.3584		0.5973	
B(A.M.)	0.9	0.9	0.45	0.45	6	0.4629	29%	0.5143	13.9%
B(H.M.)	0.5	0.5	0.4	0.4	6	0.3732	4.1%	0.4665	21.9%
U	1.5	0.3	0.6	0.3	10	0.3007		0.5011	
B(A.M.)	0.9	0.9	0.45	0.45	10	0.3635	21%	0.4039	19.4%
B(H.M.)	0.5	0.5	0.4	0.4	10	0.3180	5.8%	0.3975	20.7%

Abbreviations:-

U = Unbalanced regenerator, B = Balanced regenerator.

B(A.M.) = Balanced regenerator defined using arithmetic mean of unbalanced regenerator parameters.

B(H.M.) = Balanced regenerator defined using harmonic mean of unbalanced regenerator parameters.

TABLE 7

FURTHER TEST RESULTS FROM PROGRAM 1

Program Parameters:- m=3, e_1=0.002 (unless otherwise stated).

Example Number	N_1	N_2	$\frac{N_1}{N_2}$	M_1	M_2	$\frac{M_1}{M_2}$	Ω	$\dot{H}^*$	$E\dot{H}^*$	η_R
9	4.5	0.9	5	2.0	0.2	10	10	0.3183	±1.8%	0.7956
10	4.5	0.9	5	2.0	0.4	5	10	0.3778	±2.1%	0.4723
11	4.5	0.9	5	2.0	1.0	2	10	0.3977	±2.2%	0.1988
12	4.5	0.9	5	1.6	0.8	2	10	0.3952	±2.1%	0.2470
13	4.5	0.9	5	1.2	0.6	2	10	0.390	±1.8%	0.325
14	4.5	0.9	5	0.8	0.4	2	10	+	+	+
	4.5	0.9	5	0.8	0.4	2	10	0.3760**	±1.45%**	0.4699**
14^I	0.9	4.5	0.2	0.4	0.8	0.5	10	0.3761	±1.4%	0.4701
15	4.5	0.9	5	0.4	0.2	2	10	0.3124	±0.5%	0.7809
15^I	0.9	4.5	0.2	0.2	0.4	0.5	10	0.3149	±0.75%	0.7871

Notes 1. + Example 14 : m=3 solutions not in range -1 to +1.

2. ** Example 14 : valid solutions obtained with m=6.

3. I Indicates 'invert' regenerator.

4. Example 15 : n=30 results were of poor accuracy and were omitted from the analyses to calculate $\dot{H}^*$ and η_R.

(c) Some Further Tests

It has been noted in 6.2.2(a) that the largest numerical error in the predicted values of η_R occurs when the individual parameter values were at the maximum values considered, i.e. for $N_1 = 1.5$, $N_2 = 0.3$, $M_1 = 0.6$, $M_2 = 0.3$, $\Omega = 10$ (see Curve A_1, FIG.15). Whereas these latter values are believed to represent the maximum values of practical interest, a few additional tests were carried out with the first four of these parameters increased well beyond these figures. This was done simply to obtain an appreciation of the extent to which computational accuracy, as measured by the maximum numerical error in η_R, is affected when these parameters take more extreme values.

The parameter values selected for these further tests, and the results obtained, are summarised in Table 7. All of the examples tested, which are numbered 9 to 15, had the same Biot number values viz. $N_1 = 4.5$, $N_2 = 0.9$, these being five times the largest values previously considered. All of the examples had the same dimensionless period, $\Omega = 10$. However the parameters M_1 and M_2 were varied as indicated in Table 7, the maximum values considered being $M_1 = 2$, $M_2 = 1$.

As expected, in almost all cases the numerical errors $E\dot{H}^*$, in the predicted values of $\dot{H}^*$ and η_R were greater than any of those reported in FIGS.14 and 15 for the main assessment. A maximum numerical error $E\dot{H}^*$ of $\pm$ 2.2% was obtained for Example 11, for which all five parameters were at the maximum values considered.

One slightly unexpected feature of the results presented in Table 7 concerns the group of examples 11 to 15. These all have $N_1 = 4.5$, $N_2 = 0.9$, $\Omega = 10$ but with M_1 and M_2 varied so as to maintain $\frac{M_1}{M_2} = 2$.

Examples 11, 12 and 13 were computed without difficulty with the normal program parameter settings. However, the solutions computed for Examples 14 and 15 with these settings both exhibited similar features to those originally observed for examples 2 to 8 of Table 2; i.e. the computed solutions were outside the permitted range of $-1 \leqslant f_i \leqslant +1$.

In the case of Example 14, increasing m from 3 to 6, (the technique found to be successful for the worst examples of Table 2) was again sufficient to produce acceptable solutions. However the same technique did not prove successful for Example 15, although in this case, it was only the computations at n=30 which were of an unsatisfactory accuracy. For both of these examples, the results obtained for the corresponding 'invert' example were obtained without difficulty and are included in Table 7. A fuller discussion of these particular examples and of the 'invert' regenerator theory is given in Chapters 8 and 9.

6.3 PROGRAM 1 : OPERATING DETAILS

One important aspect not included in the preceding assessment concerns program computation times. In order to round-off the assessment the following details relating to program operation and computation times are presented at this

point, rather than in the formal documentation of Program 1 which is presented in Appendix 5.

(a) Input/Output

For convenience, the input data to Program 1 is read from a separately prepared data file. For each example the input data 'set' consists of the three program parameters, n, m, e_1, followed by the five regenerator parameters Ω , N_2, N_1, M_2, M_1. The data set is completed by either a zero (indicating the end of the data file), or a 'one' (to indicate that a further data set is to be read).

A typical Program 1 output takes the form shown in Table 8. The initial table of results contains the computed fluid temperatures throughout the regenerator for a complete cycle. Each line of the output table gives the fluid temperatures at any instant, at seven equally-spaced distances along the regenerator length (levels -3 to +3). For each period there are (n+1) such lines corresponding to the (n+1) equally-spaced times(τ) which divide each period.

The output is completed with a summary of the input data, the computed mean fluid exit temperatures $\bar{f}_2(+1)$, $\bar{f}_1(-1)$, the dimensionless heat-transfer rates $\dot{H}_2$, $\dot{H}_1$, and finally, the heat-balance discrepancy.

For convenience of comparison and discussion at a later stage, the corresponding output for the 'invert' of Example 1 is included as Table 9.

Explanation

COMPUTED TEMPERATURES IN REGENERATOR

Explanation

$\zeta = \frac{1}{3}$(LEVEL VALUE)

Dimensionless Time, τ	LEVEL -3	-2	-1	0	+1	+2	+3
COLD FLUID							
0	-1.000000	-0.745267	-0.513158	-0.300886	-0.106224	0.072574	0.236740
0.2x Ω	-1.000000	-0.779978	-0.557476	-0.358238	-0.172241	0.001400	0.163388
0.4x Ω	-1.000000	-0.779468	-0.572218	-0.377510	-0.194656	-0.023042	0.137848
0.6x Ω	-1.000000	-0.784964	-0.581824	-0.390122	-0.209391	-0.039190	0.120870
0.8x Ω	-1.000000	-0.789257	-0.589353	-0.400038	-0.221016	-0.051976	0.107367
1.0x Ω	-1.000000	-0.793010	-0.595950	-0.408747	-0.231248	-0.063260	0.095414
HOT FLUID							
0	0.076622	0.252294	0.377632	0.536590	0.673495	0.818752	0.999999
0.2x Ω	0.215221	0.362556	0.501698	0.633727	0.760001	0.891981	1.000001
0.4x Ω	0.255323	0.397988	0.536134	0.664301	0.784812	0.897367	1.000000
0.6x Ω	0.281662	0.420345	0.558210	0.683446	0.799896	0.906391	0.999999
0.8x Ω	0.302379	0.443361	0.575259	0.698043	0.811137	0.912951	1.000000
1.0x Ω	0.320545	0.459643	0.590008	0.710518	0.820628	0.918401	1.000000

$f_2(\zeta,\tau) = -f_1^I(-\zeta,\tau)$

$f_1(\zeta,\tau) = -f_2^I(-\zeta,\tau)$

See Table 9 for 'invert' example results denoted by superscript I .

SUMMARY OF DATA AND COMPUTED RESULTS

NUMBER OF TIME INTERVALS =	5		n
NUMBER OF DISTANCE INTERVALS =	6		2m
SERIES FRACTIONAL ERROR BOUND =	0.0020		e_1
DIMENSIONLESS PERIOD =	0.4176000		Ω
DIMENSIONLESS PARAMETER N (COOLING PERIOD) =	0.2327660		N_2
DIMENSIONLESS PARAMETER N (HEATING PERIOD) =	1.3634590		N_1
DIMENSIONLESS PARAMETER M (COOLING PERIOD) =	0.3365800		M_2
DIMENSIONLESS PARAMETER M (HEATING PERIOD) =	0.5149430		M_1
AVERAGE COLD FLUID EXIT TEMPERATURE =	0.1373995		$\bar{f}_2(+1)$
AVERAGE HOT FLUID EXIT TEMPERATURE =	0.2555711		$\bar{f}_1(-1)$
HEAT TO COLD FLUID =	0.3828259		$\dot{H}_2$
HEAT FROM HOT FLUID =	0.3833385		$\dot{H}_1$
COMPUTED HEAT BALANCE =	0.133888	PER CENT	H.B.D.

TABLE 8 PROGRAM 1 OUTPUT FOR EXAMPLE 1

Explanation

COMPUTED TEMPERATURES IN REGENERATOR

Explanation

Dimensionless Time, τ	LEVEL	-3	-2	-1	0	+1	+2	+3	
				COLD FLUID					
0		-1.000000	-0.918952	-0.673495	-0.536590	-0.397632	-0.252298	-0.098622	
0.2 x Ω		-1.000000	-0.861981	-0.760001	-0.633727	-0.501698	-0.362555	-0.215221	$f_2^I(\zeta,\tau)$
0.4 x Ω		-1.000000	-0.897367	-0.788812	-0.668301	-0.536134	-0.399988	-0.255323	
0.6 x Ω		-1.000000	-0.906391	-0.799896	-0.683466	-0.558210	-0.424345	-0.281662	
0.8 x Ω		-1.000000	-0.912951	-0.811137	-0.698043	-0.575259	-0.443361	-0.302379	
1.0 x Ω		-1.000000	-0.918401	-0.820628	-0.710518	-0.590008	-0.459943	-0.320545	
				HOT FLUID					
0		-0.236749	-0.072574	0.106224	0.300086	0.513154	0.745267	1.000000	
0.2 x Ω		-0.163384	-0.001400	0.172241	0.358238	0.557476	0.770998	1.000000	$f_1^I(\zeta,\tau)$
0.4 x Ω		-0.137848	0.023042	0.198656	0.377510	0.572218	0.779468	1.000000	
0.6 x Ω		-0.120870	0.039190	0.209391	0.390122	0.581024	0.784963	1.000000	
0.8 x Ω		-0.107367	0.051976	0.221016	0.400038	0.589353	0.789257	1.000000	
1.0 x Ω		-0.095414	0.063260	0.231248	0.408747	0.595950	0.793018	1.000000	

Explanation

$\zeta = \frac{1}{3}$(LEVEL VALUE)

I signifies 'invert' of Example 1.

SUMMARY OF DATA AND COMPUTED RESULTS

NUMBER OF TIME INTERVALS	=	5
NUMBER OF DISTANCE INTERVALS	=	6
SERIES FRACTIONAL ERROR BOUND	=	0.0020
DIMENSIONLESS PERIOD	=	0.4176000
DIMENSIONLESS PARAMETER H (COOLING PERIOD)	=	1.3638590
DIMENSIONLESS PARAMETER N (HEATING PERIOD)	=	0.2327860
DIMENSIONLESS PARAMETER M (COOLING PERIOD)	=	0.5149630
DIMENSIONLESS PARAMETER M (HEATING PERIOD)	=	0.3365800
AVERAGE COLD FLUID EXIT TEMPERATURE	=	-0.2555711
AVERAGE HOT FLUID EXIT TEMPERATURE	=	-0.1373995
HEAT TO COLD FLUID	=	0.3033385
HEAT FROM HOT FLUID	=	0.3020259
COMPUTED HEAT BALANCE	=	0.133887 PER CENT

$\bar{f}_2^I(+1)$

$\bar{f}_1^I(-1)$

A_1^I

$\dot{H}_2^I$

TABLE 9 PROGRAM 1 OUTPUT FOR THE 'INVERT' OF EXAMPLE 1

TABLE 10

PROGRAM 1 EXECUTION TIMES FOR EXAMPLE 1

n	m	e_1	C.P.U. Time MIN : SECS	Used for	
				Figs 14,15	Table 7
5	3	0.002	0:1.65	Yes	Yes
10	3	0.002	0:3.31	Yes	Yes
30	3	0.002	0:39.31	Yes	Yes
30	6	0.002	0:59.92	No	Yes(Ex.14)
5	6	0.002	0:1.74	No	Yes(Ex.14)
5	24	0.002	0:2.56	No	No
5	48	0.002	0:18.49	No	No
30	48	0.002	4:45.41	No	No

(b) Computation Times

On the DEC System 20 computer used for these studies, the period taken to compute one regenerator example, i.e. one set of input data as stipulated in (a) above, is referred to as the C.P.U. or execution time. Such periods do not include the time needed for program compilation or for the printing of results.

Execution times for Program 1 depend for the greatest part on the number of time and distance steps (n and m) specified in the input data. Table 10 indicates how C.P.U. times vary for different values of n and m.

For $n \leqslant 10$ and $m \leqslant 24$, the C.P.U. times are relatively small; being of the order of 4 seconds or less. However, for larger values of these parameters, execution times increase considerably, attaining about 4.75 minutes for the largest n and m values tried. As may be observed from Table 10, only the combinations n=5, m=3; n=10, m=3 and n=30, m=3 are required for normal computations, although an m value of six was used with n values of 5, 10 and 30 for example 14 of Table 7.

PART 2

DEVELOPMENTS RELATING TO THE GENERAL THEORY FOR WHICH THE REVERSAL PERIODS ARE NOT NECESSARILY EQUAL

CHAPTER 7

DEVELOPMENT OF PROGRAM 2 FOR THE MORE GENERAL THEORY

7.1 SPECIFICATION FOR PROGRAM 2

Following the successful development of Program 1 for computing the fluid temperature distributions in regenerators which operate with heating and cooling periods of equal duration, attention was turned to developing a second program, which is capable of carrying out similar computations for regenerators in which the heating and cooling times are not necessarily the same.

As previously stated, the motivation for such a development was to enable the non-iterative method to be more meaningfully applied to the computation of blast-furnace regenerators which normally operate with different heating and cooling times.

The general requirements for the second program, which for convenience we call Program 2, were the same as those for Program 1. That is, for a high-level language program, capable of giving fast and accurate results over a range of regenerator parameters of practical interest. However, in the case of Program 2, this latter requirement was to apply specifically for parameters which are representative of modern blast-furnace stoves, and as such, would include different values for the dimensionless heating period, Ω_1, and the dimensionless cooling period, Ω_2.

As far as the method of computation was concerned, we have seen that the non-iterative approach being investigated in this research study had been extended by Edwards [37] ,

in an earlier investigation, to cope with regenerators operating with unequal period times. For this more general case, Edwards showed that the fluid temperatures within the regenerator could, as for the theory derived for equal period times, be obtained by solving a pair of integro-differential equations, namely (2-13) and (2-14).

A method for computing the required fluid temperatures by solving these equations numerically had also been formulated in the original investigation [74]. The method was developed along similar lines to that used in Program 1, with the computation process consisting of three main stages.

The first of these stages involves the calculation of the four matrices $\underline{B}_1$, $\underline{B}_2$, $\underline{D}_1$ and $\underline{D}_2$, which arise from the numerical integration (i.e. quadrature) of the time integrals in equations (2-13) and (2-14). The mathematical procedures used for the quadrature, together with the forms derived for the elements of these four matrices, have been reviewed in Section 2.3 of Chapter 2, which also indicates the procedures needed for the other two stages of the computation.

In the second stage, matrices $\underline{B}_1$, $\underline{B}_2$, $\underline{D}_1$ and $\underline{D}_2$ are combined as indicated in equations (2-39) to (2-42), to form the matrix $\underline{P}_1$ of equations (2-37) and (2-38). Then, in the final stage, the system of differential equations (2-37) are solved by numerical integration along the regenerator length.

In basing Program 2 on this method of computation, any problems to be resolved were expected to arise at the

application stage. This was because, neither the solution method nor the more general theory developed by Edwards, had been tested under the conditions of practical interest. The single test calculation which had been carried out in the study by Edwards et al [74], had only applied the more general theory to an example for which the periods were equal: the example used was example 1 of Table 2. Even then, the results were not particularly accurate, thereby indicating that considerable further development would be needed to obtain results of an acceptable accuracy for the range of regenerator parameters referred to above.

One of the reasons given for the limited accuracy of the test calculation was that it had not been possible for the infinite series $Q_i(u)$ and $R_i(u)$ of equations (A2.2-3) and (A2.2-4), which were used to calculate the elements of the matrices $\underline{B}_1$, $\underline{B}_2$, $\underline{D}_1$ and $\underline{D}_2$, to be summed with sufficient accuracy. The first step in the formulation of Program 2 was, therefore, to rectify this deficiency by developing mathematical techniques which would ensure the accurate summation of all required infinite series. The techniques derived to do this are described in Section 7.2.1.

Furthermore, because of the similarities between the solution method to be used for Program 2 and that already incorporated in Program 1, it was reasonable to assume that, as well as the summation errors considered in the preceding paragraph, the various other types of numerical error identified in Chapter 3 as affecting the 'equal-period' theory solutions, would also be present and affect the accuracy of

the Program 2 predictions.

Without doubt, the most significant cause of numerical inaccuracy in the Program 1 calculations was the assumption that the functions $X_1(\zeta, z')$ and $X_2(\zeta, z')$ are linear functions of z', within each time interval. Moreover, the ability to select a suitably small time step for each program computation was found to be essential in order to control such errors. Because, in the more general case, similar assumptions are made with regard to the 'corresponding' functions $\phi_1(\zeta, v)$ and $\phi_2(\zeta, v)$ (see Appendix 2), it was clearly prudent to design Program 2 with a similar facility for enabling the time step $h(= \frac{1}{n})$ to be changed from one computation to the next.

In fact, as a result of the experience gained in the PART 1 investigations, both of the numerical integration techniques featured in the more general solution process have been programmed to allow the use of different step sizes. In practice this is achieved by specifying appropriate values for the parameters m and n in the program input data. Also as in Program 1, the maximum acceptable fractional error, e_1, for each calculated infinite series, is specified as input data to Program 2.

Two other features which were found to have a beneficial effect on the accuracy of solutions computed from the 'equal-period' theory, were also incorporated into Program 2, at the design stage. Thus, to prevent the possible build-up of round-off errors in the second stage

matrix calculations, the analysis leading to the formation of matrix $\underline{P}_1$ of equation (2-38) was re-developed to simplify the matrix expressions to be evaluated. Details of the revised analysis needed to achieve this simplification are given in Section 7.2.2.

Finally, in the third stage of the computation, the Crank-Nicolson method was again used for the numerical integration along the regenerator.

7.2 MATHEMATICAL DEVELOPMENTS

7.2.1 Accuracy of Summation of Infinite Series $Q_i(u)$ and $R_i(u)$

The method developed below to ensure that the sums of all Q- and R-series are within a specified accuracy requires firstly, that all terms used for summation are evaluated to within the specified accuracy, and secondly that the summation process for each series is continued until the error in each sum is less than the specified maximum.

We consider first the accuracy of all series terms, and commence by noting from equations (A2.2-3) and (A2.2-4) that the s-th terms of both the $Q_i(u)$ and $R_i(u)$ series are functions of u, Ω_i and β_s, where β_s is the s-th root of $\sqrt{\beta}\ \tan\sqrt{\beta} = 1$.

For given values of u and Ω_i (i.e. for a given series), the accuracy with which each s-th term is evaluated is therefore governed by the accuracy with which β_s is determined.

Now, for Program 2, and for a given value of s, it is shown in equations (A7-1) to (A7-8) that the root β_s is bounded by the values $\beta_{s\ min}$ and $\beta_{s\ max}$, where the difference between the values of these two bounds can be made progressively smaller by repeated application of the iterative method specified by these equations.

Therefore it follows that, in principle, by taking $\beta_s = \frac{1}{2}(\beta_{s\ min} + \beta_{s\ max})$, and by continuing the iterative process until the difference between $\beta_{s\ min}$ and $\beta_{s\ max}$ is sufficiently small, the value of β_s, and hence that of each s-th term, can be determined within any given accuracy.

Using this approach, it is shown in Appendix 6, Sections A6.1 and A6.2, that the terms of all Q- and R-series can be calculated to within a specified accuracy by ensuring that $\beta_{s\ min}$ and $\beta_{s\ max}$ are close enough to satisfy the two conditions given as Tests A and B, below. These tests relate to the terms of the Q- and R-series, respectively, and are stated as follows:

TEST A: The fractional error in the s-th term of every $Q_i(u)$ series will be less than a pre-selected value e_1, if each term is calculated with β_s set equal to the mean of the values of $\beta_{s\ min}$ and $\beta_{s\ max}$ for which

$$\left\{\frac{\beta_{s\ max}}{\beta_{s\ min}}\cdot\frac{2+\beta_{s\ max}}{2+\beta_{s\ min}}\cdot\frac{1-\exp\left[-(\Omega_1+\Omega_2)\beta_{s\ max}\right]}{1-\exp\left[-(\Omega_1+\Omega_2)\beta_{s\ min}\right]}\right. \times$$

$$\left.\frac{\exp(h\Omega_i\beta_{s\ max})-1-h\Omega_i\beta_{s\ min}}{\exp(h\Omega_i\beta_{s\ min})-1-h\Omega_i\beta_{s\ max}}\cdot\exp\left[(\Omega_1+\Omega_2)(\beta_{s\ max}-\beta_{s\ min})\right]\right\} - 1 < e_1$$

..... (7-1)

TEST B: The fractional error in the s-th term of every required $R_i(u)$ series will be less than a pre-selected value e_1, if each term is calculated with β_s set equal to the mean of the values of $\beta_{s\ min}$ and $\beta_{s\ max}$ for which

$$\left\{ \frac{\beta_{s\ max}}{\beta_{s\ min}} \cdot \frac{2+\beta_{s\ max}}{2+\beta_{s\ min}} \cdot \frac{1-\exp\left[-(\Omega_1+\Omega_2)\beta_{s\ max}\right]}{1-\exp\left[-(\Omega_1+\Omega_2)\beta_{s\ min}\right]} \right. \times$$

$$\frac{\exp(-h\Omega_i\beta_{s\ min})-1+h\Omega_i\beta_{s\ max}}{\exp(-h\Omega_i\beta_{s\ max})-1+h\Omega_i\beta_{s\ min}} \cdot \exp\left[(\Omega_1+\Omega_2-h\Omega_i)\right.$$

$$\left.\left.(\beta_{s\ max}-\beta_{s\ min})\right]\right\}-1 < e_1 \qquad \ldots\ldots (7\text{-}2)$$

In (7-1) and (7-2), i = 1 for terms of $Q_1(u)$ and $R_1(u)$ and i = 2 for terms of $Q_2(u)$ and $R_2(u)$.

Dealing next with the summation of each series, a comparison of the convergence rates of the various Q- and R-series has been carried out in Section A6.3 of Appendix 6. This comparison and subsequent analysis shows that the sums of all the Q- and R-series can be determined to within a pre-selected accuracy provided the following single condition is satisfied:

TEST C: Suppose the first s terms of every series have been summed. Then, if all further terms are neglected in every series, the fractional residue of every series will be less than a pre-selected value e_1, provided the fractional residue in the series $R_i(0)$ is less than e_1.

This latter condition will be satisfied when s is large enough to ensure that

$$\frac{\frac{2}{\pi^2\Omega_i}\left[\frac{\pi^2}{6} - \sum_{q=1}^{s-1}\frac{1}{q^2}\right]}{\bar{S}_s\left[R_i(0)\right]} < e_1 \qquad \ldots\ldots (7\text{-}3)$$

where $\bar{S}_s\left[R_i(0)\right]$ represents the sum of the first s terms of $R_i(0)$.

Tests A and B above have been incorporated directly into Stage 1 of Program 2. However, because the series $R_i(0)$ (for i=1,2) were both found to converge slowly, TEST C was not used in Program 2. Instead, the following method has been developed to ensure that each series $R_i(0)$ is summed to the required accuracy.

We start by assuming that the first s terms of $R_i(0)$ have been summed, and let the sum and residue at that stage be represented by $\bar{S}_s\left[R_i(0)\right]$ and $\bar{R}_s\left[R_i(0)\right]$ respectively. (The residue $\bar{R}_s$ is defined in equation (A6.3-11) to be the sum of the remaining terms of $R_i(0)$ after the first s terms have been added).

Next we define RESMIN and RESMAX to be values which span the value of $\bar{R}_s\left[R_i(0)\right]$. That is

$$\text{RESMIN} < \bar{R}_s\left[R_i(0)\right] < \text{RESMAX} \qquad \ldots\ldots (7\text{-}4)$$

The analysis given in Section A6.3(d) shows that RESMAX is given by the relationship (A6.3-17). Also, following a

similar procedure to that presented in (A6.3(d)), it can be shown for $\Omega_i < 1$, that

$$\text{RESMIN} > \frac{2}{1+\pi^2} \sum_{q=s+1}^{\infty} \frac{1}{q^2} = \frac{2}{1+\pi^2}\left[\frac{\pi^2}{6} - \sum_{q=1}^{s} \frac{1}{q^2}\right] \quad \ldots\ldots \quad (7\text{-}5)$$

For $\Omega_i \geqslant 1$, RESMIN is taken to be zero.

As each new term is added to the sum of $R_i(0)$, the values of RESMIN and RESMAX can be up-dated using (A6.3-17) and (7-5). In this way, the interval containing $\overline{R}_s[R_i(0)]$ becomes successively smaller as the summation proceeds. It follows that if, after s terms have been summed, the value of $R_i(0)$ is taken as

$$\overline{S}_s[R_i(0)] + \overline{R} \quad \ldots\ldots \quad (7\text{-}6)$$

where $\overline{R}$ is an estimated value of $\overline{R}_s[R_i(0)]$ given by

$$\overline{R} = \frac{1}{2}(\text{RESMIN} + \text{RESMAX}) \quad \ldots\ldots \quad (7\text{-}7)$$

then the maximum fractional error in the sum given by (7-6) will not exceed

$$\frac{\overline{R} - \text{RESMIN}}{\overline{S}_s[R_i(0)] + \text{RESMIN}}$$

We therefore conclude that if the summation of $R_i(0)$ is continued until s is large enough to ensure

$$\frac{\frac{1}{2}(\text{RESMAX-RESMIN})}{\bar{S}_s[R_i(0)]+\text{RESMIN}} < e_1 \qquad \ldots\ldots (7\text{-}8)$$

then the value of $R_i(0)$ given by (7-6) will have a fractional error less than e_1.

7.2.2 A Simplified Matrix Analysis for Stage 2

To achieve the desired simplification, we first replace $\underline{\phi}_1(\zeta)$ and $\underline{\phi}_2(\zeta)$ in equations (2-35) and (2-36) by their equivalent forms obtained from equations (2-16) and (2-17). This leads to the equations

$$-\frac{M_1\Omega_1}{a_1}(\underline{B}_1+d_1\underline{I})\frac{\partial \underline{F}_1}{\partial\zeta}+\frac{\Omega_2 M_2}{a_2}\underline{D}_1\frac{\partial \underline{F}_2}{\partial\zeta}=\left[\Omega_1(\underline{B}_1+d_1\underline{I})-a_1\underline{I}\right]\underline{F}_1$$

$$+\Omega_2\underline{D}_1\underline{F}_2. \qquad \ldots\ldots (7\text{-}9)$$

and

$$-\frac{M_1\Omega_1}{a_1}\underline{D}_2\frac{\partial \underline{F}_1}{\partial\zeta}+\frac{M_2\Omega_2}{a_2}(\underline{B}_2+d_2\underline{I})\frac{\partial \underline{F}_2}{\partial\zeta}=\Omega_1\underline{D}_2\underline{F}_1+$$

$$\left[\Omega_2(\underline{B}_2+d_2\underline{I})-a_2\underline{I}\right]\underline{F}_2. \qquad \ldots\ldots (7\text{-}10)$$

If matrices $\underline{K}_1$, $\underline{K}_2$, $\underline{K}_3$, $\underline{K}_4$, $\underline{C}_1$, $\underline{C}_2$, $\underline{C}_3$ and $\underline{C}_4$ are then defined as shown in equations (7-19) to (7-26), equations (7-9) and (7-10) may be written as

$$\underline{K}_2\frac{\partial \underline{F}_2}{\partial\zeta}+\underline{K}_1\frac{\partial \underline{F}_1}{\partial\zeta}=\underline{C}_2\underline{F}_2+\underline{C}_1\underline{F}_1 \qquad \ldots\ldots (7\text{-}11)$$

$$\underline{K}_4\frac{\partial \underline{F}_2}{\partial\zeta}+\underline{K}_3\frac{\partial \underline{F}_1}{\partial\zeta}=\underline{C}_4\underline{F}_2+\underline{C}_3\underline{F}_1 \qquad \ldots\ldots (7\text{-}12)$$

This pair of equations can then be expressed as the single matrix equation

$$\left[\begin{array}{c|c} \underline{K}_2 & \underline{K}_1 \\ \hline \underline{K}_4 & \underline{K}_3 \end{array}\right] \left[\begin{array}{c} \frac{\partial \underline{F}_2}{\partial \zeta} \\ \\ \frac{\partial \underline{F}_1}{\partial \zeta} \end{array}\right] = \left[\begin{array}{c|c} \underline{C}_2 & \underline{C}_1 \\ \hline \underline{C}_4 & \underline{C}_3 \end{array}\right] \left[\begin{array}{c} \underline{F}_2 \\ \\ \underline{F}_1 \end{array}\right] \qquad \ldots\ldots (7\text{-}13)$$

This in turn, can be written even more concisely as

$$\underline{R}_1 \frac{\partial \underline{F}}{\partial \zeta} = \underline{S}_1 \underline{F} \qquad \ldots\ldots (7\text{-}14)$$

to give

$$\frac{\partial \underline{F}}{\partial \zeta} + \underline{P}_1' \underline{F} = 0 \qquad \ldots\ldots (7\text{-}15)$$

where $\underline{P}_1' = -\underline{R}_1^{-1} \underline{S}_1$ $\qquad \ldots\ldots (7\text{-}16)$

In equation (7-16), we see that

$$\underline{R}_1 = \left[\begin{array}{c|c} \underline{K}_2 & \underline{K}_1 \\ \hline \underline{K}_4 & \underline{K}_3 \end{array}\right] \qquad \ldots\ldots (7\text{-}17)$$

and

$$\underline{S}_1 = \left[\begin{array}{c|c} \underline{C}_2 & \underline{C}_1 \\ \hline \underline{C}_4 & \underline{C}_3 \end{array}\right] \qquad \ldots\ldots (7\text{-}18)$$

where $\underline{K}_1 = \frac{-M_1 \Omega_1}{a_1} (\underline{B}_1 + d_1 \underline{I})$ $\qquad \ldots\ldots (7\text{-}19)$

$$\underline{K}_2 = \frac{M_2\Omega_2}{a_2}\ \underline{D}_1 \qquad \ldots\ldots (7\text{-}20)$$

$$\underline{K}_3 = \frac{-M_1\Omega_1}{a_1}\ \underline{D}_2 \qquad \ldots\ldots (7\text{-}21)$$

$$\underline{K}_4 = \frac{M_2\Omega_2}{a_2}\ (\underline{B}_2+d_2\underline{I}) \qquad \ldots\ldots (7\text{-}22)$$

$$\underline{C}_1 = \Omega_1(\underline{B}_1+d_1\underline{I}) - a_1\underline{I} \qquad \ldots\ldots (7\text{-}23)$$

$$\underline{C}_2 = \Omega_2\underline{D}_1 \qquad \ldots\ldots (7\text{-}24)$$

$$\underline{C}_3 = \Omega_1\underline{D}_2 \qquad \ldots\ldots (7\text{-}25)$$

$$\underline{C}_4 = \Omega_2(\underline{B}_2+d_2\underline{I}) - a_2\underline{I} \qquad \ldots\ldots (7\text{-}26)$$

It is evident from equations (7-17) to (7-26) that the calculation of the sub-matrices contained in $\underline{R}_1$ and $\underline{S}_1$ requires the matrix operations of addition and scalar multiplication only. Matrix inversion is needed just once, to form $\underline{R}_1^{-1}$. This alternative analysis has therefore been programmed for Stage 2 of the more general program, in preference to the scheme described by equations (2-38) to (2-42).

7.3 STRUCTURE OF PROGRAM 2

A description of the main features of Program 2 is given in Appendix 7. This contains details of the program operation together with a series of flowcharts which provide a step-by-step breakdown of the entire computation.

The first flowchart, which illustrates the broad structure of the program, shows that the calculations for each of the three main stages of the computation are carried out by separate subroutines. This arrangement was selected to facilitate the development and testing of the program and differs slightly from that of Program 1, in which the corresponding stages were combined into a single subroutine.

The flowcharts given for each of the Program 2 subroutines are fully annotated with references to appropriate sections of the text, in order to indicate the mathematical techniques used in each part of the computation. However, two points merit further comment.

Firstly, we note that for simplicity of programming a different numerical procedure from that used in Program 1 has been used to compute the roots of $\sqrt{\beta} \tan \sqrt{\beta} = 1$. Secondly, in contrast to the last point, it is worth mentioning that the mathematical and computational procedures used for the third stage of the computation are identical in both Program 1 and Program 2. This occurs because the final systems of differential equations to be solved in each case have identical forms and boundary conditions.

CHAPTER 8

ASSESSMENT OF THE MORE GENERAL METHOD OF SOLUTION

(RESULTS FROM PROGRAM 2)

8.1 OVERVIEW

We have seen from earlier comments that the only previous attempt to apply the Edwards' generalisation of the non-iterative method of solution was limited to a single computation of a regenerator system for which the heating and cooling periods were of equal duration. It was important, therefore, that this further assessment of the more general form of solution should involve a range of regenerator systems, with particular attention being given to those having different heating and cooling times. It may seem surprising therefore, that the first group of examples to be tested in this assessment, all featured dimensionless heating and cooling periods of equal value ($\Omega_1 = \Omega_2$). The reason for doing this was simply to enable the results computed by the more general method of solution, as incorporated in Program 2, to be checked with the corresponding Program 1 results calculated using the original theory, which applies only to systems having $\Omega_1 = \Omega_2$.

The scope of the assessment was then widened by testing the more general theory with a second group of examples for which, in most cases, the dimensionless heating and cooling periods had different values. The regenerator parameter values used for these examples were selected to cover a range of values of practical interest.

Finally, in order to make these tests as realistic as possible, Program 2 was used to compute two examples

representing typical blast-furnace stoves. That is, the values of the regenerator parameters $N_1, N_2, M_1, M_2, \Omega_1$ and Ω_2 were calculated from physical and operating data derived from two actual blast-furnace stoves.

Within these three groups of tests, two further issues required particular attention. The first of these concerned the numerical accuracies of the computed fluid temperatures, which as previously discussed are governed by the extent to which numerical errors accumulate throughout the computation process. In this context, we have seen from Chapter 7, that various techniques were built-in to Program 2, with a view to controlling the growth of such numerical errors. Although similar techniques have been shown to be effective in controlling the accuracy of the Program 1 solutions, it was clearly necessary to examine their effectiveness in the case of the Program 2 calculations.

The second issue which required special attention, concerned the applicability of the method for predicting the regenerator effectiveness η_R, from the solutions computed by Program 2. As will be explained below, the procedure for predicting η_R given in Chapter 4, needs some modification for examples in which $\Omega_1 \neq \Omega_2$.

8.2 COMPARISON OF PREDICTIONS FROM PROGRAM 1 AND PROGRAM 2 FOR SYSTEMS WITH EQUAL REVERSAL PERIODS (i.e. $\Omega_1 = \Omega_2 = \Omega$).

The regenerator parameter values selected for this first group of test examples are summarised in Table 11. In each example, the dimensionless reversal periods Ω_1 and Ω_2

were given a common value Ω, the value of Ω being varied from one example to the next to cover the range $0.5 \leq \Omega \leq 10$. The parameters N_1, N_2, M_1 and M_2 were set at the values given in Table 2 for Example 1, for all computations.

The effectiveness values computed via Program 1 for each of these examples have already been reported in FIG.11, but are repeated in Table 11 to facilitate the present comparison. The maximum numerical error ($E\eta_R$), associated with each of the η_R values predicted by Program 1 is also given in Table 11.

Each of the Table 11 examples was then computed by Program 2 with n set successively to the values 5,10,15,20, 25, and then 30. Subsequent examinations of the graphs of $\dot{H}_1^n$ and $\dot{H}_2^n$ versus $\frac{1}{n}$, plotted from the results of these computations, revealed that these were identical in form to those previously obtained from Program 1 computations. This meant that the procedures detailed in Chapter 4, and in particular equations (4-3), (4-4) and (4-9) for obtaining $\dot{H}^*$, $E\dot{H}^*$ and η_R, were directly applicable to these results from Program 2. Application of these procedures then yielded the Program 2 effectiveness values, together with the associated maximum fractional error values $E\eta_R$, listed in Table 11.

Comparison of corresponding η_R values in Table 11 confirms that the effectiveness values predicted by both versions of this non-iterative method were in good agreement for all examples tested. The entries in the

final column of the table indicate a maximum difference in any pair of η_R values of just under 0.4%. Inspection of the corresponding pairs of fractional errors $E\eta_R$ shows that the effectiveness predictions from the Program 2 results have slightly greater associated errors than those derived from the Program 1 solutions.

Now in all of the computations carried out to obtain the results reported in Table 11, the program parameters e_1 and m were set at their 'normal' values $e_1 = 0.002$ and m=3. It was of interest therefore, as far as Program 2 was concerned, to examine the extent to which the computed mean heat-transfer rates $\dot{H}_i$, and hence the predicted effectiveness values, were changed when these program parameters were given different values.

To do this, an additional series of examples were computed with Program 2 only, (a similar assessment for Program 1 having already been reported in Chapter 4), to check the effect of firstly, changing m from 3 to 48 with e_1 invariant at 0.002, and secondly, of decreasing e_1 from 0.002 to 0.001, with m retained equal to three. Analysis of these additional tests confirmed that, just as for Program 1 (see Section 4.2), such changes in the program parameters produced extremely small variations in the computed mean heat-transfer rates $\dot{H}_1$ and $\dot{H}_2$, and therefore also in the predicted $\dot{H}^*$ and η_R values.

TABLE 11

COMPARISON OF REGENERATOR EFFECTIVENESS VALUES
COMPUTED BY PROGRAM 1 AND PROGRAM 2

Regenerator Parameters:- N_1=1.363459, N_2=0.232786, M_1=0.514943, M_2=0.33658

Program Parameters:- m=3, e_1=0.002

$\Omega_1=\Omega_2=\Omega$	PROGRAM 1		PROGRAM 2		Difference = η_R(Program 1) $-\eta_R$(Program 2)
	η_R	$E\eta_R$	η_R	$E\eta_R$	
0.5	0.5650	±0.1%	0.5651	±0.2%	0.02%
1.0	0.5591	±0.1%	0.5593	±0.2%	0.04%
1.5	0.5555	±0.15%	0.5560	±0.2%	0.09%
2.5	0.5476	±0.2%	0.5479	±0.3%	0.05%
5.0	0.5169	±0.4%	0.5181	±0.6%	0.23%
7.5	0.4743	±0.6%	0.4754	±1.0%	0.23%
10.0	0.4274	±1.0%	0.4290	±1.3%	0.37%

Finally, as a general observation on this first set of tests, it was concluded that, apart from the small differences identified in Table 11, the Program 2 solutions for examples having $\Omega_1 = \Omega_2$ exhibited identical characteristics to those previously described for Program 1.

8.3 APPLICATION OF PROGRAM 2 TO SYSTEMS WITH UNEQUAL REVERSAL PERIODS (i.e. $\Omega_1 \neq \Omega_2$)

8.3.1 Predicting the Regenerator Effectiveness

For examples in which $\Omega_1 = \Omega_2$, the method used to predict the regenerator effectiveness relies on the fact that the mean heat-transfer rates $\dot{H}_1^n$ and $\dot{H}_2^n$ obtained from a computation which uses n time-intervals, approach a common limit, $\dot{H}^*$, as the value of n is successively increased. However for regenerators operating with heating and cooling periods of different durations ($\Omega_1 \neq \Omega_2$), the mean rate of heat transfer in the heating period will have a quite different value to that in the cooling period. Consequently, for regenerators operating in this mode, the computed values of $\dot{H}_1$ and $\dot{H}_2$ will not converge to a common limiting value, and as such, the method introduced in Chapter 4 for predicting the regenerator effectiveness, will not be applicable.

In modifying the method of Chapter 4 to cater for examples for which $\Omega_1 \neq \Omega_2$, instead of the dimensionless heat-transfer rates $\dot{H}_1$ and $\dot{H}_2$, we consider the quantities $H_{T,1}$ and $H_{T,2}$ defined in equations (8-1) and (8-2).

$$H_{T,1} = M_1 \left[1 - \bar{f}_1(-1) \right] \Omega_1 \qquad \ldots\ldots (8\text{-}1)$$

$$H_{T,2} = M_2 \left[\bar{f}_2(+1) + 1 \right] \Omega_2 \qquad \ldots\ldots (8\text{-}2)$$

Comparing the dimensionless terms in these equations with the corresponding terms of equations (2-43) and (2-44), we see that $H_{T,1}$ and $H_{T,2}$ represent on a dimensionless scale, the actual amounts of heat transferred in the heating and cooling periods, respectively. In a computation free from numerical errors, whether the dimensionless periods are equal or not, these quantities should have the same value, which we designate as H_T^*.

Now in the Program 2 tests reported later in this chapter, involving examples in which $\Omega_1 \neq \Omega_2$, most examples were computed several times with the time-step parameter n set successively to the values given by n = 5(5)30. Plotting the computed values of $H_{T,1}$ and $H_{T,2}$ against the corresponding values of $\frac{1}{n}$, has shown that both $H_{T,1}$ and $H_{T,2}$ are linearly related to $\frac{1}{n}$, the plotted graphs being similar to, but not always of the same arrangement as, the convergence graphs depicted in FIG. 9. In fact, as will be apparent from Section 8.3.2(b), five different 'types' of convergence graphs were obtained from the Program 2 results for examples in which $\Omega_1 \neq \Omega_2$.

The five types of graph have been designated types A,B,C,D and E, and are illustrated diagrammatically in FIG. 16. The classification of the graphs into these five types was based on whether the values of $H_{T,1}$ were greater or less than the corresponding values of $H_{T,2}$, and also according to the sign of the gradient of the 'best' line through the $H_{T,i}$ versus $\frac{1}{n}$ results.

Despite the somewhat greater diversity in the types of convergence graphs obtained from the Program 2 results, it nevertheless follows that in much the same way as the convergence graphs of $\dot{H}_1$ and $\dot{H}_2$ versus $\frac{1}{n}$ are used to determine $\dot{H}^*$ for examples with $\Omega_1 = \Omega_2$, the corresponding convergence plots of $H_{T,1}$ and $H_{T,2}$ versus $\frac{1}{n}$ can be used to determine H_T^*, for examples having $\Omega_1 \neq \Omega_2$.

Hence, using a procedure similar to that presented in Section 4.2 of Chapter 4, but with $\dot{H}_1$, $\dot{H}_2$ and $\dot{H}^*$, replaced by $H_{T,1}$, $H_{T,2}$ and H_T^* respectively, the value of H_T^* can be obtained, for each of the five types of graphs, from the following formulae:-

Graph Types A and D

$$H_T^* = \frac{1}{2}\left[H_{T,1}^{30} + H_{T,2}^{30}\right] \qquad \ldots\ldots (8\text{-}3)$$

$$EH_T^* = \pm \frac{1}{2}\left[H_{T,1}^{30} - H_{T,2}^{30}\right] \qquad \ldots\ldots (8\text{-}4)$$

Graph Type B

$$H_T^* = \frac{1}{2}\left[(H_{T,i}^{\infty})_{min} + H_{T,1}^{30}\right] \qquad \ldots\ldots (8\text{-}5)$$

$$EH_T^* = \pm \frac{1}{2}\left[H_{T,1}^{30} - (H_{T,i}^{\infty})_{min}\right] \qquad \ldots\ldots (8\text{-}6)$$

Graph Type E

Apply (8-5) and (8-6) but with $H_{T,1}^{30}$ replaced by $H_{T,2}^{30}$.

Graph Type C

$$H_T^* = \frac{1}{2}\left[(H_{T,i}^{\infty})_{max} + H_{T,1}^{30}\right] \qquad \ldots\ldots (8\text{-}7)$$

$$EH_T^* = \pm\frac{1}{2}\left[(H_{T,i}^{\infty})_{max} - H_{T,1}^{30}\right] \qquad \ldots\ldots (8\text{-}8)$$

It also follows that, for computations for which $\Omega_1 \neq \Omega_2$, the heat-balance discrepancy has to be calculated from the formula

$$H.B.D. = \frac{|H_{T,1} - H_{T,2}|}{(H_{T,i})_{min}} \times 100 \qquad \ldots\ldots (8\text{-}9)$$

Cooling-Period Effectiveness, $\eta_{R,C}$

Considering the definition given in equation (4-5), we see that for systems in which $\Omega_1 \neq \Omega_2$, the regenerator effectiveness η_R is given by

$$\eta_R = \frac{M_1\Omega_1\left[\bar{f}_1(+1)-\bar{f}_1(-1)\right]}{(M_i\Omega_i)_{min}\left[\bar{f}_1(+1)-\bar{f}_2(-1)\right]} = \frac{M_2\Omega_2\left[\bar{f}_2(+1)-\bar{f}_2(-1)\right]}{(M_i\Omega_i)_{min}\left[\bar{f}_1(+1)-\bar{f}_2(-1)\right]}$$

$$= \frac{M_1\Omega_1\left[1-\bar{f}_1(-1)\right]}{2(M_i\Omega_i)_{min}} = \frac{M_2\Omega_2\left[\bar{f}_2(+1)+1\right]}{2(M_i\Omega_i)_{min}} \qquad \ldots\ldots (8\text{-}10)$$

However, for the regenerator systems examined in Section 8.3.2, $(M_i\Omega_i)_{min}$ is equal to $M_1\Omega_1$ for certain examples but $M_2\Omega_2$ for others. Because of this, the values of η_R calculated from equation (8-10) varied over only a fairly narrow range, and as such they did not give a very clear picture of how the amount of heat transferred in each period is affected by changes in the regenerator parameters.

To avoid this difficulty, for all the examples having $\Omega_1 \neq \Omega_2$, overall regenerator performance has been expressed in terms of the cooling-period effectiveness, denoted by $\eta_{R,C}$, where

$$\eta_{R,C} = \frac{M_2\Omega_2\left[\bar{f}_2(+1)-\bar{f}_2(-1)\right]}{M_2\Omega_2\left[\bar{f}_1(+1)-\bar{f}_2(-1)\right]} = \frac{M_2\Omega_2\left[\bar{f}_2(+1)+1\right]}{2M_2\Omega_2} \quad \ldots\ldots \quad (8\text{-}11)$$

Simplifying equation (8-11) gives the alternative form,

$$\eta_{R,C} = \frac{1}{2}\left[\bar{f}_2(+1)+1\right] \quad \ldots\ldots \quad (8\text{-}12)$$

It is clear from the latter equation that the range of $\eta_{R,C}$ is zero to unity, and that a cooling-period effectiveness of unity represents the situation in which the cold fluid is heated to the same temperature, as that of the incoming hot fluid.

Combining equations (8-2) and (8-11) we obtain

$$\eta_{R,C} = \frac{H_{T,2}}{2M_2\Omega_2} \quad \ldots\ldots \quad (8\text{-}13)$$

Noting that for any particular computation, $H_{T,2}$ in equation (8-13) will be the value of H_T^* obtained by the method described earlier, we then have from equation (8-13)

$$\eta_{R,C} = \frac{H_T^*}{2M_2\Omega_2} \quad \ldots\ldots \quad (8\text{-}14)$$

Finally, we see from equations (8-10) and (8-11) that for

$M_2\Omega_2 < M_1\Omega_1$, $\eta_R = \eta_{R,C}$ $\ldots\ldots$ (8-15)

but for $M_1\Omega_1 < M_2\Omega_2$, $\eta_R = \left(\frac{M_2\Omega_2}{M_1\Omega_1}\right)\eta_{R,C}$ $\ldots\ldots$ (8-16)

8.3.2 Program 2 Tests Covering a Range of Regenerator Examples

(a) Selection of Test Examples

As stated earlier, the principal aim of this second series of tests was to investigate the results obtained from Program 2, for examples having $\Omega_1 \neq \Omega_2$. Also, with a view to the application of the program to practical regenerator calculations, the ranges of regenerator parameters to be studied needed to vary around the following values, which are considered to be typical of modern blast-furnace stoves:- $N_1 = 0.63$, $N_2 = 0.44$, $M_1 = 0.021$, $M_2 = 0.035$, $\Omega_1 = 8$, $\Omega_2 = 4$ (see Table 13 for further details).

To meet these requirements, five different groups of examples were drawn-up, each group having a different ratio of $\Omega_1:\Omega_2$. The five ratios considered were $\Omega_1:\Omega_2$ = 10:4, 8:4, 6:4, 5:4 and 4:4, where the first and second numbers of each ratio are the actual values of Ω_1 and Ω_2 used in the calculations.

To provide some indication of the effect of changes in M_1 and M_2 on the calculated regenerator performance, each of the above groups were arranged to contain five examples. Within any group, each example was given a different value of M_1 chosen from M_1 = 0.02, 0.04, 0.06, 0.08 or 0.1; the corresponding value of M_2 being determined such that $M_2 = 2M_1$.

The values of N_1 and N_2 used for the entire set of examples were 1.5 and 0.3 respectively. It will be noted from these figures that unlike the other five parameter values featured in these tests, the value of N_1 was somewhat larger than the corresponding 'typical' value quoted in the first paragraph. The reason for hoosing the higher value was related to the question of the numerical accuracy of the effectiveness predictions. Recalling from the Program 1 assessment (see FIGS. 14 and 15), that the largest numerical errors in the predicted η_R-values occurred in examples for which N_1 was largest, the same value viz. $N_1 = 1.5$, was selected for these Program 2 computations. Assuming the same situation would prevail, the expectation was that, for corresponding examples having smaller values of N_1, the fractional error in any predicted $\eta_{R,C}$ value would not exceed those determined for these selected test examples.

(b) Analysis of Results

Following the computation of these five sets of examples by Program 2, analysis of the results commenced with an examination of the convergence graphs constructed from the computed values of $H_{T,1}$ and $H_{T,2}$. The occurrence of each of the five types of convergence graph, depicted in FIG. 16, is summarised in Table 12.

We see from Table 12 that the type of graph obtained for a given example was principally determined by the ratio of $\Omega_1:\Omega_2$. Thus for $\Omega_1/\Omega_2 \geq 2$, all of the graphs were of Type A, whereas those for $\Omega_1/\Omega_2 = 1$ were of Type D. However, for

TABLE 12

TYPES OF CONVERGENCE GRAPHS OBTAINED FROM THE PROGRAM 2 COMPUTATION OF EXAMPLES HAVING $\Omega_1 \neq \Omega_2$

Ω_1	Ω_2	M_1	0.02	0.04	0.06	0.08	0.1
		M_2	0.04	0.08	0.12	0.16	0.2
10	4		A	A	A	A	A
8	4		A	A	A	A	A
6	4		D	C	*	A	B
5	4		D	D	D	E	E
4	4		**	D	D	D	D

* $H_{T,1}$ and $H_{T,2}$ lines were virtually co-incident.

** No graph possible.

$N_1 = 1.5$, $N_2 = 0.3$ in all examples tested.

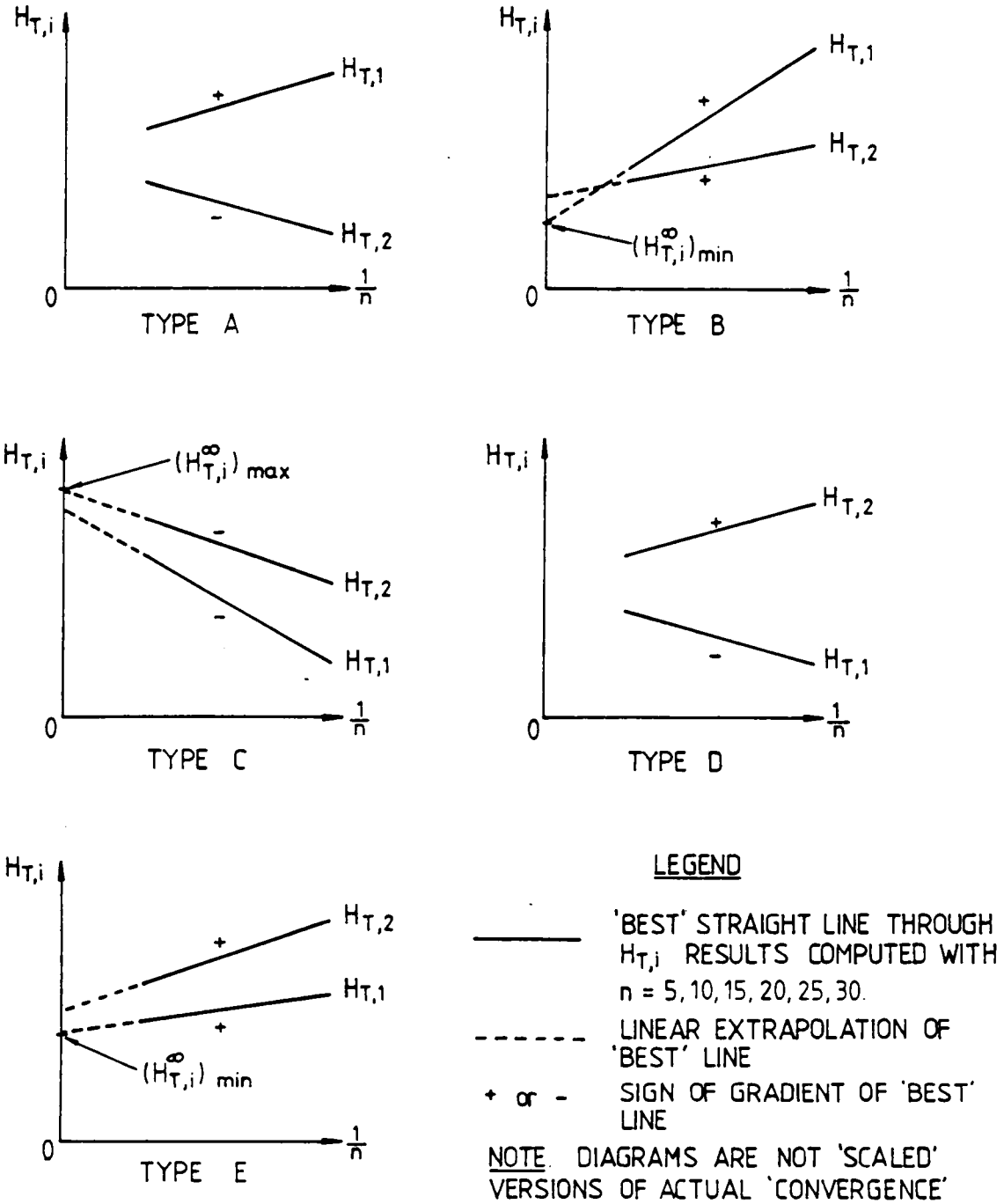

FIG. 16 DIAGRAMS (PLOTTED ON LINEAR - LINEAR GRAPH PAPER) SHOWING THE TYPES OF $H_{T,i}$ V. $\frac{1}{n}$ 'CONVERGENCE' GRAPHS OBTAINED FROM THE PROGRAM 2 PREDICTIONS

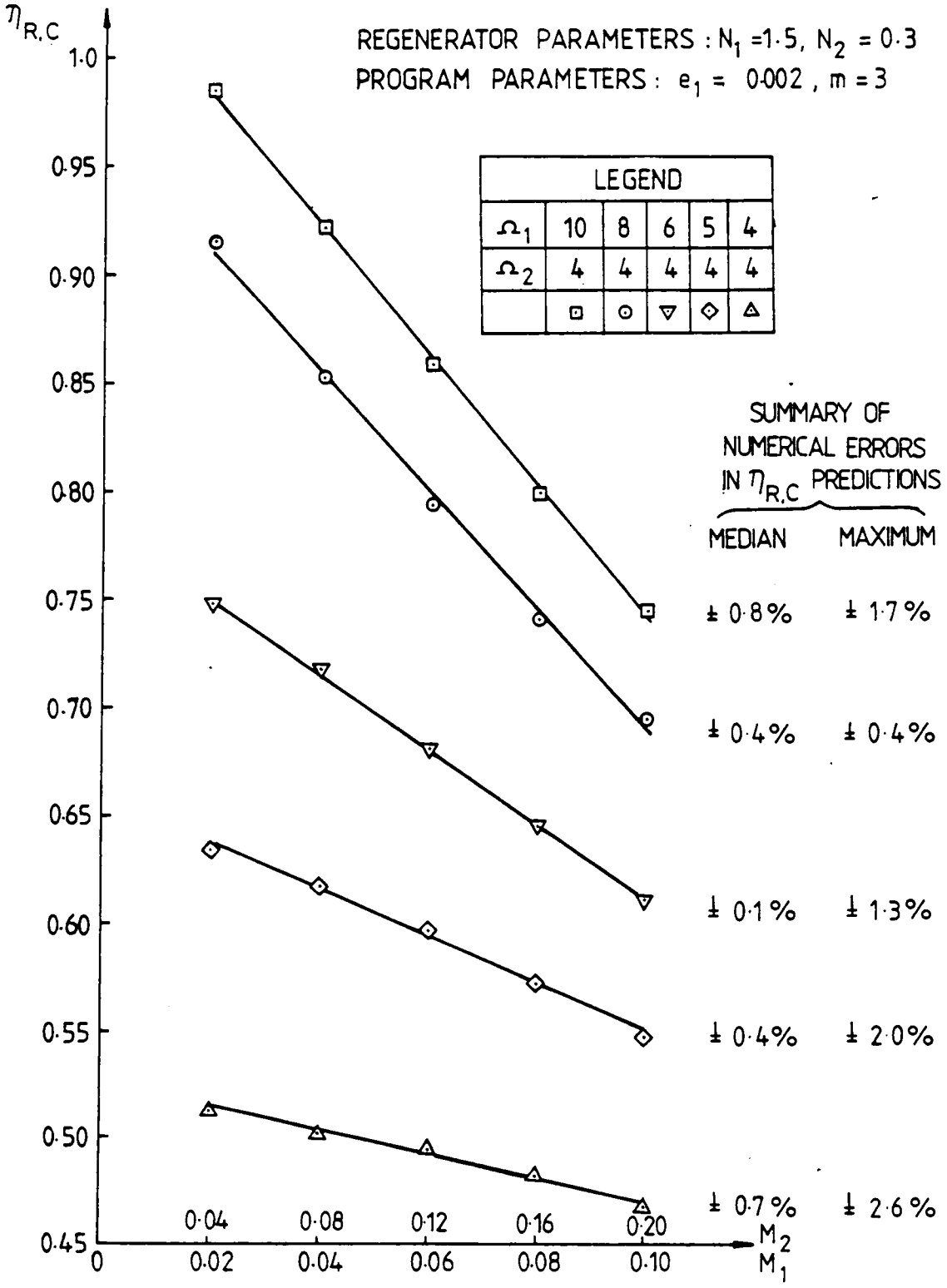

FIG. 17 EFFECT OF VARYING M_i AND Ω_i ON THE PREDICTED COOLING-PERIOD EFFECTIVENESS, $\eta_{R,C}$

$1 < \frac{\Omega_1}{\Omega_2} < 2$, the type of graph varied from A through to E, according to the values of M_1 and M_2.

Next, applying the appropriate formula from equations (8-3) to (8-8), and then incorporating each H_T^* value into equation (8-14), the effectiveness $\eta_{R,C}$ was determined for each example. These results are shown in graphical form in FIG. 17, the five curves in this diagram containing the results from each of the five groups of examples considered.

The quantitative increase in the cooling-period effectiveness brought about by increasing the ratio $\Omega_1:\Omega_2$ from 1 through to 2.5, with M_1, M_2, N_1 and N_2 invariant, is immediately evident from the FIG. 17 curves. In a more practical interpretation, for a regenerator operating with constant fluid flow rates and invariant heat-transfer coefficients, the curves indicate the extent to which $\eta_{R,C}$ (and hence the pre-heat temperature) rises by increasing the ratio of the heating-period time to the cooling-period time.

Considering now the individual curves in FIG. 17, it is intriguing to observe that, over the ranges considered, the predicted effectiveness values varied linearly with M_1 (and hence also with M_2, because $M_2 = 2M_1$), with the largest values of $\eta_{R,C}$ occurring at the smallest values of M_1 and M_2. Hence for a given regenerator system operating within the conditions specified for these tests, the cooling-period effectiveness therefore increases linearly as the hot and cold fluid flow rates both decrease.

With the exception of the curve for $\Omega_1:\Omega_2 = 8:4$, the maximum fractional error associated with each of the $\eta_{R,C}$ values plotted in FIG. 17 showed considerable variation along each curve. For all curves, except the one just mentioned, the largest error value occurred at the left-hand end of the curve (for the example with $M_1 = 0.02$, $M_2 = 0.04$), and in every case this value was considerably higher than those for other examples on the curve. To reflect these variations, the summary of the fractional errors in $\eta_{R,C}$ given in FIG. 17 therefore quotes the maximum error and also the median error obtained for each curve.

Inspection of these latter figures reveals that although the predicted $\eta_{R,C}$ values were in error by up to $\pm 2.6\%$, the median values were below 1% for all curves. We also note that the fractional errors relating to the predictions for the curve having $\Omega_1:\Omega_2 = 8:4$ were consistently less than 0.5%, although the reasons for these lower values are not clear.

Finally, it should be mentioned that of the entire set of examples investigated for FIG. 17, all but one were successfully computed by Program 2. The single exception was the example defined by $\Omega_1 = \Omega_2 = 4$, $M_1 = 0.02$, $M_2 = 0.04$, for which the program produced absurd solutions. Because the periods were equal, the same example was re-computed with Program 1, but this also gave solutions of unsatisfactory accuracy. However, computation of the corresponding 'invert'*

*See Appendix 8 for theory of 'invert' regenerator.

example (with both programs) provided solutions free from all anomalies; those obtained from Program 2 being entered in FIG. 17.

This particular example, together with Example 15 of Table 7 for which Program 1 had also given solutions of poor accuracy, are examined in more detail in Chapter 9.

8.4 COMPUTATION OF TYPICAL STOVE SYSTEMS

To complete this assessment of the more general version of the non-iterative solution method, Program 2 was used to calculate two examples which are considered to be typical of blast-furnace stove systems. The regenerator parameters for these examples, which we refer to as examples 16 and 17, have been derived, in the case of example 16, from data available in the technical literature, and for example 17, from data communicated directly to the author. This latter data refer to a stove in operation at the time of writing.

A summary of these parameters is given in Table 13. A third system is included in Table 13 simply for comparison purposes, but no computations have been carried out for this system, which is considered to be less representative of modern equipment.

Computation by Program 2 and subsequent analysis by the procedure given in Section 8.3.1 yielded the results presented in Table 14. For comparison the values of $\eta_{R,C}$ and $\bar{f}_2(+1)$ predicted by Hausen's theory [36], have been included in Table 14. For both examples tested, the

results obtained from these two 'analytical' methods of solution are in good agreement. However the high values of $\eta_{R,C}$, and hence of $\bar{f}_2(+1)$, are a somewhat surprising feature of both examples.

TABLE 13

REGENERATOR PARAMETERS FOR BLAST-FURNACE STOVES

Example Number	REGENERATOR PARAMETERS						Source of Data
	N_1	N_2	M_1	M_2	Ω_1	Ω_2	
16	0.815	0.589	0.0349	0.0631	8.6	4.69	[83]
17	0.632	0.441	0.0207	0.0346	8	4	[84]
-	0.28	0.23	0.02	0.037	15.84	9.36	[85]

TABLE 14

PROGRAM 2 RESULTS FOR EXAMPLES 16 AND 17

Method	PROGRAM 2			HAUSEN	
Example	$\eta_{R,C}$	$E\eta_{R,C}$	$\bar{f}_2(+1)$	$\eta_{R,C}$	$\bar{f}_2(+1)$
16	0.916	±0.3%	0.8316	0.918	0.835
17	0.989	±1.4%	0.978	0.985	0.97

CHAPTER 9

DISCUSSION

Prior to the commencement of this research, closed-form solutions of the equations of the regenerator, 3-D, cyclic equilibrium, linear model had been derived by Collins and Daws [72] and Edwards [37] respectively, to cater for the following two cases of regenerator operation:- (a) heating and cooling periods of equal duration only - the 'equal-period' theory, and (b) heating and cooling periods of equal or of unequal duration - the 'generalised' theory. Additional mathematical techniques were also developed by Edwards et al [74] for calculating, from these 'closed' solutions, the hot and cold fluid temperature histories at selected regenerator positions, over a complete cycle. However, a feasibility study [74] , which was restricted almost exclusively to the 'equal-period' theory, whilst giving encouraging results in certain cases, had highlighted serious deficiencies. These deficiencies clearly inhibited the use of this theoretical approach for meaningful design calculations.

As a result of the studies reported in the preceding chapters, it is now known that these deficiencies arose because no effective procedures existed for controlling the numerical accuracy of a given set of computed solutions. At that time, the factors which affected the numerical accuracy of a computation were not clearly understood and an assessment of the accuracy of any computation was limited to the application of a final heat-balance check. This simply tested the difference between the heat-transfer rates computed for successive periods. Even on this basis,

however, it was found that many of the selected test computations were not of an acceptable accuracy because the computed solutions were not thermally well-balanced. Large heat-balance discrepancies were a consistent feature of examples in which the dimensionless period, Ω , was large. Also, for certain examples, some having small values of Ω , technologically meaningless solutions were computed for no obvious reason.

From this starting position, techniques have been developed for controlling the numerical accuracy of computed solutions. Application of these techniques has enabled all of the previously reported computational difficulties to be resolved satisfactorily. In addition, methods have also been developed which it is believed enable the regenerator effectiveness, η_R, to be predicted more accurately for examples computed using either of the two theories.

A procedure has also been developed for estimating the numerical error ($E\eta_R$) in each predicted value of η_R. Because of this, the numerical accuracy of predictions from the non-iterative method no longer relies solely on the application of a final heat-balance test, although the attainment of a small heat-balance discrepancy is still an important requirement in any computation.

Now we have seen that the computation of regenerator fluid temperatures using either the 'equal-period' theory or

the more general theory requires the application of three quite separate numerical procedures. These are firstly, the evaluation of a number of infinite series; secondly, the use of numerical methods to approximate certain definite integrals (i.e. numerical quadrature); and thirdly, the numerical integration of a set of linear, simultaneous differential equations. This research has confirmed that the two 'closed' theories being studied can only be applied successfully provided the numerical errors - predominantly truncation errors - inherent in each of these three processes, together with any round-off errors which are accumulated during the computation, are all controlled to suitably small values.

Provided arithmetical computations are carried out with suitable precision, accumulated round-off errors have not been found to have a marked effect on the numerical accuracy of computed solutions. However, for examples 4 to 8 of Table 2 the introduction of a simplified matrix analysis in order to reduce the number and complexity of the matrix calculations (and thereby any associated round-off errors), did improve computational accuracy. An appropriate simplified analysis has therefore been used for both theories.

As far as the summation of infinite series is concerned, it was already known from previous work on the 'equal-period' theory by Edwards et al [74], that the accurate evaluation of all relevant infinite series was a necessary but not a sufficient condition for computing solutions which were

thermally well-balanced. In the earlier study, Edwards derived a number of tests for the 'equal-period' theory, which could be applied during the summation calculations to ensure that the fractional error in the calculated sum of every infinite series did not exceed a pre-selected value, e_1. In the course of these further studies, an additional set of tests has been developed to ensure that the calculated value of every infinite series needed for the 'generalised' theory can also be determined with a fractional error not exceeding e_1. The programs written to compute solutions from the 'equal-period' theory and the more general theory, Programs 1 and 2, respectively, have therefore incorporated these tests, as appropriate. In each program the value of e_1 can be set to any desired level in the program input data, and detailed checks carried out with both programs have shown that, for thermally well-balanced results, e_1 should not exceed 0.002. However, setting e_1 to lower values than this has little further beneficial effect either on the heat-balance discrepancy or on the accuracy of the η_R predictions.

Truncation errors which occur when the systems of differential equations (3-21) or (7-15) are solved by finite-difference techniques have been shown to be readily controlled by a suitable choice of algorithm and distance-step size. In almost all examples tested, predicted effectiveness values of an acceptable numerical accuracy were obtained by applying the Crank-Nicolson finite-difference approximations with the regenerator length divided into six intervals (m=3).

However, for a small number of examples, which are discussed in more detail below, double the number of distance intervals were required in order to obtain satisfactory results. Increasing the value of m above six had only a very small effect on the values predicted for η_R.

In the present development, the method used to approximate the integrals in equations (2-5), (2-6), (2-13) and (2-14) is the one which the earlier feasibility study [74] had shown to be the most successful for producing solutions which were thermally well-balanced. Even so, it was known that application of the method with the dimensionless period Ω divided into five time steps, (n=5), had failed consistently to produce thermally well-balanced solutions for any example for which Ω was greater than unity. However, experiments carried out with Program 1 have confirmed that the large heat-balance discrepancies obtained for such examples were directly attributable to inaccuracies which occurred because only five time steps were used for the numerical integrations. Increasing the accuracy of the integrations, by carrying out the computation process with a larger value of n, has proved to be an effective way of attaining heat-balance discrepancies below one per cent for examples having Ω as high as ten, the largest value of practical interest.

Thus on the basis of attaining a final heat-balance discrepancy of less than one per cent, it appeared at first that a single computation using appropriate values of e_1, m and n would be sufficient to enable predictions of a

satisfactory accuracy to be obtained from both closed theories. However, later investigations indicated that this criterion is not satisfactory in many cases. This is because, even with n=30, the computed values of $\dot{H}_i$ (equal-period theory) and $H_{T,i}$ (generalised theory) will not have converged sufficiently for these (n=30) values to be taken as the numerically correct (i.e. the zero step-size or fully-converged) values of these parameters. Because computations with higher values of n are not practicable with either Program 1 or Program 2, the required zero step-size values of these variables, $\dot{H}^*$ and H_T^*, generally have to be obtained by extrapolating the linear relationships which were found to exist between $\dot{H}_i$ and $\frac{1}{n}$, (see FIG.9), and between $H_{T,i}$ and $\frac{1}{n}$.

In practice, therefore, in order to establish the linear relationships needed to predict $\dot{H}^*$ or H_T^* (and hence η_R) for any regenerator example, three separate computations have to be made with each set of regenerator data. Each computation uses a different value of n (either 5, 10 or 30), the values of e_1 and m being the same, usually 0.002 and 3 respectively, for each computation.

As evidenced from FIGS. 14, 15 and 17, application of this procedure has enabled predictions with acceptably small values of $E\eta_R$ to be obtained, from both closed theories, for a large number of examples. These cover a wide range of regenerator parameter values of practical interest.

In spite of this, however, the need to perform three complete computations for each η_R prediction is disappointing

because it elaborates the prediction procedure and consequently increases the computer time needed for each prediction. Moreover, the need to resort to small step sizes, reflects the relatively poor accuracy of the method used for the numerical quadratures, a factor which has also prevented the predicted values of η_R being obtained with a greater degree of certainty (i.e. to a known degree of numerical accuracy).

An analysis of the computing times recorded for many of the examples whose results are included in FIGS. 14 and 15 has shown that for the 'equal-period' theory, the total computer time needed to predict the regenerator effectiveness, for a given example, will be close to 44 seconds. This figure is obtained from the typical set of times recorded with Program 1, as displayed in Table 10, and is the sum of the times for computations with n=5, 10 and 30. It is quite clear from these figures that the need to include a computation with n=30 makes a significant adverse contribution to the total computation time.

For computations carried out with the 'generalised' theory, the total computer time needed for each η_R prediction is about 205 seconds, almost five times longer than the corresponding Program 1 time. Now the first stage of the Program 2 computation involves considerably more calculations than the corresponding stage of the Program 1 computation. Computation times with Program 2 are therefore inevitably longer than those for Program 1. However, this factor alone does not seem sufficient to explain the observed five-fold

increase in computation time. A possible explanation may lie in the use in Program 2 of a simpler but perhaps slower method for calculating the roots, β_s, of equation (2-12), c.f. Appendices 7 and 5. This particular aspect clearly merits further examination with a view to reducing the computer times for Program 2.

Because, up to this stage, the main consideration has been to obtain valid predictions from both theories, no particular efforts have been made to minimise the computation times or the computer memory requirements for either Programs 1 or 2. However, in the light of the studies undertaken so far, both these aspects could be improved. For instance the use of pre-calculated values of β_s, accessed from a data file, would be much faster than the procedure currently adopted, which is to evaluate all the required roots every time the programs are run. Summing each infinite series to a fixed number of terms, and also reducing the maximum number of distance steps catered for in each program from 96 to 12, would simplify both programs and lead to a considerable diminution in the memory space needed for each program.

Although the introduction of the first of these suggestions would be of some benefit in reducing computing times, it is felt that the only way of making a significant improvement in this area would be to avoid the use of very small step sizes by using a more accurate method for approximating the integrals in equations (2-5), (2-6), (2-13) and (2-14). This implies the use of an accurate quadrature

formula having a small associated error term. Although many such formulae exist, their application within these closed theories is not a straight-forward exercise, principally because of the possible occurrence of divergent infinite series (see [37]).

A major factor in deciding whether or not to pursue any of the above 'time-saving' suggestions is the extent to which the computer times reported above for Programs 1 and 2 are faster or slower than those required for the alternative, completely iterative, i.e. 'open' methods of computation.

Several investigators [61, 62, 67, 68] have reported the application of 'open' methods for solving the equations of the regenerator, 3-D model, but the only computation times quoted for these methods appear to be those given, for one example, by Khandwawala and Chawla [62] . These authors report computing times of 31 seconds and 33 seconds for calculations made using the Alternating Direction Approximation (A.D.A.) and the Dufort and Frankel methods, respectively. The example concerned had equal heating and cooling periods and comparison with the times quoted in Table 10, for similar examples, shows that the 'closed-method' times recorded when Program 1 was executed with 5 or 10 time steps were much shorter than the above 'open-method' times. However, the total computer time needed to determine η_R using the 'closed' method is longer than both of the 'open-method' times.

Although interesting, this one-off comparison could be quite misleading, firstly because the competing methods were

tested on different computers and with different examples, and secondly, because the extent to which the 'open-method' times vary for different combinations of regenerator parameters is not known. On this latter point, Willmott et al [51] noted when solving the 2-D model equations by an open method, that the convergence to cyclic equilibrium with certain parameter combinations can be extremely slow, with correspondingly long computational times. In order to make a valid comparison, and thereby clarify the direction of future work, it is suggested that the A.D.A. (open) method be programmed for the computer used for the closed-method studies, and the program used to compute a range of the examples already evaluated by Programs 1 and 2.

Carrying out this suggestion would have the additional benefit of providing a detailed comparison of the solutions computed by each method. Up to this stage, it has been possible only to check the values of η_R predicted by the 3-D, 'closed' theories against those predicted by Nusselt's theory [24] for very small values of Ω, and by Hausen's analytical method [36] for larger values of this parameter. The values of η_R presented in FIGS. 14 and 15 are in good agreement with those predicted from Nusselt's theory in all cases tested. However, comparisons with Hausen's method have given conflicting results. Table 14 shows that predictions obtained for two examples using the 'generalised' theory, each example having quite large values of Ω_1 and Ω_2, were in close agreement with the corresponding Hausen predictions. However, predictions obtained from the

'equal-period' theory are only in good agreement with the corresponding Hausen predictions for values of Ω less than about three. For larger values of Ω , the Hausen effectiveness predictions are consistently higher than those obtained via equation (4-3). In the worst case found, at $\Omega = 10$, the predictions differed by about 12%. This disagreement could be due to inaccuracies in either or both methods and it remains a possibility that the extrapolation method, described in Chapter 4, for predicting $\dot{H}^*$ and hence η_R, could be underestimating these parameters. The suggested comparison with an 'open' method should resolve this point.

In earlier chapters, attention has been drawn to a small number of examples for which the normal computational procedure has given rise to a catastrophic error growth and thereby produced technologically-impossible values for the fluid temperatures, f_i. The computations which produced such 'absurd' solutions were:-

examples 2*,3,14 using e_1=0.002, m=3 and n=5 in Program 1.
example 15* using e_1=0.002, m=6,12,24* or 48 and n=5 or 10* in Program 1.
example 18 using e_1=0.002, m=12,24 or 48 and n=5 in Programs 1 and 2.

In certain cases, namely examples 2, 3 and 14, acceptable solutions were obtained by increasing the value of m used in the computations from 3 to 6, whereas for example 15 (Table 7) the required results were determined by computing the

corresponding 'invert' example. However for example 18, which is defined by the parameters N_1=1.5, N_2=0.3, M_1=0.02, M_2=0.04, $\Omega_1=\Omega_2=\Omega$=4, neither of these techniques produced entirely satisfactory solutions.

Investigation of these cases has revealed that the extremely large values of f_i are specifically due to a failure to calculate accurate solutions to the system of algebraic equations (A3-10). In the case of example 15 using n=10 and m=6, and of example 18 using m=24 or m=48 (with Program 2), the determinant of the coefficient matrix $\underline{\beta}$ was computed to be zero (to seven places of decimals), indicating that equations (A3-10) were near-singular. Secondly, checks on the computations identified with an asterisk, in the above list, have shown that the system of equations (A3-10) were grossly ill-conditioned. Both of these conditions lead to large errors in the solutions computed for equations (A3-10), and hence in the required f_i-values.

It is interesting to note that a similar problem of ill-conditioning was encountered by Willmott and Kulakowski [60] when they also used matrix inversion to solve a set of linear algebraic equations. However, as previously mentioned, Kulakowski et al [50] appeared to resolve this difficulty by using a different numerical method to solve the pertinent algebraic equations. In this respect, despite the ill-conditioning, the effect of solving equations (A3-10) by alternative direct or iterative methods could be worth checking.

It also remains a possibility that the ill-conditioning described above occurs because under certain circumstances the Crank-Nicolson method used to integrate equations (3-21) and (7-15) is numerically unstable. The necessary theoretical basis for assessing the stability of the method in a given computation has been determined [86]. However, the computer software needed to carry out the necessary calculations has only recently become available. Despite the small number of examples involved in this category, it is considered that, for completeness, this aspect should also be checked.

As far as the writer is aware, computation of the more comprehensive 3-D, non-linear regenerator model has been contemplated but not attempted. Further development of both 'open' and 'closed' solution methods in this direction is therefore a possible course for further study. However, the development of more elaborate regenerator theories must be weighed against inaccuracies which arise in the regenerator performance predicted by such theories due to the limited nature of the physical data needed for the theoretical calculations. In the high-temperature field, this might particularly apply to convective heat-transfer coefficients, bearing in mind that many designers still refer to experimental data produced some fifty years ago [87,88]. A morefruitful avenue for further research would therefore be the up-dating of such information, coupled with the correlation of actual regenerator performance with that predicted by existing theories.

CHAPTER 10

CONCLUSIONS AND RECOMMENDATIONS

10.1 CONCLUSIONS

1. A non-iterative, 'closed' method for predicting the thermal performance of a regenerator operating at cyclic equilibrium has been developed to the stage where it can be usefully applied to regenerators which operate with equal or with unequal heating and cooling periods.

   The method involves the application of the closed-form solutions derived by earlier workers for the regenerator, three-dimensional thermal model.

2. Two different closed-form 'theories' have been investigated and separately programmed. The first applies only to regenerators which operate with equal heating and cooling periods, whereas the second, more general theory, applies to regenerators for which successive periods are of equal or of unequal duration.

   Each FORTRAN program outputs the computed hot and cold fluid temperature histories, at selected positions along the regenerator length, for a complete cycle. A summary of the overall heat-transfer performance is also an output.

3. The successful application of both 'closed' theories - when assessed by the criterion that the heat-transfer predictions for the heating and cooling

periods should be thermally well-balanced - has been found to depend on the ability to limit the effect of the numerical errors which are an inherent feature of the computational process.

The necessary control of these errors has been achieved by:-

(i) developing mathematical tests to ensure that all relevant infinite series are summed to a pre-selected accuracy;

(ii) selecting suitable methods and step sizes firstly, for numerical quadrature and secondly, for numerical integration of a system of first-order differential equations; and

(iii) simplifying certain matrix calculations.

4. (a) Comprehensive tests, covering a wide range of regenerator parameter values of practical interest, have established that, apart from a few exceptional cases (see 12 below), a final heat-balance discrepancy of less than one per cent can be obtained by setting $m=3$ and $e_1=0.002$ in the program input data. This sets the distance step size for numerical integration equal to one sixth of the regenerator dimensionless length and ensures that each infinite series sum is calculated to an accuracy of 0.2%. However, to maintain this degree of thermal balance, the pre-set value of n, which

governs the step size used for all numerical quadratures, has to be increased progressively from 5 to 30 as the dimensionless period Ω increases in the range $0 < \Omega \leqslant 10$.

(b) These tests have also confirmed that for examples in which $\Omega > 1$, the failure by earlier workers to compute solutions which were thermally well-balanced was due to the inaccuracies which occurred because the numerical quadratures were performed using too large a time-step size.

5. Numerical experiments have shown that for m=3, $e_1 = 0.002$ and $5 \leqslant n \leqslant 30$:-

(a) The values of the mean rates of heat transfer in each period, $\dot{H}_1$ and $\dot{H}_2$, computed by the 'equal-period' theory, and the quantities of heat transferred in each period, $H_{T,1}$ and $H_{T,2}$, computed by the more general theory, are each related linearly to $\frac{1}{n}$, and hence also to the magnitude of the time step used for the numerical quadratures.

(b) The method used to carry out the numerical quadratures (the best of several tried) is not accurate enough to enable the effectiveness of a given regenerator to be predicted from computations which only involve small values of n.

(c) Even when the time step is reduced to a value defined by n=30, it is not possible to determine the regenerator effectiveness to a precise accuracy.

6. For the majority of examples, a method has been devised for predicting the regenerator effectiveness based on an extrapolation of the linear relationships referred to in 5(a). A procedure has also been developed for estimating the numerical error in each effectiveness prediction.

7. On the basis of the methods referred to in 3 and 6 above, extensive numerical tests have demonstrated that technologically useful regenerator predictions can be obtained from both theories for a wide range of regenerator parameter values of practical interest.

8. For each example evaluated by the 'equal-period' theory, a total computer time of about 44 seconds is required in order to predict the corresponding regenerator effectiveness. However, when the 'generalised' theory is used, a total computer time of around 205 seconds is needed for each effectiveness prediction.

Whereas the former time is considered to be reasonable for this application, the latter is unacceptably long.

9. The need to use an extrapolation method in order to predict the regenerator effectiveness has increased the computer time required for each prediction, and has also lessened the confidence with which each prediction is made (see 5(c)).

A more accurate method for numerical quadrature would be required in order to realise the maximum benefits offered by both 'closed' theories in terms of the accuracy of each effectiveness prediction and of the computer time needed for each effectiveness prediction.

10. Analysis of the predictions obtained using the 'equal-period' theory has shown that:-

(a) the regenerator effectiveness increases as the dimensionless period Ω is decreased, but that the extent to which the effectiveness increases for a given change in Ω is much greater for Ω less than about 1.0; and

(b) at very small values of Ω, the 'closed-theory' effectiveness predictions are in good agreement with those predicted from Nusselt's completely analytical solution [24] for the case of infinitesimally-short periods.

11. Analysis of predictions obtained from the 'generalised' theory has shown that:-

(a) for examples in which $\Omega_1 = \Omega_2$, the corresponding effectiveness values predicted from the two 'closed' theories are in good agreement; and

(b) for fixed Biot numbers N_1 and N_2 and provided the ratio Ω_1/Ω_2 is constant in the range $1 \leqslant \frac{\Omega_1}{\Omega_2} \leqslant 2.5$, and provided also that the value of M_2 is double that of M_1 for $0.02 \leqslant M_1 \leqslant 0.1$, the predicted cooling-period effectiveness values decrease linearly with M_2 (and hence with M_1).

12. For a small number of examples, the fluid temperatures computed by the closed-theory programs using certain combinations of the parameters e_1, m and n are technologically impossible. This phenonomenon has been shown to occur because in these cases the system of algebraic equations which are solved to determine the fluid temperatures are either near-singular or severely ill-conditioned, thereby preventing the calculation of accurate solutions.

With the exception of one case, satisfactory results have been obtained for these examples by changing the number of distance steps used for the computation or by computing the corresponding 'invert' example.

10.2 RECOMMENDATIONS

1. A fast, 'open' method for solving the equations of the regenerator model considered in this study should be programmed for a DEC 20 computer and used to obtain a direct comparison of predicted results and also of the numerical efficiency of the 'closed' and 'open' methods of regenerator computation.

2. Improvements to the numerical efficiency and to the numerical accuracy of the predictions obtained from the existing 'closed-method' programs should be attempted by:-

   (i) developing a more accurate method for numerical quadrature; and

   (ii) simplifying the procedures used for the summation of infinite series.

3. The much longer times needed to compute each example using the 'generalised-theory' program should be investigated with a view to reducing them to values much closer to those obtained with the 'equal-period' program.

4. The stability of the numerical method used for solving a system of first-order differential equations should be examined particularly for those computations which produced 'absurd' results.

REFERENCES

1. Reay, D.A., 'Industrial Energy Conservation', Pergamon Press, Oxford, 1977.

2. Shah, R.K., 'Classification of Heat Exchangers' in 'Heat Exchangers, Thermal-Hydraulic Fundamentals and Design', Hemisphere Publishing Corporation, New York, McGraw-Hill, pp. 9-46, 1981.

3. Hausen, H., 'Heat Transfer in Counterflow, Parallel Flow and Cross Flow', (English Translation), McGraw-Hill Inc., New York, 1983.

4. Fraas, A.P., Ozisik, M.N., 'Heat Exchanger Design', J. Wiley and Sons, New York, 1965.

5. Norton, C.L., 'Pebble Heater - New Heat Transfer Unit For Industry', Chemical and Metallurgical Engineering, pp. 116-119, July, 1946.

6. Schneller, J., Hlavacka, V., 'Moving Bed Heat Exchangers and Regenerators - A Summary of New Design Theory' in 'Heat Exchangers: Design and Theory Sourcebook', Scripta Book Co., Washington D.C., McGraw-Hill, pp. 695-707, 1974.

7. Edwards, J.V., Probert, S.D., 'Regenerator and Recuperator Design', Chemical and Process Engineering - Heat Transfer Survey, pp. 46-53, 1969.

8. Shah, R.K., 'Heat Exchanger Design Methodology - An Overview', in 'Heat Exchangers, Thermal-Hydraulic Fundamentals and Design', Hemisphere Publishing Corporation, New York, McGraw-Hill, pp. 455-459, 1981.

9. Schofield, M., 'The Regenerative Gas Furnace of Siemens', Iron and Coal, pp. 143-144, Jan. 20th, 1961.

10. Clark-Monks, C., 'The Cost of Regenerator Efficiency', Glass Technology, 18, No.3, pp. 66-71, 1977.

11. Smith, J.L., 'Thermal Regenerators in the Glass Industry', in Symposium: 'Low Cost Heat Recovery by Thermal Regenerators', Inst. Chem. Eng., Yorkshire Branch, Leeds, Nov., 1976.

12. Evans, J.L., 'Furnace Design and Operations - Key to Refractory Performance', Refractories Journal, 4, pp. 9-16, 1980.

13. Scott, R.B., 'Cryogenic Engineering', D.Van Nostrand Co., New Jersey, 1967.

14. Orr, N.B., 'The Rotary Regenerative Preheater, A Low Cost Mechanism For Heat Recovery', in Symposium: 'Low Cost Heat Recovery by Thermal Regenerators', Inst. Chem. Eng., Yorkshire Branch, Leeds, Nov., 1976.

15. Butler, P., 'Use the Munter Wheel to Recover Your Heat and Make Big Savings', The Engineer, p. 24, 20th Nov., 1975.

16. Rahnke, C.J.R., 'Structural Design of Ceramic Rotary Heat Exchangers', in 'Compact Heat Exchangers - History, Technological Advancement and Mechanical Design Problems', A.S.M.E. Symposium, Chicago, pp. 153-159, Nov., 1980.

17. Penny, R.N., 'Regenerators For High Temperature Gas Turbine Engines', Proc. Inst. Mech. Engs., 183, pp. 110-120, 1968-69.

18. Hryniszak, W., 'Heat Exchangers', Butterworths Publications Ltd., London, 1958.

19. Thornley, D.L., 'Heat Recovery Techniques', The Electricity Council Conference: 'Energy - The Economics and Techniques of Efficient Use', London, April, 1976.

20. Dunkle, R.V., Banks, P.J., 'Wound Parallel Plate Exchangers For Air-Conditioning Applications' in 'Compact Heat Exchangers - History, Technological Advancement and Mechanical Design Problems', A.S.M.E. Symposium, Chicago, pp. 65-71, Nov., 1980.

21. O'Neill, J.S., 'Seals for Rotary Regenerative Heat Exchangers', Tribology Int., 10, No.2, pp. 86-92, April, 1977.

22. Hansrani, S.P., 'British Steel Recuperates', Energy Manager, pp. 50-53, Nov., 1982.

23. Mondt, J.R., 'Correlating The Effects of Longitudinal Heat Conduction on Exchanger Performance' in 'Compact Heat Exchangers - History, Technological Advancement and Mechanical Design Problems', A.S.M.E. Symposium, Chicago, pp. 123-134, Nov., 1980.

24. Nusselt, W., 'Die Theorie des Winderhitzers', Zeitschr. Verein. deutscher Ing., 71, No. 3, pp. 85-91, Jan., 1927.

25. Jakob, M., 'Heat Transfer', Vol. II, J. Wiley and Sons, New York, 1957.

26. Coppage, J.E., London, A.L., 'The Periodic-Flow Regenerator-A Summary of Design Theory', Trans. Amer. Soc. Mech. Engs., 75, pp. 779-787, July, 1953.

27. Anzelius, A., 'Uber Erwarmung vermittels durchstromender Medien', Zeitschr. f. angew. Math. und Mech., 6, No. 4, pp. 291-294, Aug., 1926.

28. Schumann, T.E.W., 'Heat Transfer: A Liquid Flowing Through a Porous Prism', Journ. Franklin Inst., 28, pp. 405-416, 1929.

29. Nusselt, W., 'Der Beharrungszustand im Winderhitzer', Zeitschr. Verein. deutscher Ing., 72, No. 30, pp. 1052-1054, July, 1928.

30. Hausen, H., 'Uber die Theorie des Warmeaustausches in Regeneratoren', Z.A.M.M., 9, No. 3, pp. 173-200, June 1929. Available in English as Library Translation No. 126, of the Royal Aircraft Establishment.

31. Hausen, H., 'Naherungsverfahren zur Berechnung des Warmeaustausches in Regeneratoren', Z.A.M.M., 11, No.2, pp. 105-114, April, 1931.

32. Heiligenstaedt, W., 'Die Berechnung von Warmespeichern', Arch. fur das Eisenhuttenw., 4, pp. 217-222, 1928.

33. Schmeidler, W., 'Mathematische Theorie der Warmespeicher', Z.A.M.M., 8, No. 5, pp. 385-393, Oct., 1928.

34. Rummel, K., 'The Calculation of the Thermal Characteristics of Regenerators', J. Inst. Fuel, pp. 160-173, Feb. 1931.

35. Schack, A., 'Die Berechnung der Regeneratoren', Archiv. fur das Eisenhuttenw., 17, No. 5/6, pp. 101-118, Nov./Dec., 1943.

36. Hausen, H., 'Improved Calculations for Heat Transfer in Regenerators', Z.V.D.I., 2, pp. 31-43, 1942. (Iron and Steel Institute English Translation No. 138).

37. Edwards, J.V.,'Computation of Transient Temperatures in Regenerators at Cyclic Equilibrium', M.Sc. Thesis, University of Wales, 1968.

38. Schack, A., 'Industrial Heat Transfer', Chapman and Hall, London, 1965.

39. Razelos, P., 'History and Advancement of Regenerator Thermal Design Theory', 'Compact Heat Exchangers - History, Technological Advancement and Mechanical Design Problems', A.S.M.E., (Winter Meeting), pp. 91-100, Nov., 1980.

40. Tipler, W., 'A Simple Theory of the Heat Regenerator', Shell Technical Report ICT/14 (1947); Proc. 7th Int. Congr. Appl. Mech., Section III, p. 196, London, 1948.

41. Schalkwijk, W.F., 'A Simplified Regenerator Theory', British Chemical Engineering, pp. 33-34, Jan., 1960.

42. Traustel, S., 'Auslegung von Regeneratoren', Brennstoff-Warme-Kraft, 24, pp. 14-16, 1972.

43. Saunders, O.A., Smoleniec, S., 'Theory of Heat Regenerators', VII International Congress of Applied Mechanics, 3, pp. 91-105, 1948.

44. Allen, D.N. de G., 'The Calculation of the Efficiency of Heat Regenerators', Quart. Journ. Mech. and Appl. Math., 5, Pt.4, 455-461, 1952.

45. Lambertson, T.J., 'Performance Factors of a Periodic-Flow Heat Exchanger', Trans. Am. Soc. Mech. Eng., 159, pp. 586-592, April, 1958.

46. Willmott, A.J., 'Digital Computer Simulation of a Thermal Regenerator', J. Heat Mass Transfer, 7, pp. 1291-1302, 1964.

47. Bahnke, G.D., Howard, C.P., 'The Effect of Longitudinal Heat Conduction on Periodic-Flow Heat Exchanger Performance', Trans. A.S.M.E., J. of Engr. for Power, Series A, 86, pp. 105-120, April, 1964.

48. Iliffe, C.E., 'Thermal Analysis of the Contra-flow Regenerative Heat Exchanger', Proc. Inst. Mech. Eng., 159, pp. 363-372, 1948.

49. Nahavandi, A.N., Weinstein, A.S., 'A Solution to the Periodic-Flow Regenerative Heat Exchanger Problem', Appl. Sci. Res., A10, No. 5, pp. 335-348, 1961.

50. Kulakowski, B., Anielewski, J., 'Application of the Closed Methods of Computer Simulation to Nonlinear Regenerator Problems', Arch. Automat. Telemech., 24, Part 1, pp. 43-63, 1979.

51. Willmott, A.J., Thomas, R.J., 'Analysis of the Long Contra-flow Regenerative Heat Exchanger', J. Inst. Maths. Applics., 14, pp. 267-280, 1974.

52. Phillips., G.M., Taylor, P.J., 'Theory and Applications of Numerical Analysis', Academic Press, London, 1973.

53. Willmott, A.J., Duggan, R.C., 'Refined Closed Methods for the Contra-flow Thermal Regenerator Problem', Int. J. Heat Mass Transfer, 23, pp. 655-662, 1980.

54. Romie, F.E., 'Periodic Thermal Storage: The Regenerator', Trans. A.S.M.E., 101, Part 4, pp. 726-731, Nov., 1979.

55. Willmott, A.J., 'Simulation of a Thermal Regenerator Under Conditions of Variable Mass Flow', Int. J. Heat Mass Transfer, 11, pp. 1105-1116, 1968.

56. Willmott, A.J., 'Operation of Cowper Stoves Under Conditions of Variable Flow: A Computer Study', J. Iron Steel Inst., 206, pp. 33-38, Jan., 1968.

57. Hofmann, E.E., Kappelmayer, A., 'Mathematical Model of a Hot-blast Stove with External Combustion Chamber' in 'Mathematical Models in Metallurgical Process Development', Iron and Steel Institute Conference, London, Feb., 1969.

58. Razelos, P., Benjamin, M.K., 'Computer Model of Thermal Regenerators with Variable Mass Flow Rates', Int. J. Heat Mass Transfer, 21, pp. 735-743, 1978.

59. Razelos, P., Benjamin, M.K., 'Thermal Analysis of Blast Furnace Stove Regenerator System by Computer Simulation', Proc. Heat and Mass Transfer in Metallurgical Systems, Int. Cent. of Heat and Mass Transfer Seminar, Dubrovnik, Sept., 1979.

60. Willmott, A.J., Kulakowski, B., 'Numerical Acceleration of Thermal Regenerator Simulations', Int. J. Numerical Methods in Engineering, 11, pp. 533-551, 1977.

61. Manrique, J.A., Cardenas, R.S., 'Digital Simulation of a Regenerator', 5th Int. Heat Transfer Conference, Tokyo, pp. 190-194, Sept., 1974.

62. Khandwawala, A.I., Chawla, O.P., 'Digital Simulation of Counterflow Regenerator Two-dimensional Model by Two Relatively New Techniques', Int. J. Heat Fluid Flow, 2, No. 2, pp. 67-75, 1980.

63. Ames, W.F., 'Numerical Methods for Partial Differential Equations', 2nd Ed., Thomas Nelson and Sons, 1977.

64. Crank, J., Nicolson, P., 'A Practical Method for Numerical Evaluation of Solutions of Partial Differential Equations of the Heat-Conduction Type', Proc. Camb. Phil. Soc., 34, pp. 50-76, 1947.

65. Mitchell, A.R., Pearce, R.P., 'High Accuracy Difference Formulae for the Numerical Solution of the Heat Conduction Equation', Computer J., 5, pp. 142-146, 1962.

66. Carpenter, K.J., 'An Investigation of Thermal Regenerator Design', Ph.D. Thesis, University of Leeds, 1976.

67. Heggs, P.J., Carpenter, K.J., 'Prediction of a Dividing Line Between Conduction and Convection Effects in Regenerator Design', Trans. I. Chem. E., 56, No. 2, pp. 86-90, 1978.

68. Willmott, A.J., 'The Regenerative Heat Exchanger Computer Representation', Int. J. Heat Mass Transfer, 12, pp. 997-1014, 1969.

69. Razelos, P., Lazaridis, A., 'A Lumped Heat-Transfer Coefficient For Periodically-Heated Hollow Cylinders', Int. J. Heat Mass Transfer, 10, pp. 1373-1387, 1967.

70. Hinchcliffe, C., Willmott, A.J., 'Lumped Heat-Transfer Coefficients for Thermal Regenerators', Int.J. Heat Mass Transfer, 24, pp. 1229-1236, 1981.

71. Heggs, P.J., Carpenter, K.J., 'A Modification of the Thermal Regenerator Infinite Conduction Model to Predict the Effects of Intraconduction', Trans. I. Chem. E., 57, pp. 228-236, 1979.

72. Collins, R.D., Daws, L.F., Taylor, J.V., 'Heat Transfer in Regenerators', British Iron and Steel Research Association Report SM/A/169/55, 1955.

73. Kardas, A., 'On a Problem in The Theory of the Uni-directional Regenerator', Int. J. Heat Mass Transfer, 9, pp. 567-579, 1966.

74. Edwards, J.V., Evans, R., Probert, S.D., 'Computation of Transient Temperatures in Regenerators', Int. J. Heat Mass Transfer, 14, pp. 1175-1202, 1971.

75. Ralston, A., Wilf, H.S., 'Mathematical Methods for Digital Computers', Vol. 1, J. Wiley and Sons, New York, 1960.

76. Forsythe, G.E., Malcolm, M.A., Moler, C.B., 'Computer Methods for Mathematical Computations', Prentice-Hall, New York, 1977.

77. Lambert, J.D., 'Computational Methods in Ordinary Differential Equations', J. Wiley and Sons, London, 1974.

78. Lapidus, L., Seinfeld, J.H., 'Numerical Solution of Ordinary Differential Equations', Academic Press, London, 1971.

79. I.B.M. Corporation, 1130 Scientific Subroutine Package, (1130-CM-02X). Programmer's Manual - Fifth Edition, I.B.M. Technical Publications Dept., New York, 1970.

80. Bayley, F.J., Owen, J.M., Turner, A.B., 'Heat Transfer', T. Nelson and Sons Ltd., London, 1972.

81. Cox, M., Stevens, R.K.P., 'The Regenerative Heat Exchanger for Gas-Turbine Power-plant', Proc. I. Mech.E., 163, pp. 193-205, 1950.

82. Shah, R.K., 'Thermal Design Theory for Regenerators', in 'Heat Exchangers, Thermal-Hydraulic Fundamentals and Design', Hemisphere Publishing Corporation, New York, Mc-Graw Hill, pp 721-764, 1981.

83. Butterfield, P., Schofield, J.S., Young, P.A., 'Hot-Blast Stoves, Part II', J. Iron Steel Inst., 201, pp. 497-508, 1963.

84. Workman, G. - Private Communication.

85. Schofield, J.S., Butterfield, P., Young, P.A., 'Hot-Blast Stoves, Part I', J. Iron Steel Inst., 199, pp. 229-240, 1961.

86. Miles, R.G.,-Private Communication.

87. Kistner, H., 'Determination of Heat-transfer Coefficients and Pressure Losses in Staggered and Straight-Through Basket-Weave Checkers', Arch. Eisenhuttenw., 3, No. 12, pp. 751-768, 1930, British Iron and Steel Research Association Translation, SM/AH/127/56, August 1956.

88. Bohm, H.H.,'Versuche zur Ermittlung der konvektiven Warmeubergangszahlen an gemauerten engen Kanalen', Arch. Eisenhuttenw., 6, pp. 423-431, 1933.

APPENDIX 1

MATHEMATICAL MODEL DERIVED BY COLLINS AND DAWS FOR A REGENERATOR OPERATING WITH EQUAL HEATING AND COOLING PERIODS

MATHEMATICAL MODEL DERIVED BY COLLINS AND DAWS

Collins and Daws considered an equivalent single channel regenerator operating at cyclic equilibrium, with equal heating and cooling periods, as described in Chapter 2.

They made the following assumptions, which are common to most regenerator theories:-

(a) The mass flow rate of each fluid is large enough to permit the use of the approximation:-

$$W_i S_i \frac{\partial t}{\partial y} + w_i S_i \frac{\partial t}{\partial \theta} \simeq W_i S_i \frac{\partial t}{\partial y} .$$

(b) Conduction through the chequer walls is negligible in the direction of fluid flow.

(c) The flow regime is sufficiently turbulent to achieve a uniform fluid temperature in any plane perpendicular to the direction of the fluid flow.

(d) Chequer wall dimensions are constant throughout the regenerator.

(e) Physical properties of the chequer material and of the hot and cold fluids are invariant in both space and time.

(f) In the heating and cooling periods, the heat transfer rate is assumed to be proportional to the temperature difference between the chequer wall surface and the adjacent fluid.

(g) Heat transfer coefficients are also invariant in both space and time.

(h) Fluid mass flow rates are constant throughout each period.

With these assumptions, the regenerator model was derived in the forms stated in equations (A1-1) to (A1-6) below [72]. These forms were eventually obtained following the introduction of dimensionless temperatures, and the use of the normalising substitutions indicated in equations (2-1) to (2-3) of the main text.

Heat flow within the chequer walls is described by the unidirectional form of the heat-conduction equation

$$\frac{\partial^2 E}{\partial \xi^2} = \frac{\partial E}{\partial z} \text{ , for } 0 \leqslant \xi \leqslant 1, -1 \leqslant \zeta \leqslant +1 \text{ and } z \geqslant 0 \qquad \ldots\ldots \text{(A1-1)}$$

The associated boundary conditions are, firstly,

$$\frac{\partial E}{\partial \xi} = 0, \text{ for } \xi = 1 \text{ and } z \geqslant 0 \qquad \ldots\ldots \text{(A1-2)}$$

which specifies zero heat flow at the centre-line of the chequer wall.

Secondly, the heat transferred at the wetted-surface of the chequer walls is described by the equations,

$$\frac{\partial E}{\partial \xi} = N_1(E - \chi) = -M_1 \frac{\partial \chi}{\partial \zeta} \text{ , for } 2\bar{n}\Omega \leqslant z \leqslant (2\bar{n}+1)\Omega,$$

$$\text{and } \xi = 0 \qquad \ldots\ldots \text{(A1-3)}$$

$$\frac{\partial E}{\partial \xi} = N_2(E - \chi) = M_2 \frac{\partial \chi}{\partial \zeta} \text{ , for } (2\bar{n} + 1)\Omega \leq z \leq (2\bar{n} + 2)\Omega,$$

$$\text{and } \xi = 0 \qquad \ldots\ldots \text{(A1-4)}$$

where

$$\left.\begin{aligned} \chi(\zeta,z) &= \chi_1(\zeta,z) \\ \text{and} \qquad & \\ \chi(1,z) &= \chi_1(1,z) \end{aligned}\right\} \quad \text{for } 2\bar{n}\Omega \leq z \leq (2\bar{n} + 1)\Omega \qquad \ldots\ldots \text{(A1-5)}$$

Also

$$\left.\begin{aligned} \chi(\zeta,z) &= \chi_2(\zeta,z) \\ \text{and in particular} \qquad & \\ \chi(-1,z) &= \chi_2(-1,z) \end{aligned}\right\} \quad \text{for } (2\bar{n} + 1)\Omega \leq z \leq (2\bar{n}+2)\Omega \qquad \ldots\ldots \text{(A1-6)}$$

Given the fluid entry temperatures $\chi_1(1,z)$ for $0 \leq z \leq \Omega$, and $\chi_2(-1,z)$ for $\Omega \leq z \leq 2\Omega$, the problem then is to solve equation (A1-1) subject to the boundary conditions (A1-2) to (A1-4), together with the reversal condition, to determine all E, $\chi_1(\zeta,z)$ and $\chi_2(\zeta,z)$.

APPENDIX 2

EDWARDS et al METHOD FOR NUMERICAL INTEGRATION IN THE TIME DOMAIN

NUMERICAL INTEGRATION IN THE TIME DOMAIN

A2.1 Method of Integration Used When Reversal Periods are Equal. (Formation of Matrices $\underline{A}_1'$ and $\underline{A}_2'$).

The solution scheme described in Section 2.2 of Chapter 2, starts by dividing the dimensionless period Ω by (n+1) equally spaced times $\tau = r\frac{\Omega}{n} = rh$, $0 \leqslant r \leqslant n$. For a given ζ, equations (2-5) and (2-6) are then applied at each of these discrete times. This provides two sets each of (n+1) equations, which contain the definite integrals shown in $I_{1,r}$ and $I_{2,r}$ respectively, where

$$I_{1,r} = 2\int_{z'=0}^{rh} X_1(\zeta,z')\eta_1(rh-\Omega-z')dz' +$$

$$2\int_{z'=rh}^{\Omega} X_1(\zeta,z')\eta_1(rh-z')dz' \qquad \ldots\ldots \text{(A2.1-1)}$$

$$\simeq \sum_{s=0}^{n} X_{1s}\ell_{rs} \quad , 0 \leqslant r \leqslant n \qquad \ldots\ldots \text{(A2.1-2)}$$

and

$$I_{2,r} = 2\int_{z'=0}^{rh} X_2(\zeta,z')\eta_2(rh-\Omega-z')dz' -$$

$$2\int_{z'=rh}^{\Omega} X_2(\zeta,z')\eta_2(rh-z')dz' \qquad \ldots\ldots \text{(A2.1-3)}$$

$$\simeq \sum_{s=0}^{n} X_{2s}\ell'_{rs} \quad , 0 \leqslant r \leqslant n \qquad \ldots\ldots \text{(A2.1-4)}$$

In these equations, $X_{1s} = X_1(\zeta,sh)$, $X_{2s} = X_2(\zeta,sh)$, $0 \leqslant s \leqslant n$, and the time step $h = \frac{\Omega}{n}$.

To obtain matrices $\underline{A}_1'$ and $\underline{A}_2'$, the integrals appearing in $I_{1,r}$ and $I_{2,r}$ then have to be written in the approximate forms shown in equations (A2.1-2) and (A2.1-4), respectively. The Edwards et al method for doing this is illustrated for $I_{1,r}$.

With the period Ω divided into n equal intervals, $(r'-1)h \leq z' \leq r'h$, $1 \leq r' \leq n$, $I_{1,r}$ was written as

$$I_{1,r} = \sum_{r'=1}^{r} \delta I'_{1,r'} + \sum_{r'=r+1}^{n} \delta I''_{1,r'} \quad , \quad 1 \leq r \leq n-1 \qquad \ldots\ldots \text{(A2.1-5)}$$

where

$$\delta I'_{1,r'} = 2\int_{(r'-1)h}^{r'h} X_1(\zeta,z')\eta_1(rh-\Omega-z')dz', \quad 1 \leq r' \leq r \qquad \ldots\ldots \text{(A2.1-6)}$$

and

$$\delta I''_{1,r'} = 2\int_{(r'-1)h}^{r'h} X_1(\zeta,z')\,\eta_1(rh-z')dz', \quad r+1 \leq r' \leq n \qquad \ldots\ldots \text{(A2.1-7)}$$

Because both of these integrals have the form

$\int_{(r'-1)h}^{r'h} X_1(\zeta,z')\eta_1(C-z')dz'$, where C is a particular value of z', it is sufficient to consider just

$$\frac{1}{2}\delta I_{1,r'} = \int_{(r'-1)h}^{r'h} X_1(\zeta,z')\eta_1(C-z')dz' \qquad \ldots\ldots \text{(A2.1-8)}$$

Integrating the right-hand side by parts, gives

$$\frac{1}{2}\,\delta I_{1,r'} = \left[X_1(\zeta,z')\int \eta_1(C-z')dz'\right]_{(r'-1)h}^{r'h}$$

$$-\int_{(r'-1)h}^{r'h} \frac{\partial X_1(\zeta,z')}{\partial z'}\left[\int \eta_1(C-z')dz'\right]dz' \qquad \ldots\ldots \text{(A2.1-9)}$$

Edwards et al then assumed that, at a given ζ, and for each of the n equal time intervals dividing the reversal period, the functions $X_i(\zeta,z')$, i=1,2, are linear functions of z', so that

$$X_i(\zeta,z') = Az'+B \ , \ (r'-1)h \leqslant z' \leqslant r'h, \ 1 \leqslant r' \leqslant n \qquad \ldots\ldots \text{(A2.1-10)}$$

where A and B depend on ζ and on r'.

Putting $U_1(C,z') = \int \eta_1(C-z')dz'$ ..... (A2.1-11)

and $\bar{U}_1(C,r'h) = \frac{1}{h}\int_{(r'-1)h}^{r'h} U_1(C,z')dz'$ ..... (A2.1-12)

and using (A2.1-10), equation (A2.1-9) takes the form

$$\frac{1}{2}\,\delta I_{1,r'} = X_1(\zeta,(r'-1)h)\left[\bar{U}_1(C,r'h) - U_1(C,(r'-1)h)\right]$$

$$- X_1(\zeta,r'h)\left[\bar{U}_1(C,r'h) - U_1(C,r'h)\right] \qquad \ldots\ldots \text{(A2.1-13)}$$

For i=1 or 2, using equations (2-9), (2-10) and (A2.1-11), we have

$$U_i(C,z') = \sum_{s=1}^{\infty} \frac{b_s}{\beta_s} \frac{\exp[-\beta_s(C+\Omega-z')]}{1+(-1)^i\exp(-\beta_s\Omega)} \qquad \ldots\ldots \text{(A2.1-14)}$$

Applying this result in (A2.1-12), then gives

$$\bar{U}_i(C,r'h) = \sum_{s=1}^{\infty} \frac{b_s \exp[-\beta_s(C+\Omega-r'h)][1-\exp(-h\beta_s)]}{h\beta_s^2\,[\,1+(-1)^i\exp(-\beta_s\Omega)\,]} \qquad \ldots\ldots \text{(A2.1-15)}$$

Finally with i=1, using (A2.1-14) and (A2.1-15) in (A2.1-13) and then applying it to (A2.1-5) for r=0,1,2,3,....,n successively, Edwards et al obtained for the matrix $\underline{A}_1'$,

$$\underline{A}_1' = \begin{bmatrix} H_1(\Omega), & H_2[(n-1)h], & H_2[(n-2)h], & H_2[(n-3)h],\ldots,H_2(h), & H_3(h) \\ H_1(h), & H_3(h)+H_1(\Omega), & H_2[(n-1)h], & H_2[(n-2)h],\cdots,H_2(2h), & H_3(2h) \\ H_1(2h), & H_2(h), & H_3(h)+H_1(\Omega), & H_2[(n-1)h]\ldots, & \vdots \\ H_1(3h), & H_2(2h), & H_2(h), & H_3(h)+H_1(\Omega)\ldots, & \vdots \\ \vdots & \vdots & \vdots & & \vdots \\ H_1[(n-1)h], & H_2[(n-2)h], & \vdots & H_3(h)+H_1(\Omega), & H_3(\Omega) \\ H_1(\Omega), & H_2[(n-1)h], & H_2[(n-2)h], & H_2(h), & H_3(h) \end{bmatrix}$$

..... (A2.1-16)

where

$$H_1(Nh) = 2\sum_{s=1}^{\infty} \frac{b_s}{h\beta_s^2} \frac{\exp(-Nh\beta_s)}{[1-\exp(-\Omega\beta_s)]}[\exp(h\beta_s)-1-h\beta_s], \text{ for } 1 \leq N \leq n$$

..... (A2.1-17)

$$H_2(Nh) = 2\sum_{s=1}^{\infty} \frac{b_s}{h\beta_s^2} \frac{\exp[-(N+1)h\beta_s]}{[1-\exp(-\Omega\beta_s)]}[\exp(h\beta_s)-1]^2 \text{ for } 1 \leq N \leq n-1$$

..... (A2.1-18)

and

$$H_3(Nh) = 2\sum_{s=1}^{\infty} \frac{b_s}{h\beta_s^2} \frac{\exp(-Nh\beta_s)}{[1-\exp(-\Omega\beta_s)]}[h\beta_s\exp(h\beta_s)-\exp(h\beta_s)+1]$$

for $1 \leq N \leq n$.

..... (A2.1-19)

Similarly with i=2,

$$\underline{A}_2' = \begin{bmatrix} -H_4(\Omega), & -H_5[(n-1)h], & -H_5[(n-2)h],..,-H_5(2h), & & -H_6(2h) \\ H_4(h), & H_6(h)-H_4(\Omega), & -H_5[(n-1)h],..,-H_5(h), & & -H_6(h) \\ H_4(2h), & H_5(h), & H_6(h)-H_4(\Omega)..., & & \\ & H_5(2h), & H_5(h)..., & & \\ & & & & \\ & & & & \\ & & & & \\ & & & & \\ & & & & \\ & & & , -H_5[(n-1)h], & -H_6[(n-1)h] \\ H_4[(n-1)h], & H_5[(n-2)h], & H_5[(n-3)h].., & H_6(h)-H_4(\Omega), & -H_6(\Omega) \\ H_4(\Omega), & H_5[(n-1)h], & H_5[(n-2)h].., & H_5(h), & H_6(h) \end{bmatrix}$$

..... (A2.1-20)

where

$$H_4(Nh) = 2 \sum_{s=1}^{\infty} \frac{b_s}{h\beta_s^2} \frac{\exp(-Nh\beta_s)}{[1+\exp(-\Omega\beta_s)]} [\exp(h\beta_s)-1-h\beta_s], \text{ for } 1 \leq N \leq n$$

..... (A2.1-21)

$$H_5(Nh) = 2 \sum_{s=1}^{\infty} \frac{b_s}{h\beta_s^2} \frac{\exp[-(N+1)h\beta_s]}{[1+\exp(-\Omega\beta_s)]} [\exp(h\beta_s)-1]^2, \text{ for } 1 \leq N \leq n-1$$

..... (A2.1-22)

and

$$H_6(Nh) = 2 \sum_{s=1}^{\infty} \frac{b_s}{h\beta_s^2} \frac{\exp(-Nh\beta_s)}{[1+\exp(-\Omega\beta_s)]} [h\beta_s\exp(h\beta_s)-\exp(h\beta_s)+1],$$

for $1 \leq N \leq n$.

..... (A2.1-23)

A2.2 Method of Integration Used When Reversal Periods are Un-equal (Formation of Matrices $\underline{B}_i$ and $\underline{D}_i$).

Notation

In this section, the suffices i and j are used to denote integer values 1 or 2. In the case of the symbol i, the two values do not, as in the main text, refer to the heating and cooling periods.

The notation $\underline{B}_i(I,J)$ and $\underline{D}_i(I,J)$ is used to denote the element in the I^{th} row and J^{th} column of matrices $\underline{B}_i$ and $\underline{D}_i$, respectively.

The letter h again denotes the time step which for $\Omega_1 \neq \Omega_2$ is given by $h = \frac{1}{n}$.

Method

In this case the integrals to be approximated are those contained in equations (2-13) and (2-14).

The range of the dimensionless time v, $0 \leqslant v \leqslant 1$, is divided into (n+1) equally-spaced times. Applying equations (2-13) and (2-14) at each of the (n+1) times, and assuming that the functions $\phi_1(\zeta,v)$ and $\phi_2(\zeta,v)$ are linear functions of v within each separate interval defined by

$$rh \leqslant v \leqslant (r+1)h, \quad 0 \leqslant r \leqslant n-1$$

Edwards et al [37, 74] used a method of approximation, similar to that described in the preceding section, to obtain the elements of matrices $\underline{B}_i$ and $\underline{D}_i$, i = 1,2, as follows:-

Matrices $\underline{B}_i(I,J)$

$$\underline{B}_i(0,0) = Q_i[1 + \frac{\Omega_j}{\Omega_i}]$$

$$\underline{B}_i(I,I) = R_i[0] + Q_i[1 + \frac{\Omega_j}{\Omega_i}] \ , \ 1 \leq I \leq n-1.$$

$$\underline{B}_i(n,n) = R_i[0]$$

$$\underline{B}_i(0,J) = R_i[1 + \frac{\Omega_j}{\Omega_i} - J\,h] + Q_i[1 + \frac{\Omega_j}{\Omega_i} - Jh],$$

$$1 \leq J \leq n-1$$

$$\underline{B}_i(0,n) = R_i[\frac{\Omega_j}{\Omega_i}]$$

$$\underline{B}_i(I,n) = R_i[Ih + \frac{\Omega_j}{\Omega_i}] \ , \ 1 \leq I \leq n-1$$

$$\underline{B}_i(I,J) = R_i[1 + \frac{\Omega_j}{\Omega_i} + (I-J)h] + Q_i[1 + \frac{\Omega_j}{\Omega_i} + (I-J)h];$$

$$1 \leq I \leq n-2, \ I+1 \leq J \leq n-1$$

$$\underline{B}_i(I,J) = R_i[(I-J)h] + Q_i\,[(I-J)h] \ ,$$

$$1 \leq J \leq n-1, \ J+1 \leq I \leq n.$$

$$\underline{B}_i(I,0) = Q_i[Ih] \ , \ 1 \leq I \leq n$$

(A2.2-1)

Matrices $\underline{D}_i$

$$\left.\begin{aligned}
\underline{D}_i(I,0) &= Q_j\left[\frac{\Omega_i}{\Omega_j}\, Ih + 1\right], \quad 0 \leq I \leq n \\
\underline{D}_i(I,n) &= R_j\left[\frac{\Omega_i}{\Omega_j}\, Ih\right], \quad 0 \leq I \leq n \\
\underline{D}_i(I,J) &= R_j\left[\frac{\Omega_i}{\Omega_j}.Ih + 1 - Jh\right] + Q_j\left[\frac{\Omega_i}{\Omega_j}.Ih + 1 - Jh\right], \\
&\qquad 0 \leq I \leq n,\ 1 \leq J \leq n-1
\end{aligned}\right\} \quad \text{(A2.2-2)}$$

In these equations, j=2 when i=1 and j=1 when i=2.

Also

$$Q_i(u) = \frac{n}{\Omega_i^2} \sum_{s=1}^{\infty} \frac{b_s}{\beta_s^2} \frac{\exp(-\Omega_i \beta_s u)}{1-\exp[-\beta_s(\Omega_1+\Omega_2)]} [\exp(h\beta_s\Omega_i)-1-h\beta_s\Omega_i] \quad \text{..... (A2.2-3)}$$

and

$$R_i(u) = \frac{n}{\Omega_i^2} \sum_{s=1}^{\infty} \frac{b_s}{\beta_s^2} \frac{\exp(-\Omega_i \beta_s u)}{1-\exp[-\beta_s(\Omega_1+\Omega_2)]} [\exp(-h\beta_s\Omega_i)-1+h\beta_s\Omega_i] \quad \text{..... (A2.2-4)}$$

APPENDIX 3

SOLUTION OF COUPLED DIFFERENCE EQUATIONS

SOLUTION OF COUPLED DIFFERENCE EQUATIONS

We consider the coupled difference equations specified by equation (2-33) of Chapter 2, i.e.

$$\underline{F}_{r+1} = \underline{Q}\underline{F}_r \quad , \quad -m \leq r \leq m \qquad \ldots\ldots \text{(A3-1)}$$

where the (2n+2)x1 column matrix $\underline{F}_r = \{ \underline{F}_{2,r}, \underline{F}_{1,r} \}$, and $\underline{F}_{2,r} = \underline{F}_2(rh_L)$, $\underline{F}_{1,r} = \underline{F}_1(rh_L)$ are column matrices each of (n+1) elements. Matrix $\underline{Q}$ is defined in equation (2-34).

The system of difference equations (A3-1) has to be solved, subject to the boundary conditions which apply to a counter-flow regenerator, to determine the elements of each $\underline{F}_r$ for all relevant values of r.

The boundary conditions are those given in equations (2-29) and (2-30), re-stated here as

$$\underline{F}_{1,m} = \{(f_1)_j\} \qquad \text{where } (f_1)_j = +1, \; 1 \leq j \leq n+1 \qquad \ldots\ldots \text{(A3-2)}$$

$$\underline{F}_{2,-m} = \{(f_2)_j\} \qquad \text{where } (f_2)_j = -1, \; 1 \leq j \leq n+1 \qquad \ldots\ldots \text{(A3-3)}$$

The method of solution uses (n+2) hypothetical boundary conditions (or starting vectors), $\underline{F}_{-m}^{(s)}$, $1 \leq s \leq n+2$, defined by

$$\underline{F}_{-m}^{(s)} = \{ \underline{F}_{2,-m}, \underline{F}_{1,-m}^{(s)} \} \qquad \ldots\ldots \text{(A3-4)}$$

In this equation, $\underline{F}_{2,-m}$ is as specified in equation (A3-3), and for $1 \leq s \leq n+1$

$$\underline{F}^{(s)}_{1,-m} = \{\delta_{js}\}, \text{ where } \left.\begin{array}{l} \delta_{js} = -1 \text{ for } j = s \\ \delta_{js} = 0 \text{ for } j \neq s \end{array}\right\}, \; 1 \leq j \leq n+1$$

..... (A3-5)

Also $\underline{F}^{(n+2)}_{1,-m} = \{ \underline{F}_{2,-m}, \underline{F}_{2,-m} \}$ ..... (A3-6)

Illustrating this for n=5, the seven starting vectors would be

$$\underline{F}^{(1)}_{-m} = \{ -1,-1,-1,-1,-1,-1, \quad -1,0,0,0,0,0 \}$$

$$\underline{F}^{(2)}_{-m} = \{ -1,-1,-1,-1,-1,-1, \quad 0,-1,0,0,0,0 \}$$

$$\vdots \qquad\qquad\qquad\qquad\qquad\qquad \vdots$$

$$\underline{F}^{(6)}_{-m} = \{ -1,-1,-1,-1,-1,-1, \quad 0,0,0,0,0,-1 \}$$

$$\underline{F}^{(7)}_{-m} = \{ -1,-1,-1,-1,-1,-1, \quad -1,-1,-1,-1,-1,-1 \}$$

Formula (A3-1) is then applied recursively, with each of the (n+2) starting vectors, for all r in the range $-m \leq r \leq m$. Using $\underline{F}^{(s)}_{r}$ to represent the solution at $\zeta = rh_L$, calculated with the starting vector $\underline{F}^{(s)}_{-m}$, the true solution, $\underline{F}_r$, at this value of ζ is given by

$$\underline{F}_r = \sum_{s=1}^{n+2} K_s \underline{F}^{(s)}_r = K_1 \underline{F}^{(1)}_r + K_2 \underline{F}^{(2)}_r + \ldots + K_{n+2} \underline{F}^{(n+2)}_r .$$

..... (A3-7)

where K_1 to K_{n+2} are constants, independent of r, which we determine as follows.

The first (n+1) elements of the column matrix $\underline{F}_{-m} = \{\underline{F}_{2,-m}, \underline{F}_{1,-m}\}$ are known from (A3-3). So applying equation (A3-7) with r = -m, and equating any of the first (n+1) corresponding elements, gives

$$\sum_{s=1}^{n+2} K_s = 1 \qquad \ldots\ldots \text{(A3-8)}$$

Next, observing that the last (n+1) elements of $\underline{F}_m = \{\underline{F}_{2,m}, \underline{F}_{1,m}\}$ are known from equation (A3-2), we apply equation (A3-7) with r=m. Equating each of the last (n+1) corresponding elements gives the set of (n+1) equations,

$$\sum_{s=1}^{n+2} K_s f_{m,j}^{(s)} = 1 \quad , \; n+2 \leqslant j \leqslant 2n+2 \qquad \ldots\ldots \text{(A3-9)}$$

where $f_{m,j}^{(s)}$ is the jth element of $\underline{F}_m^{(s)}$.

Equations (A3-8) and (A3-9) form a set of (n+2) linear simultaneous equations for the (n+2) coefficients K_s. Writing these in matrix form, we have

$$\underline{\beta}\,\underline{K} = \underline{\alpha} \qquad \ldots\ldots \text{(A3-10)}$$

where the column matrices $\underline{\alpha}$ and $\underline{K}$ are

$$\underline{\alpha} = \{\alpha_s\} \text{ in which } \alpha_s = 1, \; 1 \leqslant s \leqslant n+2 \qquad \ldots\ldots \text{(A3-11)}$$

$$\underline{K} = \{K_s\} \; , \; 1 \leqslant s \leqslant n+2 \qquad \ldots\ldots \text{(A3-12)}$$

and $\underline{\beta}$ is the (n+2) square matrix defined by:-

$$\underline{\beta} = \begin{bmatrix} 1 & , 1, & 1 & , & 1, & 1 \\ f^{(1)}_{m,n+2} & , f^{(2)}_{m,n+2} & & & & f^{(n+2)}_{m,n+2} \\ f^{(1)}_{m,n+3} & , f^{(2)}_{m,n+3} & & & & f^{(n+2)}_{m,n+3} \\ \vdots & \vdots & & & & \vdots \\ f^{(1)}_{m,2n+2} & , f^{(2)}_{m,2n+2} & \cdots\cdots\cdots\cdots & & & f^{(n+2)}_{m,2n+2} \end{bmatrix}$$

..... (A3-13)

Because all the elements of $\underline{\beta}$ have been calculated using the (n+2) starting vectors with (A3-1), the unknown coefficients K_s may be obtained by solving the set of equations (A3-10) by any standard method.

In this study, equation (A3-10) was written in the form

$$\underline{K} = \underline{\beta}^{-1}\,\underline{\alpha} \qquad \text{..... (A3-14)}$$

and $\underline{K}$ obtained by evaluating $\underline{\beta}^{-1}\,\underline{\alpha}$.

Finally, with $\underline{K}$ known, a further application of (A3-7) with r=-m, enables the (n+1) unknown elements of $\underline{F}_{-m}$ to be calculated. Hence, with $\underline{F}_{-m}$ now known completely, equation (A3-1) is applied for $-m \leqslant r \leqslant m$ to compute all the required solutions.

APPENDIX 4

NUSSELT'S ANALYTICAL SOLUTION FOR A REGENERATOR OPERATING WITH INFINITESIMALLY-SHORT REVERSAL PERIODS

NUSSELT'S ANALYTIC SOLUTION FOR INFINITESIMALLY-SHORT REVERSAL PERIODS

In this Appendix we adopt the following notation originally used by Nusselt [24].

x — distance along the regenerator length, measured from the hot-fluid entry end.

F — surface area of regenerator available for heat transfer.

z_1, z_2 — duration of heating and cooling periods respectively.

α_1, α_2 — heat-transfer coefficients between fluid and regenerator wall during heating and cooling periods respectively.

u_0 — temperature of the hot fluid entering the regenerator.

v_0 — temperature of the cold fluid entering the regenerator.

W_1, W_2 — thermal capacity of the hot and cold fluids per unit time respectively.

For a regenerator operating with infinitesimally-short reversal periods, Nusselt derived the following solutions for the hot- and cold-fluid temperatures u and v, respectively.

$$u = u_0 - (u_0 - v_0) \frac{1 - \exp[-\beta x]}{1 - \frac{n}{m} \exp[-\beta F]} \quad \ldots\ldots (A4\text{-}1)$$

$$v = u_0 - (u_0 - v_0) \frac{1 - \frac{n}{m} \exp[-\beta x]}{1 - \frac{n}{m} \exp[-\beta F]} \quad \ldots\ldots (A4\text{-}2)$$

where

$$m = \frac{\alpha_1}{W_1} \left[\frac{\alpha_2 z_2}{\alpha_1 z_1 + \alpha_2 z_2} \right] \quad \ldots\ldots (A4\text{-}3)$$

$$n = \frac{\alpha_2}{W_2} \left[\frac{\alpha_1 z_1}{\alpha_1 z_1 + \alpha_2 z_2} \right] \quad \ldots\ldots (A4\text{-}4)$$

$$\beta = m - n \quad \ldots\ldots (A4\text{-}5)$$

The amount of heat transferred during each period was obtained as

$$Q_{sp} = W_1(u_0 - u_2) z_1 = W_2(v_2 - v_0) z_2 \quad \ldots\ldots (A4\text{-}6)$$

$$= \frac{(u_0 - v_0)[1 - \exp(-\beta F)]}{\frac{1}{z_1 W_1} - \frac{1}{z_2 W_2} \exp[-\beta F]} \quad \ldots\ldots (A4\text{-}7)$$

where u_2 and v_2 are the hot and cold fluid exit temperatures, respectively.

For $z_1 = z_2 = z$ say, equation (A4-7) becomes

$$Q_{sp} = \frac{(u_0 - v_0)[1 - \exp(-\beta F)] z}{\frac{1}{W_1} - \frac{1}{W_2} \exp[-\beta F]} \quad \ldots\ldots (A4\text{-}8)$$

In the ideal case, when $v_2 = u_0$, the amount of heat exchanged in each period is, from (A4-6)

$$(Q_{sp})_{max} = W_2(u_0-v_0)z \qquad \ldots\ldots \text{(A4-9)}$$

The regenerator effectiveness is therefore given by

$$\eta_R = \frac{Q_{sp}}{(Q_{sp})_{max}} = \frac{1 - \exp(-\beta F)}{\frac{W_2}{W_1} - \exp(-\beta F)} \qquad \ldots\ldots \text{(A4-10)}$$

APPENDIX 5

DOCUMENTATION FOR PROGRAM 1

PROGRAM 1 : DOCUMENTATION

Purpose To compute solutions of the integro-differential equations (2-5) and (2-6), thereby giving the hot and cold fluid temperatures $f_1(\zeta,z')$, $f_2(\zeta,z')$ at $(2m+1)$ equally-spaced distances along the regenerator length, at each of $(n+1)$ equally-spaced times within each period.

Method The method for solving equations (2-5) and (2-6), and the particular computational techniques used in Program 1 are summarised diagrammatically in the accompanying flow-chart. Details of the mathematical analysis are provided in Sections (2.2), (3.2.2), Appendices 2 and 3 and pages (ix) to (xii) below.

Input Data } **Output** } Refer to description in Chapter 6, Section (6.3)(a) and Tables 8 and 9.

Requirements On the DEC System 20 computer, memory capacity is quoted in pages, each page holding 512 words, each word containing 36 bits.

In stored form, Program 1, including its associated subroutines and subprograms occupies 20 pages of memory. During execution, an increased amount of memory

space is required, the actual amount depending on the maximum array sizes specified. Array dimensions are governed by the values of n and m, and for the maximum values incorporated in Program 1, viz. n=30, m=48, about 100 pages of memory are needed. Double-precision arithmetic is used for the function sub-program.

Restrictions Input Data: $n \leq 30$; $m = 3,6,12,24,48^{+}$

$N_1 \neq 1$, $N_2 \neq 1$.

Output: Temperatures are printed out at seven^{+} equally-spaced distances along the regenerator length (see Table 8).

+ To specify other values of m between 3 and 48 and/or to obtain (for $m > 3$) printed temperatures at more than seven positions in the regenerator, a slight modification to the existing program would be required.

Outline Flow-chart for Program 1

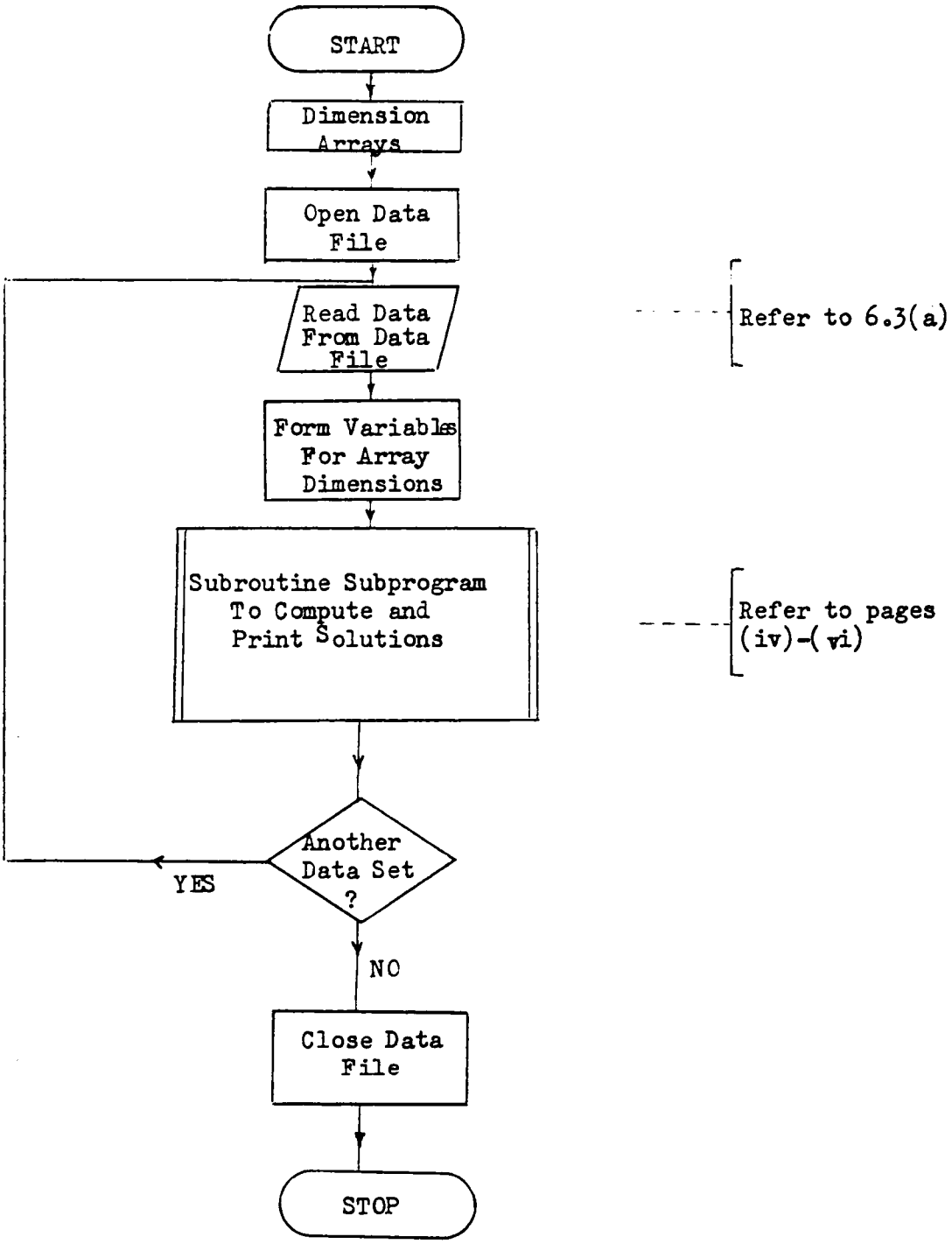

Main Line Program

Subroutine Subprogram

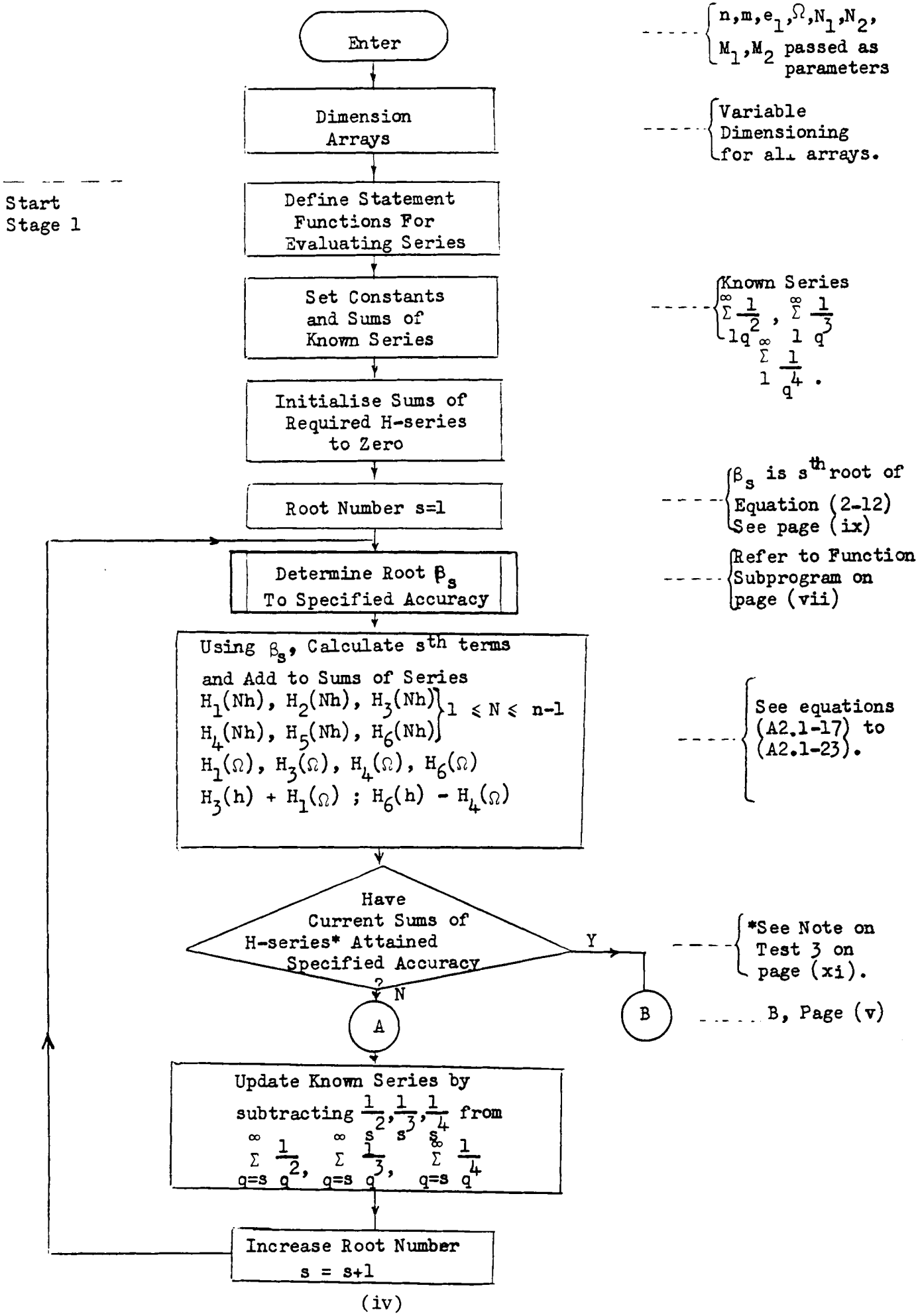

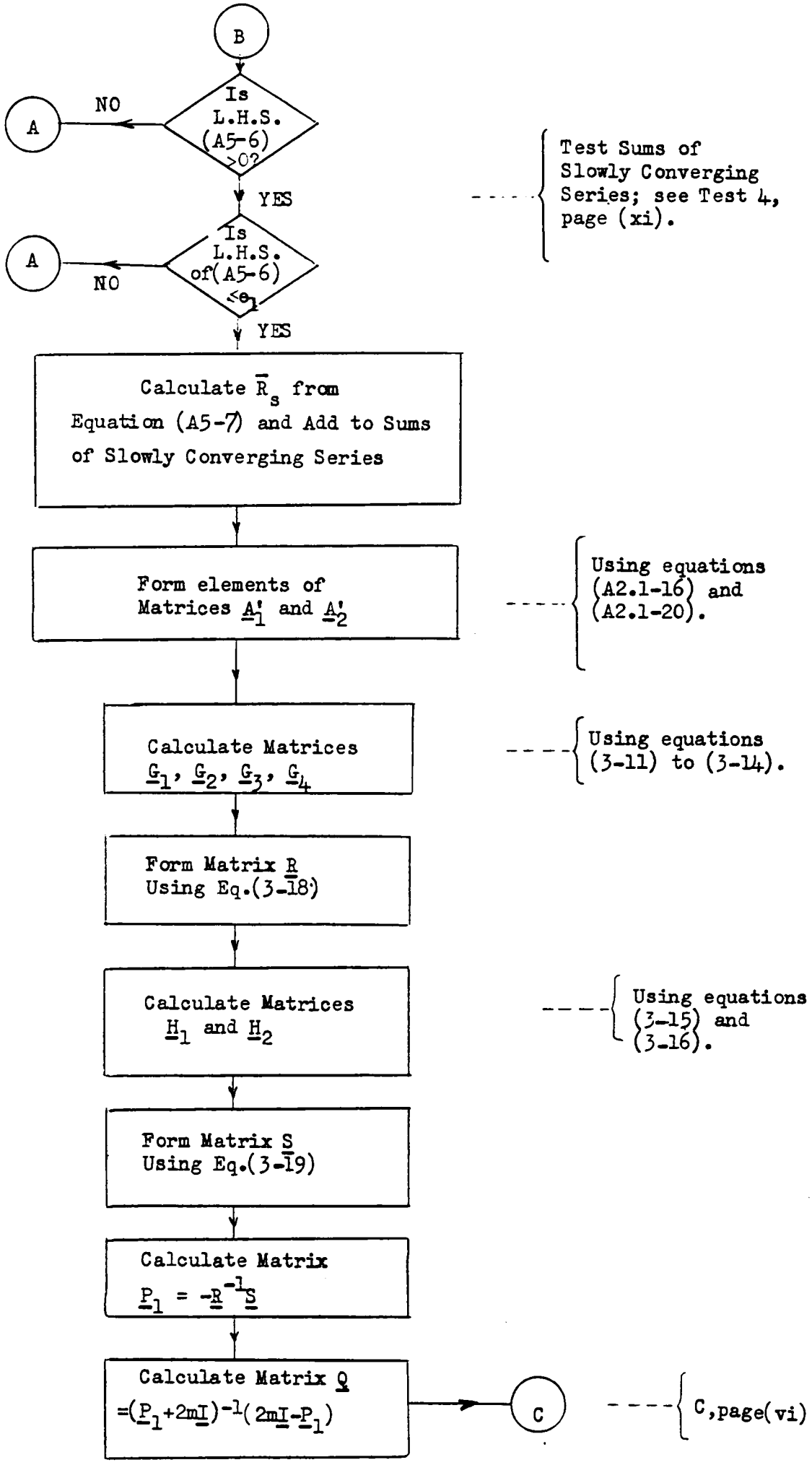
B
Is L.H.S. (A5-6) >0?
NO
A
YES
Is L.H.S. of (A5-6) ≤e1
A
NO
YES
Test Sums of Slowly Converging Series; see Test 4, page (xi).
Calculate $\bar{R}_s$ from Equation (A5-7) and Add to Sums of Slowly Converging Series
Form elements of Matrices $\underline{A}_1'$ and $\underline{A}_2'$
Using equations (A2.1-16) and (A2.1-20).
End Stage 1
Start Stage 2
Calculate Matrices $\underline{G}_1$, $\underline{G}_2$, $\underline{G}_3$, $\underline{G}_4$
Using equations (3-11) to (3-14).
Form Matrix $\underline{R}$ Using Eq.(3-18)
Calculate Matrices $\underline{H}_1$ and $\underline{H}_2$
Using equations (3-15) and (3-16).
Form Matrix $\underline{S}$ Using Eq.(3-19)
Calculate Matrix $\underline{P}_1 = -\underline{R}^{-1}\underline{S}$
Calculate Matrix $\underline{Q}$ $=(\underline{P}_1+2m\underline{I})^{-1}(2m\underline{I}-\underline{P}_1)$
C
C, page (vi)
End Stage 2

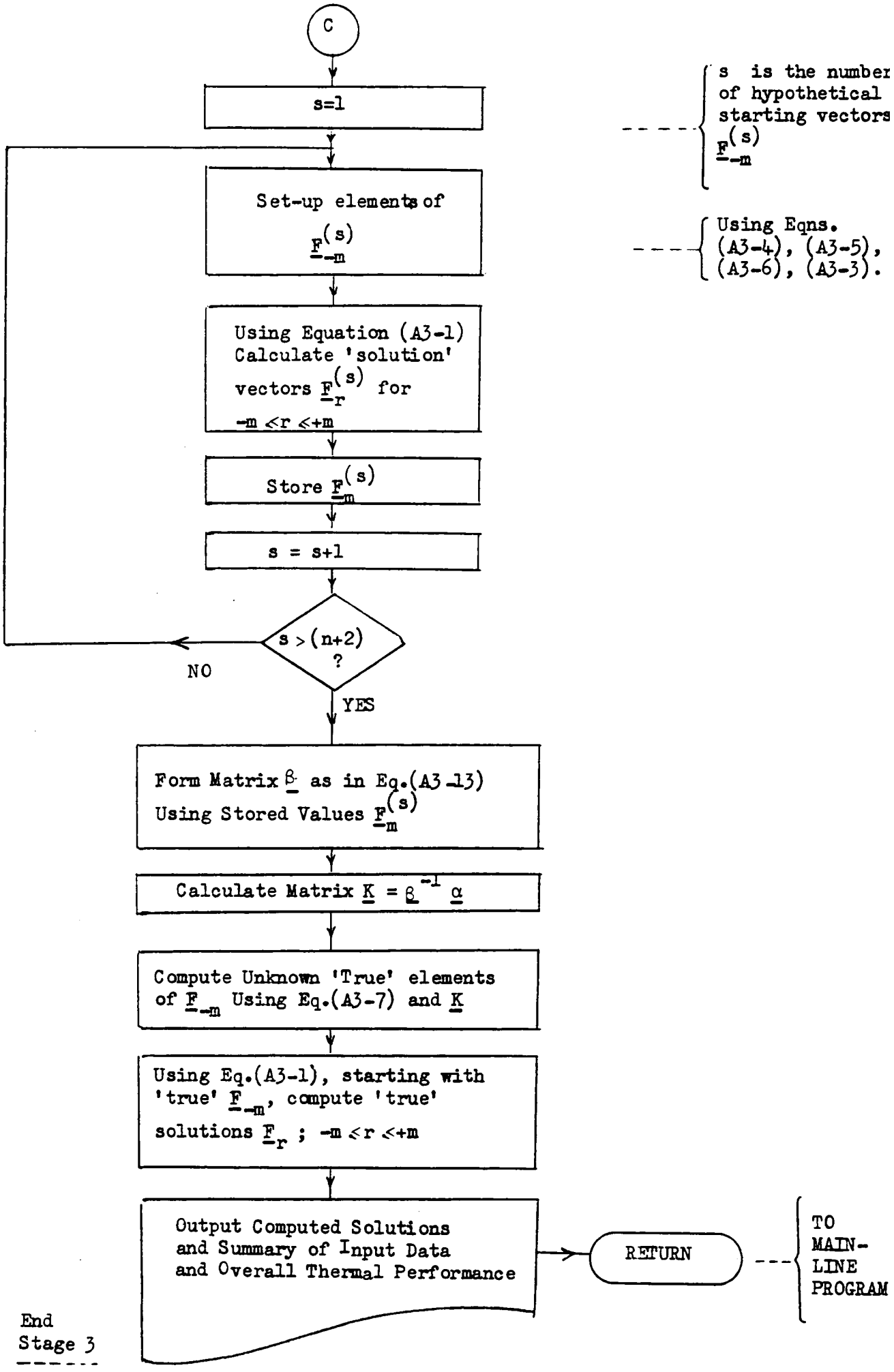
C
s=1
s is the number of hypothetical starting vectors $\underline{F}_{-m}^{(s)}$
Set-up elements of $\underline{F}_{-m}^{(s)}$
Using Eqns. (A3-4), (A3-5), (A3-6), (A3-3).
Using Equation (A3-1) Calculate 'solution' vectors $\underline{F}_{r}^{(s)}$ for $-m \leq r \leq +m$
Store $\underline{F}_{m}^{(s)}$
s = s+1
s > (n+2) ?
NO
YES
Form Matrix $\underline{\beta}$ as in Eq.(A3-13) Using Stored Values $\underline{F}_{m}^{(s)}$
Calculate Matrix $\underline{K} = \underline{\beta}^{-1}\,\underline{\alpha}$
Compute Unknown 'True' elements of $\underline{F}_{-m}$ Using Eq.(A3-7) and $\underline{K}$
Using Eq.(A3-1), starting with 'true' $\underline{F}_{-m}$, compute 'true' solutions $\underline{F}_{r}$; $-m \leq r \leq +m$
Output Computed Solutions and Summary of Input Data and Overall Thermal Performance
RETURN
TO MAIN-LINE PROGRAM
End Stage 3

Function Subprogram to Calculate Roots of $\sqrt{\beta}\tan\sqrt{\beta}=1$

For mathematical details refer to pages (ix) to (xi).

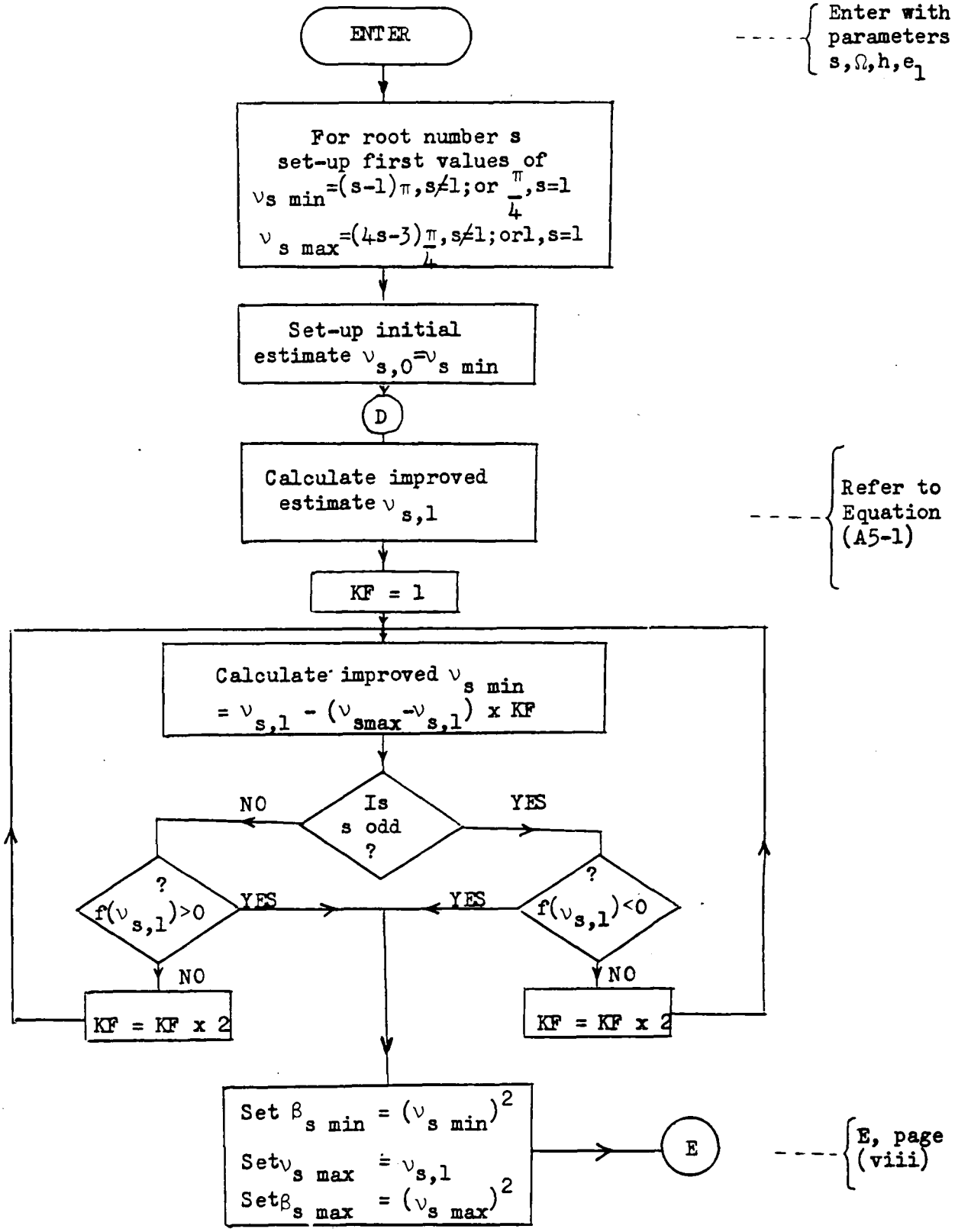

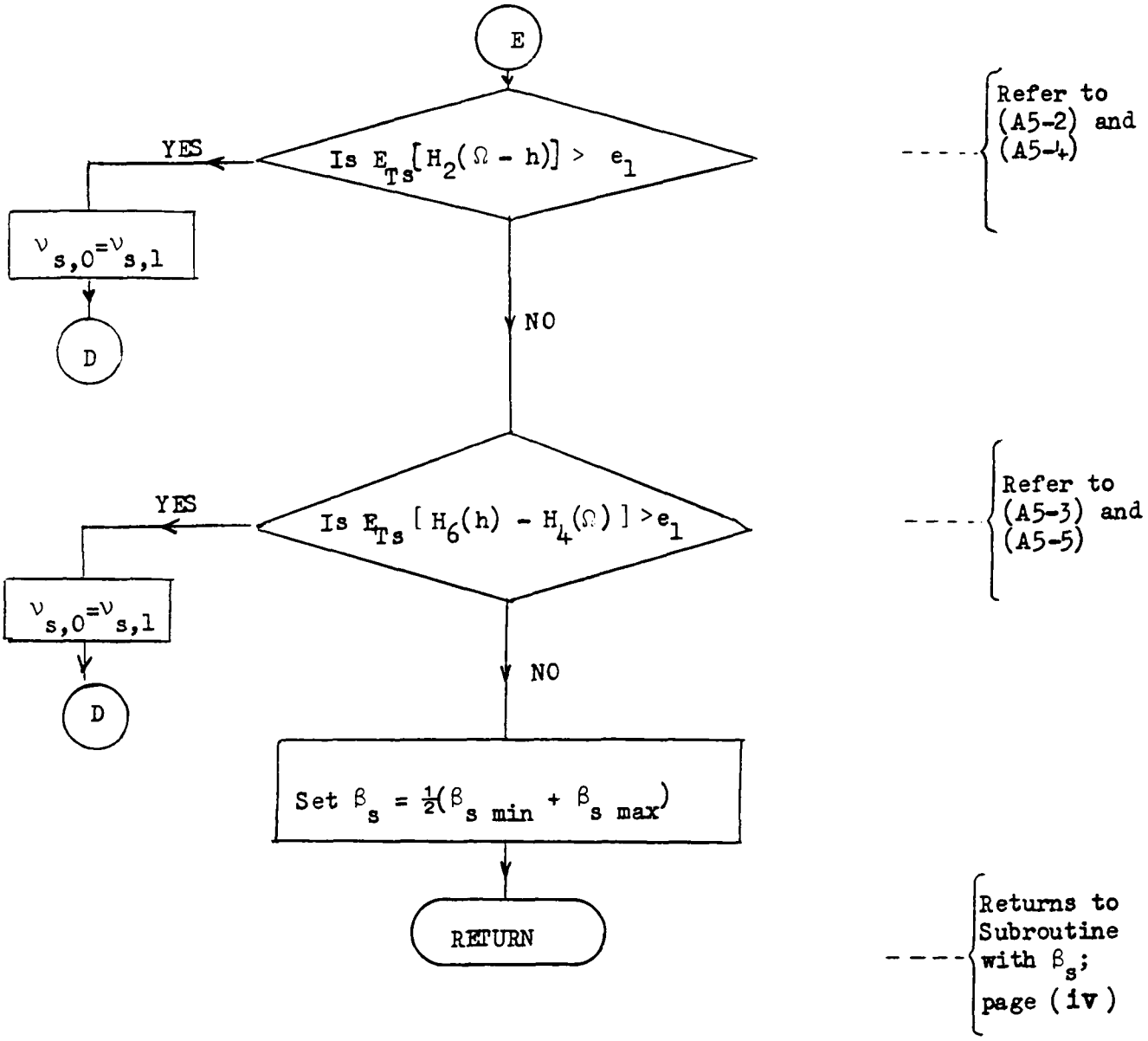
E
Is $E_{Ts}[H_2(\Omega - h)] > e_1$
YES
$\nu_{s,0}=\nu_{s,1}$
D
NO
Is $E_{Ts}[H_6(h) - H_4(\Omega)] > e_1$
YES
$\nu_{s,0}=\nu_{s,1}$
D
NO
Set $\beta_s = \frac{1}{2}(\beta_{s\ min} + \beta_{s\ max})$
RETURN
Refer to (A5-2) and (A5-4)
Refer to (A5-3) and (A5-5)
Returns to Subroutine with β_s; page (iv)

Notes on Flow-chart for Program 1 : Stage 1 calculations

The following test expressions were developed by Edwards, (see reference [37] for full derivation), to ensure that each term and each sum of all the required infinite series are computed to within a specified accuracy.

To utilise the various tests, values of $\beta_{s\ min}$, β_s and $\beta_{s\ max}$, where β_s is the s^{th} root of $\sqrt{\beta}\tan\sqrt{\beta} = 1$ and $\beta_{s\ min} < \beta_s < \beta_{s\ max}$, are determined by the function subprogram described on pages (vii) and (viii) above.

The subprogram obtains β_s as ν_s^2 where $\nu_s \tan\nu_s = 1$. Each root ν_s is computed iteratively from $f(\nu_s) = \nu_s \sin\nu_s - \cos\nu_s = 0$, using the Newton-Raphson technique. Hence

$$\nu_{s,1} = \frac{\nu_{s,0}^2 + \nu_{s,0}\tan\nu_{s,0} + 1}{\nu_{s,0} + 2\tan\nu_{s,0}} \qquad \ldots\ldots \text{(A5-1)}$$

where $\nu_{s,0}$ and $\nu_{s,1}$ are successive estimates of ν_s.

For all s, lower and upper bounds $\nu_{s\ min}$ and $\nu_{s\ max}$ are also determined such that $\nu_{s\ min} < \nu_s < \nu_{s\ max}$. Squaring $\nu_{s\ min}$ and $\nu_{s\ max}$ then gives the required values of $\beta_{s\ min}$ and $\beta_{s\ max}$, respectively.

Tests to Ensure the Accurate Computation of the Terms of Each H-series

The fractional error in the s^{th} term of all series $H_j(Nh)$, $1 \leq N \leq n$, will be less than a specified value e_1, whenever the fractional errors in the series $H_2(\Omega - h)$, denoted by $E_{Ts}[H_2(\Omega - h)]$, and in the series $H_6(h) - H_4(\Omega)$, denoted by $E_{Ts}[H_6(h) - H_4(\Omega)]$ are both less than e_1. The maximum values of these fractional errors are given by

$$E_{Ts}[H_2(\Omega-h)] = e^{\Omega(BX-BN)} \frac{2+BX}{2+BN} \cdot \frac{BX(1-e^{-\Omega BX})}{BN(1-e^{-\Omega BN})} \frac{(e^{hBX}-1)^2}{(e^{hBN}-1)^2} \quad \ldots\ldots (A5\text{-}2)$$

and

$$E_{Ts}[H_6(h)-H_4(\Omega)] = \frac{BX}{BN} \cdot \frac{2+BX}{2+BN} \cdot \frac{e^{\Omega BX}+1}{e^{\Omega BN}+1} \times$$

$$\frac{hBXe^{\Omega BX} - e^{\Omega BX} + e^{(\Omega-h)BX} - e^{hBX} + 1 + hBX}{hBNe^{\Omega BN} - e^{\Omega BN} + e^{(\Omega-h)BN} - e^{hBN} + 1 + hBN} \quad \ldots\ldots (A5\text{-}3)$$

where $BX = \beta_{s\ max}$ and $BN = \beta_{s\ min}$.

For each value of s, (each root), the iterative procedure described above for refining the values of $\beta_{s\ min}$ and $\beta_{s\ max}$ is therefore continued until both

$$E_{Ts}\,[\,H_2(\Omega-h)\,] < e_1 \quad ; \quad \text{(TEST 1)} \qquad \ldots\ldots \text{(A5-4)}$$

and

$$E_{Ts}\,[\,H_6(h) - H_4(\Omega)\,] < e_1 \quad ; \quad \text{(TEST 2)} \qquad \ldots\ldots \text{(A5-5)}$$

are satisfied.

Tests to Ensure the Accurate Summation of All H-series

Let $\sigma_s\,[H_j(Nh)]$ represent the sum of the first s terms of the series $H_j(Nh)$, $1 \leq N \leq n$.

Test 3

After summing the first s terms of all series $H_j(Nh)$, $1 \leq N \leq n$, if

$$\frac{\frac{4}{\pi^4 h}\sum_{q=s}^{\infty}\frac{1}{q^4}}{\sigma_s\,[H_4(h)]} < e_1 \qquad \ldots\ldots \text{(A5-6)}$$

then, if all further terms are neglected in summing all series, the fractional error in each series, except $H_3(h)$ and $H_6(h)$, will be less than e_1.

Test 4

For the slowly converging series $H_3(h)$, $H_6(h)$ and $H_6(h) - H_4(\Omega)$, suppose after summing the first s terms we approximate the sum of the remaining terms by $\bar{R}_s$, where

$$\bar{R}_s = \frac{4}{\pi^2}\sum_{q=s}^{\infty}\frac{1}{q^2} - \frac{2}{\pi^2}\sum_{q=s}^{\infty}\frac{1}{q^3} - \frac{2}{\pi^4 h}\sum_{q=s}^{\infty}\frac{1}{q^4} \qquad \ldots\ldots \text{(A5-7)}$$

Then if

$$\frac{\frac{2}{\pi^2}\sum_{q=s}^{\infty}\frac{1}{q^3}+\frac{2}{\pi^4 h}\sum_{q=s}^{\infty}\frac{1}{q^4}}{\sigma_s\,[H_6(h)-H_4(\Omega)]+\frac{4}{\pi^2}\sum_{q=s}^{\infty}\frac{1}{q^2}-\frac{4}{\pi^2}\sum_{q=s}^{\infty}\frac{1}{q^3}-\frac{4}{\pi^4 h}\sum_{q=s}^{\infty}\frac{1}{q^4}} < e_1 \qquad \ldots\ldots \text{(A5-8)}$$

the sums of each of these three series, obtained by adding $\bar{R}_s$ of equation (A5-7) to the appropriate partial sum $\sigma_s\,[H]$, each have a maximum fractional error of less than e_1.

APPENDIX 6

DEVELOPMENT OF METHODS FOR ENSURING THE ACCURATE SUMMATION OF ALL INFINITE SERIES $Q_j(u)$ AND $R_j(u)$

Notation: In this Appendix, except when used with the variable Ω, the sub-script i does not refer to the heating and cooling periods.

A 6.1 Accuracy of the Terms of $Q_i(u)$ Series, i=1 or 2

By substituting for b_s from equation (2-11), we can write the function $Q_i(u)$, defined in equation (A2.2-3), in the form:

$$Q_i(u) = \sum_{s=1}^{\infty} \theta(\Omega_i, \beta_s) \exp(-u\Omega_i \beta_s) = \sum_{s=1}^{\infty} q_s(u) \quad \ldots\ (A6.1\text{-}1)$$

$$\text{where } \theta(\Omega_i, \beta_s) = \frac{2[\exp(h\Omega_i \beta_s) - 1 - h\Omega_i \beta_s]}{h\Omega_i^2 \beta_s (2+\beta_s)\,[1-\exp(\Omega_T \beta_s)]} \quad \ldots\ (A6.1\text{-}2)$$

$$\text{and } \Omega_T = \Omega_1 + \Omega_2 \quad \ldots\ (A6.1\text{-}3)$$

In equation (A6.1-1), $q_s(u)$ is the s-th term of the series $Q_i(u)$, and is given by

$$q_s(u) = \theta(\Omega_i, \beta_s) \exp(-u\Omega_i \beta_s) \quad \ldots\ (A6.1\text{-}4)$$

For a given value of s, application of the iterative method described in equations (A7-1) to (A7-8) of Appendix 7 produces a convergent sequence of lower and upper bounds of β_s, the s-th root of $\sqrt{\beta} \tan \sqrt{\beta} = 1$.

If $\beta_{s\ min}$ and $\beta_{s\ max}$ represent any such pair of lower and upper bounds respectively, then we may write

$$\beta_{s\ min} \leq \beta_s \leq \beta_{s\ max} \quad \ldots\ (A6.1\text{-}5)$$

Since u, Ω_i and β_s are all positive quantities, it follows that

$$\exp(-u\Omega_i\beta_{s\ max}) \leq \exp(-u\Omega_i\beta_s) \leq \exp(-u\Omega_i\beta_{s\ min}) \quad \ldots\ (A6.1\text{-}6)$$

Also, since h is always positive, by defining

$$\left[\theta(\Omega_i,\beta_s)\right]_{min} = \frac{2\left[\exp(h\Omega_i\beta_{s\ min})-1-h\Omega_i\beta_{s\ max}\right]}{h\Omega_i^2(2+\beta_{s\ max})\beta_{s\ max}\left[1-\exp(-\Omega_T\beta_{s\ max})\right]} \quad \ldots\ (A6.1\text{-}7)$$

and

$$\left[\theta(\Omega_i,\beta_s)\right]_{max} = \frac{2\left[\exp(h\Omega_i\beta_{s\ max})-1-h\Omega_i\beta_{s\ min}\right]}{h\Omega_i^2(2+\beta_{s\ min})\beta_{s\ min}\left[1-\exp(-\Omega_T\beta_{s\ min})\right]} \quad \ldots\ (A6.1\text{-}8)$$

it may be shown that

$$\left[\theta(\Omega_i,\beta_s)\right]_{min} \leq \theta(\Omega_i,\beta_s) \leq \left[\theta(\Omega_i,\beta_s)\right]_{max} \quad \ldots\ (A6.1\text{-}9)$$

Hence, provided we use values of $\beta_{s\ min}$ and $\beta_{s\ max}$ which satisfy the relationships given in (A6.1-5), it follows from equations (A6.1-4), (A6.1-7) and (A6.1-8), together with (A6.1-6) and (A6.1-9), that the exact value of the term $q_s(u)$ is between the values of $\left[q_s(u)\right]_{min}$ and $\left[q_s(u)\right]_{max}$ as given by

$$\left[q_s(u)\right]_{min} = \left[\theta(\Omega_i,\beta_s)\right]_{min} \exp\left[-u\Omega_i\beta_{s\ max}\right] \quad \ldots\ (A6.1\text{-}10)$$

and

$$\left[q_s(u)\right]_{max} = \left[\theta(\Omega_i,\beta_s)\right]_{max} \exp\left[-u\Omega_i\beta_{s\ min}\right] \quad \ldots\ (A6.1\text{-}11)$$

That is

$$\left[q_s(u)\right]_{min} \leq q_s(u) \leq \left[q_s(u)\right]_{max} \quad \ldots\ (A6.1\text{-}12)$$

It also follows that if $q_s(u)$ is calculated using an approximate value of β_s, which is between $\beta_{s\ min}$ and $\beta_{s\ max}$, then the fractional error of the term $q_s(u)$ so calculated, is not greater than $Eq_s(u)$, where

$$Eq_s(u) = \frac{[q_s(u)]_{max} - [q_s(u)]_{min}}{[q_s(u)]_{min}}$$

$$= \frac{[\theta(\Omega_i, \beta_s)]_{max}}{[\theta(\Omega_i, \beta_s)]_{min}} . \exp[u\Omega_i(\beta_{s\ max} - \beta_{s\ min})] - 1$$

.... (A6.1-13)

It can be seen from this equation that $Eq_s(u)$ increases with u, which for the required $Q_i(u)$ series, has a maximum value of $(1 + \frac{\Omega_j}{\Omega_i})$. It follows, therefore, that if the iterative procedure of equations (A7-1) to (A7-8) is continued until the calculated values of $\beta_{s\ min}$ and $\beta_{s\ max}$ become sufficiently close to ensure that

$$Eq_s\ (1 + \frac{\Omega_j}{\Omega_i}) < e_1, \text{ where for } i=1, j=2 \text{ and for } i=2, j=1$$

.... (A6.1-14)

and if we then use $\beta_s = \frac{1}{2}(\beta_{s\ min} + \beta_{s\ max})$, where the bounds have the values that satisfy (A6.1-14), then it follows that the s-th terms of all the required $Q_i(u)$ series can be determined with a fractional error less than e_1.

So, combining (A6.1-7), (A6.1-8) and (A6.1-13), we see that the fractional error in the s-th term of all the required $Q_i(u)$ series will be less than e_1, when each term is calculated with β_s set equal to the mean of the $\beta_{s\ min}$ and $\beta_{s\ max}$ values for which

$$\left\{\frac{BX}{BN}\,\frac{(2+BX)}{(2+BN)}\,\frac{[1-\exp(-\Omega_T BX)]}{[1-\exp(-\Omega_T BN)]}\,x\right.$$

$$\left.\frac{[\exp(h\Omega_i BX)-1-h\Omega_i BN]}{[\exp(h\Omega_i BN)-1-h\Omega_i BX]}.\exp[\Omega_T(BX-BN)]\right\}-1<e_1$$

.... (A6.1-15)

where $BX \equiv \beta_{s\ max}$ and $BN \equiv \beta_{s\ min}$.

A 6.2 Accuracy of the Terms of $R_i(u)$ Series, i=1 or 2

We commence by writing the function $R_i(u)$, defined in equation (A2.2-4), in the form

$$R_i(u) = \sum_{s=1}^{\infty} \Theta(\Omega_i, \beta_s)\exp(-u\Omega_i\beta_s) = \sum_{s=1}^{\infty} r_s(u) \qquad \text{.... (A6.2-1)}$$

In this equation $r_s(u)$ is the s-th term of $R_i(u)$, given by

$$r_s(u) = \Theta_1(\Omega_i, \beta_s)\ \exp(-u\Omega_i\beta_s) \qquad \text{.... (A6.2-2)}$$

where

$$\Theta_1(\Omega_i, \beta_s) = \frac{2}{h\Omega_i^2(2+\beta_s)\beta_s}\,\frac{[\exp(-h\Omega_i\beta_s)-1+h\Omega_i\beta_s]}{[1-\exp(-\Omega_T\beta_s)]} \qquad \text{.... (A6.2-3)}$$

and Ω_T is given by equation (A6.1-3).

By adopting exactly the same procedure as in the preceding section, but with $Q_i(u)$, $q_s(u)$ and $\Theta(\Omega_i,\beta_s)$ replaced by $R_i(u)$, $r_s(u)$ and $\Theta_1(\Omega_i,\beta_s)$ respectively, it can be shown that if the term $r_s(u)$ is calculated using an approximate value of β_s which is between $\beta_{s\ min}$

and $\beta_{s\ max}$, (which satisfy A6.1-5), then the fractional error in the term $r_s(u)$ so calculated, does not exceed $Er_s(u)$, where

$$Er_s(u) = \frac{[\theta_1(\Omega_i,\beta_s)]_{max}}{[\theta_1(\Omega_i\beta_s)]_{min}} \exp[u\Omega_i(\beta_{s\ max} - \beta_{s\ min})] - 1$$

.... (A6.2-4)

In equation (A6.2-4),

$$[\theta_1(\Omega_i,\beta_s)]_{min} = \frac{2[\exp(-h\Omega_i\beta_{s\ max}) - 1 + h\Omega_i\beta_{s\ min}]}{h\Omega_i^2(2+\beta_{s\ max})\beta_{s\ max}[1 - \exp(-\Omega_T\beta_{s\ max})]}$$

.... (A6.2-5)

and

$$[\theta_1(\Omega_i,\beta_s)]_{max} = \frac{2[\exp(-h\Omega_i\beta_{s\ max}) - 1 + h\Omega_i\beta_{s\ max}]}{h\Omega_i^2(2+\beta_{s\ min})\beta_{s\ min}[1 - \exp(-\Omega_T\beta_{s\ min})]}$$

.... (A6.2-6)

Equation (A6.2-4) shows that $Er_s(u)$ also increases with u, which for the required $R_i(u)$ series has a maximum value of $(1 + \frac{\Omega_j}{\Omega_i} - h)$. Using similar reasoning to that used for the $Q_i(u)$ series, we conclude that if the iterative procedure of equations (A7-1) to (A7-8) is continued until the values of $\beta_{s\ min}$ and $\beta_{s\ max}$ are sufficiently close to ensure that

$$E\ r_s(1 + \frac{\Omega_j}{\Omega_i} - h) < e_1, \text{ where for } i=1,\ j=2 \text{ and for } i=2,\ j=1$$

.... (A6.2-7)

then the s-th terms of all the $R_i(u)$ series can be determined to this accuracy.

Combining (A6.2-4), (A6.2-5) and (A6.2-6), it follows that the fractional error in the s-th term of every required $R_i(u)$ series will be less than e_1, when each term is calculated with β_s set equal to the mean of the $\beta_{s\ min}$ and $\beta_{s\ max}$ values for which:-

$$\left\{\frac{BX}{BN}\frac{(2+BX)}{(2+BN)}\frac{[1-\exp(-\Omega_T BX)]}{[1-\exp(-\Omega_T BN)]}\ x\right.$$

$$\left.\frac{[\exp(-h\Omega_i BN)-1+h\Omega_i BX]}{[\exp(-h\Omega_i BX)-1+h\Omega_i BN]}\exp[(\Omega_1+\Omega_2-h\Omega_i)(BX-BN)]\right\}-1<e_1 \qquad \ldots\ldots \text{(A6.2-8)}$$

where $BX \equiv \beta_{s\ max}$ and $BN \equiv \beta_{s\ min}$.

A 6.3 Accuracy of the Calculated Sums of All the $Q_i(u)$ and $R_i(u)$ Series, i=1 or 2

The aim of the next four sections is to develop a single test which, when satisfied, will ensure the accuracy of the calculated sums of all Q- and R- series.

(a) Convergence Rates of the $Q_i(u)$ Series

First, we consider two series $Y_1 = \sum_{s=1}^{\infty} y_s$ and $Y_2 = \sum_{s=1}^{\infty} y_s p(s)$ where $y_s > 0$ for all s and $p(s) > 0$ for $s > r_1$, and define $\bar{S}_r$ and $\bar{R}_r$ to be the partial sum and residue of any such series, so that:-

$$Y_1 = \sum_{s=1}^{r} y_s + \sum_{s=r+1}^{\infty} y_s = \bar{S}_r[Y_1] + \bar{R}_r[Y_1] \qquad \ldots\ldots \text{(A6.3-1)}$$

and

$$Y_2 = \sum_{s=1}^{r} y_s p(s) + \sum_{s=r+1}^{\infty} y_s p(s) = \bar{S}_r[Y_2] + \bar{R}_r[Y_2]$$

..... (A6.3-2)

If p(s) increases with s, and if $\bar{S}_r[Y_2]$ is positive for $s > r_2$, then Edwards [37] has proved that the fractional residue in the partial sum of Y_2 exceeds that of Y_1. That is

$$\frac{\bar{R}_r[Y_2]}{\bar{S}_r[Y_2]} > \frac{\bar{R}_r[Y_1]}{\bar{S}_r[Y_1]} \qquad \text{..... (A6.3-3)}$$

Next consider any $u^1 > h$ and put

$$Y_1 = Q_i(u^1) = \sum_{s=1}^{\infty} \psi(\Omega_i, \beta_s) \exp(-u^1 \Omega_i \beta_s) = \sum_{s=1}^{\infty} y_s$$

..... (A6.3-4)

and

$$Y_2 = Q_i(h) = \sum_{s=1}^{\infty} [\psi(\Omega_i, \beta_s) \exp(-u^1 \Omega_i \beta_s)] \exp[(u^1-h) \Omega_i \beta_s]$$

$$= \sum_{s=1}^{\infty} y_s p(s) \qquad \text{..... (A6.3-5)}$$

where $p(s) = \exp[(u^1-h) \Omega_i \beta_s]$.

Since $u^1-h > 0$ then $p(s) > 0$, and since β_s increases with s, p(s) also increases with s. Hence, applying (A6.3-3) to the series in (A6.3-4) and (A6.3-5) it follows that if, after summing the first r terms of all the required $Q_i(u)$ series, the fractional residue of the series $Q_i(h)$ is less than e_1, then if no further terms are added to the sum of each series, the fractional residue of every sum will be less than e_1.

(b) Convergence Rates of the $R_i(u)$ Series

If we repeat the procedure described in the previous section, but with $Q_i(u^1)$ replaced by $R_i(u^1)$ and $Q_i(h)$ replaced by $R_i(0)$, a similar conclusion may be reached for the $R_i(u)$ series. That is, if after summing the first r terms of all the required $R_i(u)$ series, the fractional residue of the series $R_i(o)$ is less than e_1, then if no further terms are added to the sum of each series, the fractional residue of every sum will be less than e_1.

(c) Comparison of the Convergence Rates of $Q_i(h)$ with $R_i(0)$

$$\text{Let } Y_1 = Q_i(h) = \sum_{s=1}^{\infty} \psi^1(\Omega_i, \beta_s) \left[1 - (1+h\beta_s\Omega_i)\exp(-h\Omega_i\beta_s) \right]$$

$$= \sum_{s=1}^{\infty} y_s \qquad \ldots\ldots \text{(A6.3-6)}$$

and

$$Y_2 = R_i(0) = \sum_{s=1}^{\infty} \psi^1(\Omega_i, \beta_s) \left[1 - (1+h\beta_s\Omega_i)\exp(-h\Omega_i\beta_s)p(s) \right]$$

$$= \sum_{s=1}^{\infty} y_s p(s) \qquad \ldots\ldots \text{(A6.3-7)}$$

where

$$p(s) = \frac{\left[\exp(-h\Omega_i\beta_s) - 1 + h\Omega_i\beta_s \right]}{1 - (1+h\beta_s\Omega_i)\exp(-h\Omega_i\beta_s)} \qquad \ldots\ldots \text{(A6.3-8)}$$

and $\psi^1(\Omega_i, \beta_s)$ is a function of Ω_i and β_s.

Substituting $u = h\Omega_i\beta_s$ and rearranging, then

$$p(s) = \frac{1 - e^u + ue^u}{e^u - 1 - u} \qquad \ldots\ldots \text{(A6.3-9)}$$

Replacing e^u by its Maclaurin series, readily confirms that the right-hand side of (A6.3-9) is positive for all $u > 0$.

To show that p(s) increases with s, we consider

$$\frac{dp}{du} = \frac{e^u\left[e^u - 2 + e^{-u} - u^2\right]}{(e^u - 1 - u)^2} = \frac{e^u\left[2\cosh u - 2 - u^2\right]}{(e^u - 1 - u)^2} \qquad \ldots\ldots \text{(A6.3-10)}$$

The sign of $\frac{dp}{du}$ clearly depends upon the sign of the term $2\cosh u - 2 - u^2$ which is positive for all u, because

$$2\cosh u - 2 - u^2 = 2\left[1 + \frac{u^2}{2} + \frac{u^4}{4!} + \frac{u^6}{6!} + \frac{u^8}{8!} + \ldots\right] - 2 - u^2$$

$$= 2\left[\frac{u^4}{4!} + \frac{u^6}{6!} + \frac{u^8}{8!} + \ldots\right].$$

It follows that p(s) increases with β_s, and as this increases with s, the required condition is established.

By applying (A6.3-3) to (A6.3-6) and (A6.3-7) we see that if the $R_i(0)$ series has been summed to within a fractional residue e_1, then provided the same number of terms are included in its sum, the series $Q_i(h)$ will also have a fractional residue less than e_1.

Combining this result with those of sections (a) and (b) above, we conclude that if after summing the first r terms of all $Q_i(u)$ and $R_i(u)$ series, the fractional error of the

series $R_i(0)$ is less than e_1, then, if no further terms are added, the fractional error of every series will also be less than e_1.

(d) Residue of $R_i(0)$

The residue of $R_i(0)$ after r terms have been summed is given by

$$\bar{R}_r[R_i(0)] = \sum_{s=r+1}^{\infty} \frac{b_s \left[\exp(-h\Omega_i\beta_s)-1+h\Omega_i\beta_s\right]}{h\Omega_i^2\beta_s^2\left[1-\exp(-\Omega_T\beta_s)\right]} = \sum_{s=r+1}^{\infty} y_s \qquad \ldots\ldots \text{(A6.3-11)}$$

where $\Omega_T = \Omega_1 + \Omega_2$.

Writing each term of this residue in the form

$$y_s = \frac{b_s}{\Omega_i\beta_s} - \frac{b_s\left[1-\exp(-h\Omega_i\beta_s)-h\Omega_i\beta_s\exp(-\Omega_T\beta_s)\right]}{h\Omega_i^2\beta_s^2\left[1-\exp(-\Omega_T\beta_s)\right]}$$

$$= \frac{b_s}{\Omega_i\beta_s} - Y(s).$$

we see that

$$\bar{R}_r[R_i(0)] = \sum_{s=r+1}^{\infty} \left(\frac{b_s}{\Omega_i\beta_s} - Y(s)\right) \qquad \ldots\ldots \text{(A6.3-12)}$$

If $Y(s) > 0$ for all $s \geq r+1$, it follows that

$$\bar{R}_r[R_i(0)] < \sum_{s=r+1}^{\infty} \frac{b_s}{\Omega_i\beta_s} . \qquad \ldots\ldots \text{(A6.3-13)}$$

Considering $Y(s) = \dfrac{b_s\left[1-\exp(-h\Omega_i\beta_s)-h\Omega_i\beta_s\exp(-\Omega_T\beta_s)\right]}{h\Omega_i^2\beta_s^2\left[1-\exp(-\Omega_T\beta_s)\right]}$

The denominator of this expression is clearly positive for all s, as is b_s. The sign of Y(s) therefore depends on the sign of the factor $\left\{1-\exp(-h\Omega_i\beta_s)-h\Omega_i\beta_s\exp[-(\Omega_1+\Omega_2)\beta_s]\right\}$. Because $h\Omega_i\beta_s\exp[-(\Omega_1+\Omega_2)\beta_s] < h\Omega_i\beta_s\exp(-h\Omega_i\beta_s)$, then

$$1-\exp(-h\Omega_i\beta_s)-h\Omega_i\beta_s\exp[-(\Omega_1+\Omega_2)\beta_s] > 1-\exp(-h\Omega_i\beta_s)$$

$$-h\Omega_i\beta_s\exp(-h\Omega_i\beta_s) \qquad \ldots\ldots \text{(A6.3-14)}$$

It follows that if the right-hand side of (A6.3-14) is positive, the factor in (A6.3-13) and therefore Y(s) will also be positive. Again putting $u = h\Omega_i\beta_s$, the right-hand side of (A6.3-14) becomes $1-e^{-u} - ue^{-u} = e^{-u}\left[e^u-1-u\right] =$

$e^{-u}\left[\frac{u^2}{2!} + \frac{u^3}{3!} + \frac{u^4}{4!} + \ldots.\right]$, which is positive because $u > 0$.

The relationship in (A6.3-13) is therefore valid, giving, on substituting for b_s,

$$\bar{R}_r\left[R_i(0)\right] < \sum_{r+1}^{\infty}\frac{b_s}{\Omega_i\beta_s} = \sum_{r+1}^{\infty}\frac{2}{\Omega_i(2+\beta_s)} \qquad \ldots\ldots \text{(A6.3-15)}$$

But, from equation (A7-1), for all s,

$$\beta_s = \left[v_s+(s-1)\pi\right]^2 \quad \text{where } 0 < v_s < \frac{\pi}{2}$$

$$\therefore\ 2+\beta_s > (s-1)^2\pi^2 ,$$

and $\frac{1}{2+\beta_s} < \frac{1}{(s-1)^2\pi^2}$

Combining this with (A6.3-15), we have

$$\bar{R}_r\left[R_i(0)\right] < \frac{2}{\Omega_i} \sum_{s=r+1}^{\infty} \frac{1}{(s-1)^2\pi^2}$$

Alternatively, replacing s by q for greater clarity, then

$$\bar{R}_r\left[R_i(0)\right] < \frac{2}{\pi^2\Omega_i} \sum_{q=r}^{\infty} \frac{1}{q^2} \qquad \ldots\ldots \text{(6.3-16)}$$

Using the well-known result that $\sum_{q=1}^{\infty} \frac{1}{q^2} = \frac{\pi^2}{6}$,

we can write (A6.3-16) in the form

$$\bar{R}_r\left[R_i(0)\right] < \frac{2}{\pi^2\Omega_i}\left[\frac{\pi^2}{6} - \sum_{1}^{r-1} \frac{1}{q^2}\right] \qquad \ldots\ldots \text{(A6.3-17)}$$

As the summation of $R_i(0)$ proceeds (A6.3-17) may therefore be used to test whether the fractional residue of this (and all other) series is less than the pre-selected target, e_1.

APPENDIX 7

DOCUMENTATION FOR PROGRAM 2

Purpose: To compute solutions of the integro-differential equations (2-13) and (2-14), thereby giving the hot and cold fluid temperatures $f_1(\zeta,v)$, $f_2(\zeta,v)$ at (2m+1) equally-spaced distances along the regenerator length, at each of (n+1) equally-spaced times during each period.

Method: The method for solving equations (2-13) and (2-14) is described in Chapter 2, Section 2.3, & Appendix 2, Section A2.2. Additional computational techniques are detailed in Chapter 7 and page (viii) of this Appendix.

Input Data: This is read from a previously created data file. The data needed for each regenerator example are the values of:- N_1, N_2, M_1, M_2, Ω_1, Ω_2, n, m, e_1, followed by unity if a further example is to be calculated or a zero, otherwise.

Output: The form of the output from Program 2 is almost identical to that from Program 1.

Requirements: About 21 pages of memory are needed to store the object files for Program 2 and its associated subroutines on a DEC-20 computer. During execution, for n=30, m=48, this requirement increases to about 124 pages, although this could be considerably reduced by the use of space-saving techniques. Double-precision arithmetic is needed for Subroutine 4.

Restrictions: Same as for Program 1 (see Appendix 5).

Outline Flowchart for Program 2

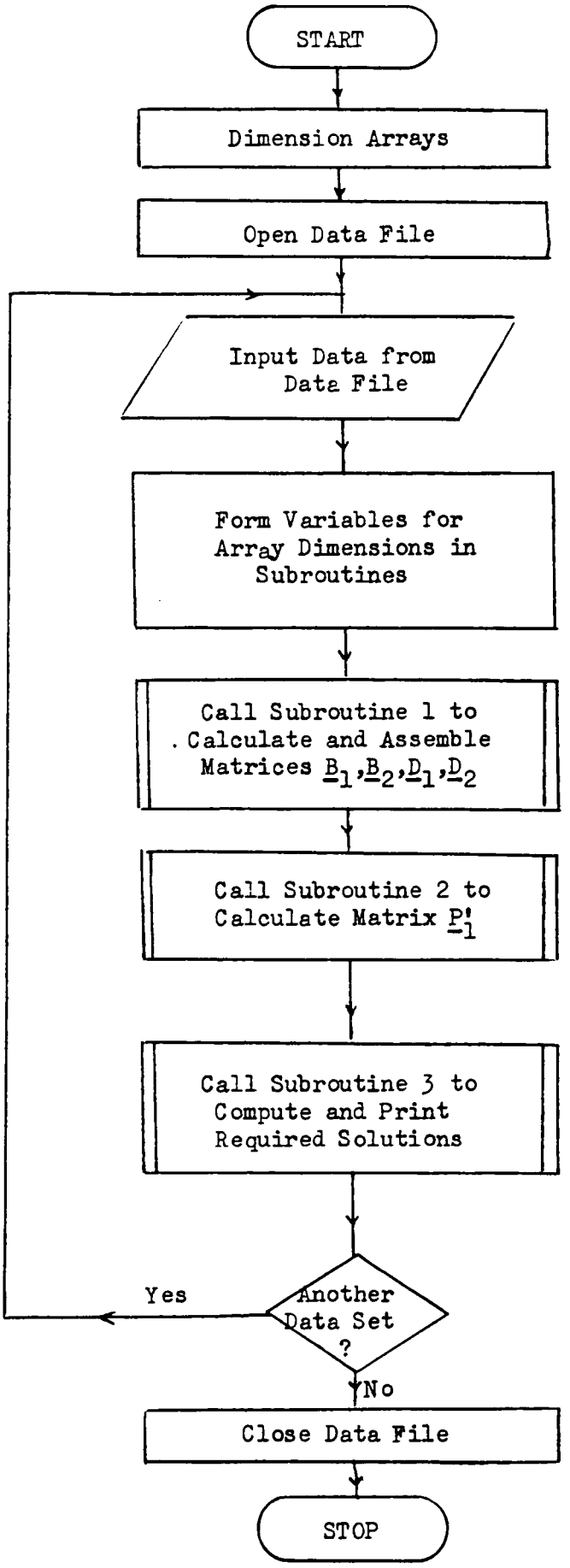

..... See page (i)

..... See page (iii)

..... See page (v)

..... See page (vi)

Main-Line Program

Subroutine 1 (Stage 1; Calculates elements of B_1, B_2, D_1, D_2)

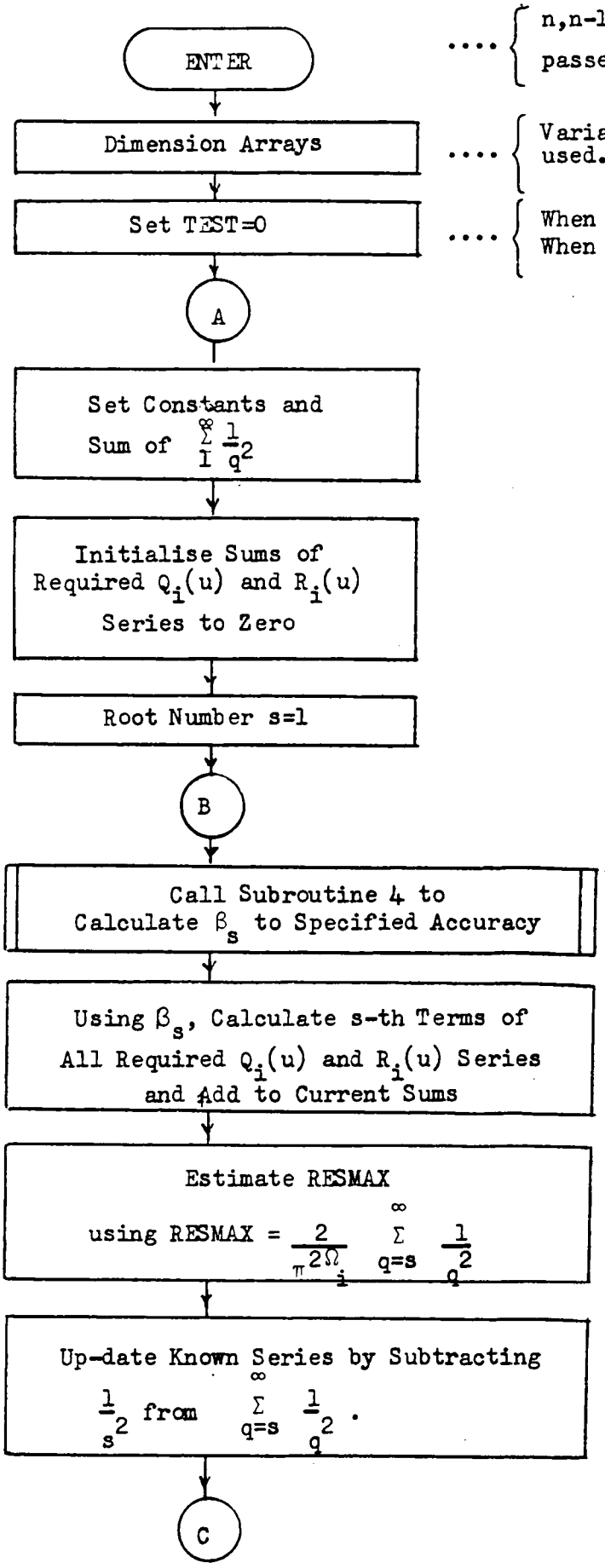

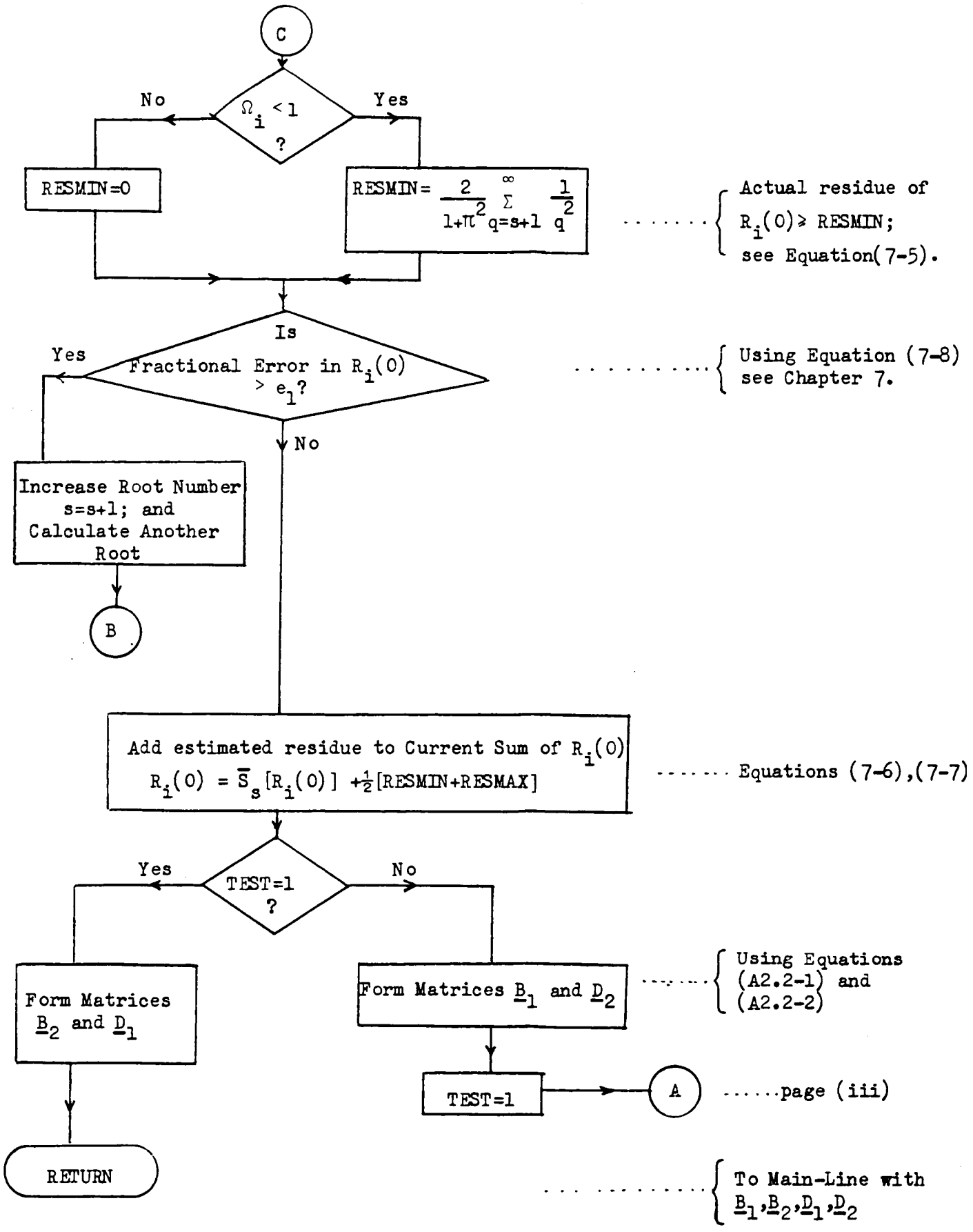
C
No
$\Omega_i < 1$?
Yes
RESMIN=0
RESMIN= $\frac{2}{1+\pi^2} \sum_{q=s+1}^{\infty} \frac{1}{q^2}$
Actual residue of $R_i(0) \geq$ RESMIN; see Equation(7-5).
Is Fractional Error in $R_i(0)$ $> e_1$?
Yes
No
Using Equation (7-8) see Chapter 7.
Increase Root Number s=s+1; and Calculate Another Root
B
Add estimated residue to Current Sum of $R_i(0)$
$R_i(0) = \bar{S}_s[R_i(0)] + \frac{1}{2}[RESMIN+RESMAX]$
Equations (7-6),(7-7)
TEST=1 ?
Yes
No
Form Matrices $\underline{B}_2$ and $\underline{D}_1$
Form Matrices $\underline{B}_1$ and $\underline{D}_2$
Using Equations (A2.2-1) and (A2.2-2)
TEST=1
A
.....page (iii)
RETURN
To Main-Line with $\underline{B}_1, \underline{B}_2, \underline{D}_1, \underline{D}_2$

Subroutine 2 (Stage 2; Calculates Matrix $\underline{P}_1'$)

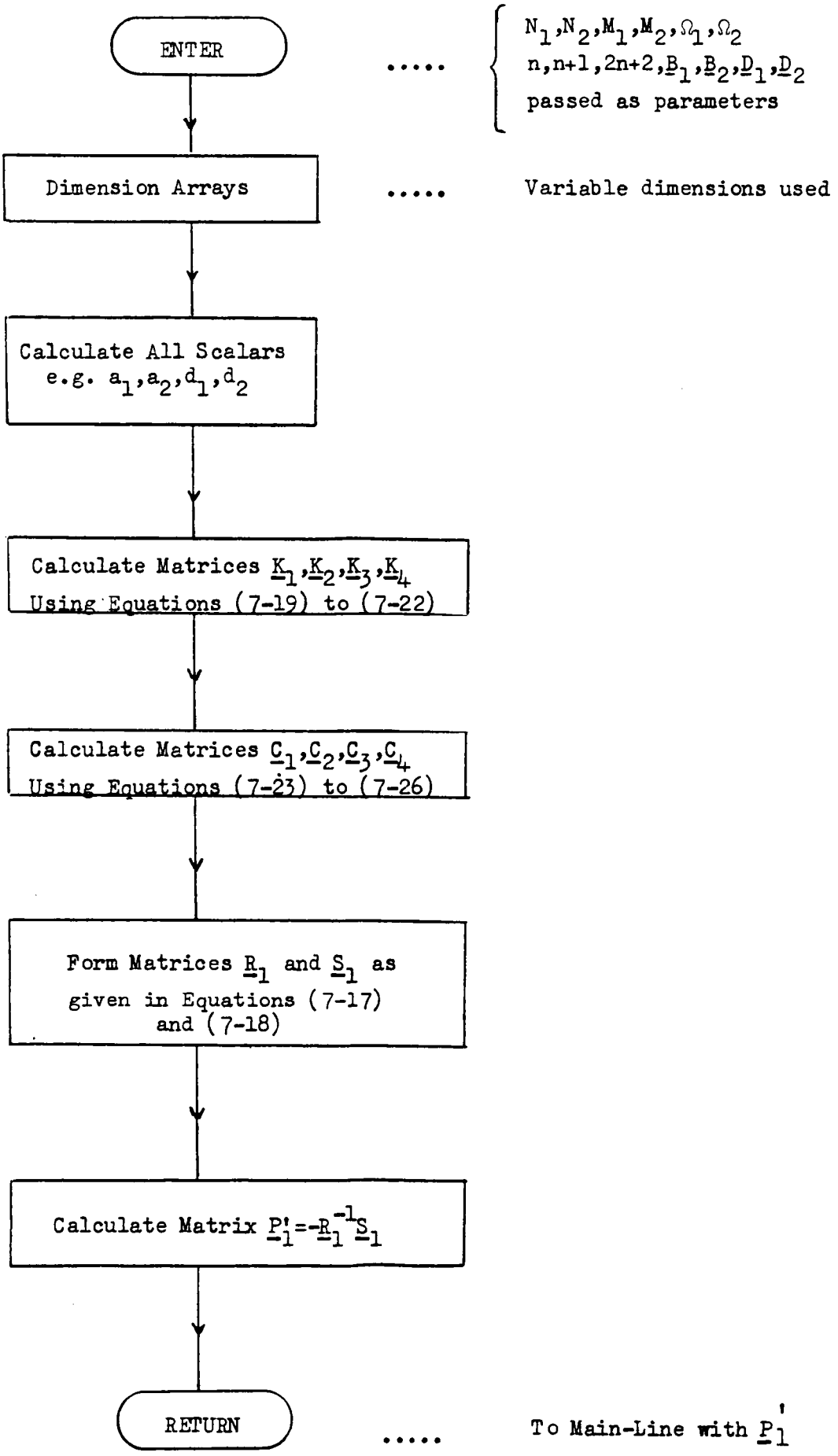

Subroutine 3 Stage 3; Computes and Prints Solutions

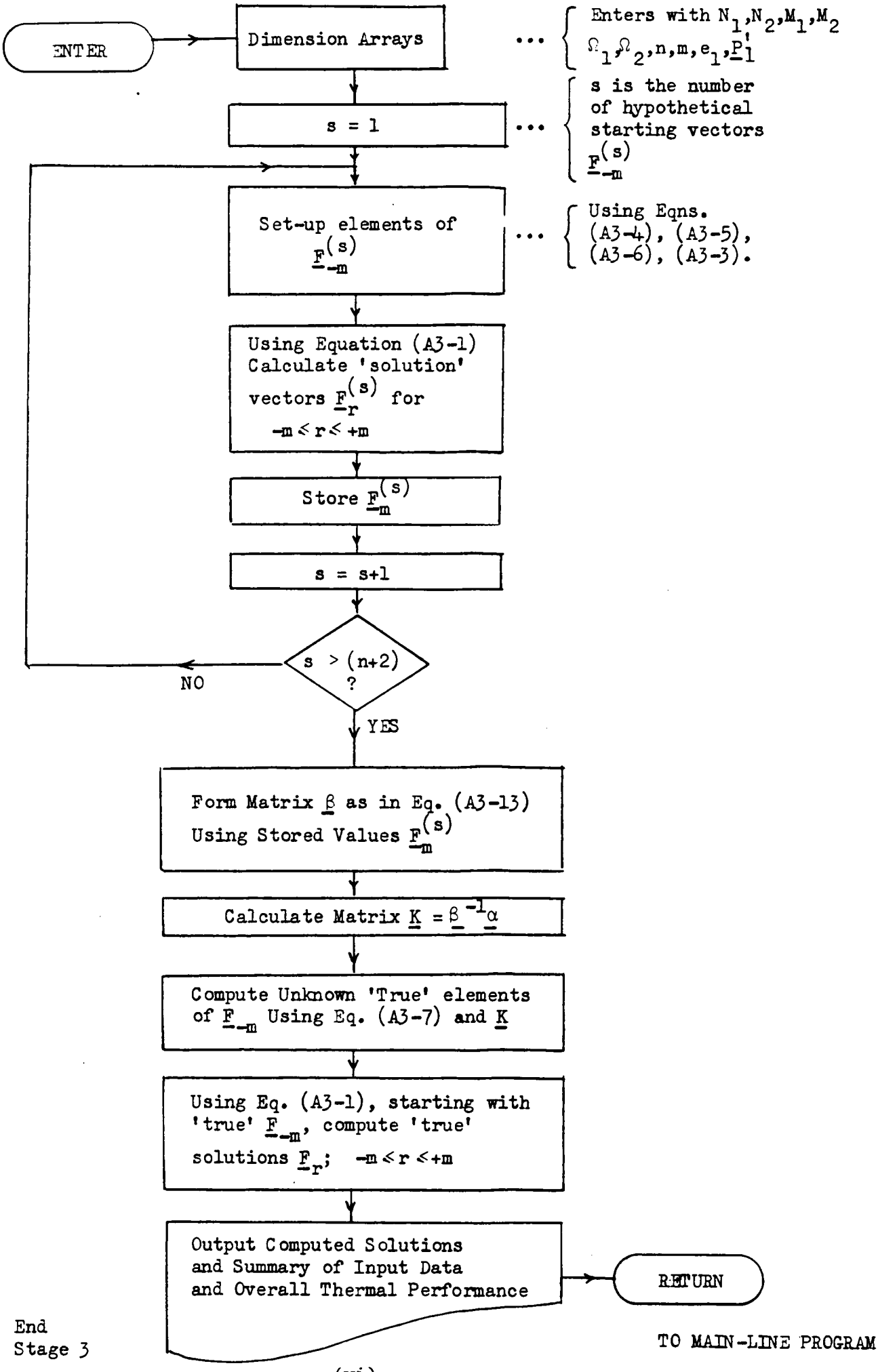

End Stage 3

TO MAIN-LINE PROGRAM

Subroutine 4 Calculates Roots of $\sqrt{\beta}\tan\sqrt{\beta}=1$ - See next page

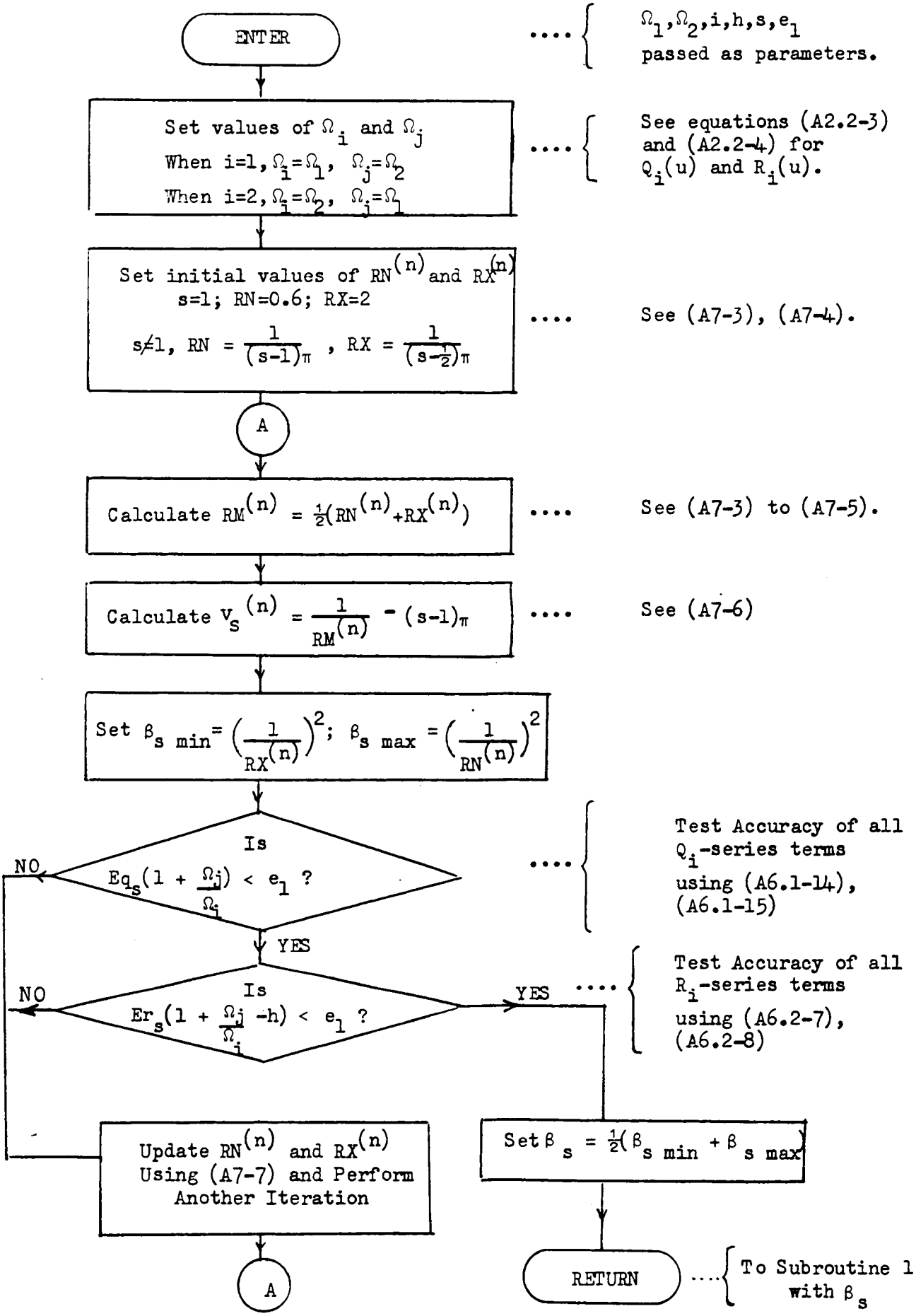

Note on Calculation of Roots of $\sqrt{\beta}\tan\sqrt{\beta} = 1$

Putting $\sqrt{\beta} = v+(s-1)\pi$ the equation to be solved becomes

$$\tan v = \frac{1}{v+(s-1)\pi} \quad , \quad 0 < v < \frac{\pi}{2} \qquad \ldots\ldots \text{(A7-1)}$$

Let $v_s^{(n)}$ denote the n-th estimate of the s-th root of (A7-1), and suppose $v_s^{(n)}$ is between $v_{s\,min}^{(n)}$ and $v_{s\,max}^{(n)}$, so that

$$v_{s\,min}^{(n)} \leqslant v_s \leqslant v_{s\,max}^{(n)} \qquad \ldots\ldots \text{(A7-2)}$$

If we write, for brevity,

$$RN^{(n)} = \frac{1}{v_{s\,max}^{(n)} + (s-1)\pi} \qquad \ldots\ldots \text{(A7-3)}$$

$$RX^{(n)} = \frac{1}{v_{s\,min}^{(n)} + (s-1)\pi} \qquad \ldots\ldots \text{(A7-4)}$$

and $$RM^{(n)} = \tfrac{1}{2}\left[RN^{(n)} + RX^{(n)}\right] \qquad \ldots\ldots \text{(A7-5)}$$

then it can be shown that

$$v_s^{(n)} = \frac{1}{(RM)^n} - (s-1)\pi \qquad \ldots\ldots \text{(A7-6)}$$

This estimate can then be refined by the following procedure:-

$$\left.\begin{array}{l} \text{If } RM^{(n)} > \tan v_s^{(n)}, \text{ replace } RX^{(n)} \text{ by } RM^{(n)} \\ \text{If } RM^{(n)} < \tan v_s^{(n)}, \text{ replace } RN^{(n)} \text{ by } RM^{(n)} \end{array}\right\} \ldots\ldots \text{(A7-7)}$$

At any stage of the calculation we have

$$\beta_{s\ min} = \left[\frac{1}{RX(n)}\right]^2 \quad \text{and} \quad \beta_{s\ max} = \left[\frac{1}{RN(n)}\right]^2 \qquad \ldots\ldots \text{(A7-8)}$$

APPENDIX 8

THE THERMAL 'INVERT' OF A GIVEN REGENERATOR

A8.1 Analysis Based On The 'Equal-Period' Theory

Using the notation introduced in Chapter 2, we consider two physically-identical regenerators, A and B, and assume that the thermal performance of regenerator A is defined by parameters N_1, N_2, M_1, M_2 and Ω, whilst that of regenerator B is defined by the parameters $N_{1,B}$, $N_{2,B}$, $M_{1,B}$, $M_{2,B}$ and Ω.

In the usual way, fluid temperatures in both regenerators are referred to dimensionless distance and time axes ζ and τ respectively, where $-1 \leqslant \zeta \leqslant +1$ and $0 \leqslant \tau \leqslant \Omega$. However, to clarify the analysis presented below, we let the temperatures of the fluids during the heating and cooling periods, at any position ζ and at any time τ, be denoted by $f_1(\zeta,\tau)$ and $f_2(\zeta,\tau)$ for regenerator A, and by $f_{1,B}(\zeta,\tau)$ and $f_{2,B}(\zeta,\tau)$ for regenerator B.

It is further assumed that the fluid entry temperatures are such that

$$f_1(1,\tau) = f_{1,B}(1,\tau) \qquad , 0 \leqslant \tau \leqslant \Omega$$

and

$$f_2(-1,\tau) = f_{2,B}(-1,\tau) \qquad , 0 \leqslant \tau \leqslant \Omega$$

Regenerator A

We have seen in Chapter 2 that the fluid temperatures $f_1(\zeta,\tau)$ and $f_2(\zeta,\tau)$ can be obtained by solving the integro-differential equations (2-5) and (2-6), with the known

fluid entry temperatures as boundary conditions.

Introducing some algebraic simplifications, and also incorporating the expressions given in equations (2-7) and (2-8) for the functions $X_1(\zeta,z')$ and $X_2(\zeta,z')$, the integro-differential equations (2-5) and (2-6) may be written in the following more convenient forms+:

$$f_1(\zeta,\tau) + f_2(\zeta,\tau) - \frac{M_1}{N_1}\frac{\partial f_1}{\partial \zeta}(\zeta,\tau) + \frac{M_2}{N_2}\frac{\partial f_2}{\partial \zeta}(\zeta,\tau)$$

$$+\int_0^I \left\{ -\left[\frac{M_1}{a_1}\frac{\partial f_1}{\partial \zeta} + f_1\right] + \left[\frac{M_2}{a_2}\frac{\partial f_2}{\partial \zeta} - f_2\right] \right\} \eta_1(\tau-\Omega-z')\,dz'$$

$$+\int_\tau^\Omega \left\{ -\left[\frac{M_1}{a_1}\frac{\partial f_1}{\partial \zeta} + f_1\right] + \left[\frac{M_2}{a_2}\frac{\partial f_2}{\partial \zeta} - f_2\right] \right\} \eta_1(\tau-z')\,dz' = 0$$

..... (A8-1)

and

$$-f_1(\zeta,\tau) + f_2(\zeta,\tau) + \frac{M_1}{N_1}\frac{\partial f_1(\zeta,\tau)}{\partial \zeta} + \frac{M_2}{N_2}\frac{\partial f_2(\zeta,\tau)}{\partial \zeta}$$

$$+\int_0^\tau \left\{ \left[\frac{M_1}{a_1}\frac{\partial f_1}{\partial \zeta} + f_1\right] + \left[\frac{M_2}{a_2}\frac{\partial f_2}{\partial \zeta} - f_2\right] \right\} \eta_2(\tau-\Omega-z')\,dz'$$

$$-\int_\tau^\Omega \left\{ \left[\frac{M_1}{a_1}\frac{\partial f_1}{\partial \zeta} + f_1\right] + \left[\frac{M_2}{a_2}\frac{\partial f_2}{\partial \zeta} - f_2\right] \right\} \eta_2(\tau-z')\,dz' = 0$$

..... (A8-2)

+ For greater clarity in this Appendix, the use of functional notation will be restricted to the first line of each equation.

where for equations (A8-1) and (A8-2), $-1 \leqslant \zeta \leqslant +1$, $0 \leqslant \tau \leqslant \Omega$ and

$$a_1 = \frac{N_1}{N_1 - 1} \quad , \quad a_2 = \frac{N_2}{N_2 - 1} \qquad \ldots\ldots \text{(A8-3)}$$

To determine the fluid temperatures $f_1(\zeta,\tau)$ and $f_2(\zeta,\tau)$ at all relevant values of ζ and τ, equations (A8-1) and (A8-2) have to be solved simultaneously subject to the boundary conditions:

$$f_1(1,\tau) = +1 \quad , \quad 0 \leqslant \tau \leqslant \Omega \qquad \ldots\ldots \text{(A8-4)}$$

$$f_2(-1,\tau) = -1 \quad , \quad 0 \leqslant \tau \leqslant \Omega \qquad \ldots\ldots \text{(A8-5)}$$

Regenerator B

Proceeding as for regenerator A, but amending the notation to that appropriate for regenerator B, we see that the fluid temperatures in regenerator B may be obtained as the solutions of equations (A8-6) and (A8-7), subject to the boundary conditions stated in equations (A8-9) and (A8-10).

$$f_{1,B}(\zeta,\tau) + f_{2,B}(\zeta,\tau) - \frac{M_{1,B}}{N_{1,B}} \frac{\partial f_{1,B}}{\partial \zeta}(\zeta,\tau) + \frac{M_{2,B}}{N_{2,B}} \frac{\partial f_{2,B}}{\partial \zeta}(\zeta,\tau)$$

$$+ \int_0^{\tau} \left\{ - \left[\frac{M_{1,B}}{a_{1,B}} \frac{\partial f_{1,B}}{\partial \zeta} + f_{1,B} \right] + \left[\frac{M_{2,B}}{a_{2,B}} \frac{\partial f_{2,B}}{\partial \zeta} - f_{2,B} \right] \right\} \eta_1(\tau - \Omega - \varepsilon') \, d\varepsilon'$$

$$+ \int_{\tau}^{\Omega} \left\{ - \left[\frac{M_{1,B}}{a_{1,B}} \frac{\partial f_{1,B}}{\partial \zeta} - f_{1,B} \right] + \left[\frac{M_{2,B}}{a_{2,B}} \frac{\partial f_{2,B}}{\partial \zeta} - f_{2,B} \right] \right\} \eta_1(\tau - \varepsilon') \, d\varepsilon' = 0$$

..... (A8-6)

$$- f_{1,B}(\zeta,\tau) + f_{2,B}(\zeta,\tau) + \frac{M_{1,B}}{N_{1,B}} \frac{\partial f_{1,B}}{\partial \zeta}(\zeta,\tau) + \frac{M_{2,B}}{N_{2,B}} \frac{\partial f_{2,B}}{\partial \zeta}(\zeta,\tau)$$

$$+ \int_0^{\tau} \left\{ \left[\frac{M_{1,B}}{a_{1,B}} \frac{\partial f_{1,B}}{\partial \zeta} + f_{1,B} \right] + \left[\frac{M_{2,B}}{a_{2,B}} \frac{\partial f_{2,B}}{\partial \zeta} - f_{2,B} \right] \right\} \eta_2(\tau - \Omega - \varepsilon') \, d\varepsilon'$$

$$- \int_{\tau}^{\Omega} \left\{ \left[\frac{M_{1,B}}{a_{1,B}} \frac{\partial f_{1,B}}{\partial \zeta} + f_{1,B} \right] + \left[\frac{M_{2,B}}{a_{2,B}} \frac{\partial f_{2,B}}{\partial \zeta} - f_{2,B} \right] \right\} \eta_2(\tau - \varepsilon') \, d\varepsilon' = 0$$

..... (A8-7)

For equations (A8-6) and (A8-7), $-1 \leqslant \zeta \leqslant +1$, $0 \leqslant \tau \leqslant \Omega$ and

$$a_{1,B} = \frac{N_{1,B}}{N_{1,B} - 1} \quad , \quad a_{2,B} = \frac{N_{2,B}}{N_{2,B} - 1} \qquad \text{..... (A8-8)}$$

The boundary conditions for equations (A8-6) and (A8-7) are:

$$f_{1,B}(1,\tau) = +1 \quad , \quad 0 \leqslant \tau \leqslant \Omega \qquad \ldots\ldots \text{(A8-9)}$$

$$f_{2,B}(-1,\tau) = -1 \quad , \quad 0 \leqslant \tau \leqslant \Omega \qquad \ldots\ldots \text{(A8-10)}$$

The Thermal 'Invert' of Regenerator A

We define regenerator B to be the thermal 'invert' of regenerator A if the following relationships are valid:

$$N_{1,B} = N_2,\ N_{2,B} = N_1,\ M_{1,B} = M_2,\ M_{2,B} = M_1 \qquad \ldots\ldots \text{(A8-11)}$$

In this special case, it follows from equations (A8-3) and (A8-8) that

$$a_{1,B} = a_2 \quad \text{and} \quad a_{2,B} = a_1 \qquad \ldots\ldots \text{(A8-12)}$$

Introducing the relationships given in (A8-11) and (A8-12) into equations (A8-6) and (A8-7), the integro-differential equations for the 'invert' regenerator B become,

$$f_{1,B}(\zeta,\tau) + f_{2,B}(\zeta,\tau) - \frac{M_2}{N_2}\frac{\partial f_{1,B}}{\partial \zeta}(\zeta,\tau) + \frac{M_1}{N_1}\frac{\partial f_{2,B}}{\partial \zeta}(\zeta,\tau)$$

$$+\int_0^{\tau}\left\{-\left[\frac{M_2}{a_2}\frac{\partial f_{1,B}}{\partial \zeta} + f_{1,B}\right] + \left[\frac{M_1}{a_1}\frac{\partial f_{2,B}}{\partial \zeta} - f_{2,B}\right]\right\}\eta_1(\tau-\Omega-\varepsilon')\,d\varepsilon'$$

$$+\int_{\tau}^{\Omega}\left\{-\left[\frac{M_2}{a_2}\frac{\partial f_{1,B}}{\partial \zeta} + f_{1,B}\right] + \left[\frac{M_1}{a_1}\frac{\partial f_{2,B}}{\partial \zeta} - f_{2,B}\right]\right\}\eta_1(\tau-\varepsilon')\,d\varepsilon' = 0$$

$$\ldots\ldots \text{(A8-13)}$$

and

$$-f_{1,B}(\zeta,\tau) + f_{2,B}(\zeta,\tau) + \frac{M_2}{N_2}\frac{\partial f_{1,B}}{\partial \zeta}(\zeta,\tau) + \frac{M_1}{N_1}\frac{\partial f_{2,B}}{\partial \zeta}(\zeta,\tau)$$

$$+\int_0^{\tau}\left\{\left[\frac{M_2}{a_2}\frac{\partial f_{1,B}}{\partial \zeta} + f_{1,B}\right] + \left[\frac{M_1}{a_1}\frac{\partial f_{2,B}}{\partial \zeta} - f_{2,B}\right]\right\}\eta_2(\tau-\Omega-\varepsilon')\,d\varepsilon'$$

$$-\int_{\tau}^{\Omega}\left\{\left[\frac{M_2}{a_2}\frac{\partial f_{1,B}}{\partial \zeta} + f_{1,B}\right] + \left[\frac{M_1}{a_1}\frac{\partial f_{2,B}}{\partial \zeta} - f_{2,B}\right]\right\}\eta_2(\tau-\varepsilon')\,d\varepsilon' = 0$$

..... (A8-14)

with boundary conditions

$$f_{1,B}(1,\tau) = +1 \quad , \; 0 \leqslant \tau \leqslant \Omega \qquad \ldots\ldots \text{(A8-15)}$$

$$f_{2,B}(-1,\tau) = -1 \quad , \; 0 \leqslant \tau \leqslant \Omega \qquad \ldots\ldots \text{(A8-16)}$$

We now introduce the change of variable $\zeta^* = -\zeta$, such that the fluid temperatures $f_{i,B}(\zeta,\tau)$ transform to $f_{i,I}(\zeta^*,\tau)$. Also, to simplify the presentation, we put $F_{i,I}(\zeta^*,\tau) = -f_{i,I}(\zeta^*,\tau)$. Incorporating these changes into equations (A8-13) to (A8-16), we have, after some re-arrangement

$$F_{1,I}(\zeta^*,\tau) + F_{2,I}(\zeta^*,\tau) - \frac{M_1}{N_1}\frac{\partial F_{2,I}}{\partial \zeta^*}(\zeta^*,\tau) + \frac{M_2}{N_2}\frac{\partial F_{1,I}}{\partial \zeta^*}(\zeta^*,\tau)$$

$$+\int_0^{\tau}\left\{-\left[\frac{M_1}{a_1}\frac{\partial F_{2,I}}{\partial \zeta^*} + F_{2,I}\right] + \left[\frac{M_2}{a_2}\frac{\partial F_{1,I}}{\partial \zeta^*} - F_{1,I}\right]\right\}\eta_1(\tau-\Omega-\varepsilon')\,d\varepsilon'$$

$$+\int_{\tau}^{\Omega}\left\{-\left[\frac{M_1}{a_1}\frac{\partial F_{2,I}}{\partial \zeta^*} + F_{2,I}\right] + \left[\frac{M_2}{a_2}\frac{\partial F_{1,I}}{\partial \zeta^*} - F_{1,I}\right]\right\}\eta_1(\tau-\varepsilon')\,d\varepsilon' = 0$$

..... (A8-17)

$$-F_{2,I}(\zeta^*,\tau) + F_{1,I}(\zeta^*,\tau) + \frac{M_1}{N_1}\frac{\partial F_{2,I}}{\partial \zeta^*}(\zeta^*,\tau) + \frac{M_2}{N_2}\frac{\partial F_{1,I}}{\partial \zeta^*}(\zeta^*,\tau)$$

$$+\int_0^{\tau}\left\{\left[\frac{M_1}{a_1}\frac{\partial F_{2,I}}{\partial \zeta^*} + F_{2,I}\right] + \left[\frac{M_2}{a_2}\frac{\partial F_{1,I}}{\partial \zeta^*} - F_{1,I}\right]\right\}\eta_2(\tau-\Omega-\varepsilon')\,d\varepsilon'$$

$$-\int_{\tau}^{\Omega}\left\{\left[\frac{M_1}{a_1}\frac{\partial F_{2,I}}{\partial \zeta^*} + F_{2,I}\right] + \left[\frac{M_2}{a_2}\frac{\partial F_{1,I}}{\partial \zeta^*} - F_{1,I}\right]\right\}\eta_2(\tau-\varepsilon')\,d\varepsilon' = 0$$

..... (A8-18)

In equations (A8-17) and (A8-18) the ranges of ζ^* and τ are $-1 \leqslant \zeta^* \leqslant +1$ and $0 \leqslant \tau \leqslant \Omega$, respectively.

The boundary conditions given in equations (A8-15) and (A8-16) transform to

$$F_{1,I}(-1,\tau) = -1 \quad , \; 0 \leqslant \tau \leqslant \Omega \qquad \text{..... (A8-19)}$$

$$F_{2,I}(1,\tau) = +1 \quad , \; 0 \leqslant \tau \leqslant \Omega \qquad \text{..... (A8-20)}$$

Comparison of equations (A8-17) to (A8-20) for the 'invert' regenerator (B), with equations (A8-1), (A8-2), (A8-4) and (A8-5) for the given regenerator (A), shows that the former equations can be obtained immediately from the latter by replacing f_1, f_2 and ζ by $F_{2,I}$, $F_{1,I}$ and ζ^*, respectively. It follows from this that, in a computation free from numerical error, the solutions obtained from equations (A8-1), (A8-2), (A8-4) and (A8-5) for f_1 and f_2 at $\zeta = \zeta_r$ and $\tau = \tau_s$ (for regenerator A)[+], will also be the solutions for $F_{2,I}$ and $F_{1,I}$ at $\zeta = \zeta_r$ and $\tau = \tau_s$, for the 'invert' regenerator equations (A8-17) to (A8-20).

We have, therefore, for all relevant values of τ

$$\left.\begin{aligned} & f_1(\zeta,\tau) = F_{2,I}(\zeta^*,\tau) = -f_{2,I}(\zeta^*,\tau) = -f_{2,I}(-\zeta,\tau) \\ \text{and} \\ & f_2(\zeta,\tau) = F_{1,I}(\zeta^*,\tau) = -f_{1,I}(\zeta^*,\tau) = -f_{1,I}(-\zeta,\tau) \end{aligned}\right\} \quad \ldots\ldots \text{(A8-21)}$$

In particular, we can write

$$\left.\begin{aligned} & f_1(-1,\tau) = -f_{2,I}(+1,\tau) \\ \text{and} \\ & f_2(+1,\tau) = -f_{1,I}(-1,\tau) \end{aligned}\right\} \; 0 \leqslant \tau \leqslant \Omega \qquad \ldots\ldots \text{(A8-22)}$$

[+] ζ_r and τ_s are particular values of ζ and τ.

These relationships which have been shown to exist between the fluid temperatures calculated for a given regenerator and its thermal 'invert' are demonstrated for Example 1 of Table 2, by the Program 1 results presented in Tables 8 and 9.

Substituting the relationships given in equations (A8-21) and (A8-22) into equations (2-45), (2-46) and (4-8), and again using the sub-script I to represent quantities relevant to the 'invert' regenerator, it is easily shown that:

$$\dot{H}_1 = (\dot{H}_2)_I \qquad \ldots\ldots \text{(A8-23)}$$

$$\dot{H}_2 = (\dot{H}_1)_I \qquad \ldots\ldots \text{(A8-24)}$$

$$\eta_R = (\eta_R)_I \qquad \ldots\ldots \text{(A8-25)}$$

A8.2 Analysis Based on the 'Generalised' Theory

According to the more general theory developed by Edwards [37], the fluid temperatures in a given regenerator can be obtained (even when successive periods are not of equal duration), by solving the integro-differential equations (2-13) and (2-14), subject to the boundary conditions $f_1(1, \frac{\tau}{\Omega_1}) = +1$ and $f_2(-1, \frac{\tau}{\Omega_1}) = -1$, for $0 \leqslant \tau \leqslant \Omega_1$.

Proceeding in a similar way to that given in Section A8.1, but with the thermal performance of regenerator A defined by the parameters N_1, N_2, M_1, M_2, Ω_1, Ω_2 and that of regenerator B by parameters $N_{1,B}$, $N_{2,B}$, $M_{1,B}$, $M_{2,B}$, $\Omega_{1,B}$ and $\Omega_{2,B}$, we

define regenerator B to be the thermal 'invert' of regenerator A if the following relationships are satisfied:

$$\left.\begin{aligned} &N_{1,B} = N_2,\ N_{2,B} = N_1,\ M_{1,B} = M_2,\ M_{2,B} = M_1, \\ &\Omega_{1,B} = \Omega_2,\ \Omega_{2,B} = \Omega_1. \end{aligned}\right\} \quad \ldots\ldots \text{(A8-26)}$$

Introducing appropriate changes to the variables ζ and τ in equations (2-13), (2-14) and the associated boundary conditions, and using a similar analysis to that given in A8.1, the following relationships can be deduced:

$$f_1(\zeta, \frac{\tau}{\Omega_1}) = -f_{2,I}(-\zeta, \frac{\tau}{\Omega_1}) \quad \ldots\ldots \text{(A8-27)}$$

$$f_2(\zeta, \frac{\tau}{\Omega_1}) = -f_{1,I}(-\zeta, \frac{\tau}{\Omega_1}) \quad \ldots\ldots \text{(A8-28)}$$

where $-1 \leqslant \zeta \leqslant +1$ and $0 \leqslant \tau \leqslant \Omega_1$.

By incorporating these relationships into equations (8-1), (8-2), (8-12) and (8-10), and using the notation introduced in the previous section, the following further relationships can be established for computations carried out using the more general theory:

$$H_{T,1} = (H_{T,2})_I \quad \ldots\ldots \text{(A8-29)}$$

$$H_{T,2} = (H_{T,1})_I \quad \ldots\ldots \text{(A8-30)}$$

$$\eta_{R,C} = \frac{M_1\Omega_1}{M_2\Omega_2} (\eta_{R,C})_I \quad \ldots\ldots \text{(A8-31)}$$

$$\eta_R = (\eta_R)_I \quad \ldots\ldots \text{(A8-32)}$$